

# IAEA HUMAN HEALTH SERIES

No. 16

## Atlas of Bone Scintigraphy in the Developing Paediatric Skeleton: The Normal Skeleton, Variants and Pitfalls



**IAEA**

International Atomic Energy Agency

## **IAEA HUMAN HEALTH SERIES PUBLICATIONS**

The mandate of the IAEA human health programme originates from Article II of its Statute, which states that the “Agency shall seek to accelerate and enlarge the contribution of atomic energy to peace, health and prosperity throughout the world”. The main objective of the human health programme is to enhance the capabilities of IAEA Member States in addressing issues related to the prevention, diagnosis and treatment of health problems through the development and application of nuclear techniques, within a framework of quality assurance.

Publications in the IAEA Human Health Series provide information in the areas of: radiation medicine, including diagnostic radiology, diagnostic and therapeutic nuclear medicine, and radiation therapy; dosimetry and medical radiation physics; and stable isotope techniques and other nuclear applications in nutrition. The publications have a broad readership and are aimed at medical practitioners, researchers and other professionals. International experts assist the IAEA Secretariat in drafting and reviewing these publications. Some of the publications in this series may also be endorsed or co-sponsored by international organizations and professional societies active in the relevant fields.

There are two categories of publications in this series:

### **IAEA HUMAN HEALTH SERIES**

Publications in this category present analyses or provide information of an advisory nature, for example guidelines, codes and standards of practice, and quality assurance manuals. Monographs and high level educational material, such as graduate texts, are also published in this series.

### **IAEA HUMAN HEALTH REPORTS**

Human Health Reports complement information published in the IAEA Human Health Series in areas of radiation medicine, dosimetry and medical radiation physics, and nutrition. These publications include reports of technical meetings, the results of IAEA coordinated research projects, interim reports on IAEA projects, and educational material compiled for IAEA training courses dealing with human health related subjects. In some cases, these reports may provide supporting material relating to publications issued in the IAEA Human Health Series.

All of these publications can be downloaded cost free from the IAEA web site:

<http://www.iaea.org/Publications/index.html>

Further information is available from:

Marketing and Sales Unit  
International Atomic Energy Agency  
Vienna International Centre  
PO Box 100  
1400 Vienna, Austria

Readers are invited to provide their impressions on these publications. Information may be provided via the IAEA web site, by mail at the address given above, or by email to:

[Official.Mail@iaea.org](mailto:Official.Mail@iaea.org).



ATLAS OF BONE SCINTIGRAPHY  
IN THE DEVELOPING  
PAEDIATRIC SKELETON:  
THE NORMAL SKELETON,  
VARIANTS AND PITFALLS

The following States are Members of the International Atomic Energy Agency:

AFGHANISTAN	GHANA	NORWAY
ALBANIA	GREECE	OMAN
ALGERIA	GUATEMALA	PAKISTAN
ANGOLA	HAITI	PALAU
ARGENTINA	HOLY SEE	PANAMA
ARMENIA	HONDURAS	PARAGUAY
AUSTRALIA	HUNGARY	PERU
AUSTRIA	ICELAND	PHILIPPINES
AZERBAIJAN	INDIA	POLAND
BAHRAIN	INDONESIA	PORTUGAL
BANGLADESH	IRAN, ISLAMIC REPUBLIC OF	QATAR
BELARUS	IRAQ	REPUBLIC OF MOLDOVA
BELGIUM	IRELAND	ROMANIA
BELIZE	ISRAEL	RUSSIAN FEDERATION
BENIN	ITALY	SAUDI ARABIA
BOLIVIA	JAMAICA	SENEGAL
BOSNIA AND HERZEGOVINA	JAPAN	SERBIA
BOTSWANA	JORDAN	SEYCHELLES
BRAZIL	KAZAKHSTAN	SIERRA LEONE
BULGARIA	KENYA	SINGAPORE
BURKINA FASO	KOREA, REPUBLIC OF	SLOVAKIA
BURUNDI	KUWAIT	SLOVENIA
CAMBODIA	KYRGYZSTAN	SOUTH AFRICA
CAMEROON	LATVIA	SPAIN
CANADA	LEBANON	SRI LANKA
CENTRAL AFRICAN REPUBLIC	LESOTHO	SUDAN
CHAD	LIBERIA	SWEDEN
CHILE	LIBYAN ARAB JAMAHIRIYA	SWITZERLAND
CHINA	LIECHTENSTEIN	SYRIAN ARAB REPUBLIC
COLOMBIA	LITHUANIA	TAJIKISTAN
CONGO	LUXEMBOURG	THAILAND
COSTA RICA	MADAGASCAR	THE FORMER YUGOSLAV REPUBLIC OF MACEDONIA
CÔTE D'IVOIRE	MALAWI	TUNISIA
CROATIA	MALAYSIA	TURKEY
CUBA	MALI	UGANDA
CYPRUS	MALTA	UKRAINE
CZECH REPUBLIC	MARSHALL ISLANDS	UNITED ARAB EMIRATES
DEMOCRATIC REPUBLIC OF THE CONGO	MAURITANIA	UNITED KINGDOM OF GREAT BRITAIN AND NORTHERN IRELAND
DENMARK	MAURITIUS	UNITED REPUBLIC OF TANZANIA
DOMINICAN REPUBLIC	MEXICO	UNITED STATES OF AMERICA
ECUADOR	MONACO	URUGUAY
EGYPT	MONGOLIA	UZBEKISTAN
EL SALVADOR	MONTENEGRO	VENEZUELA
ERITREA	MOROCCO	VIETNAM
ESTONIA	MOZAMBIQUE	YEMEN
ETHIOPIA	MYANMAR	ZAMBIA
FINLAND	NAMIBIA	ZIMBABWE
FRANCE	NEPAL	
GABON	NETHERLANDS	
GEORGIA	NEW ZEALAND	
GERMANY	NICARAGUA	
	NIGER	
	NIGERIA	

The Agency's Statute was approved on 23 October 1956 by the Conference on the Statute of the IAEA held at United Nations Headquarters, New York; it entered into force on 29 July 1957. The Headquarters of the Agency are situated in Vienna. Its principal objective is "to accelerate and enlarge the contribution of atomic energy to peace, health and prosperity throughout the world".

ATLAS OF BONE SCINTIGRAPHY  
IN THE DEVELOPING  
PAEDIATRIC SKELETON:  
THE NORMAL SKELETON,  
VARIANTS AND PITFALLS

## **COPYRIGHT NOTICE**

All IAEA scientific and technical publications are protected by the terms of the Universal Copyright Convention as adopted in 1952 (Berne) and as revised in 1972 (Paris). The copyright has since been extended by the World Intellectual Property Organization (Geneva) to include electronic and virtual intellectual property. Permission to use whole or parts of texts contained in IAEA publications in printed or electronic form must be obtained and is usually subject to royalty agreements. Proposals for non-commercial reproductions and translations are welcomed and considered on a case-by-case basis. Enquiries should be addressed to the IAEA Publishing Section at:

Marketing and Sales Unit, Publishing Section  
International Atomic Energy Agency  
Vienna International Centre  
PO Box 100  
1400 Vienna, Austria  
fax: +43 1 2600 29302  
tel.: +43 1 2600 22417  
email: [sales.publications@iaea.org](mailto:sales.publications@iaea.org)  
<http://www.iaea.org/books>

© IAEA, 2011

Printed by the IAEA in Austria  
April 2011  
STI/PUB/1491

### **IAEA Library Cataloguing in Publication Data**

Atlas of bone scintigraphy in the developing paediatric skeleton : the normal skeleton, variants and pitfalls. — Vienna : International Atomic Energy Agency, 2011.

p. ; 29 cm. — (IAEA human health series, ISSN 2075-3772 ; no. 16)  
STI/PUB/1491

ISBN 978-92-0-112710-5

Includes bibliographical references.

1. Children development — Radioisotope scanning — Atlases.
  2. Children development — Nuclear medicine. 3. Children development — Musculoskeletal system — Abnormalities — Radionuclide imaging.
- I. International Atomic Energy Agency. II. Series.

IAEAL

11-00671

# FOREWORD

Since the introduction of  $^{99\text{m}}$ technetium polyphosphate in 1972 by Dr. M. Subramanian, bone scintigraphy has become an integral part of the evaluation of paediatric musculoskeletal disorders. Using the current high resolution gamma cameras and  $^{99\text{m}}$ technetium-methylene diphosphonate ( $^{99\text{m}}\text{Tc-MDP}$ ) or  $^{99\text{m}}\text{Tc}$  2,3-dicarboxypropane-1,1-diphosphonate ( $^{99\text{m}}\text{Tc-DPD}$ ), the quality of images available for interpretation is high. From the very earliest days, there has been a certain confusion over normal bone physiology, as depicted by the bone scintigram in paediatric patients. This has resulted in a number of difficulties in detecting subtle abnormalities, especially near the dynamically changing scintigraphic presentation of the physes (growth zones). Examples of abnormalities that might be confused with normal bone activity are osteomyelitis, bucket handle fractures of the long bones, as well as neuroblastoma and leukaemic metastases.

The aim of this publication is to provide structured information about the maturation and normal appearance of the skeleton from infancy to adulthood. As such, it reflects the current status of bone scintigraphy. It is hoped that this work will contribute to an enhanced understanding of the dynamic process of naturally occurring metabolic bone changes, which will, in turn, improve the quality of reporting of paediatric bone scans. As the majority of paediatric bone scintigrams are interpreted by non-paediatric nuclear physicians, the availability of this reference atlas should improve the care of children.

This atlas is intended to address the needs of nuclear medicine physicians, both residents and specialists. It is intended to serve as an illustrative reference to those not having sufficient exposure to paediatric bone scan investigations, to enable them to maintain adequate competency in this particular application. Experts in paediatric nuclear medicine are often consulted for their opinion on bone scans obtained in their respective countries. It became obvious that only physicians who were experienced in paediatric nuclear medicine could immediately recognize the appearance of a 'normal' bone scan. Maintaining high quality bone images is an important issue that needs constant attention at various operational levels of the nuclear medicine department.

The above consideration provided the stimulus leading the Paediatric Task Group of the EANM in 1992 to compile and publish the first edition of the Atlas of Bone Scintigraphy in the Developing Paediatric Skeleton as one of its collaborative projects. More than 17 years later, the need for an updated edition of this reference publication is more relevant than ever.

There has been a consensus among leading professionals in the field of paediatric nuclear medicine, particularly among those involved in teaching and reporting activities, that it is an important endeavour to disseminate the know-how concentrated in this atlas among as many specialists and scholars as possible. The IAEA acknowledges the contributions made to this publication by the Paediatric Task Group of the European Association of Nuclear Medicine and by other experts in the field. Permission to publish an updated edition of this atlas was granted by the authors and by Springer Verlag.

The IAEA officer responsible for this publication was J.J. Zaknun of the Division of Human Health.

## *EDITORIAL NOTE*

*Although great care has been taken to maintain the accuracy of information contained in this publication, neither the IAEA nor its Member States assume any responsibility for consequences which may arise from its use.*

*The use of particular designations of countries or territories does not imply any judgement by the publisher; the IAEA, as to the legal status of such countries or territories, of their authorities and institutions or the delimitation of their boundaries.*

*The mention of the name of specific companies or products (whether or not indicated as registered) does not imply any intention to infringe proprietary rights, nor should it be construed as an endorsement or recommendation on the part of the IAEA.*

# CONTENTS

1.	INTRODUCTION .....	1
1.1.	Background.....	1
1.2.	Objective.....	1
1.3.	Scope.....	1
1.4.	Structure .....	1
1.5.	Principles of bone scanning .....	2
1.5.1.	Bone physiology and structure .....	2
1.5.2.	Tracer localization.....	2
1.5.3.	Effect of age and gender on skeletal maturation.....	2
1.5.4.	Effect of immobilization.....	2
1.5.5.	Causes of increased or decreased tracer uptake .....	3
1.5.6.	Indications for bone scanning in children.....	3
1.6.	Functional anatomical correlation.....	4
1.6.1.	Anterior whole body bone scan .....	4
1.6.2.	Posterior whole body bone scan .....	5
1.7.	Patients and methods.....	5
1.7.1.	Inclusion criteria .....	5
1.7.2.	Radiopharmaceuticals.....	6
1.7.3.	Blood pool images .....	6
1.7.4.	Bone scan images .....	6
1.7.5.	Immobilization during imaging .....	6
1.7.6.	Sedation.....	7
1.7.7.	Image recording and graphical production .....	7
2.	AGE 0–6 MONTHS.....	11
3.	AGE 6–12 MONTHS.....	23
4.	AGE 1–2 YEARS.....	35
5.	AGE 2–3 YEARS.....	49
6.	AGE 3–4 YEARS.....	65
7.	AGE 4–5 YEARS.....	83
8.	AGE 5–6 YEARS.....	99
9.	AGE 6–7 YEARS.....	115
10.	AGE 7–8 YEARS.....	131
11.	AGE 8–9 YEARS.....	149
12.	AGE 9–10 YEARS.....	167
13.	AGE 10–11 YEARS.....	187
14.	AGE 11–12 YEARS.....	205



15. AGE 12–13 YEARS.....	223
16. AGE 13–14 YEARS.....	239
17. AGE 14–15 YEARS.....	255
18. AGE 15–17 YEARS.....	271
19. AGE 17–22 YEARS.....	285
20. KNEES.....	297
21. HIPS.....	317
22. CONCLUDING REMARKS.....	343
APPENDIX: PAEDIATRIC DOSAGE OF RADIOPHARMACEUTICALS .....	345
CONTRIBUTORS TO DRAFTING AND REVIEW.....	349

# 1. INTRODUCTION

## 1.1. BACKGROUND

The clinical value of bone scanning was established in the late 1960s. Over time, advances in imaging instrumentation and the introduction of  $^{99m}\text{Tc}$  labelled bone seeking radiopharmaceuticals have led to shortened procedure time, improved image quality and acceptance among clinicians, thereby consolidating the clinical value of dynamic and static bone scanning for the management of a long list of indications comprising non-communicative and communicative diseases.

## 1.2. OBJECTIVE

The objective of this atlas is to provide a source of illustrated reference material and structured illustrated information about the maturation and normal appearance of the skeleton from infancy to adulthood. It is intended that this atlas will contribute to an enhanced understanding of the dynamic process of naturally occurring metabolic bone changes, which will, in turn, improve the quality of reporting of paediatric bone scans. As the majority of paediatric bone scintigrams are interpreted by non-paediatric nuclear medicine physicians, the availability of this reference atlas should contribute to supporting and improving the diagnostic process, with the aim of improving the standard of health care received by children referred to bone scanning.

## 1.3. SCOPE

This atlas addresses the needs of nuclear medicine physicians, both residents and specialists. It serves as an illustrative reference to nuclear medicine professionals and to those having insufficient access to paediatric bone scanning, thereby maintaining an adequate level of competence in order to address more fully indications, optimizing imaging protocols and enhancing the overall quality of reporting in this particular application.

## 1.4. STRUCTURE

The atlas is subdivided into three major parts. An introductory section covers theoretical and practical aspects related to bone scanning. These aspects include biochemistry, physiology and conditions affecting the normal distribution of technetium labelled phosphonates in healthy and diseased tissue. Section 1 provides a list of indications for performing bone scanning in children. Practical advice is provided, including hands-on techniques to facilitate immobilization and optimal positioning of newborn, child and juvenile patients to achieve best possible imaging results; these are supported by illustrations and the advice of experts in the field. Section 1.7 summarizes the inclusion criteria and methodology endorsed for the process of selecting 'normal' scans and the reproduction of the figures. As a relevant accessory to the methodology, the fraction of administered adult dose to paediatric patients is provided separately in Appendix I. In the second part of the publication, Sections 2–19 provide scintigraphic 'blood pool' tissue and delayed bone scans of the developing skeleton for different age groups, from the newborn to patients of 22 years of age.

A medical knowledge of the normal appearance of the knee and hip joints on bone scans is essential in order to identify subtle changes caused by benign or malignant processes affecting these areas. For this purpose, the third part of the atlas (Sections 20 and 21) provides highly detailed scans of knee and hip joints that appear normal and Section 22 provides concluding remarks.

## 1.5. PRINCIPLES OF BONE SCANNING

### 1.5.1. Bone physiology and structure

Bone tissue is a complex viable dynamic structure comprising protein and minerals coexisting in equilibrium, in which the osteocytes and vascular structures are suspended. Bone mineral is deposited in the collagen by osteocytes. Bone mineral accounts for approximately 70% of bone mass, of which about two thirds are a calcium–magnesium–phosphate complex of hydroxyapatite crystals. In addition to bone collagen and calcium hydroxyapatite crystals, bone contains ions of sodium, magnesium, strontium, fluorine, barium, lead, gallium and trace amounts of caesium. Numerous factors in the healthy and diseased body affect bone metabolism and, therefore, impact on this equilibrium and turnover in an anabolic or a catabolic fashion. These factors include, among others, physical activity, vitamins and nutrition, hormones and steroids, inflammatory processes and medications. Increased bone turnover is present at sites of growing bone and following bone injury. Following intravenous injection of  $^{99m}\text{Tc}$  methylene diphosphonate (MDP), approximately 40% of the tracer will localize to the bone within several hours, whilst the remaining activity will undergo renal elimination.

### 1.5.2. Tracer localization

Factors affecting bone localization of bone seeking radiopharmaceuticals include:

- (a) Bone blood flow;
- (b) Extracellular fluid space of bone;
- (c) Ion exchange (between the tracer and ions in the bone);
- (d) Diffusion of the tracer within bone tissue;
- (e) Increased surface absorption to bone.

### 1.5.3. Effect of age and gender on skeletal maturation

The paediatric skeleton is in a constant state of growth and maturation from birth to adulthood. This maturation involves the growth of every bone, growth being principally located at the epiphyseal plates. Since the  $^{99m}\text{Tc}$  bone scanning agents are adsorbed onto the hydroxyapatite, accumulated activity on the bone scan reflects higher bone turnover. In the developing skeleton, the appearance of the rapidly growing areas is, therefore, different at different stages of maturation. Early in the course of interpreting bone scintigrams in children, it was realized that there was a significant difference in the appearance of the physes in the first years of life compared to that in a more mature child. The growth zone is globular at birth and becomes discoid later in childhood. The process is completed in about two years. The maturation of the physes varies considerably, especially between males and females. As the growth zone fuses, there is a blurring of the normal linear pattern, until eventually the adult appearance emerges. The time at which this occurs varies according to the child's degree of physical activity and their state of health and nutrition. As shown in this atlas, there is an obvious general pattern to the closure of the growth zones. It is extremely important to understand this information, in order to determine whether there is premature closure secondary to focal disease or therapy. It is also extremely important to be aware of the presence of normal apophyses, sychondroses and sutures.

### 1.5.4. Effect of immobilization

An important observation is that a child who ceases to use a limb for even as little as 24 hours, particularly one who has not reached skeletal maturity, will suffer as much as 50% reduction in bone activity in that limb. This can be due simply to pain, even if it is not related to a musculoskeletal problem. In such circumstances, it is necessary to question the child or their guardians carefully in order to determine whether or not there is a reason for the reduction in the use of the limb.

### 1.5.5. Causes of increased or decreased tracer uptake

Increased uptake is found in:

- (a) Normal states: growing metaphyses and epiphyses, costochondral junctions, facial bones, spine sternoclavicular joints, scapulae, shoulders, sacroiliac joints, elbows, and knees.
- (b) Normal variants: persistent ossification centres.
- (c) Soft tissue abnormalities: myositis ossificans, calcinosis cutis, calcific tendinitis, onychomycosis, healing wounds, sites of intramuscular injections, sites of bone marrow biopsy or aspiration.
- (d) Pathological conditions of bone:
  - Benign: bone tumours, hyperostosis, congenital fusion of vertebrae, fibrous dysplasia, eosinophilic granuloma, hypertrophic osteodystrophy, regional osteoporosis, arthritis, fractures, osteomyelitis, gout, Paget's disease, hyperparathyroidism, ischemic necrosis of hip, systemic mastocytosis and bone infarction.
  - Malignant: primary and metastatic tumours, multiple myeloma and lymphomas.

Decreased uptake is found in:

- (a) Pathological conditions: bone cyst, gangrene.
- (b) Non-pathological conditions: artefacts, such as metallic fillings for teeth, gold teeth, pacemaker, prostheses and overlying oral contrast media.
- (c) Iatrogenic: site of external beam radiation therapy.

### 1.5.6. Indications for bone scanning in children

Bone scintigraphy shows high sensitivity in the detection of changes in bone metabolism associated with pathology and is therefore useful in the early localization of sites of pathology. Common clinical indications for bone scanning are:

- (a) Infection or inflammation:
  - Acute osteomyelitis;
  - Differentiation between soft tissue inflammation (cellulitis) and osteomyelitis;
  - Subacute and chronic osteomyelitis;
  - Septic arthritis complicating osteomyelitis;
  - Aseptic arthritis.
- (b) Bone tumours:
  - Benign bone tumours, e.g. osteoid osteoma;
  - Malignant bone tumours;
  - Tumor-like lesions, e.g. Langerhans histiocytosis;
  - Bone metastases.
- (c) Aseptic necrosis:
  - Legg–Calvé–Perthes disease;
  - Sickle cell disease.
- (d) Trauma:
  - Equivocal X ray findings after trauma;
  - Stress fractures;
  - Child abuse (battered child syndrome);
  - Polytrauma;
  - Complications of fractures and therapy.
- (e) Other clinical situations in paediatrics:
  - Pain, possibly due to bone pathology;
  - Limp or backache;
  - Fever of unknown origin;
  - Metabolic bone disease.

For additional reading, the European Association of Nuclear Medicine’s (EANM) web portal provides two relevant guidelines on performing bone scintigraphy. These guidelines have considered and integrated the recommendations of the American Society of Nuclear Medicine guideline on the same topic. The first guideline aimed at performing bone scintigraphy in the paediatric population<sup>1</sup>.

The second guideline is directed predominantly at the adult oncology patients<sup>2</sup>.

### 1.6. FUNCTIONAL ANATOMICAL CORRELATION

#### 1.6.1. Anterior whole body bone scan

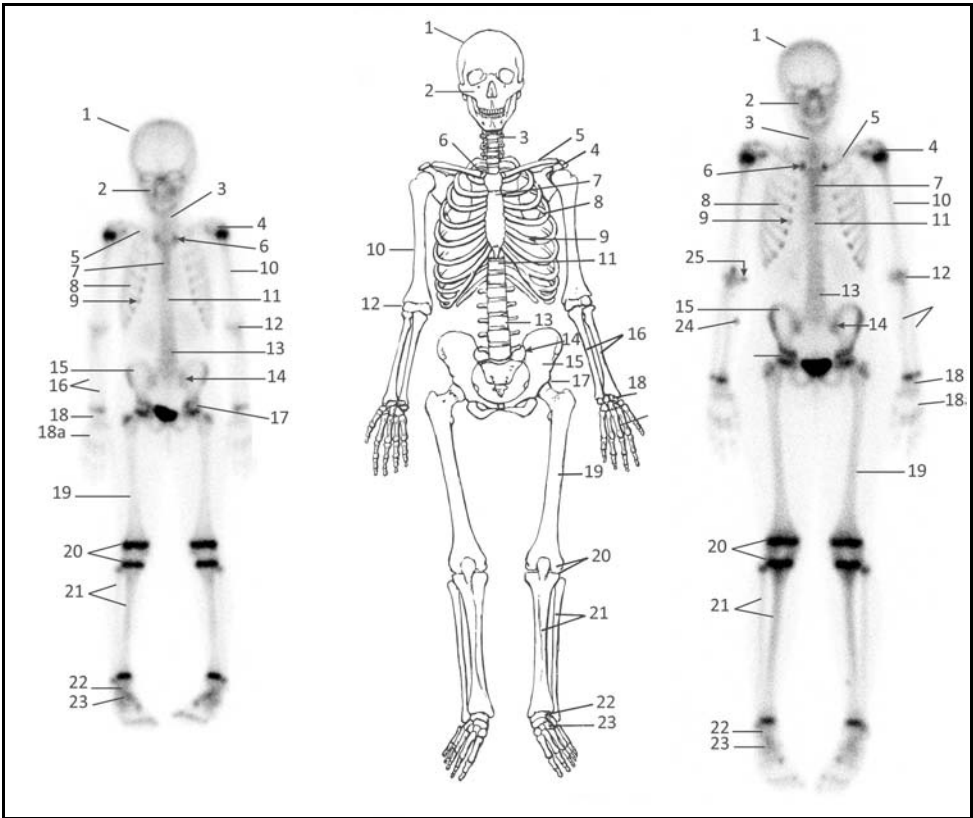


**FIG. 1.** Schematic presentation of the human skeleton, anterior whole body bone scan images acquired in 6- and 12-year-old children.

1. Skull	10. Humerus	19. Femur
2. Facial bones	11. Thoracic spine	20. Knee metaphyses and epiphyses
3. Cervical spine	12. Elbow	21. Tibia and fibula
4. Shoulder	13. Lumbar spine	22. Ankle
5. Clavicle	14. Sacroiliac joint	23. Foot
6. Sternoclavicular joint	15. Pelvis	24. Injection site
7. Sternum	16. Radius and ulna	25. Lymph node accumulation
8. Ribs	17. Hip	
9. Costochondral joints	18. Wrist	
	18a. Hand	

<sup>1</sup> [https://www.eanm.org/scientific\\_info/guidelines/gl\\_paed\\_bone\\_scin.pdf](https://www.eanm.org/scientific_info/guidelines/gl_paed_bone_scin.pdf).

<sup>2</sup> [https://www.eanm.org/scientific\\_info/guidelines/gl\\_onco\\_bone.pdf](https://www.eanm.org/scientific_info/guidelines/gl_onco_bone.pdf).

### 1.6.2. Posterior whole body bone scan

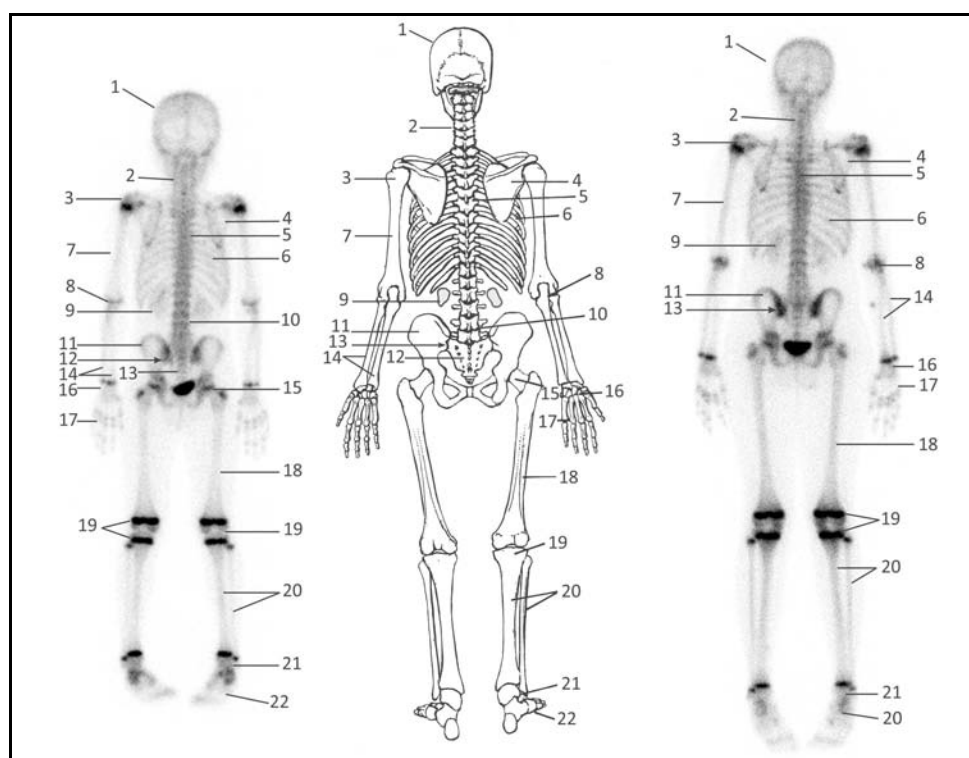


FIG. 2. Schematic presentation of the human skeleton, posterior whole body bone scan images acquired in 6- and 12-year-old children.

1. Skull	9. Kidney	17. Hand
2. Cervical spine	10. Lumbar spine	18. Femur
3. Shoulder	11. Pelvis, iliac bone	19. Knee metaphyses and epiphyses
4. Scapula	12. Sacroiliac joint	20. Tibia and fibula
5. Thoracic spine	13. Sacrum	21. Ankle
6. Ribs	14. Radius and ulna	22. Foot
7. Humerus	15. Hip	
8. Elbow	16. Wrist	

## 1.7. PATIENTS AND METHODS

This section describes the methodology applied in the process of selecting ‘normal’ patients, pharmaceuticals, acquisition parameters and methods used for producing final graphical illustrations.

### 1.7.1. Inclusion criteria

No ‘healthy’ children underwent bone scans, the scans included here are, rather, from the children who had undergone bone scintigraphy for clinical reasons, but in whom it was considered highly probable that the skeleton was normal. EANM’s Paediatric Task Group defined the following groups of children for inclusion:

- (a) *Focal symptoms*: These are thought to be due to bone pathology in a healthy child, if the child did not have any skeletal pathology on follow-up and if the cause of the symptoms was found to lie outside the skeleton. This group underwent bone scans mainly for suspected infection or trauma.

- (b) *Generalized symptoms*: Bone scintigraphy was carried out if the diagnosis was not clear. Only those children who had undergone bone scans within 72 h after the onset of symptoms were included. All of these children were ambulatory and not confined to bed prior to the bone scan. There was no alteration of skeletal metabolism or radionuclide uptake. Clinical follow-up in all of these children ensured that none of the children included were later found to have any malignancy or bone pathology.
- (c) *Known malignancy*: Children with certain solid tumours, such as rhabdomyosarcoma, teratoma, Wilms' and yolk sac tumours were included only if the bone scan had been carried out prior to the administration of any chemotherapeutic agents. These patients were ambulatory prior to, and at the time of, the scintigraphy.
- (d) *Localized benign bone tumours*: Only those parts of the skeleton not affected by the benign bone tumours were included.
- (e) *Suspected fracture*: If whole body images were obtained in those children with suspected single acute fracture, the images from the non-affected areas were included.
- (f) *Children with localized pain, but without certain evidence of bone disease*: Most of these children were suffering from backache.
- (g) *Children with ichthyosis*.

In age, the 'normal' children ranged from neonates to 22-year-olds.

### 1.7.2. Radiopharmaceuticals

The radiopharmaceuticals used were  $^{99m}\text{Tc}$ -MDP or  $^{99m}\text{Tc}$  dicarboxypropane diphosphonate (DPD). The dose used followed the recommendations of the updated EANM Paediatric Dosage Card provided in Appendix I (Tables 1 and 2). The minimum amount of activity injected was 40 MBq; this should guarantee good quality images. The radiopharmaceutical was administered strictly intravenously via an indwelling catheter or a butterfly needle, and thereafter flushed slowly with normal saline. The butterfly, unless otherwise indicated, was removed before starting the imaging.

### 1.7.3. Blood pool images

Static gamma camera images were completed within 5–10 min of the injection. The minimum acquired count rate was 100 000 counts. The maximum time per image was 3 min. For acquiring whole body scans, imaging was started directly after the injection of the radiopharmaceutical, using a camera scan speed of 25–30 cm/min.

### 1.7.4. Bone scan images

The images were acquired no sooner than 3 h post-injection, with a minimum count rate of 50 000 counts for hands and feet, 100 000 counts for the knee joint and 200 000 counts for the skull. Between 250 000 and 500 000 counts were acquired for images of the pelvis and the remaining skeleton. Static images were acquired with Elscint, Picker or Siemens gamma cameras, with the child lying directly on top of the head of the gamma camera (Figs 1.3 and 1.4).

Whole body scans were acquired with speeds of 8 cm/min in children up to the age of 8 years, 10 cm/min in children ranging from 8 to 12 years and 12 cm/min in children ranging from 12 to 16 years. For patients older than this, the scan speed was 15 cm/min. Whole body scans were acquired on an Elscint, Siemens or GE system equipped with low energy, high resolution collimators (Fig. 1.5).

### 1.7.5. Immobilization during imaging

For infants and young children, adaptive techniques to achieve direct positioning on top of the camera head are shown in Fig. 1.3. Accessories to be used to support the positioning and immobilization of infants are presented in Fig. 1.4. These can be produced locally or in-house and commonly include sand bags of different shapes and self-adhesive bands of different lengths adapted to fit infants or children. The Plexiglas triangle shown in Fig. 1.5 is used to fix the foot of the older child to achieve an internal rotation of the lower limb. This position of the lower limb provides optimal visualization of the fibula and of the hip joint and proximal femur.



### 1.7.6. Sedation

There was no routine sedation. If required, mild sedation with Dominal (prothipendyl) or Dormicum (midazolam) was used.

### 1.7.7. Image recording and graphical production

The majority of the primary images were recorded on X ray film, transparent foils and photographic paper. All selected images were prepared in the same film laboratory in the Klinik für Nuklearmedizin, University Hospital, Mainz, Germany. The more recent scintigraphic images, pictures and schemes were recorded digitally.



*FIG. 3. Adapting a wooden plate (2 cm thick) with a circular opening tightly fitted to the head of a single headed gamma camera can provide a comfortable surface for conducting scintigraphic investigations on children. The minimal distance between the body (organ) and the camera will allow production of high quality images while maintaining the greatest possible comfort for the child.*

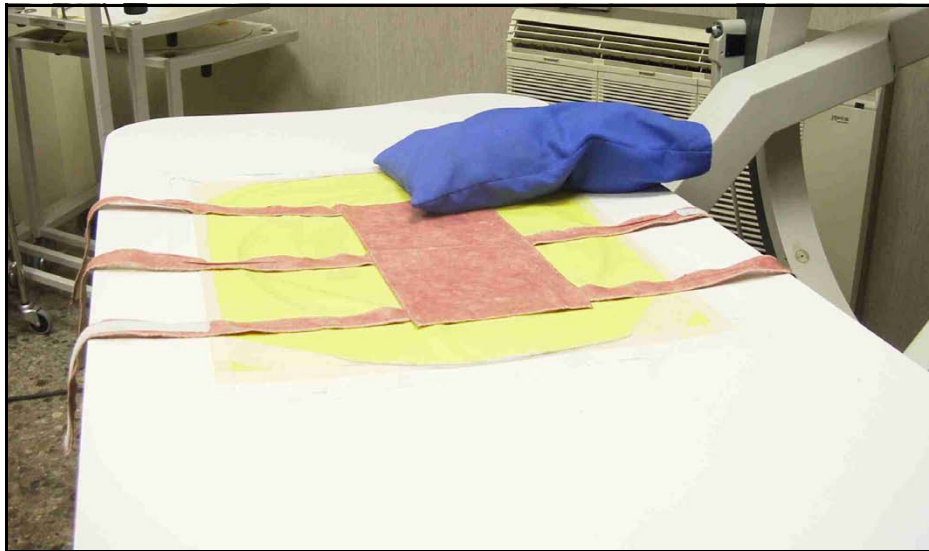


*FIG. 4. Avoiding motion artifact is essential for good quality images. Tools to achieve immobilization of a baby may include sand bags and adhesives (Velcro®) bands. These can be produced locally or in-house and are implemented successfully by the nuclear medicine technologists (courtesy of I. Roca, Val d'Hebron Hospital, Spain).*



*FIG. 5. Correct positioning of a child for whole body scanning. Fixing the feet with internal rotation is achieved by the use of a Plexiglas triangle. This positioning ensures optimal visualization of the fibulae. Note that the butterfly needle or the Venflon used for injecting the radiopharmaceutical should be removed prior to the start of scanning (courtesy of M.D. Mann, Red Cross Children's Hospital, Cape Town, South Africa).*

*FIG. 1. ....*

*FIG. 4. ....*

*FIG. 2. ....*

*FIG. 5. ....*

*FIG. 3. ....*

*FIG. 6. ....*

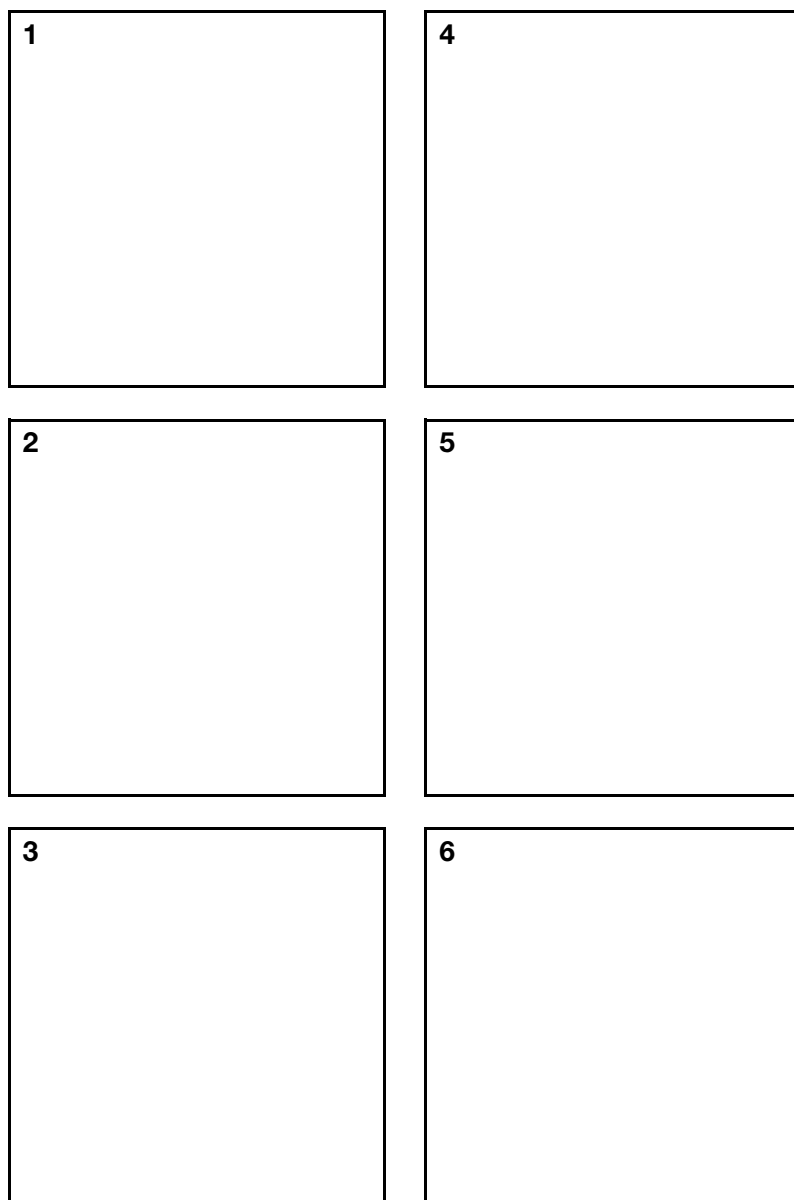


*FIG. 6. The orientation of images and their captions as displayed throughout the atlas.*

## **2. AGE 0–6 MONTHS**



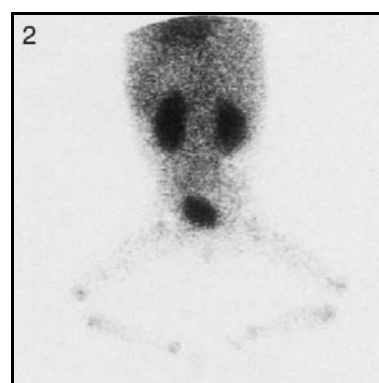
## 2: Age 0–6 months

## Blood pool images

*FIG. 1. Posterior view of skull, upper limbs and thorax.*



*FIG. 2. Posterior view of spine, pelvis and lower limbs.*



### Technical comments

Note the sagittal suture in the skull in Fig. 1.

Note the extravasation of isotope at the site of injection in the scalp in Fig. 1.



*FIG. 4. Posterior view of skull, thorax and upper limbs.*

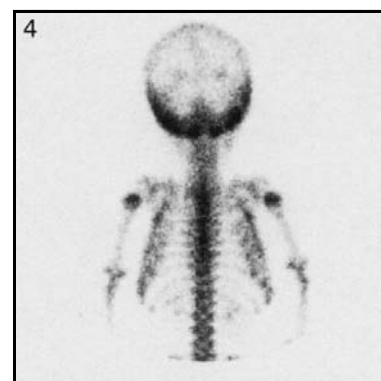


*FIG. 2. Right lateral view and anterior view of thorax and upper limbs.*

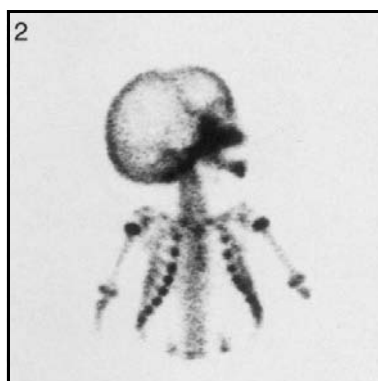
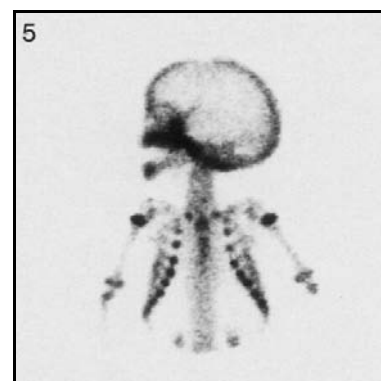


*FIG. 5. Left lateral view and anterior view of thorax and upper limbs.*



### **Technical comments**

The coronal suture is seen in Figs 2 and 5. Note the difference in uptake between the left and the right sides. The transverse sinus is clearly seen in Fig. 4.

Note the increased activity at the growing ends of the bone, i.e. costochondral junctions and the epiphyseal plates of the upper humeri.

The indistinct lateral aspects of the ribs in Fig. 4 are due to 'shine through' from the costochondral junctions.

### **Potential pitfalls**

Decreased activity is noted in the region of the anterior fontanelle in Figs 2 and 5. This should not be mistaken for a depressed fracture of the skull.

Posterior thorax shows increased activity laterally in Fig. 4 which should not be mistaken for multiple rib fractures. This increased activity is not in line with the posterior ribs and is due to increased activity from the costochondral junctions.

## 2: Age 0–6 months

## Skull, thorax, upper limbs and pelvis

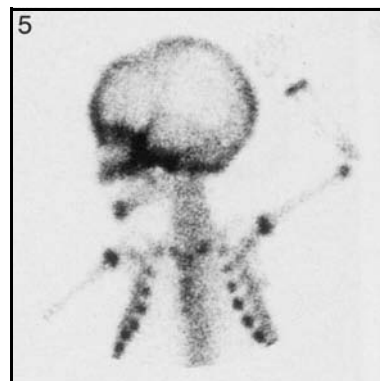
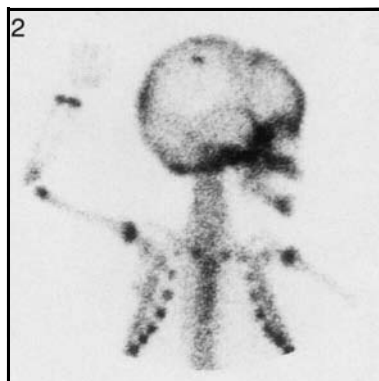
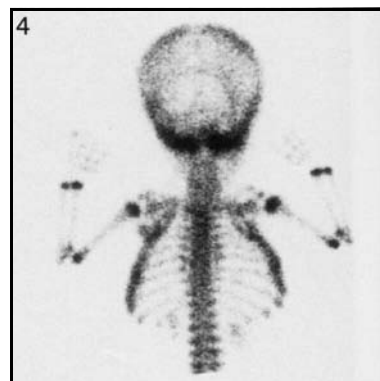
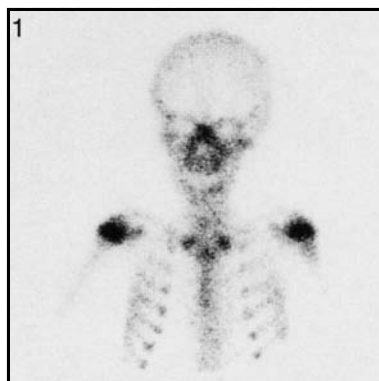
*FIG. 1. Anterior view of skull and thorax.*

*FIG. 4. Posterior view of skull and upper limbs.*

*FIG. 2. Right lateral view of skull, right upper limb and anterior left upper limb and anterior view of thorax.*

*FIG. 5. Left lateral view of skull, left upper limb and anterior view of thorax.*

*FIG. 3. Anterior view of thorax, pelvis and upper limbs.*



### Technical comments

At this age, the upper limbs may be imaged either with the skull (Figs 2 and 5) or thorax (Fig. 3). Good positioning allows clear separation of the distal radius from the ulna.

Note the extravasation of isotope at the site of the injection in the scalp in Fig. 2.

### Potential pitfalls

Decreased activity is noted in the region of the anterior fontanelle in Figs 2 and 5. This should not be mistaken for a depressed fracture of the skull.

Increased activity seen laterally in Fig. 4 should not be mistaken for multiple fractures. This increased activity is not in line with the posterior ribs and is due to the increased activity in the region of the costochondral junctions.

## 2: Age 0–6 months

## Skull, thorax, spine and pelvis

FIG. 1. Left lateral view of skull and anterior view of thorax.

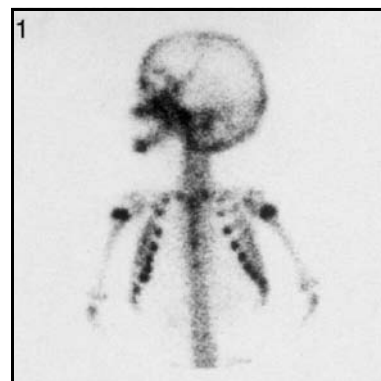


FIG. 2. Left lateral view of skull and anterior view of thorax.

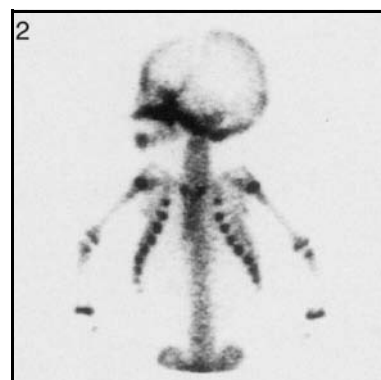
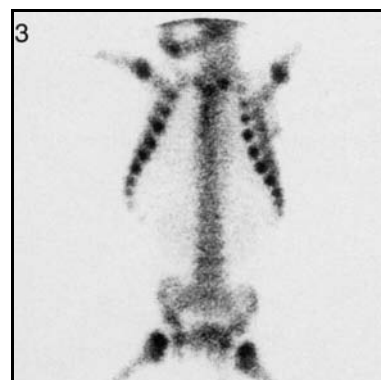


FIG. 3. Left lateral view of skull and anterior view of thorax.



### Technical comment

Note the clarity of the lower lumbar spine in the anterior view in Fig. 3.

### Potential pitfall

Note the difference in activity in the coronal suture in Figs 1 and 2. This variation makes the diagnosis of suture fusion difficult.

## 2: Age 0–6 months

## Thorax and pelvis

*FIG. 1. Right anterior oblique view of thorax and pelvis.*

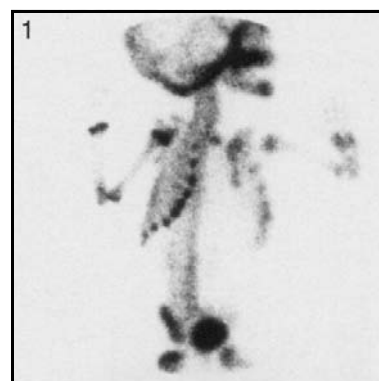
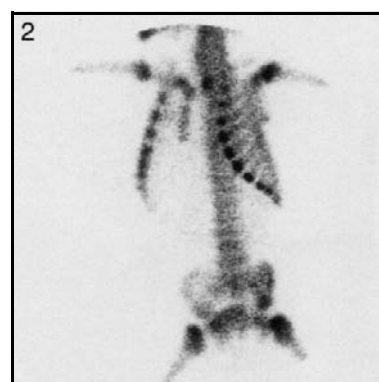


*FIG. 2. Left anterior view of thorax and pelvis.*



### Technical comments

The sternum is well seen in both images.

Note the high activity in the full bladder in Fig. 1.

The anterior view of the pelvis should not be obtained at the same time as the oblique views of the thorax.

## 2: Age 0–6 months

## Thorax, spine, pelvis and upper limbs

FIG. 1. Posterior view of thorax, spine, pelvis and upper limbs.



FIG. 2. Posterior view of thorax, spine, pelvis and upper limbs.

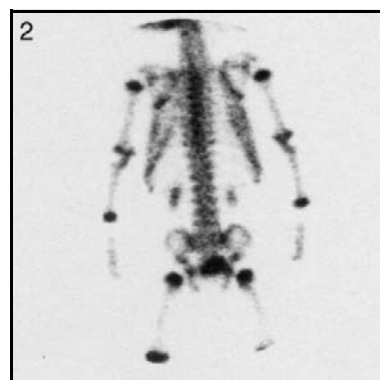
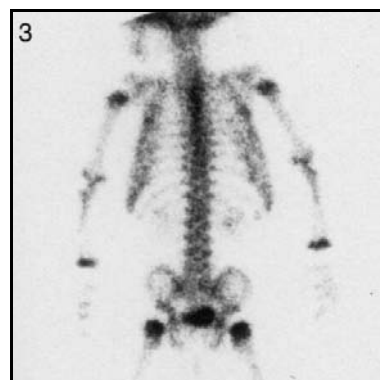


FIG. 3. Posterior view of thorax, spine, pelvis and upper limbs.



### Technical comments

The epiphysis of the scapula is seen in Fig. 2.

Note the difference in renal excretion. In Fig. 2, both kidneys are clearly seen. This is within normal limits.

Note the lack of differentiation between the distal radius and the ulna owing to poor positioning of the hands in all images.

### Potential pitfall

Note the loss of clarity of the ribs in the axilla on all three images. This is due to the increased activity at the costochondral junctions and is not pathological.

## 2: Age 0–6 months

## Spine, pelvis and lower limbs

*FIG. 1. Anterior view of spine and pelvis.*

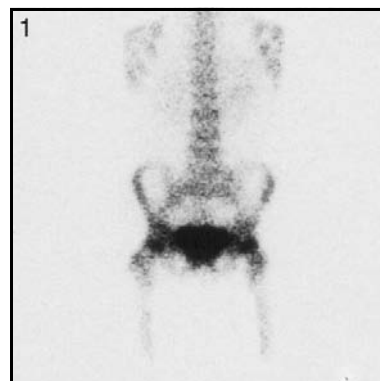


*FIG. 2. Anterior view of pelvis and lower limbs.*

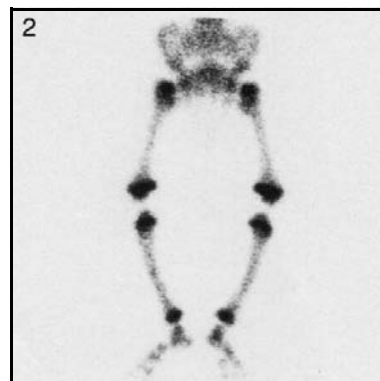
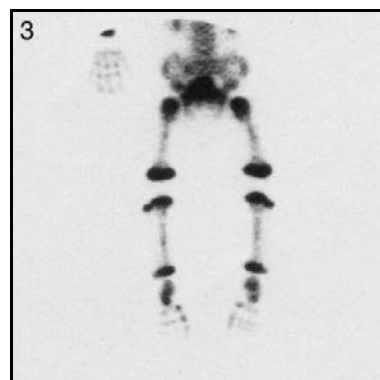


*FIG. 3. Anterior view of pelvis and lower limbs.*



### Technical comments

The full bladder in Figs 1 and 3 precludes adequate visualization of the hips.

Note that in Fig. 2 the feet are facing laterally whilst in Fig. 3 the toes are facing medially, the radiographic neutral position. This is the reason why the fibulae are clearly seen in Fig. 3 but not in Fig. 2.

## 2: Age 0–6 months

## Thorax, spine and lower limbs

*FIG. 1. Posterior view of thorax, spine and pelvis.*

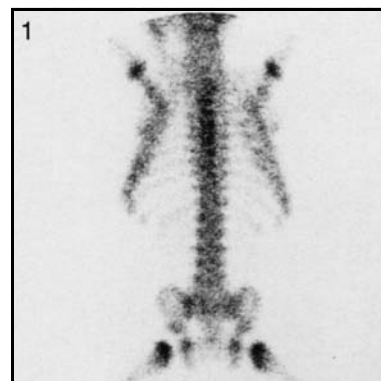


*FIG. 2. Posterior view of pelvis and lower limbs.*

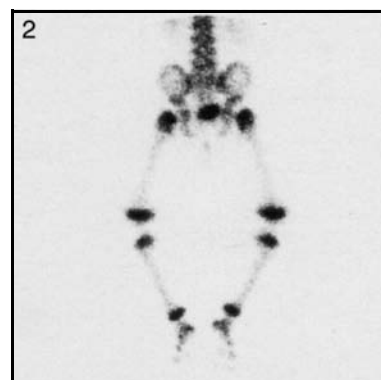
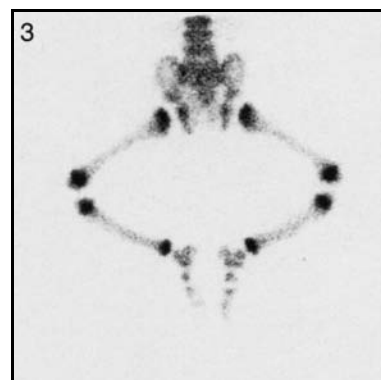


*FIG. 3. Posterior view of pelvis and lateral view of lower limbs.*



### Technical comments

Urine contamination of the nappy below the pelvis is seen in Fig. 2.

Figure 3 shows the projection which is required for imaging the feet. This position is not ideal for imaging the knees (see Section 19: Knees).



## 2: Age 0–6 months

## 'Babygram' views

*FIG. 1. Posterior view of thorax, spine, pelvis and lower limbs.*

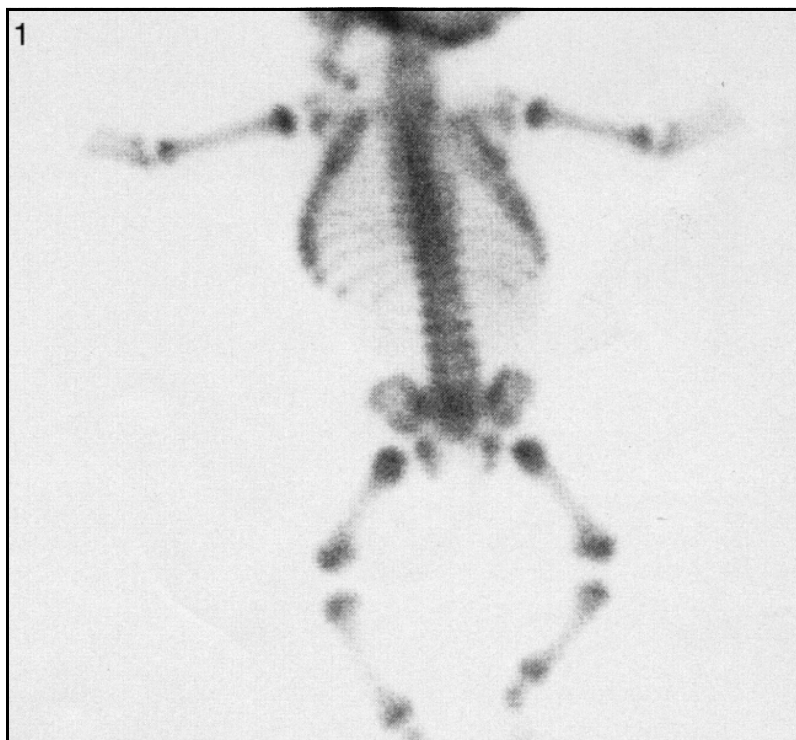
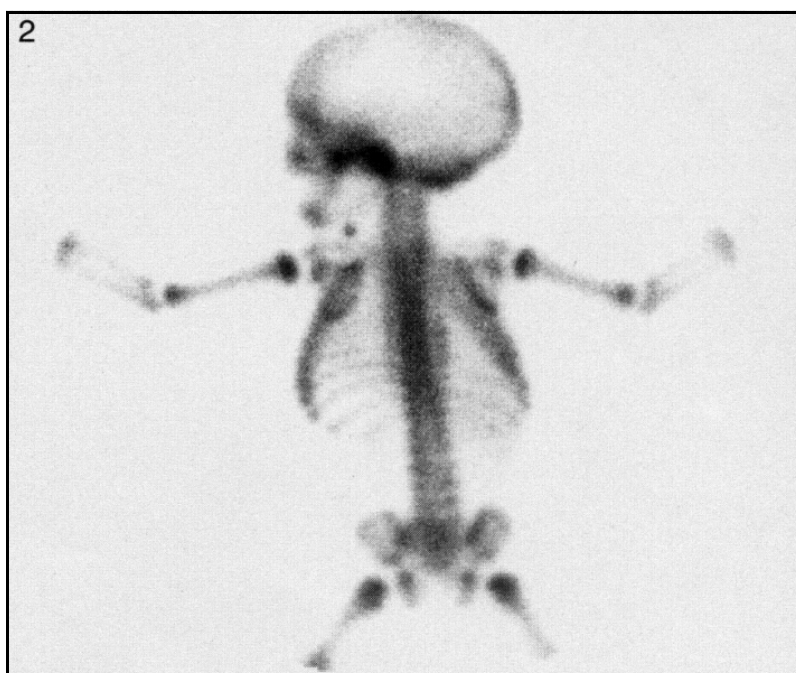


*FIG. 2. Left lateral view of skull and posterior view of upper limbs, thorax, spine and pelvis.*



### Technical comments

Although it is tempting to obtain whole body imaging on a large field of view gamma camera at this age, the quality of the images is unacceptable.

Spot images, with appropriate patient positioning and use of magnification, are preferable.



### **3. AGE 6–12 MONTHS**



### 3: Age 6–12 months

### Blood pool images

*FIG. 1. Posterior view of skull and thorax.*

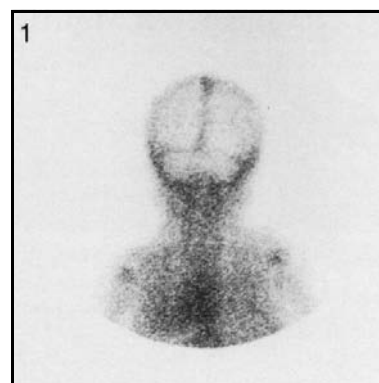


*FIG. 2. Left lateral view of skull and posterior view of thorax.*

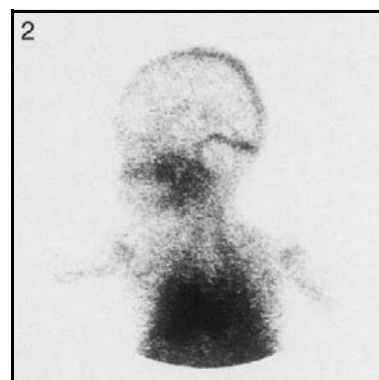
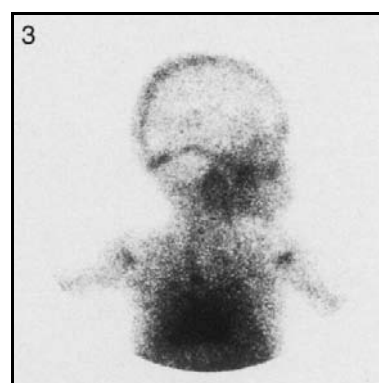


*FIG. 3. Right lateral view of skull and posterior view of thorax.*



### Technical comments

Note the clarity of the venous sinuses in all the views.

The 'hot' epiphyseal plates at the upper ends of the humeri are also clearly seen. This is normal.

### 3: Age 6–12 months

### Blood pool images

*FIG. 1. Posterior view of thorax, spine, pelvis and upper limbs.*

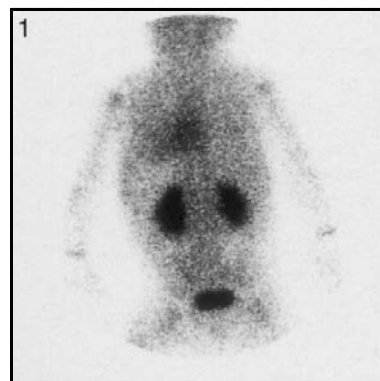


*FIG. 2. Posterior view of thorax, spine, pelvis and upper limbs.*

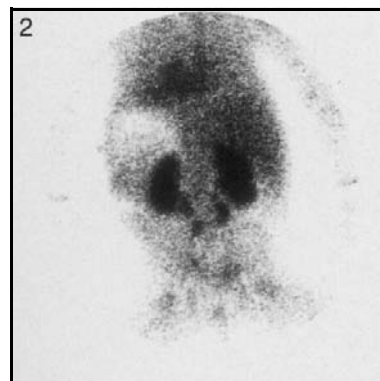
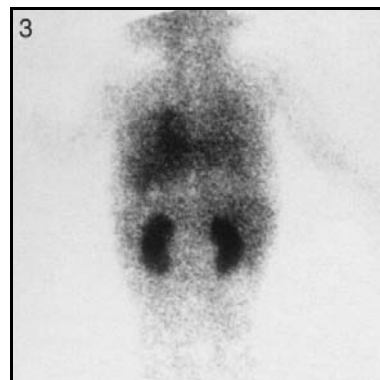


*FIG. 3. Posterior view of thorax, spine and pelvis.*



#### Technical comments

Figure 3 is an image taken 1 min after injection of tracer and no activity is visible in the bladder, whereas Figs 1 and 2 are at 4–5 min and activity is clearly visible in the bladder.

Figure 2 shows a photon deficient area above the left kidney. This is due to a full stomach.

#### Potential pitfall

Curvilinear radioactivity between and below the kidneys in Fig. 2 is probably due to a tortuous ureter. This is normal.

### 3: Age 6–12 months

### Blood pool images

*FIG. 1. Posterior view of pelvis and lower limbs.*

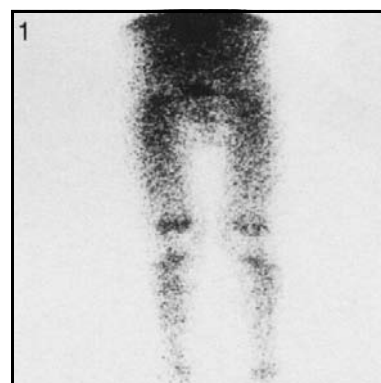
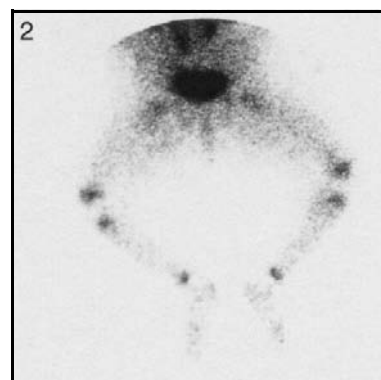


*FIG. 2. Posterior view of pelvis and lateral view of lower limbs.*



#### Technical comments

Note the normal increased perfusion of the epiphyseal plates of the lower limbs.

The position of the lower limbs in Fig. 1 is ideal for the knees and tibiae, while in Fig. 2 the position is ideal for the feet.

Bladder activity is noted in Fig. 2.

### 3: Age 6–12 months

### Skull, thorax and upper limbs

*FIG. 1. Anterior view of skull and thorax.*

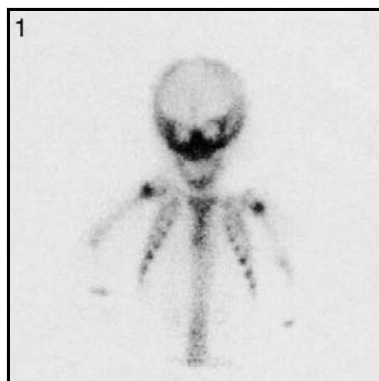


*FIG. 4. Posterior view of skull and thorax.*

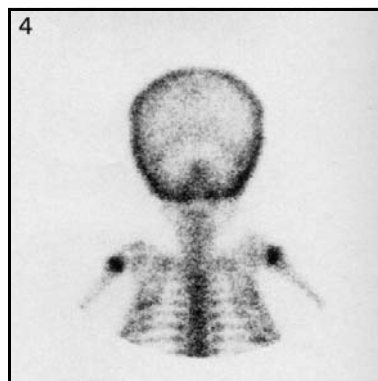


*FIG. 2. Right lateral view of skull, left upper limb and posterior view of thorax.*

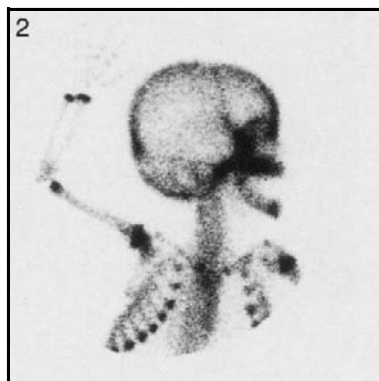
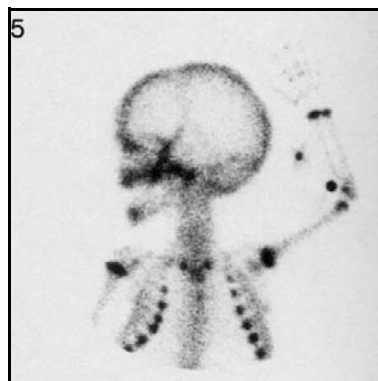


*FIG. 5. Left lateral view of skull, right upper limb and posterior view of thorax.*



#### Technical comment

Note the difference between the coronal sutures on the lateral images in Figs 2 and 5.

#### Potential pitfalls

Figure 1 shows asymmetry in the activity of the skull vault. This is due to rotation and should not be mistaken for a subdural haematoma.

Focal increased activity is seen over the ribs laterally of Figs 2, 4 and 5. This is due to activity from the costochondral junctions.



### 3: Age 6–12 months

### Skull, thorax and upper limbs

*FIG. 1. Anterior view of skull and thorax.*

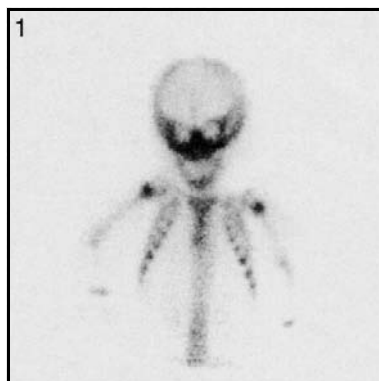


*FIG. 4. Posterior view of skull and thorax.*

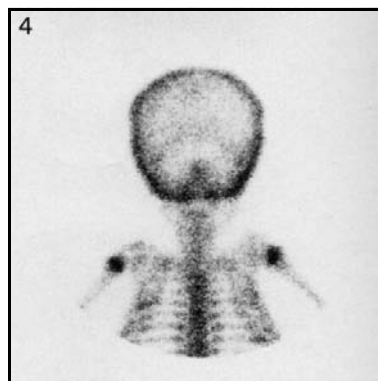


*FIG. 2. Right lateral view of skull, left upper limb and posterior view of thorax.*

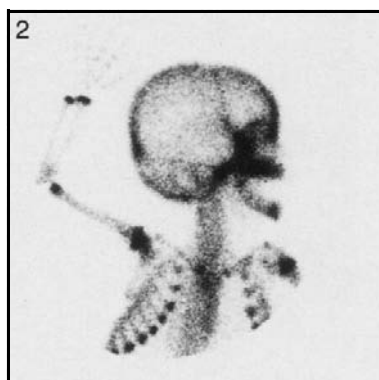
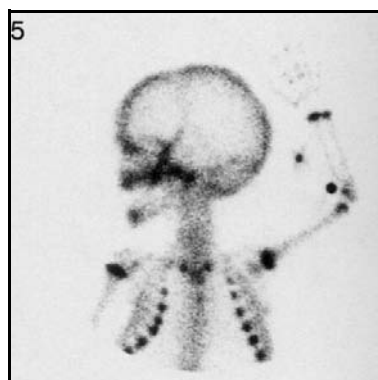


*FIG. 5. Left lateral view of skull, right upper limb and posterior view of thorax.*



#### Technical comments

Focal increased activity is seen over the ribs laterally in Fig. 4. This is due to activity from the costochondral junctions.

Note the extravasation of isotope at the site of injection in the left elbow in Fig. 5.

### 3: Age 6–12 months

### Skull, thorax, pelvis and upper limbs

*FIG. 1. Left lateral view of skull, anterior view of thorax and both upper limbs.*

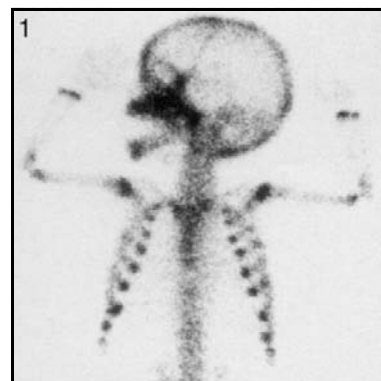


*FIG. 2. Anterior view of thorax and spine.*

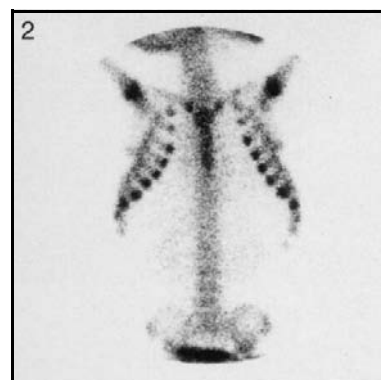
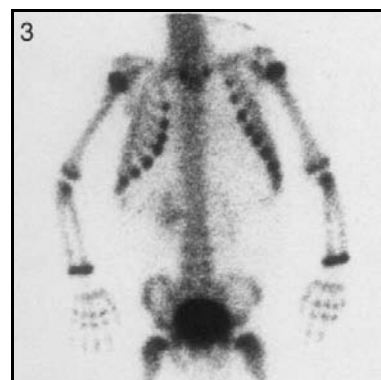


*FIG. 3. Anterior view of thorax, spine, pelvis and upper limbs.*



#### Technical comments

Note the position of the upper limbs in Fig. 1 as opposed to Fig. 3; both are adequate at this age.

There is variability in the ossification of the sternum. The entire sternum is clearly seen in Fig. 2. This is not true in Fig. 1 or Fig. 3.

In Fig. 3, the anterior thorax is obliquely positioned and the bladder is full of activity. These factors make this image difficult to interpret.

#### Potential pitfall

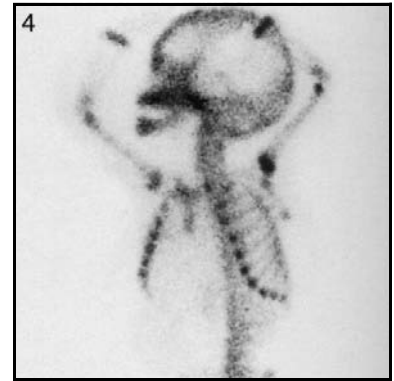
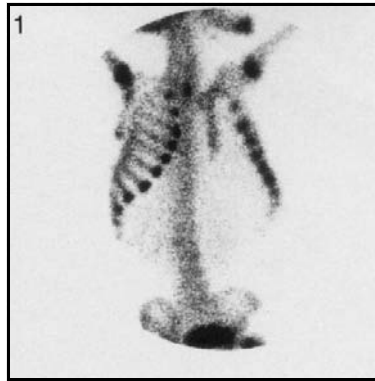
There is asymmetry between the kidneys in Fig. 3, with the right kidney having more activity than the left. This is a variation of normal.

### 3: Age 6–12 months

### Skull and thorax

*FIG. 1. Right anterior oblique view of thorax.*

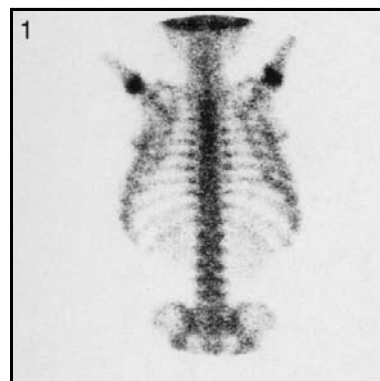
*FIG. 4. Left lateral view of skull, left anterior oblique view of thorax and upper limbs.*



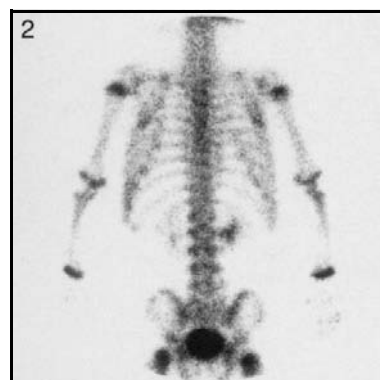
#### Technical comment

Figure 4 is poor quality because of the slight movement causing blurring of the upper limbs. The distal left radius and the ulna overlie the skull, which is not ideal.

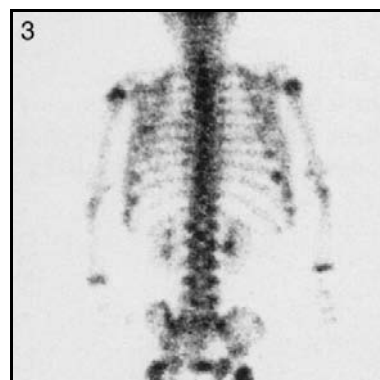
*FIG. 1. Posterior view of thorax and spine.*



*FIG. 2. Posterior view of thorax, spine, pelvis and upper limbs.*



*FIG. 3. Posterior view of thorax, spine, pelvis and upper limbs.*



### **Technical comments**

Note the different position of the upper limbs. This results in variation of the appearance of the scapulae in Fig. 1 compared with Fig. 2.

The renal activity is different between the two kidneys in Figs 2 and 3. These appearances are within normal limits.

### **Potential pitfall**

Focal patchy increased activity is noted in the lateral aspect of the ribs in all images. This is due to normal increased activity in the costochondral junctions shining through on this projection.

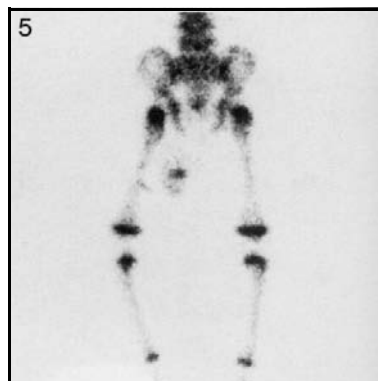
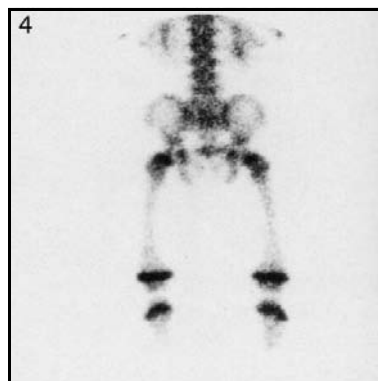
### 3: Age 6–12 months

### Spine, pelvis and lower limbs

*FIG. 1. Anterior view of pelvis and upper portion of lower limbs.*

*FIG. 4. Posterior view of spine, pelvis and upper portion of lower limbs.*

*FIG. 5. Posterior view of pelvis and lower limbs.*



#### Technical comments

Urine contamination medial to the left femur is seen in Fig. 5.

Figure 1 shows good positioning of the left knee and foot. This allows visualization of the left fibula. The fibula is not seen on the right owing to poor positioning of both the knee and the foot. The same is seen in Fig. 5.

### 3: Age 6–12 months

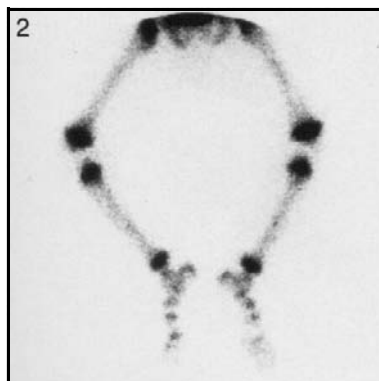
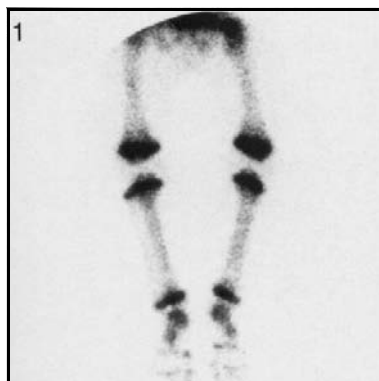
### Spine, pelvis and lower limbs

*FIG. 1. Anterior view of lower limbs and feet.*

*FIG. 4. Posterior view of lower limbs.*

*FIG. 2. Lateral view of lower limbs and feet.*

*FIG. 5. Posterior view of lower limbs and feet.*



#### Technical comments

Note the shape of the epiphyseal plates around the knees.

Figure 1 shows good positioning of the right knee and foot; this allows visualization of the right fibula. The fibula is not seen on the left owing to poor positioning of both the knee and the foot. The same is seen in Fig. 5.

Figure 2 is a lateral view of the lower limbs. This is good for the feet but inadequate for the knees.

## **4. AGE 1–2 YEARS**





#### 4: Age 1–2 years

#### Blood pool image

*FIG. 1. Posterior view of skull and thorax.*

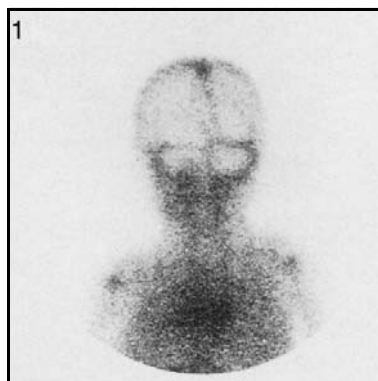


*FIG. 4. Posterior view of thorax, spine and pelvis.*

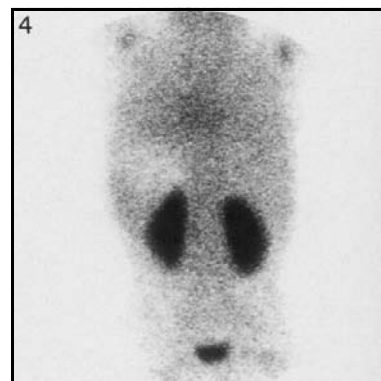


*FIG. 2. Posterior view of lower limbs.*

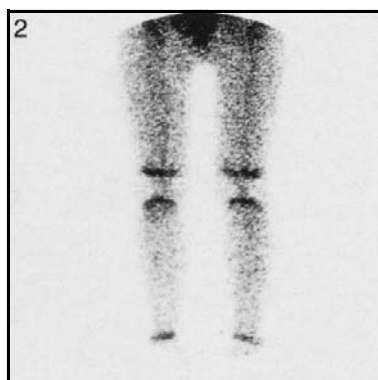
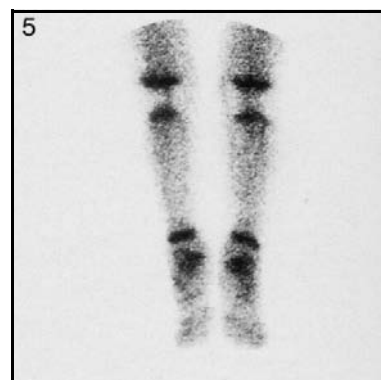


*FIG. 5. Posterior view of lower limbs.*



#### Technical comments

Note the photon deficient area above the left kidney in Fig. 4 due to full stomach.  
Slight rotation of the head in Fig. 1 causes an apparent deviation of the sagittal sinus.

#### 4: Age 1–2 years

#### Blood pool image

*FIG. 1. A double headed whole body gamma camera was used. Left image is anterior view; right image is posterior view.*



#### Technical comments

Note the rotation of the head causing apparent deviation of the sagittal sinus.  
Note the extravasation of isotope at the site of injection in the right hand.  
Marker on the right side.

#### 4: Age 1–2 years

#### Whole body scan

*FIG. 1. A single headed whole body gamma camera was used. Left image is anterior view; right image is posterior view.*

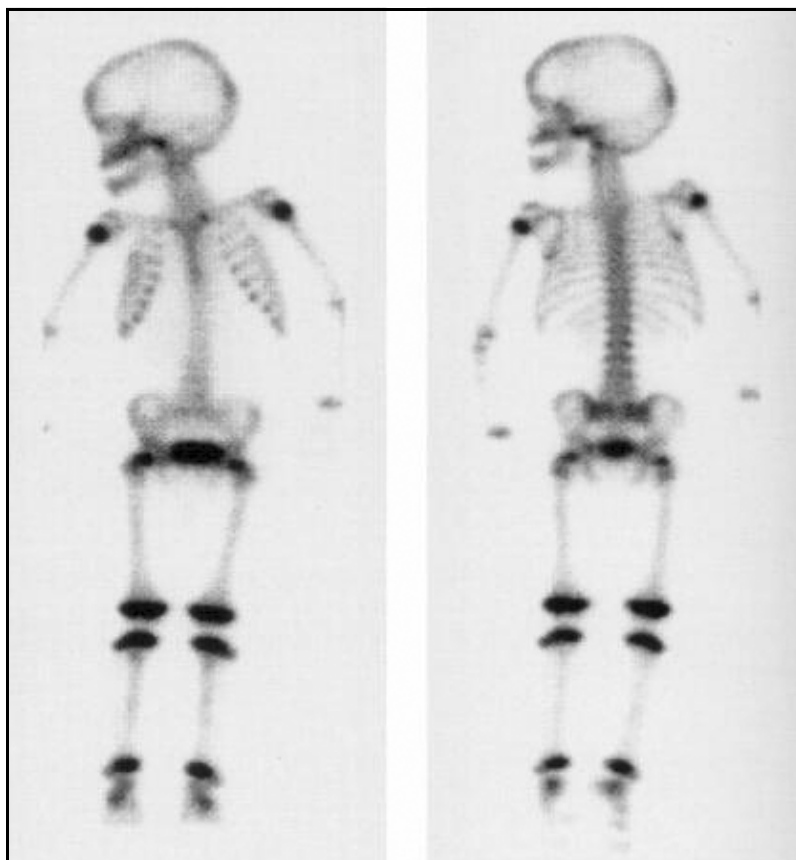
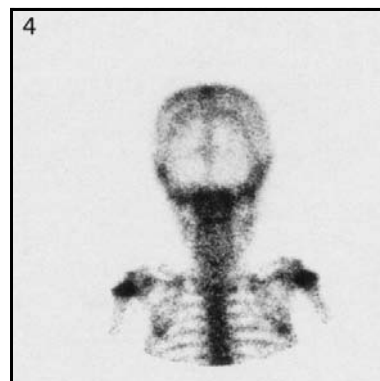
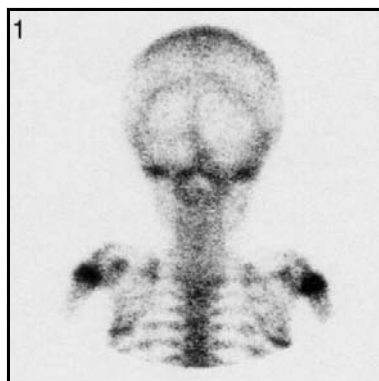


*FIG. 1. Posterior view of skull.*

*FIG. 4. Posterior view of skull with chin down and thorax.*

*FIG. 2. Right lateral view of skull and right upper limb.*

*FIG. 5. Left lateral view of skull and left upper limb.*



### **Technical comments**

Note the different appearances of the skull in the posterior projection depending on the degree of flexion of the head.

Note the clear separation of the distal radius and ulna in Figs 2 and 5.

The anterior ribs and the sternoclavicular joints are well seen in Figs 2 and 5.

The lateral views of the skull (Figs 2 and 5) were taken anteriorly.

Note the extravasation of isotope at the site of injection in the right elbow in Fig. 2.

#### 4: Age 1–2 years

#### Skull, thorax and upper limbs

*FIG. 1. Posterior view of skull and thorax.*

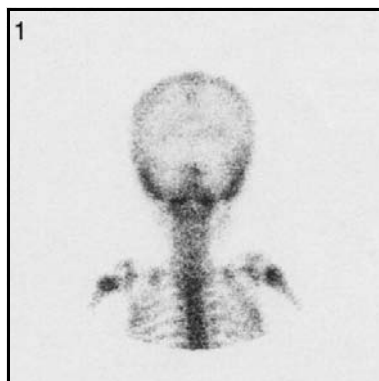


*FIG. 4. Posterior view of skull and thorax.*

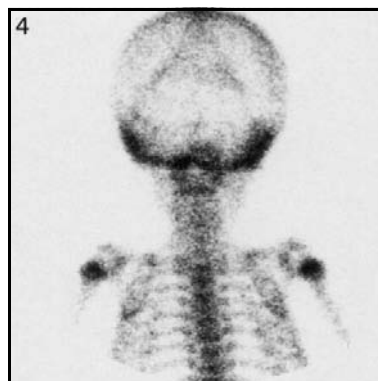


*FIG. 2. Right lateral view of skull and right upper limb.*



*FIG. 5. Left lateral view of skull and left upper limb.*



#### Technical comments

Note the different appearance of the skull in the posterior projection depending on the degree of flexion of the head. The anterior views of the skull (Figs 2 and 5) were taken anteriorly.

Note the extravasation of isotope at the site of injection in the right elbow in Fig. 2.

*FIG. 1. Anterior view of thorax and spine.*

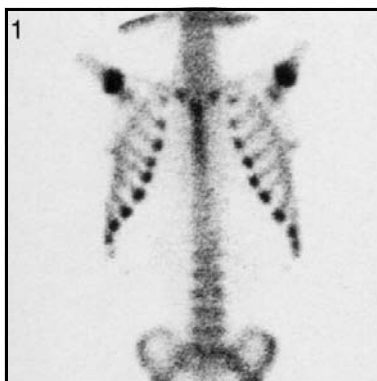


*FIG. 2. Anterior view of thorax and spine.*

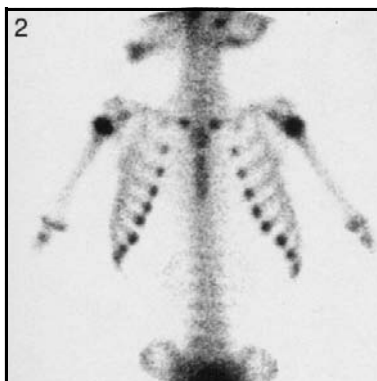
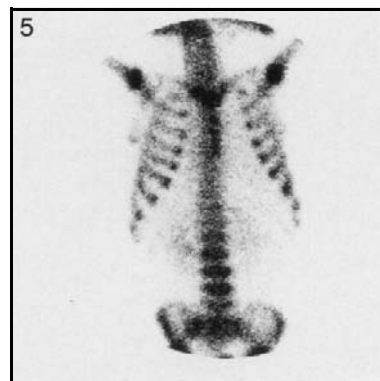


*FIG. 5. Anterior view of thorax and spine.*



**Technical comments**

Variability in the sternal ossification is clearly seen.

The lumbar vertebrae are very clearly seen in Figs 1 and 5. This appearance in the anterior thoracic view of the lumbar spine will be seen on other thoracic images.

The different positions of the upper limbs in the three images results in the scapulae having a different appearance in the images.

#### 4: Age 1–2 years

#### Thorax and spine

*FIG. 4. Posterior view of thorax and spine.*

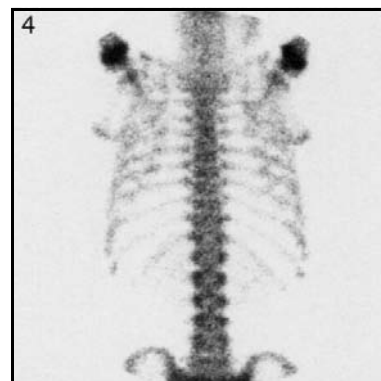


*FIG. 2. Anterior view of thorax and spine.*

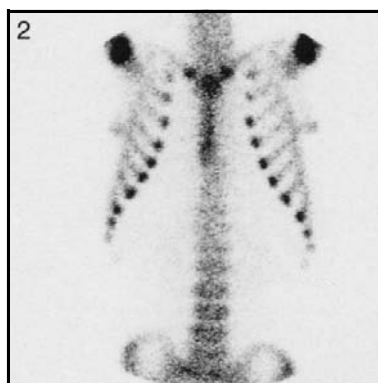


*FIG. 5. Posterior view of thorax and spine.*

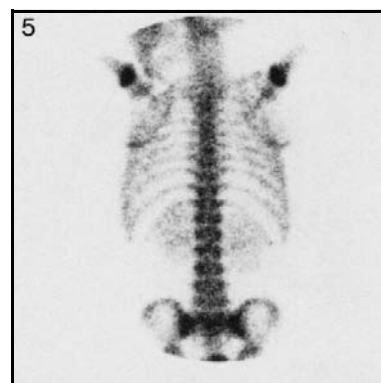
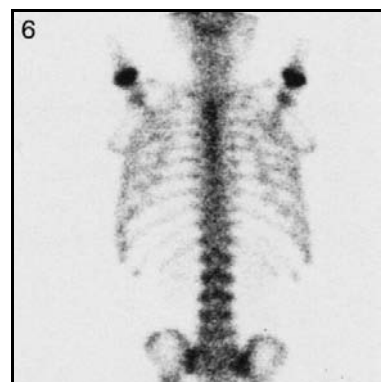


*FIG. 6. Posterior view of thorax and spine.*



#### Potential pitfall

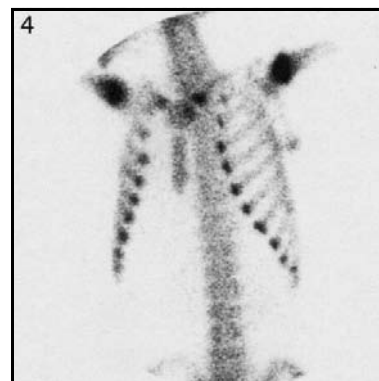
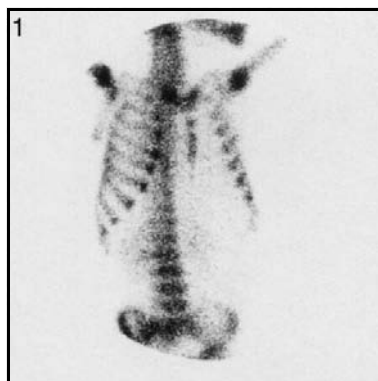
Increased activity in the lateral aspect of the ribs posteriorly is best seen in Figs 4 and 6 and is due to the normal increased activity in the costochondral junction, clearly seen in Fig. 2.

#### 4: Age 1–2 years

#### Thorax and spine

*FIG. 1. Right anterior oblique view of thorax.*

*FIG. 4. Left anterior oblique view of thorax.*



#### Technical comment

Note the variability in sternal ossification.



#### 4: Age 1–2 years

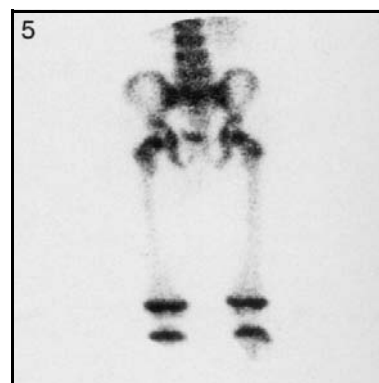
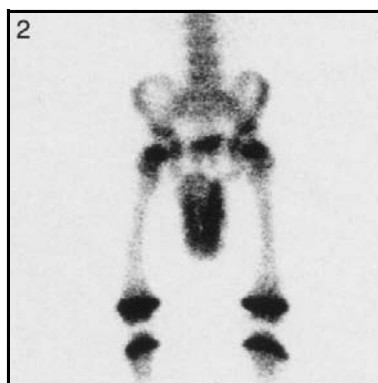
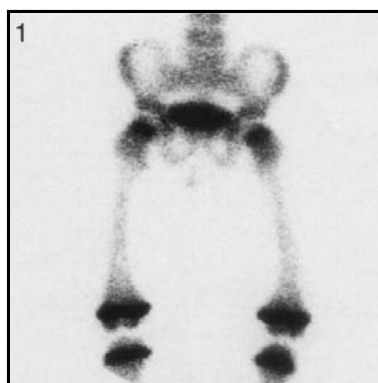
#### Pelvis and femora

*FIG. 1. Anterior view of pelvis and femora.*

*FIG. 4. Posterior view of pelvis and femora.*

*FIG. 2. Anterior view of pelvis and femora.*

*FIG. 5. Posterior view of pelvis and femora.*



#### Technical comment

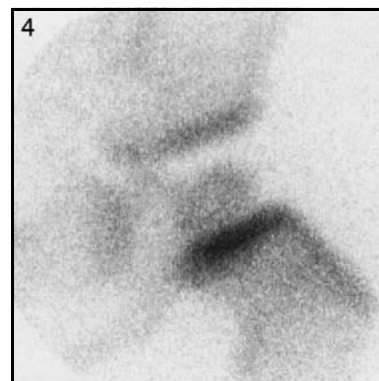
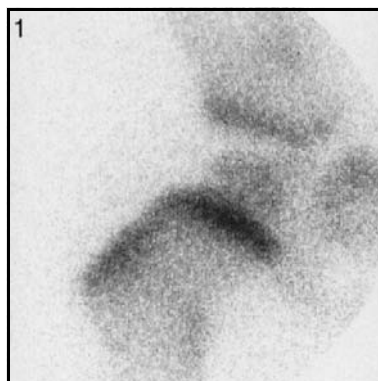
Urine contamination below the pelvis is seen in Figs 1 and 2.

#### 4: Age 1–2 years

#### Hips

*FIG. 1. Pinhole view of right hip.*

*FIG. 4. Pinhole view of left hip.*



#### 4: Age 1–2 years

#### Lower limbs

*FIG. 1. Posterior view of lower limbs and feet.*

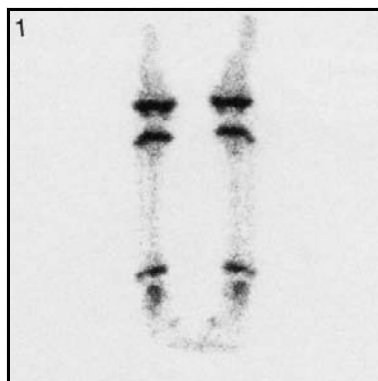


*FIG. 4. Anterior view of lower limbs and feet.*



*FIG. 2. Lateral view of lower limbs and feet.*

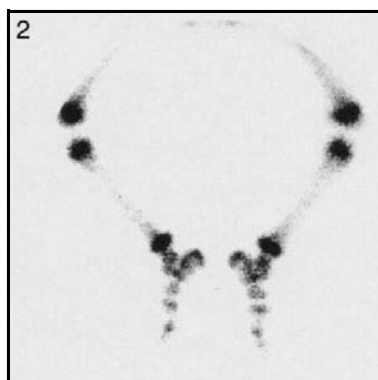
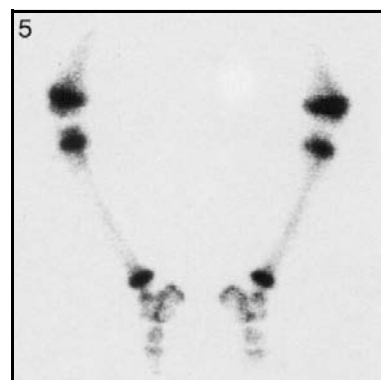


*FIG. 5. Lateral view of lower limbs and feet.*



#### Technical comments

Figures 1 and 4 show good positioning for the knees, tibia and fibulae. The fibula is clearly seen separate from the tibia.

Figures 2 and 5 show the positioning for imaging the feet. This position is inadequate for the knees since there is overlapping of the epiphyseal plate of the tibia and the fibula.



## **5. AGE 2–3 YEARS**



## 5: Age 2–3 years

## Blood pool images

*FIG. 1. Posterior view of the skull and upper limbs.*



*FIG. 4. Left lateral view of skull.*

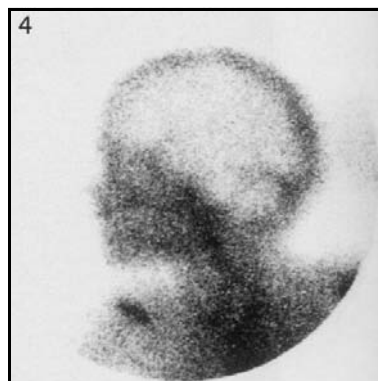


*FIG. 2. Posterior view of thorax and spine.*

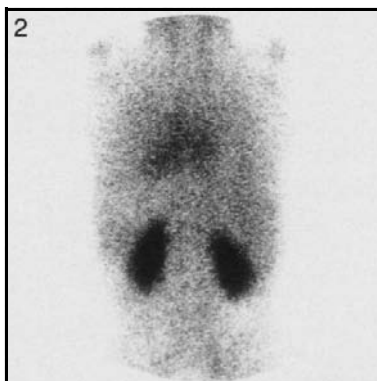
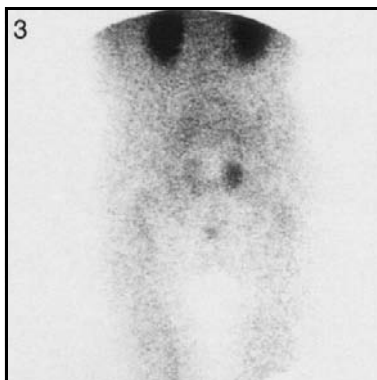


*FIG. 3. Posterior view of spine, pelvis and lower limbs.*



### Technical comments

Note the venous sinuses in Fig. 1.

Note the focal accumulation of isotope in the bladder.

Note the extravasation of isotope at the site of injection in the left hand in Fig. 1.

## 5: Age 2–3 years

## Blood pool images

*FIG. 1. Posterior view of pelvis and upper part of lower limbs.*

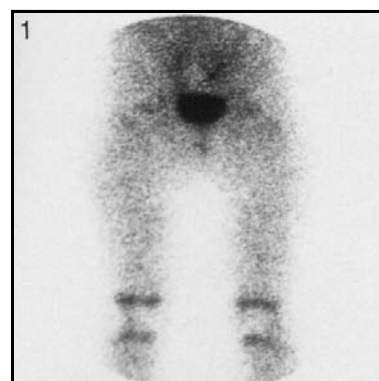
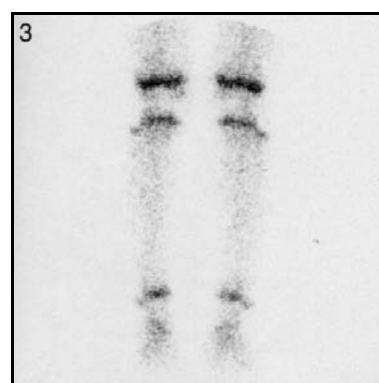


*FIG. 2. Posterior view of lower part of limbs.*



*FIG. 3. Posterior view of lower part of lower limbs.*



### Technical comments

Note the vascularity of the epiphyseal plates, showing up as areas of increased uptake of tracer.  
Note the bladder activity in Fig. 1.



## 5: Age 2–3 years

## Blood pool images

*FIG. 1. A double headed whole body gamma camera was used. Left image is anterior view; right image is posterior view.*



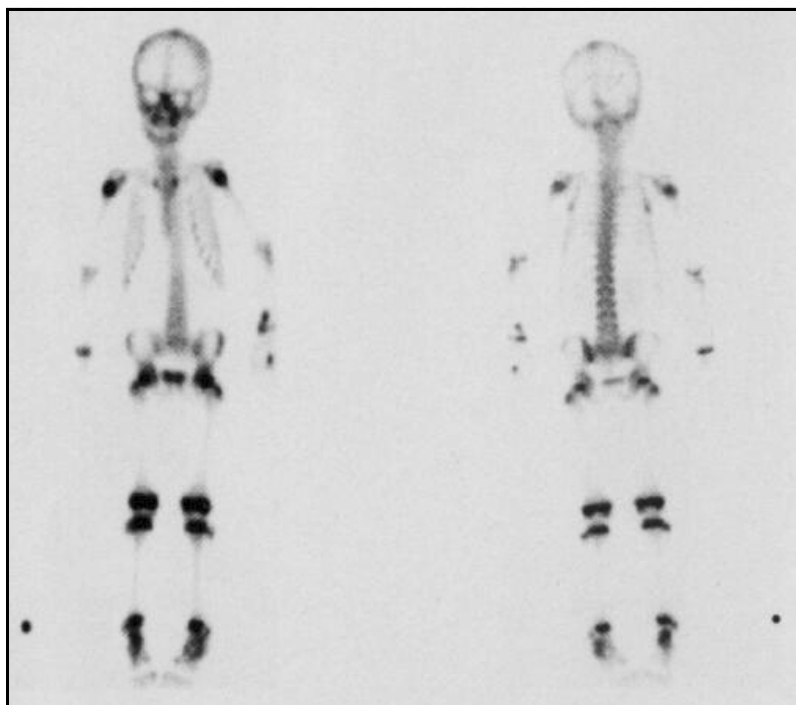
### Technical comments

Note the rotation of the head, causing apparent deviation of the sagittal sinus.

Note the extravasation of isotope at the site of injection in the left hand.

Marker on the right side.

*FIG. 1. A double headed whole body gamma camera was used. Left image is anterior view; right image is posterior view.*



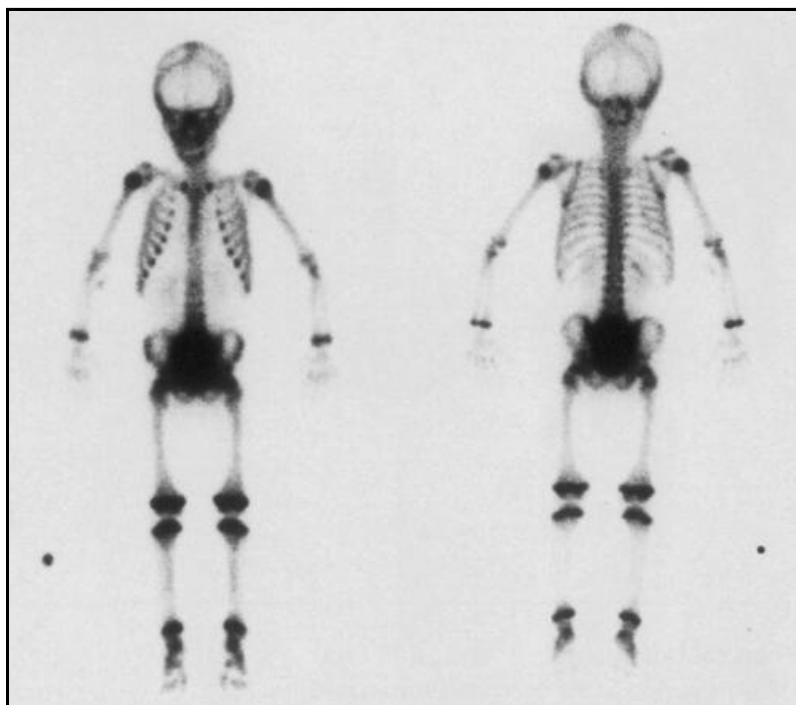
**Technical comments**

Note the rotation of the head, causing asymmetry.

Note the extravasation of isotope at the site of injection in the left hand.

Marker on the right side.

*FIG. 1. A double headed whole body gamma camera was used. Left image is anterior view; right image is posterior view.*



**Technical comments**

Note the full bladder; not an ideal situation.  
Marker on the right side.

## 5: Age 2–3 years

## Skull, thorax and upper limbs

*FIG. 1. Anterior view of skull and thorax.*



*FIG. 4. Posterior view of skull and thorax.*

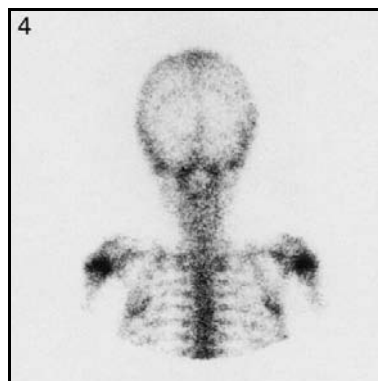


*FIG. 2. Right lateral view of skull and right upper limb.*

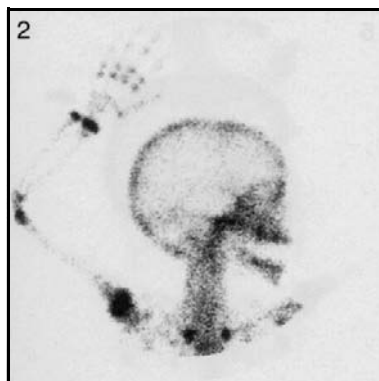
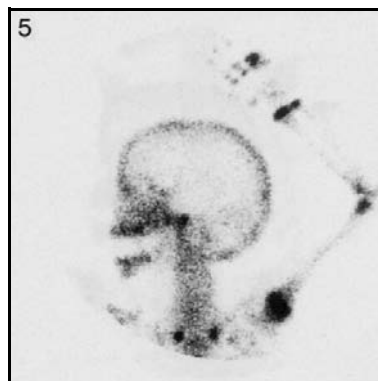


*FIG. 5. Left lateral view of skull and left upper limb.*



### Technical comments

Note focal increased activity in the 4th finger of the hand due to the extravasation of isotope at the site of injection in Fig. 5.

The lateral views of the skull (Figs 2 and 5) were taken anteriorly.

## 5: Age 2–3 years

## Skull, thorax and upper limbs

*FIG. 4. Posterior view of skull and thorax.*

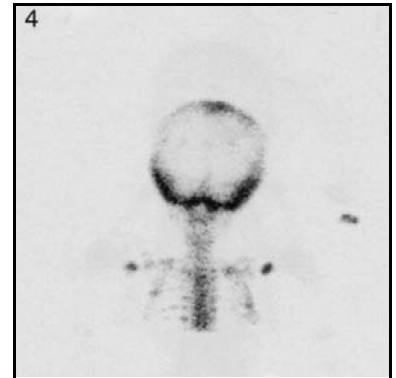


*FIG. 2. Right lateral view of skull and right upper limb.*



*FIG. 5. Left lateral view of skull and left upper limb.*



### Technical comments

Note the rather poor positioning of the hands in all three figures compared with the images on p. 56. The lateral views of the skull (Figs 2 and 5) were taken anteriorly.

*FIG. 1. Anterior view of thorax and spine.*

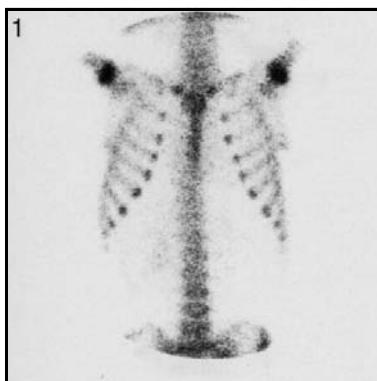


*FIG. 2. Anterior view of thorax and spine.*

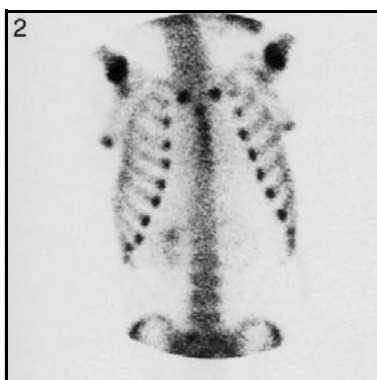
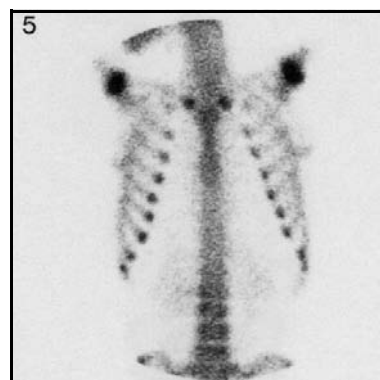


*FIG. 5. Anterior view of thorax and spine.*



**Technical comments**

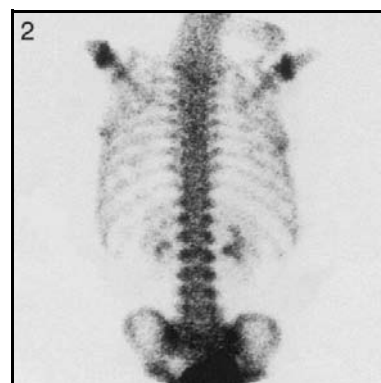
Note the right kidney in Fig. 2. This is within normal limits.

Note the clarity with which the lower lumbar spine is seen in all three images.

*FIG. 1. Posterior view of thorax and spine.*



*FIG. 2. Posterior view of thorax and spine.*



**Potential pitfall**

The focal increased activity noted in the mid-portion of the poster ribs, best seen in Fig. 1, is due to activity from the costochondral junctions and should not be mistaken for a rib fracture. This is also seen in Fig. 2.

*FIG. 1. Right anterior view of thorax.*

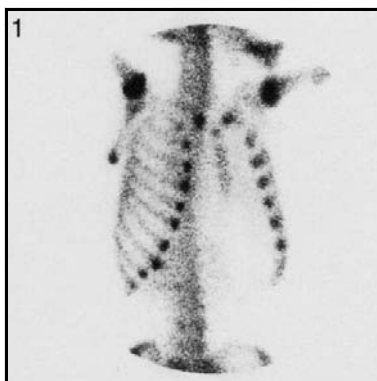


*FIG. 4. Left anterior oblique view of thorax.*

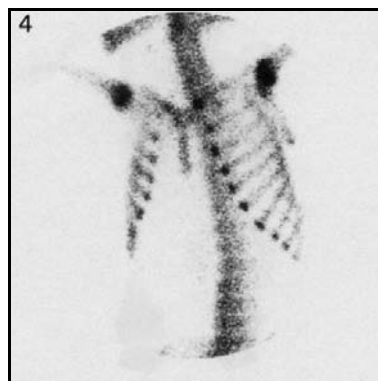


*FIG. 2. Right anterior oblique view of thorax.*

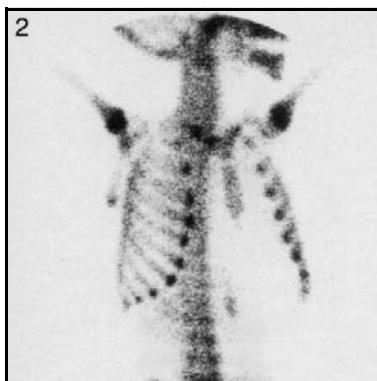
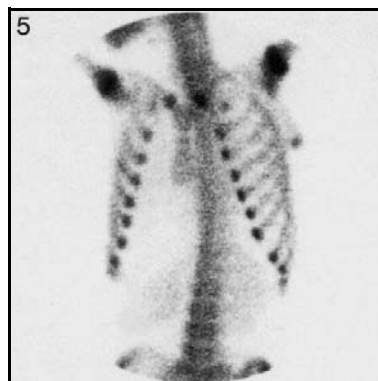


*FIG. 5. Left anterior oblique view of thorax.*



**Technical comments**

The sternum continues to show its variation but all sternal ossification centres are now present. In Fig. 2, a small amount of activity is noted in the kidney to the left of the midline. This is normal.



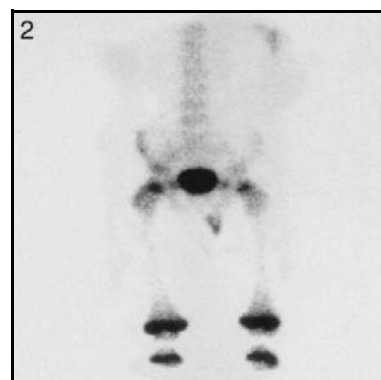
## 5: Age 2–3 years

## Spine, pelvis and femora

*FIG. 1. Anterior view of pelvis and femora.*



*FIG. 2. Anterior view of spine, pelvis and femora.*



### Technical comment

Urine contamination below the pelvis is seen in Fig. 2.

## 5: Age 2–3 years

## Spine, pelvis and femora

*FIG. 1. Posterior view of spine, pelvis and femora.*

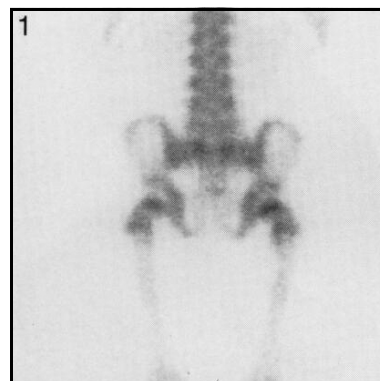


*FIG. 2. Posterior view of spine, pelvis and femora.*

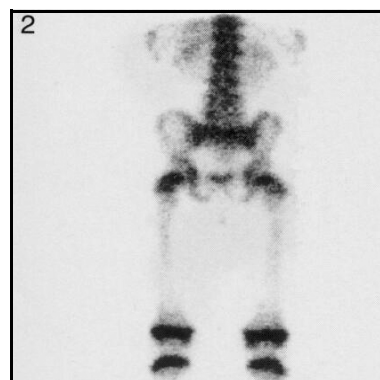
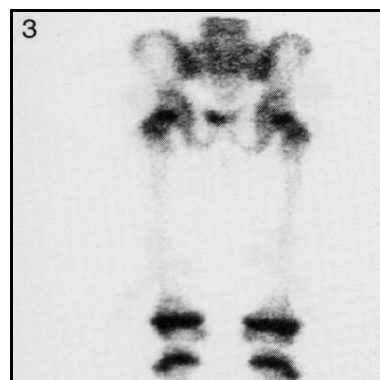


*FIG. 3. Posterior view of pelvis and femora.*



### Technical comment

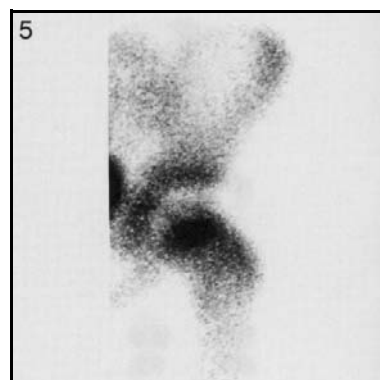
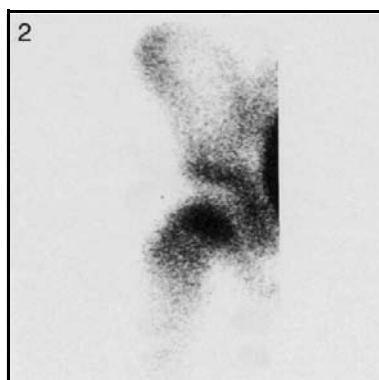
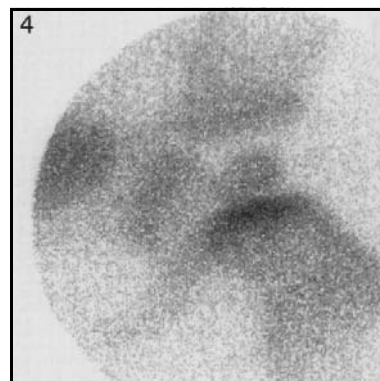
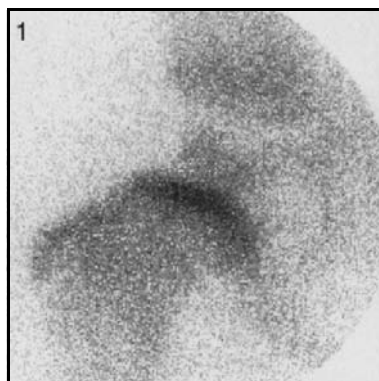
Note that the bladder is virtually empty in all three images; an ideal situation.

*FIG. 1. Pinhole view of right hip.*

*FIG. 4. Pinhole view of left hip.*

*FIG. 2. Pinhole view of right hip.*

*FIG. 5. Pinhole view of left hip.*



## 5: Age 2–3 years

## Pelvis, lower limbs and feet

*FIG. 1. Anterior view of pelvis and lower limbs.*

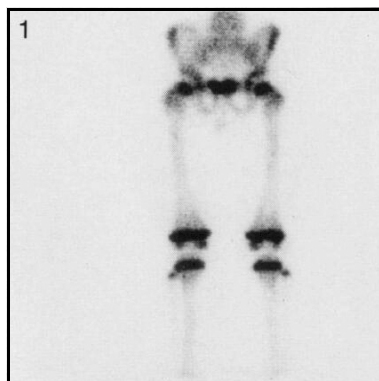


*FIG. 4. Posterior view of lower limbs.*

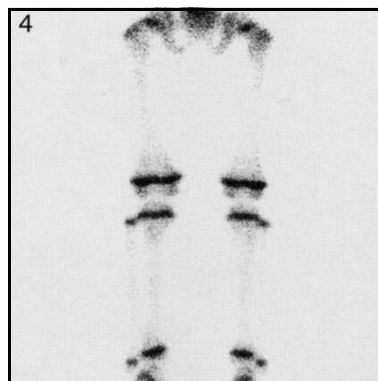


*FIG. 2. Anterior view of tibia, fibula and feet.*



*FIG. 5. Posterior view of tibia and fibula.*

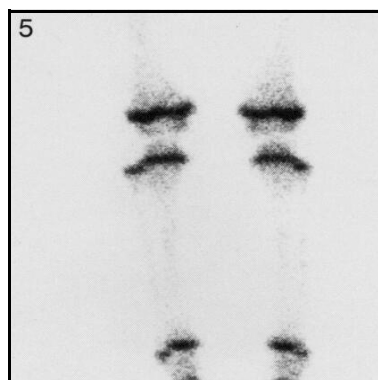
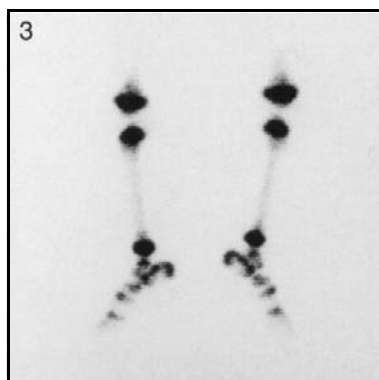


*FIG. 3. Lateral view of lower limbs and feet.*



### Technical comments

Note the clarity of the fibula separate from the tibia in Figs 1, 2, 4 and 5. This is due to the radiographic neutral position of the feet.

Lateral views of the feet (Fig. 3) are inadequate for the evaluation of the knees.

## **6. AGE 3–4 YEARS**



## 6: Age 3–4 years

## Blood pool images

*FIG. 1. Posterior view of skull and thorax.*

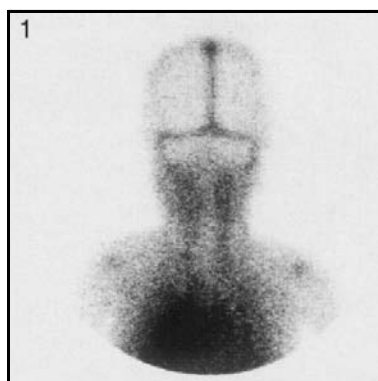


*FIG. 2. Right lateral view of skull and thorax.*

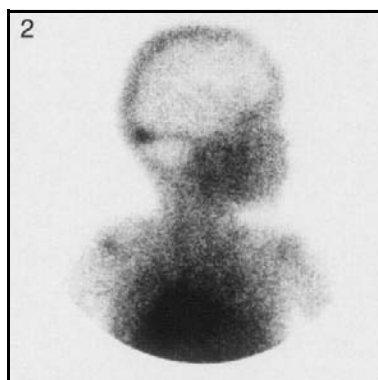
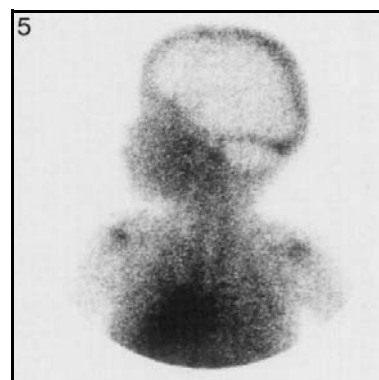


*FIG. 5. Left lateral view of skull and anterior view of thorax.*



### Technical comment

Note the high activity in the venous sinuses on all images.

## 6: Age 3–4 years

## Blood pool images

*FIG. 1. Posterior view of thorax and spine.*

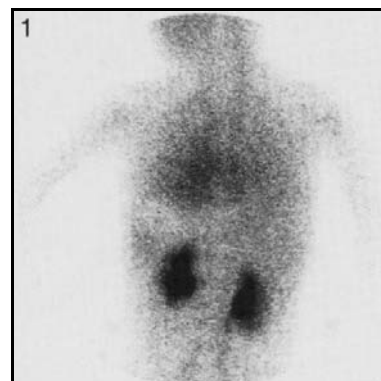


*FIG. 2. Posterior view of spine and pelvis.*

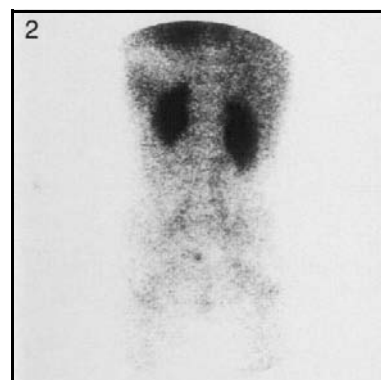
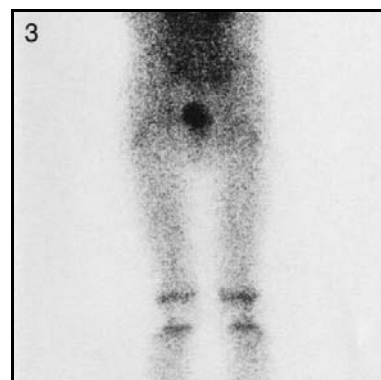


*FIG. 3. Posterior view of pelvis and lower limbs.*

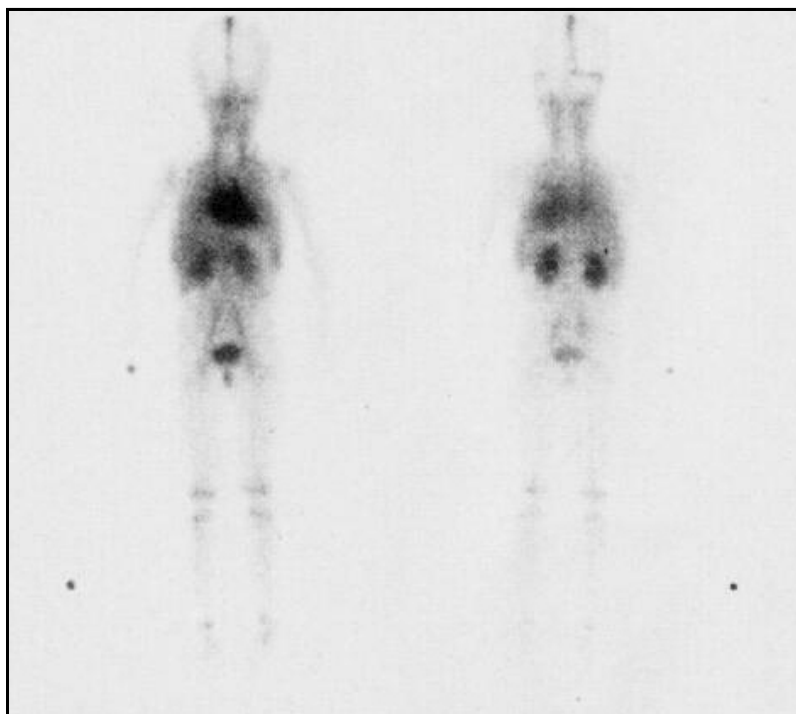


### Technical comment

Note the activity in the bladder in Fig. 3.



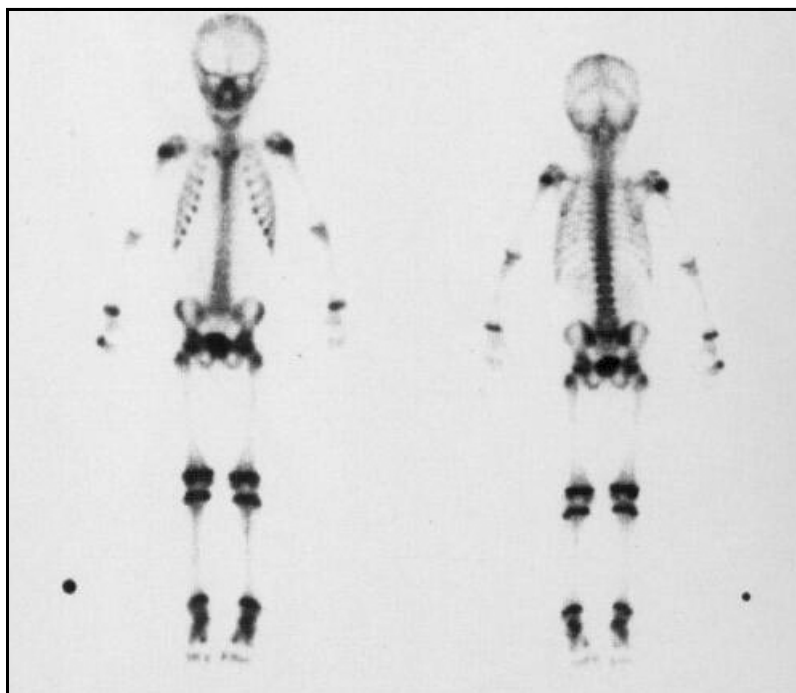
*FIG. 1. A double headed whole body gamma camera was used. Left image is anterior view; right image is posterior view.*



**Technical comments**

Note the extravasation of isotope at the site of injection in the right hand.  
Urine contamination is seen below the pelvis.  
Marker on the right side.

*FIG. 1. A double headed whole body gamma camera was used. Left image is anterior view; right image is posterior view.*



**Technical comments**

The left foot is well positioned, with the toes turned inwards, allowing good visualization of the fibula.  
Note the extravasation of isotope at the site of injection in the right hand.  
Marker on the right side.

## 6: Age 3–4 years

## Skull, thorax and upper limbs

*FIG. 1. Anterior view of skull and thorax.*



*FIG. 4. Posterior view of skull and thorax.*



*FIG. 2. Right lateral view of skull and right upper limb.*

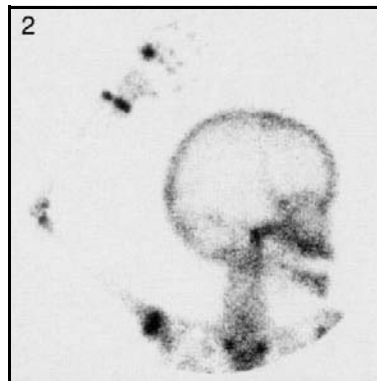
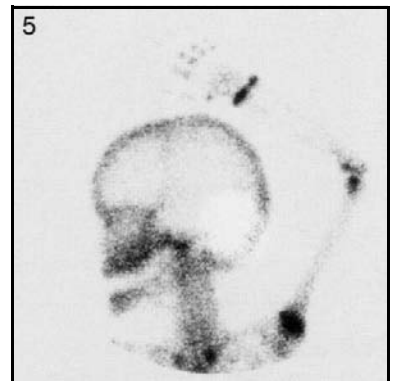


*FIG. 5. Left lateral view of skull and left upper limb.*



### Technical comments

Note the clear visualization of the coronal sutures on both lateral skull images; contrast these with the poor visualization of the sutures seen on the next page (Figs 2 and 5).

Note the extravasation of isotope at the site of injection in the right hand in Fig. 2.

The lateral views of the skull (Figs 2 and 5) were taken anteriorly.

*FIG. 1. Anterior view of skull and thorax.*



*FIG. 4. Posterior view of skull and thorax.*



*FIG. 2. Right lateral view of skull and right upper limb.*



*FIG. 5. Left lateral view of skull and left upper limb.*



**Technical comments**

Note the poor visualization of the coronal sutures on both lateral skull images; contrast these with the clarity of the sutures seen on the previous page (Figs 2 and 5).

Note the extravasation of isotope at the site of injection in the right elbow in Fig. 2.

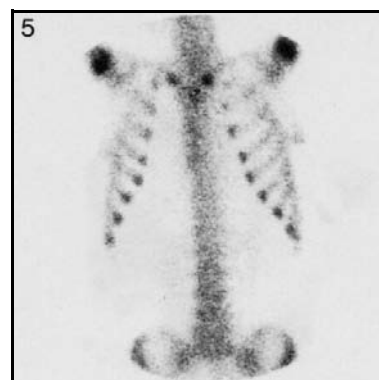
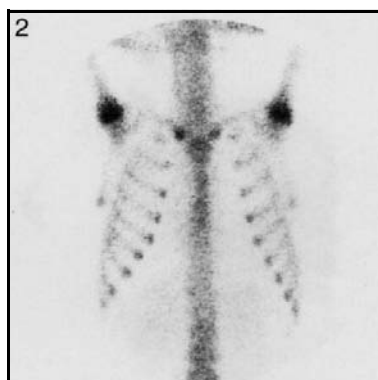
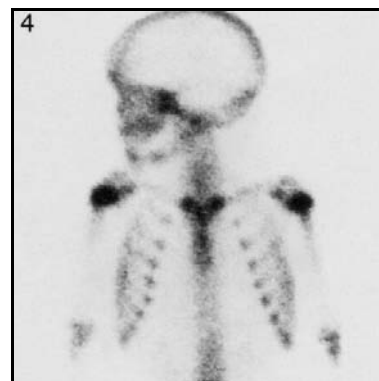
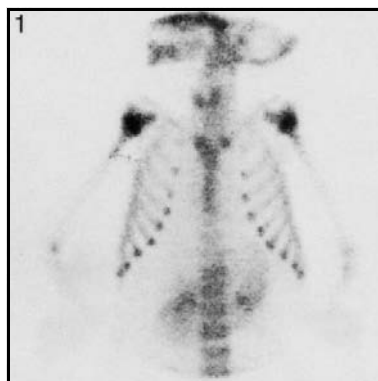
The lateral views of the skull (Figs 2 and 5) were taken anteriorly.

*FIG. 1. Anterior view of thorax spine.*

*FIG. 4. Left lateral view of skull and anterior view of thorax.*

*FIG. 2. Anterior view of thorax and spine.*

*FIG. 5. Anterior view of thorax and spine.*



### **Technical comments**

Figure 1 shows activity in the thyroid gland and also in the stomach due to the free  $^{99m}\text{Tc}$ -pertechnetate. This is rather unusual but it does occasionally occur.

Figure 1 shows the lower lumbar spine to good advantage.

Note the variation in sternal ossification.

## 6: Age 3–4 years

## Skull, thorax and upper limbs

*FIG. 1. Right lateral view of skull, posterior view of thorax, spine and upper limbs.*



*FIG. 4. Posterior view of thorax and spine.*



*FIG. 2. Posterior view of thorax and spine.*

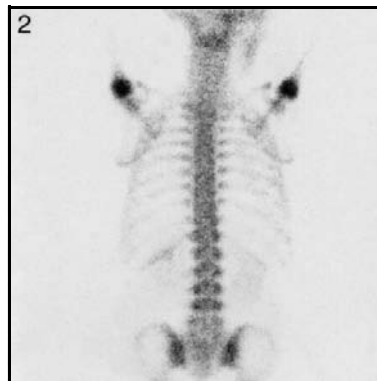
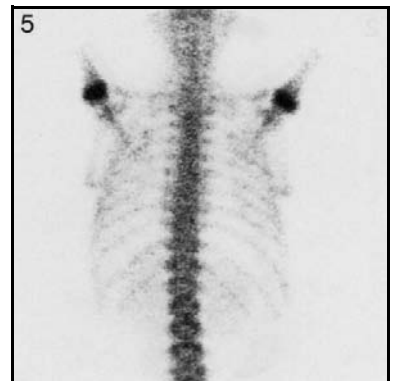


*FIG. 5. Posterior view of thorax and spine.*



### Technical comments

With the upper limbs elevated in Figs 2 and 5, the scapula clears the thorax and is well seen. Note the poor positioning of the hands in Fig. 1.

*FIG. 1. Left anterior oblique view of thorax.*

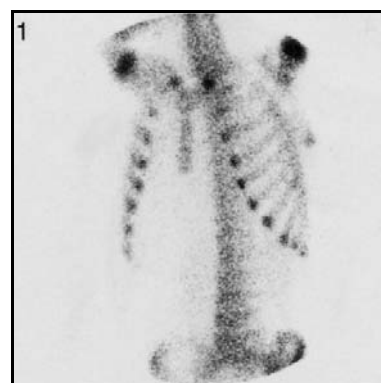
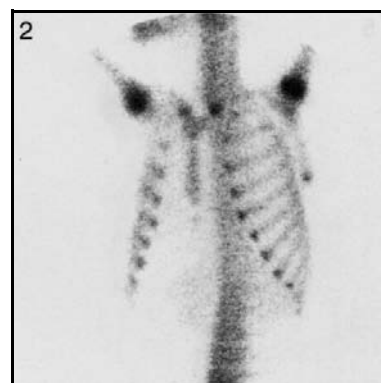


*FIG. 2. Left anterior oblique view of thorax.*



## 6: Age 3–4 years

## Spine, pelvis and femora

*FIG. 1. Anterior view of spine, pelvis and femora.*



*FIG. 4. Anterior view of spine, pelvis and femora.*



*FIG. 2. Anterior view of spine and pelvis.*

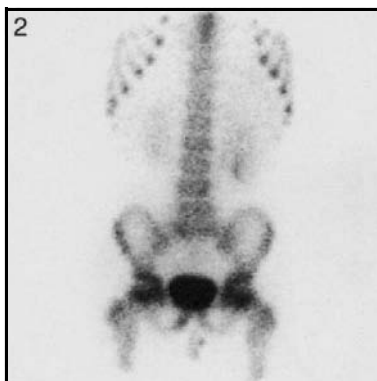
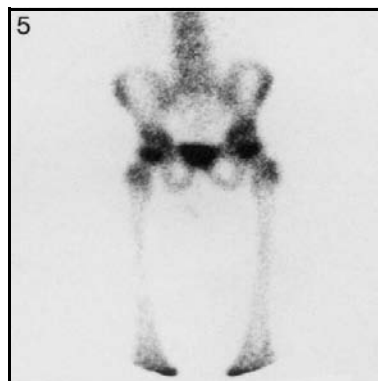


*FIG. 5. Anterior view of pelvis and femora.*



### Technical comments

Note the clarity of the lower lumbar spine on all images.

The bladder in Fig. 4 is of relatively large volume but has little activity, suggesting that the child is well hydrated.

The other three images show high activity and low volume bladders. This is not recommended.

Urine contamination below the pelvis is seen in Figs 2, 4 and 5.



## 6: Age 3–4 years

## Skull, thorax and upper limbs

*FIG. 1. Posterior view of spine, pelvis and femora.*

*FIG. 4. Posterior view of spine, pelvis and femora.*

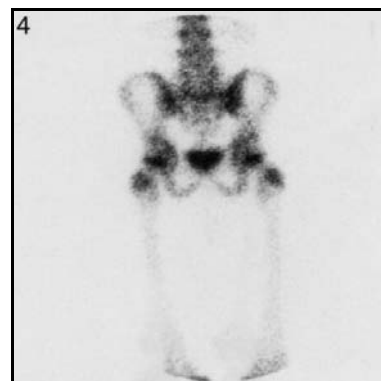
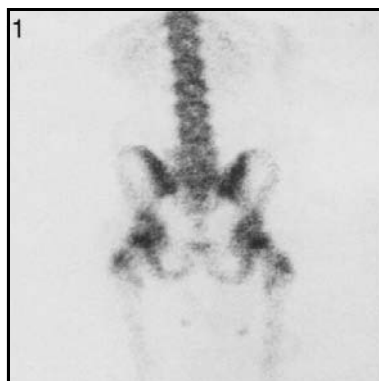
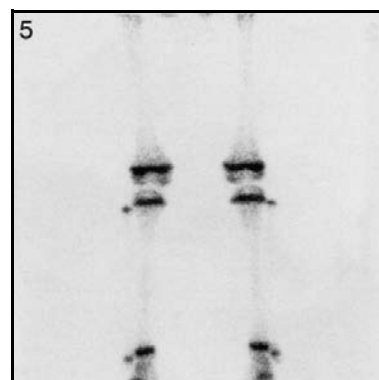
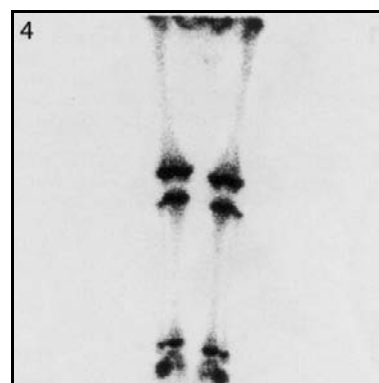


*FIG. 1. Posterior view of femora and knees.*

*FIG. 4. Posterior view of lower limbs.*

*FIG. 2. Posterior view of knees, tibia, fibula and ankles.*

*FIG. 5. Posterior view of lower limbs.*



**Technical comment**

The clarity of the fibula on all the images suggests good positioning of the feet.

FIG. 1. Pinhole view of right hip.

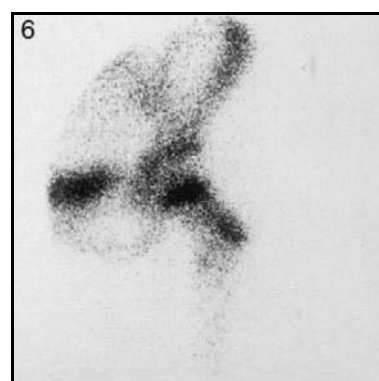
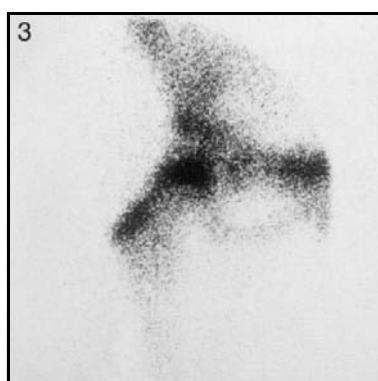
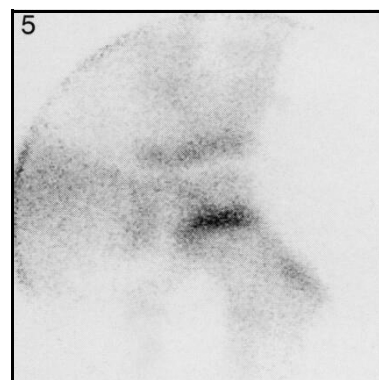
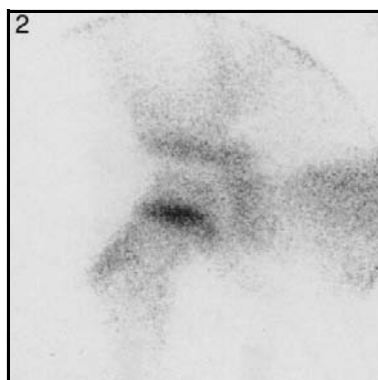
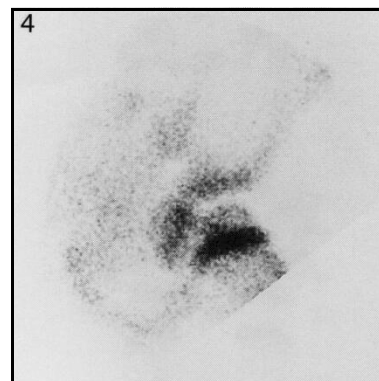
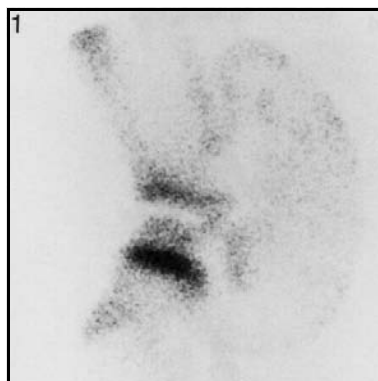
FIG. 4. Pinhole view of left hip.

FIG. 2. Pinhole view of right hip.

FIG. 5. Pinhole view of left hip.

FIG. 3. Pinhole view of right hip.

FIG. 6. Pinhole view of left hip.



### Technical comments

Different sizes of pinhole inserts give different degrees of magnification.

The position of the hips on the bottom series (Figs 3 and 6) is not as good as in the top two.

This is related to the positioning of the knees and the lack of in-turning of the feet. The radiographic neutral position of the feet and knees is essential when recording pinhole views of the hips.

*FIG. 1. Anterior view of knees.*

*FIG. 4. Posterior view of knees.*

*FIG. 2. Anterior view of knees.*

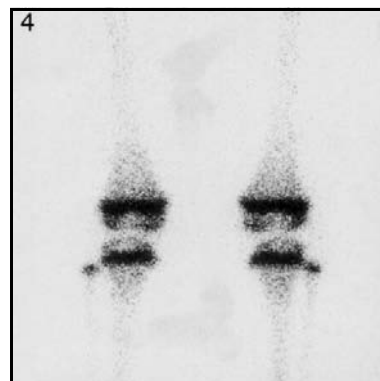


*FIG. 1. Lateral view of right knee and foot.*

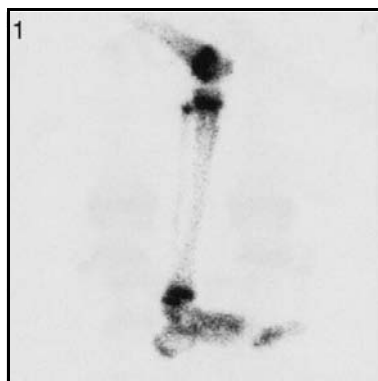


*FIG. 2. Anterior pinhole view of right knee.*

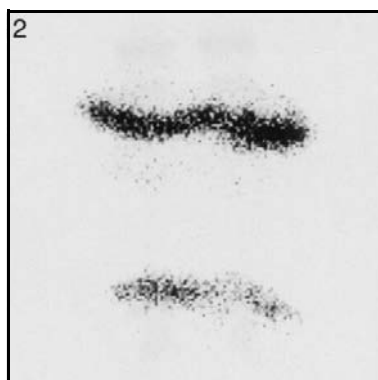


*FIG. 5. Anterior pinhole view of left knee.*



**Technical comment**

Pinhole projections are rather frequently required for clinical purposes.

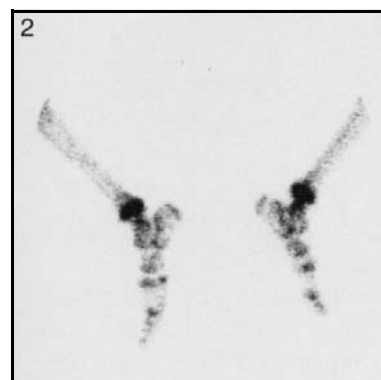
**6: Age 3–4 years**

**Tibia, fibula and feet**

*FIG. 1. Posterior view of tibia, fibula and ankles.*



*FIG. 2. Lateral view of feet.*



## **7. AGE 4–5 YEARS**





## 7: Age 4–5 years

## Blood pool images

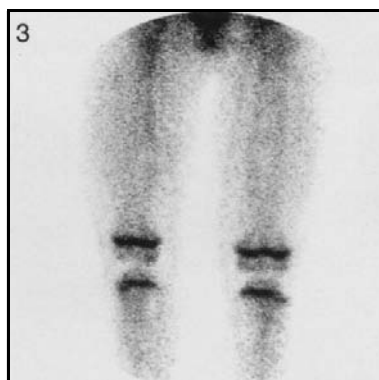
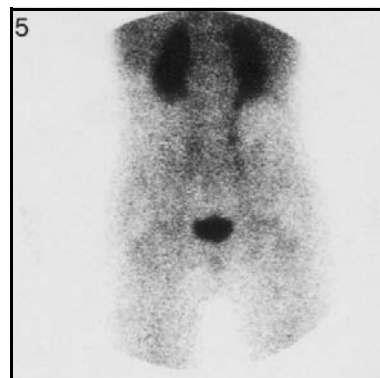
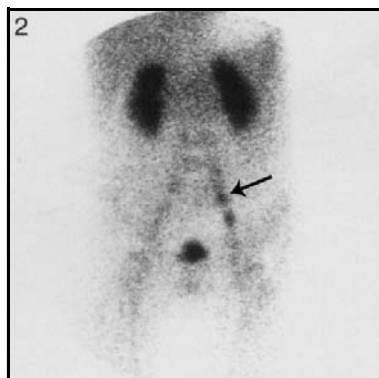
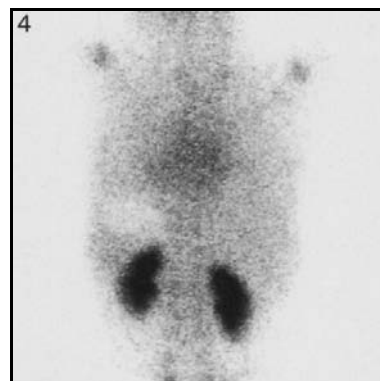
*FIG. 1. Posterior view of skull.*

*FIG. 4. Posterior view of thorax and spine.*

*FIG. 2. Anterior view of spine and pelvis.*

*FIG. 5. Posterior view of spine and pelvis.*

*FIG. 3. Anterior view of femora and knees.*

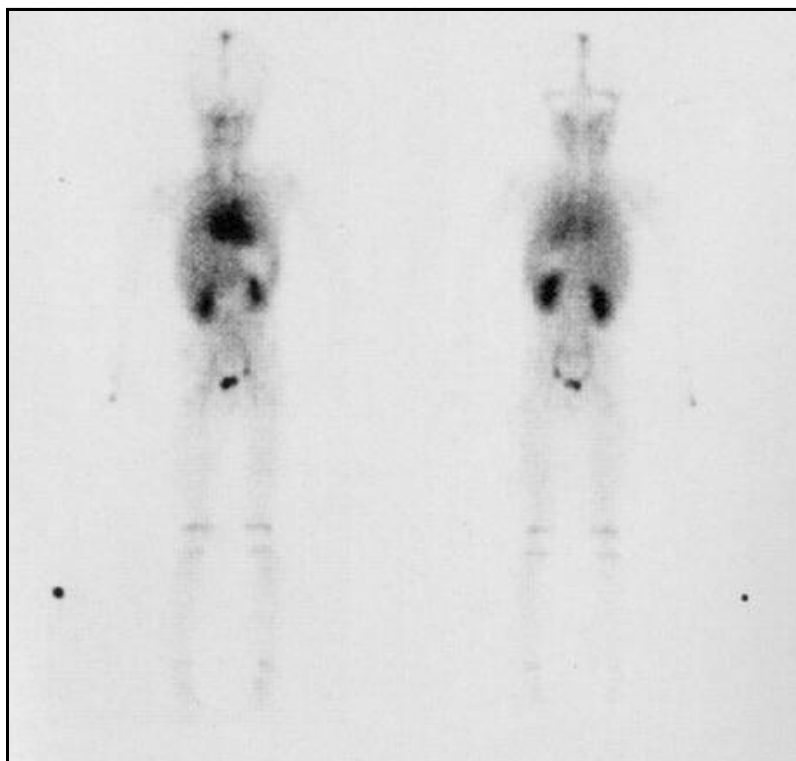


### Technical comments

The photon deficient area above the left kidney in Fig. 4 represents the stomach full of food. This is also seen in Fig. 2, immediately above the left kidney.

Figure 2 shows the focal accumulation of isotope above the bladder on the left. This may be in the ureter (arrowed).

*FIG. 1. A double headed whole body gamma camera was used. Left image is anterior view; right image is posterior view.*



**Technical comments**

Isotope is seen in both ureters.

The full stomach is seen as a photon deficient area in the anterior view above the left kidney.

Note the extravasation of isotope at the site of injection in the right hand.

Marker on the right side.

*FIG. 1. A double headed whole body gamma camera was used. Left image is anterior view; right image is posterior view.*



**Technical comments**

The left foot is better positioned than the right, with the toes turned inward allowing good visualization of the fibula.

Diffuse parenchymal renal activity is seen, no pathological cause was evident.

Note the extravasation of isotope at the site of injection in the left elbow.

Urine contamination below the pelvis is seen in the anterior view.

Marker on the right side.

## 7: Age 4–5 years

## Skull and upper limbs

*FIG. 1. Anterior view of skull.*



*FIG. 4. Posterior view of skull and thorax.*

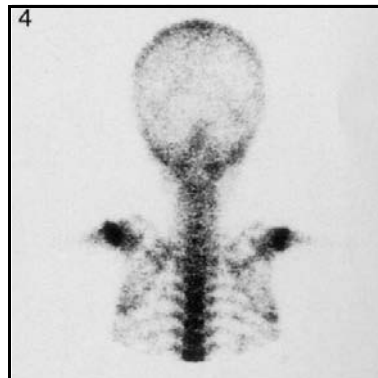


*FIG. 2. Right lateral view of skull and right upper limb.*

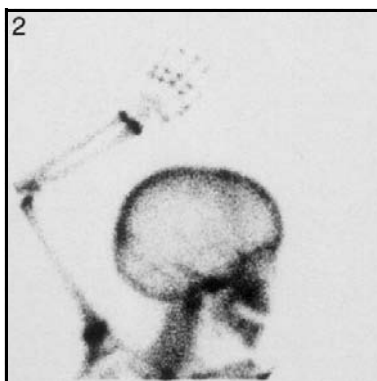


*FIG. 5. Left lateral view of skull and left upper limb.*



### Technical comments

Note the poor positioning of the left hand in Fig. 5; the thumb cannot be seen. The coronal sutures are indistinct in Figs 2 and 5; this is a variation of normality. The lateral views of the skull (Figs 2 and 5) were taken anteriorly.

## 7: Age 4–5 years

## Skull and upper limbs

*FIG. 4. Posterior view of skull and thorax.*



*FIG. 2. Right lateral view of skull and right upper limb.*



*FIG. 5. Left lateral view of skull and left upper limb.*

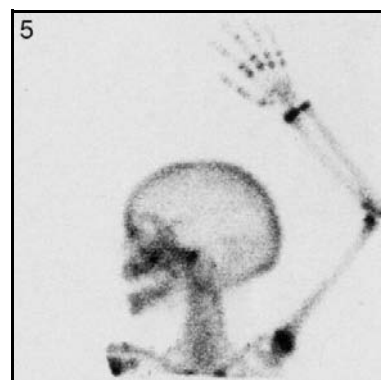


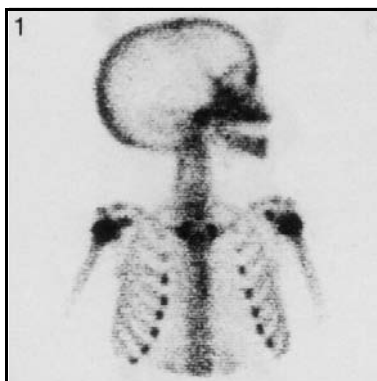
*FIG. 3. Left lateral view of skull and both upper limbs.*



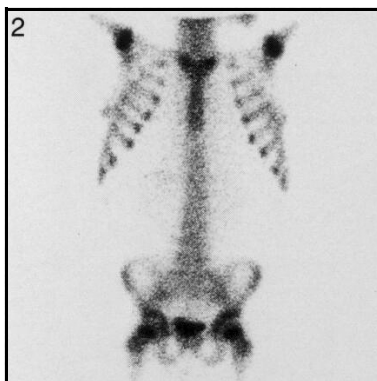
### Technical comments

Figure 3 shows the difficulty of attempting to image both hands simultaneously. Imaging of the right upper limb with the right lateral skull and the left upper limb with the left lateral skull is recommended. The lateral views of the skull (Figs 2 and 5) were taken anteriorly.

*FIG. 1. Right lateral view of skull and anterior view of thorax.*



*FIG. 2. Anterior view of spine and pelvis.*



*FIG. 5. Lateral anterior oblique view of thorax.*

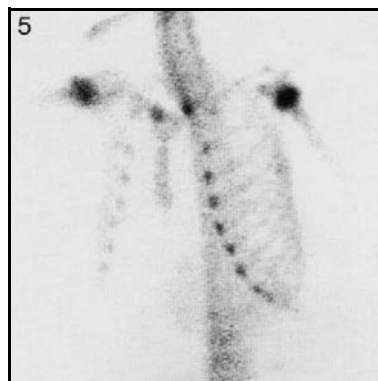
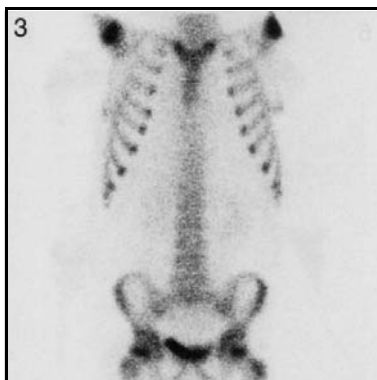


*FIG. 3. Anterior view of thorax, spine and pelvis.*



#### Technical comment

Urine contamination below the pelvis is seen in Fig. 2.

## 7: Age 4–5 years

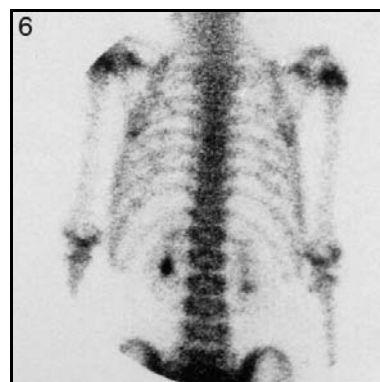
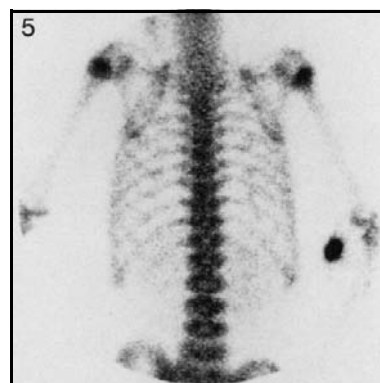
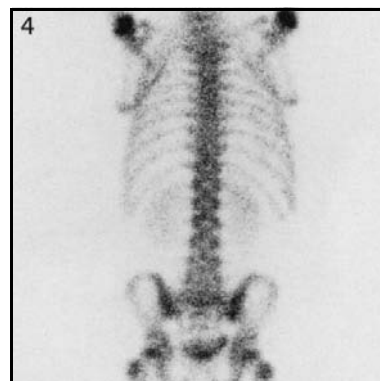
## Thorax, spine, pelvis and upper limbs

*FIG. 1. Anterior view of thorax, spine and pelvis.*

*FIG. 4. Posterior view of thorax, spine and pelvis.*

*FIG. 5. Posterior view of thorax and spine.*

*FIG. 6. Posterior view of thorax and spine.*



### Technical comments

Different positions of the upper limbs have resulted in the different appearance of the scapulae in Figs 4 and 5. Urine contamination below the pelvis is seen in Fig. 1.

Note the asymmetrical renal pelvic activity in the right renal pelvis in Fig. 1 and in the left in Fig. 6.

Note the extravasation of isotope at the site of injection in the right elbow in Fig. 5.

## 7: Age 4–5 years

## Spine, pelvis and femora

*FIG. 1. Anterior view of spine and pelvis.*

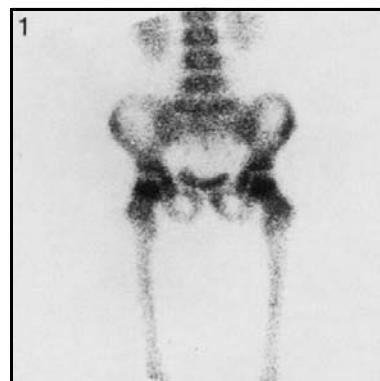


*FIG. 2. Anterior view of spine, pelvis and femora.*

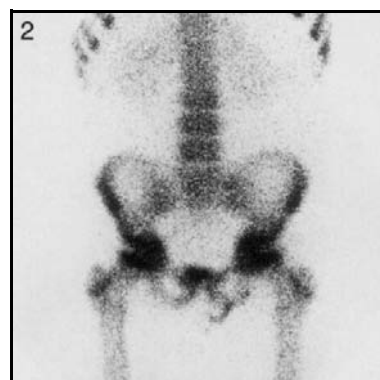
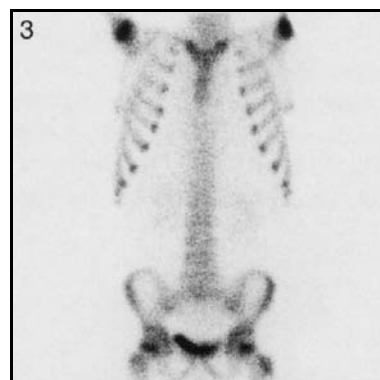


*FIG. 3. Anterior view of thorax, spine and pelvis.*



### Technical comments

Urine contamination over the right inferior pubic ramus is seen in Fig. 2. Note the clarity of the lower lumbar spine on these images.



**7: Age 4–5 years**

**Spine, pelvis and femora**

*FIG. 1. Posterior view of spine, pelvis and femora.*

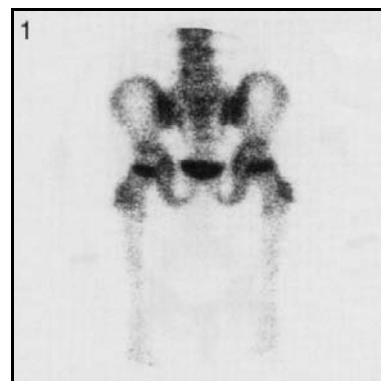


*FIG. 2. Posterior view of spine, pelvis and femora.*

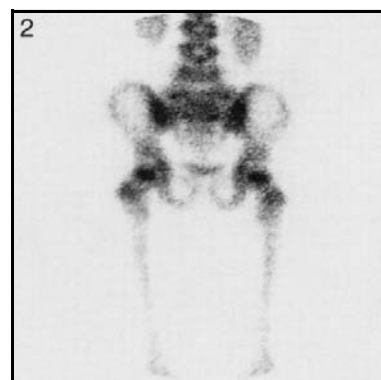


*FIG. 3. Posterior view of spine, pelvis and femora.*

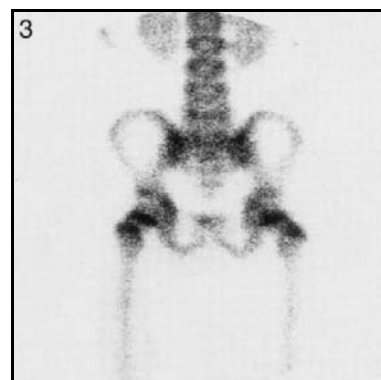
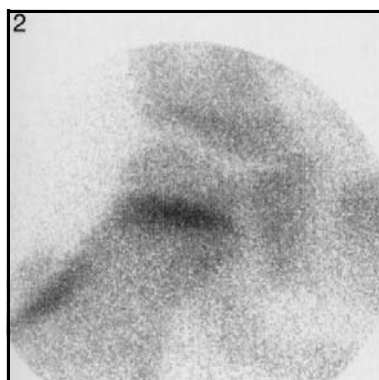
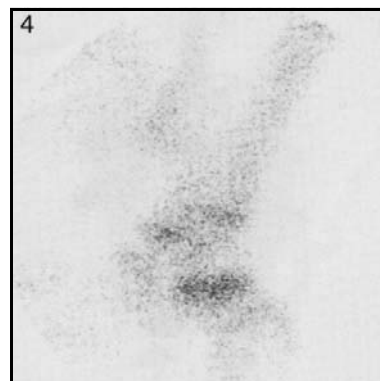
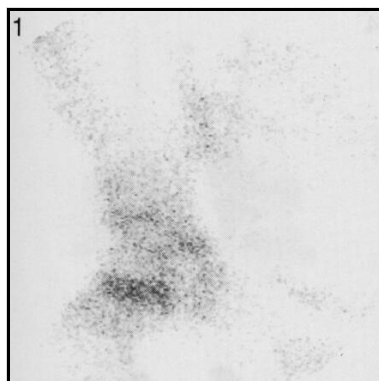


*FIG. 1. Pinhole view of right hip.*

*FIG. 4. Pinhole view of left hip.*

*FIG. 2. Pinhole view of right hip.*

*FIG. 5. Pinhole view of left hip.*



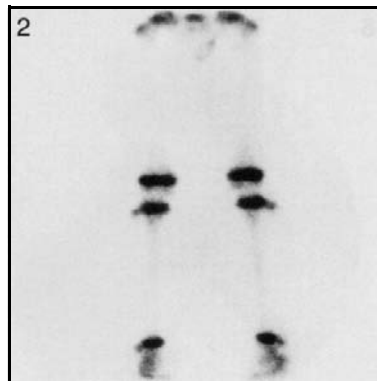
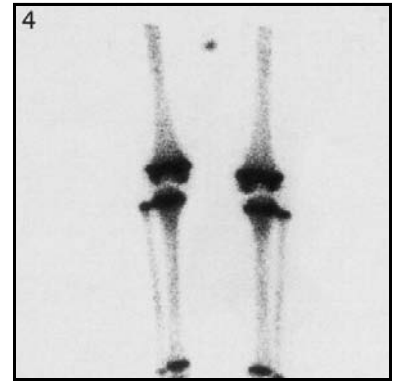
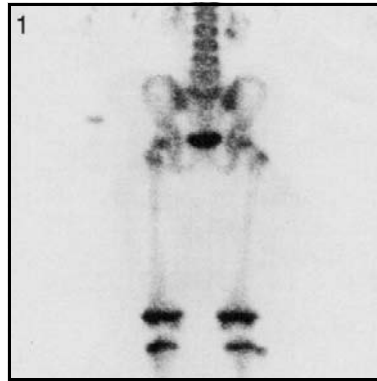
## 7: Age 4–5 years

## Pelvis and lower limbs

*FIG. 1. Posterior view of pelvis and femora.*

*FIG. 4. Posterior view of lower limbs.*

*FIG. 2. Posterior view of lower limbs.*



### Technical comments

Urine contamination is seen at the upper edge of Fig. 4.

Figure 1 shows the difference in activity between the two femoral necks. The left leg is poorly positioned, as evidenced by the lack of visualization of the head of the fibula. This has resulted in the greater trochanter rotating and being seen to overlie the femoral neck. The right side is well positioned.

### Potential pitfall

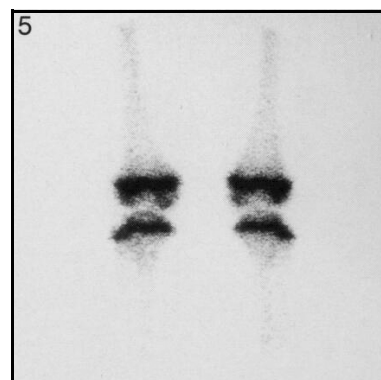
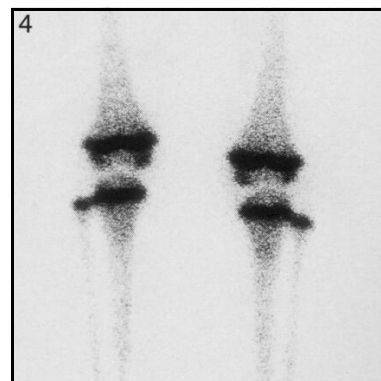
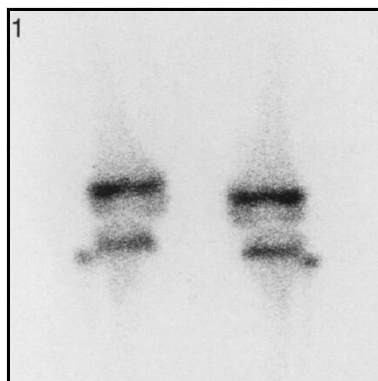
The lack of clarity of the epiphyseal plates around the knees in Fig. 4 is due to overexposure during acquisition.

FIG. 1. Posterior view of knees.

FIG. 4. Posterior view of knees.

FIG. 2. Posterior view of knees.

FIG. 5. Posterior view of knees.



### Technical comments

Note the clarity of the heads of the fibulae on all the images.

Note the clarity of the epiphyseal plates with their well-defined margins.

## 7: Age 4–5 years

## Tibia, fibula and feet

*FIG. 1. Posterior view of both tibia, fibula and ankles.*

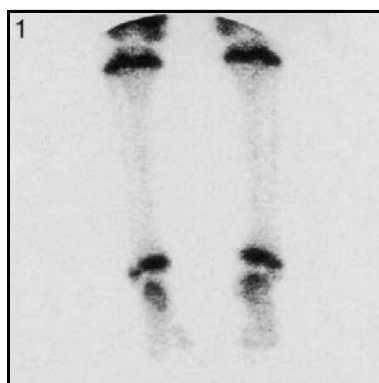


*FIG. 4. Anterior view of both feet.*

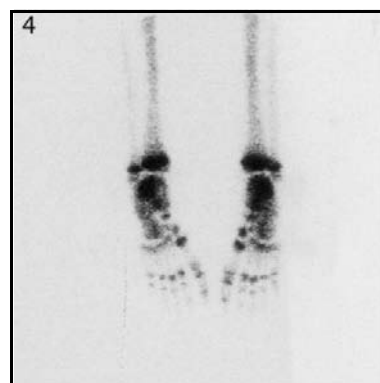


*FIG. 2. Lateral view of left lower limb.*



*FIG. 5. Lateral view of right lower limb.*

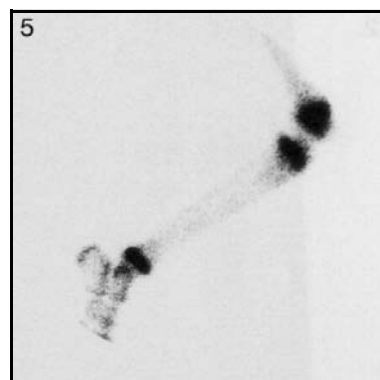
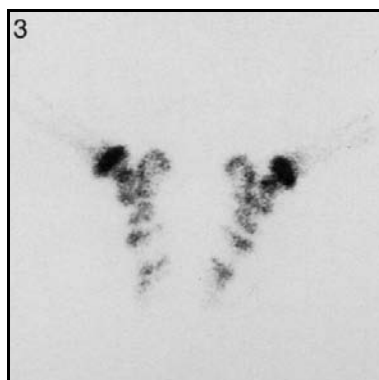


*FIG. 3. Lateral view of both feet.*



### Technical comment

The lateral views (Figs 2 and 5) are of little value for the knees.



## **8. AGE 5–6 YEARS**





*FIG. 1. Posterior view of thorax and spine.*

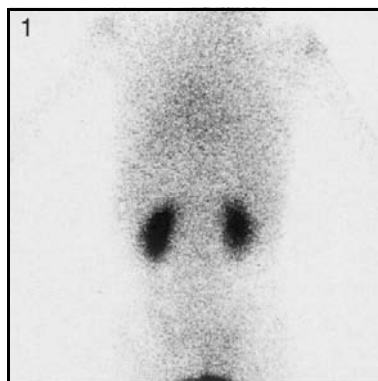


*FIG. 2. Posterior view of spine and pelvis.*

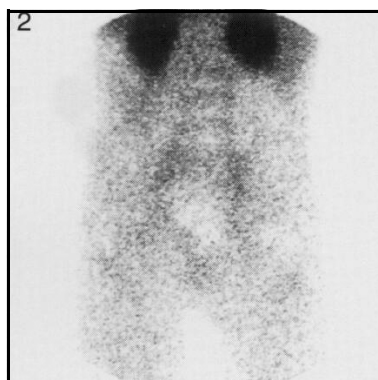


*FIG. 5. Posterior view of pelvis.*

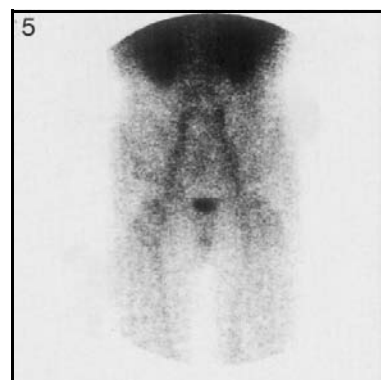


*FIG. 3. Posterior view of femora and knees.*

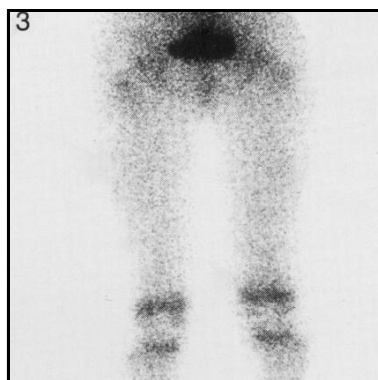
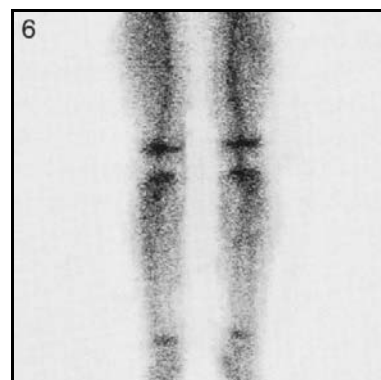


*FIG. 6. Anterior view of lower limbs.*

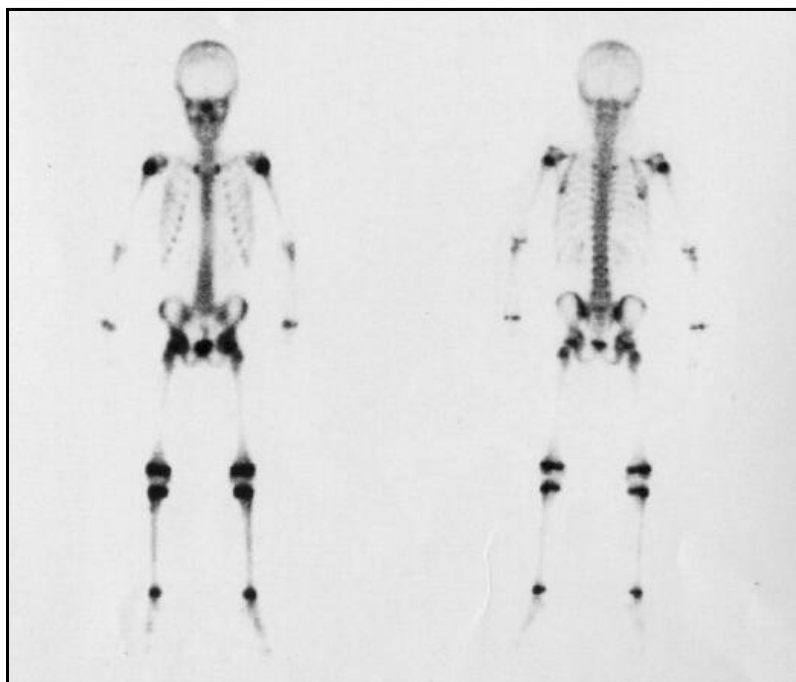


**Technical comments**

The full bladder is seen as a photon deficient area in Fig. 2.

The larger vessels are clearly seen in the anterior view in Figs 5 and 6.

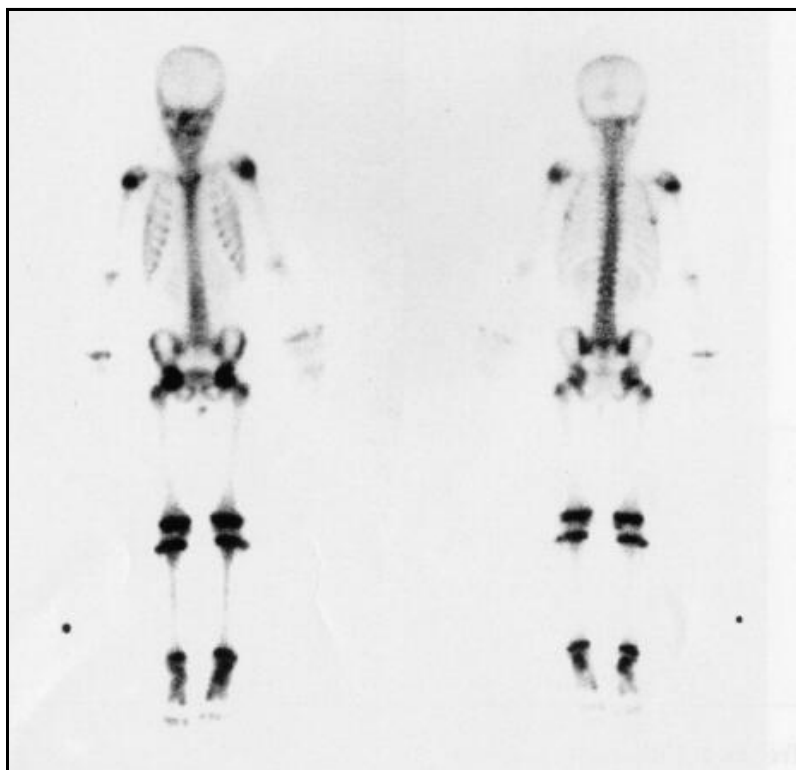
*FIG. 1. A double headed whole body gamma camera was used. Left image is anterior view; right image is posterior view.*



**Technical comment**

The feet are poorly positioned with out-turning of the toes bilaterally.

*FIG. 1. A double headed whole body gamma camera was used. Left image is anterior view; right image is posterior view.*



**Technical comments**

Both feet are well positioned with the toes turned inwards, allowing good visualization of the fibula.  
Slight movement of the upper limbs has resulted in blurring of the images of the upper limbs.  
Urine contamination below the pelvis is seen in the anterior view.  
Marker on the right side.

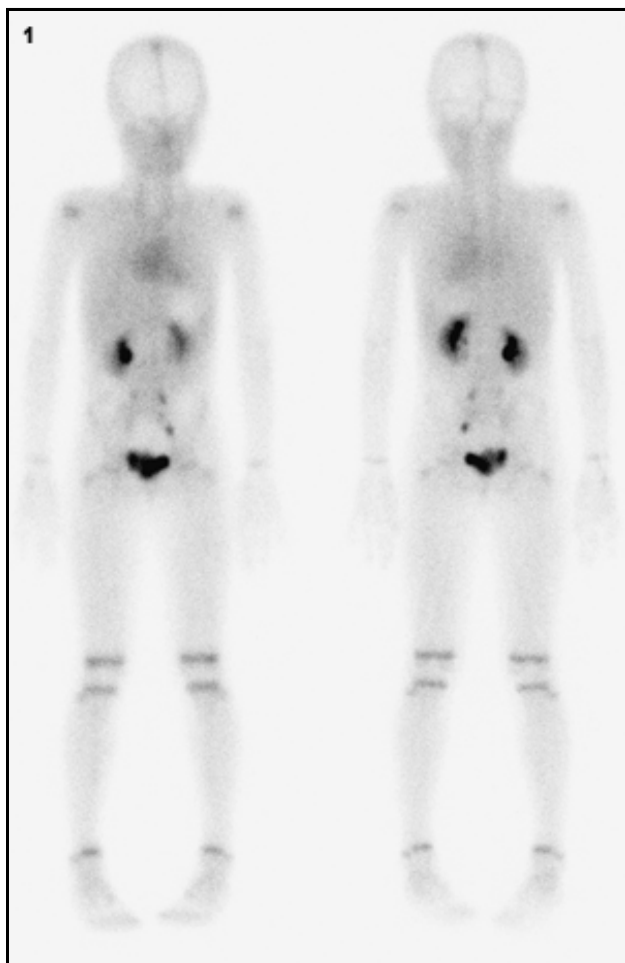


*FIG. 1. Whole body images of a 5-year-old female (22 kg body weight). Anterior and posterior blood pool whole body views.*

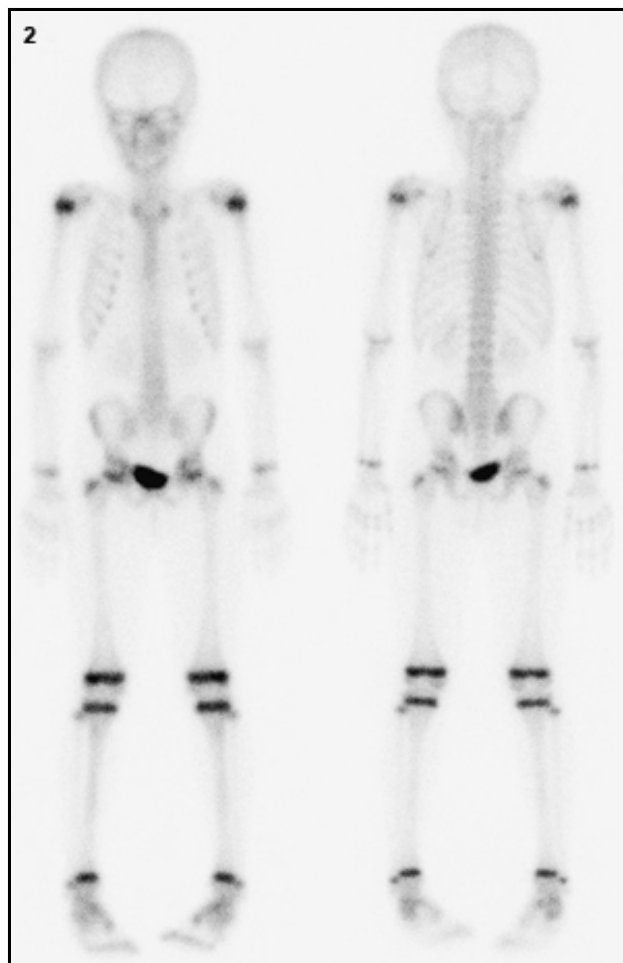


*FIG. 2. Whole body images of a 5-year-old female (22 kg body weight). Delayed anterior and posterior whole body bone scan.*

#### Technical comments

A double headed digital whole body gamma camera equipped with high resolution low energy collimator was used and the energy window width set to 15%.

Immediately following the intravenous injection of 260 MBq (0.5, fraction of adult administered activity of 500 MBq) of  $^{99m}\text{Tc}$ -MDP, whole body blood pool imaging was started at a camera scanning speed of 20 cm/min. Delayed bone scan imaging was acquired 3 hours p.i. at a camera speed of 12 cm/min.

## 8: Age 5–6 years

## Skull, thorax and upper limbs

*FIG. 1. Anterior view of skull and thorax.*



*FIG. 4. Posterior view of skull and spine.*

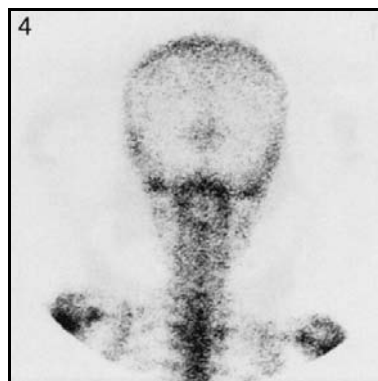


*FIG. 2. Lateral view of skull, right upper limb and posterior view of thorax.*

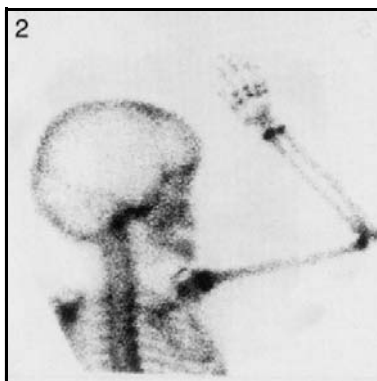


*FIG. 5. Left lateral view of skull, left upper limb and posterior view of thorax.*



### Technical comments

Note the increased activity in the region of the maxillary antra in Fig. 1. This is within normal limits. The lateral views of the skull (Figs 2 and 5) were taken posteriorly.

*FIG. 1. Right lateral view of skull, both upper limbs and posterior view of thorax.*



*FIG. 4. Left lateral view of skull and both upper limbs.*



*FIG. 2. Right lateral view of skull and right upper limb.*



*FIG. 5. Left lateral view of skull and left upper limb.*

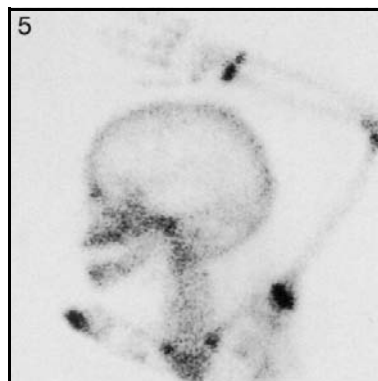
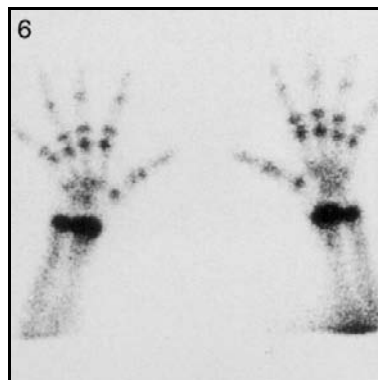


*FIG. 3. Anterior view of both hands.*



*FIG. 6. Anterior view of both hands.*



### **Technical comments**

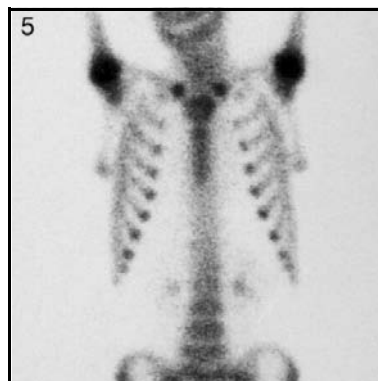
Note the difficulty of imaging both hands simultaneously in Figs 1 and 4. The lateral views of the skull (Figs 2 and 5) were taken anteriorly.

*FIG. 1. Anterior view of thorax and spine.*

*FIG. 4. Right lateral view of skull and anterior view of thorax.*

*FIG. 2. Anterior view of thorax and spine.*

*FIG. 5. Anterior view of thorax and spine.*



**Technical comments**

Note the differences in the sternum on these four images.

The lumbar spine is clearly seen in Figs 1, 2 and 5.

The scapulae appear differently in Figs 2 and 5 owing to different positions of the upper limbs.

## 8: Age 5–6 years

## Spine, pelvis and femora

*FIG. 4. Posterior view of thorax and spine.*



*FIG. 2. Left anterior oblique view of thorax.*

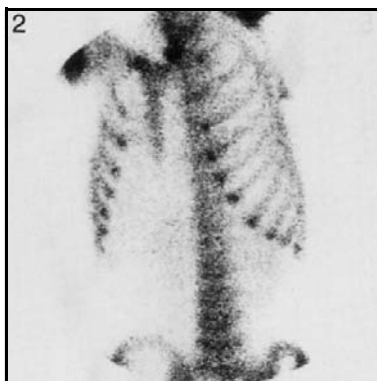
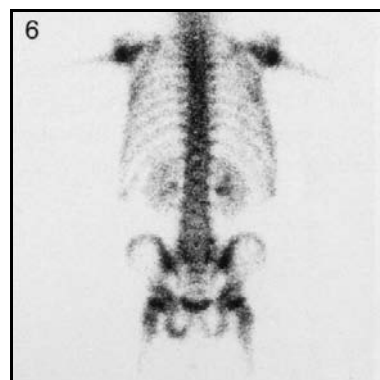


*FIG. 5. Posterior view of thorax, spine and pelvis.*



*FIG. 6. Posterior view of thorax, spine and pelvis.*



### Potential pitfall

Note the increased activity in the posterior pubic ramus and ischium in Fig. 6. This is an unusual variant of the normal spondylosis.



## 8: Age 5–6 years

## Thorax, spine and pelvis

*FIG. 1. Anterior view of spine, pelvis and femora.*



*FIG. 4. Anterior view of spine and pelvis.*

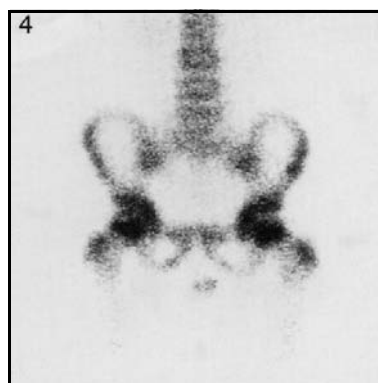


*FIG. 2. Anterior view of spine and pelvis.*

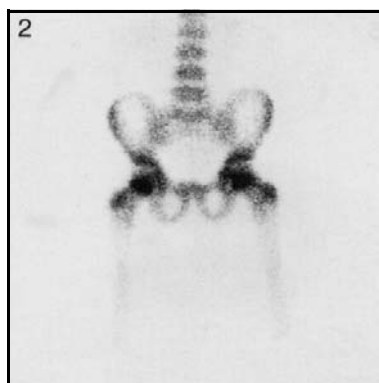
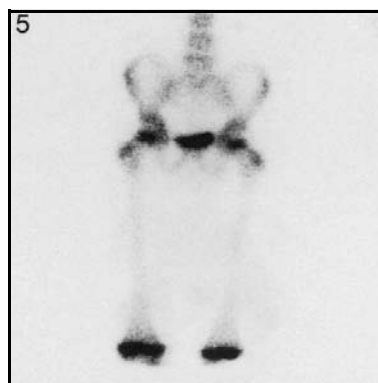


*FIG. 5. Anterior view of spine and pelvis.*



### Technical comments

Note the clarity of lumbar spine in all views.

Urine contamination below the pelvis is seen in Figs 1 and 4.

FIG. 1. Posterior view of spine and pelvis.

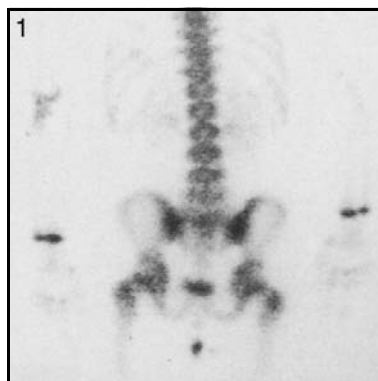


FIG. 4. Posterior view of spine, pelvis and femora.

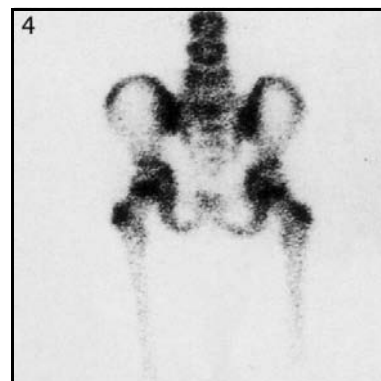


FIG. 2. Posterior view of spine and pelvis.



FIG. 5. Posterior view of spine and pelvis.

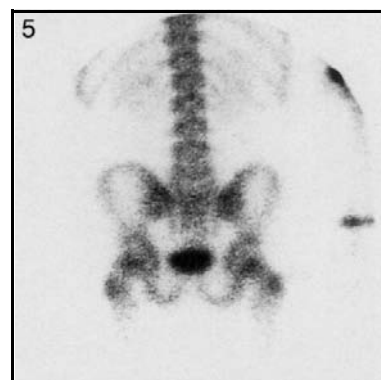


FIG. 6. Posterior view of spine and pelvis with lower limbs in abduction.



### Technical comments

Urine contamination is seen below the pelvis in Fig. 1.

Figure 6 shows the hips in abduction. This is the usual view used mainly to look for slipped capital femoral epiphysis.

FIG. 1. Pinhole view of right hip.

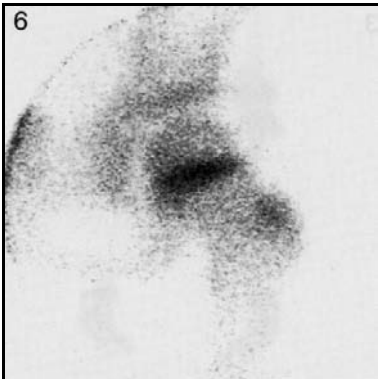
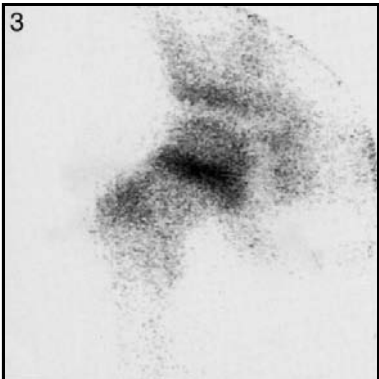
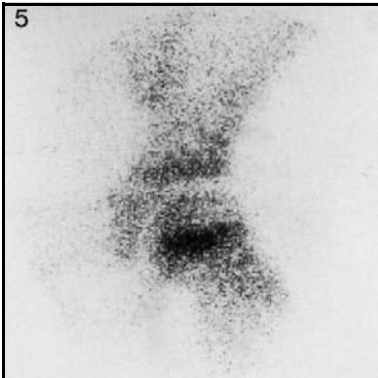
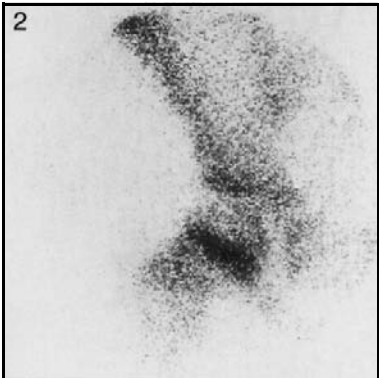
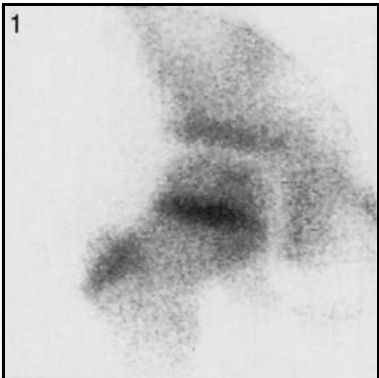
FIG. 4. Pinhole view of left hip.

FIG. 2. Pinhole view of right hip.

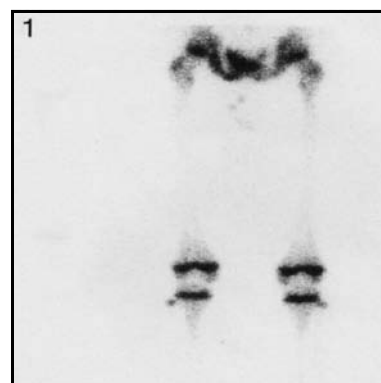
FIG. 5. Pinhole view of left hip.

FIG. 3. Pinhole view of right hip.

FIG. 6. Pinhole view of left hip.



*FIG. 1. Posterior view of lower limbs.*



*FIG. 2. Posterior view of knees, tibia, fibula and ankles.*

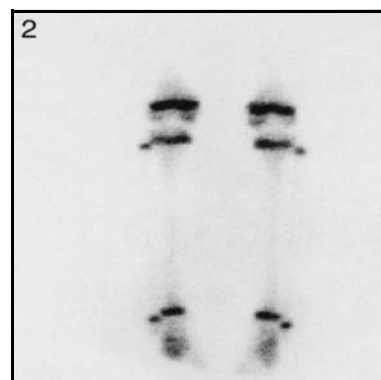
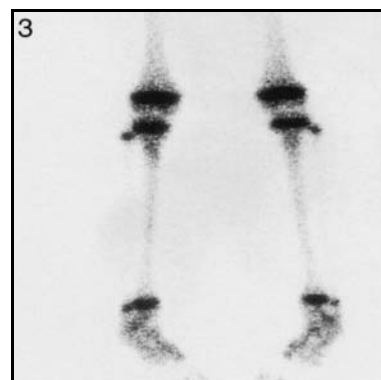


*FIG. 3. Posterior view of knees, tibia, fibula and feet.*



**Technical comment**

Note the radiographic neutral positioning of the feet in Figs 1–3, resulting in clear visualization of the fibula.

*FIG. 1. Posterior view of knees.*

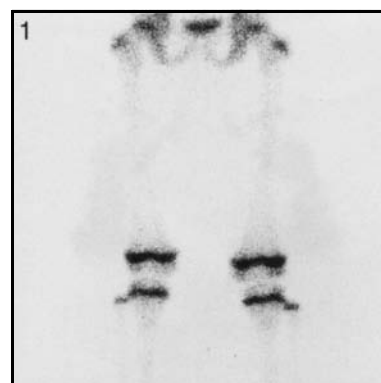


*FIG. 2. Posterior view of knees.*

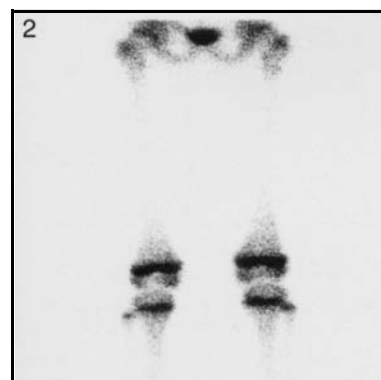
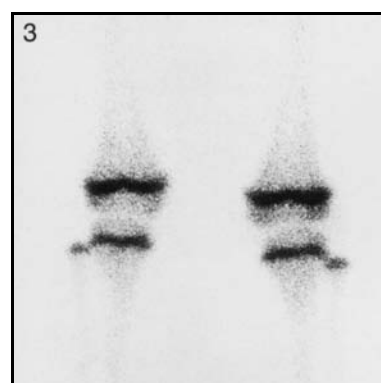


*FIG. 3. Posterior view of knees.*



**Technical comments**

The magnified view (Fig. 3) shows the epiphyseal plates to best advantage.  
The fibula is clearly seen in all figures because the toes were turned inwards during image acquisition.

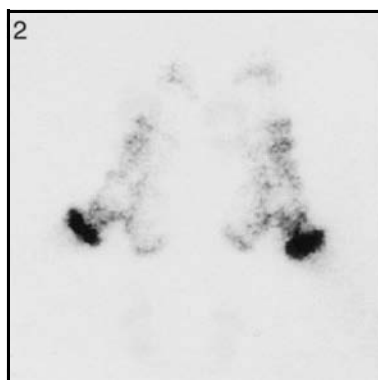
## 8: Age 5–6 years

## Ankles and feet

*FIG. 1. Lateral view of feet with straight knees.*

*FIG. 4. Anterior view of feet.*

*FIG. 2. Lateral magnified view of feet with knees flexed.*

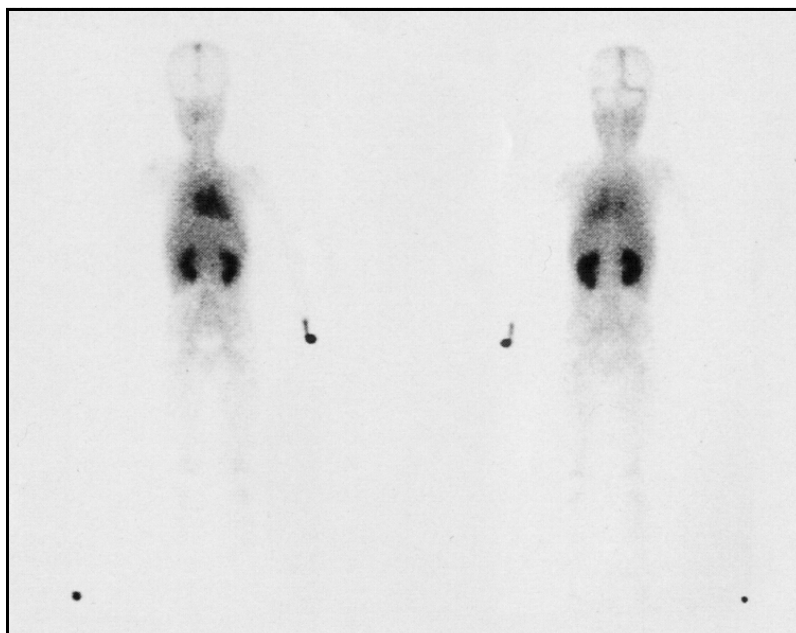


## **9. AGE 6–7 YEARS**





*FIG. 1. A double headed whole body gamma camera was used. Left image is anterior view; right image is posterior view.*



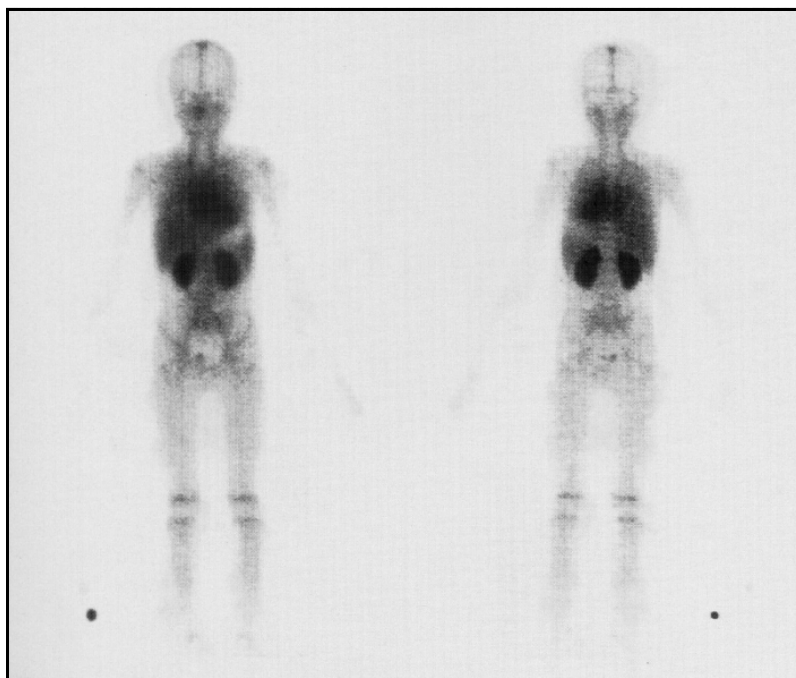
**Technical comments**

Note the extravasation of isotope at the site of injection in the left hand.  
Marker on the right side.

## 9: Age 6–7 years

## Blood pool images

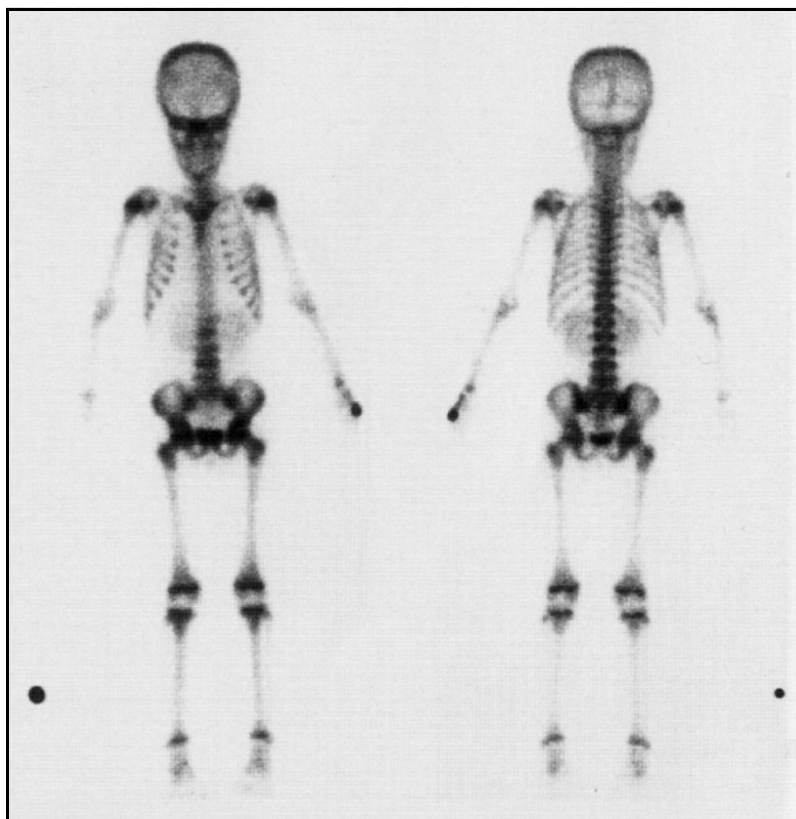
*FIG. 1. A double headed whole body gamma camera was used. Left image is anterior view; right image is posterior view.*



### Technical comments

Marker on the right side.

*FIG. 1. A double headed whole body gamma camera was used. Left image is anterior view; right image is posterior view.*



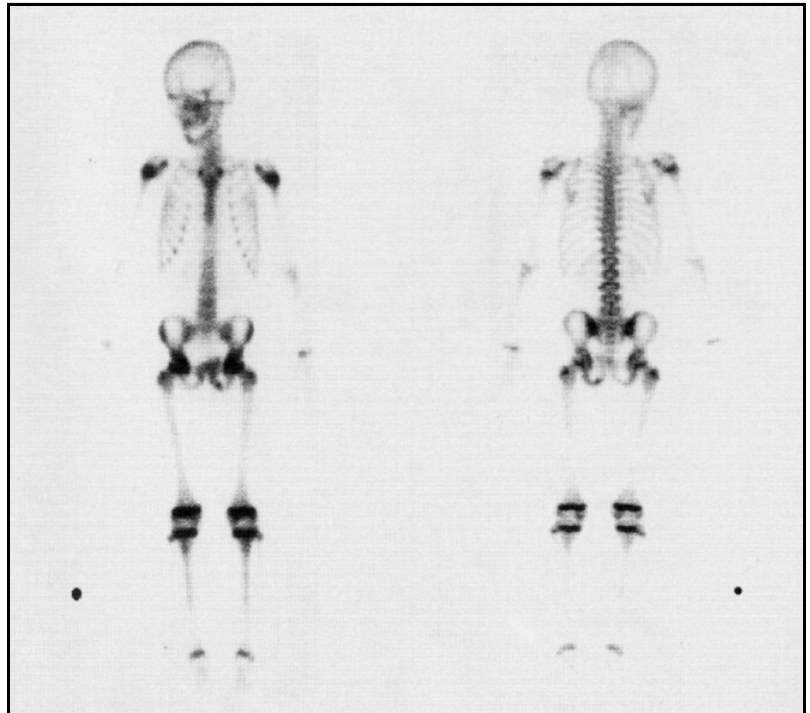
**Technical comments**

Note the extravasation of isotope at the site of injection in the left hand.  
Marker on the right side.

**Potential pitfall**

Note the band of apparent increased isotope uptake in the region of the orbits in the anterior view. This is due to the positioning of the child.

*FIG. 1. A double headed whole body gamma camera was used. Left image is anterior view; right image is posterior view.*



**Technical comments**

The child's head is rotated.  
Marker on the right side.

**Potential pitfall**

There is increased activity in the left inferior pubic ramus, best seen in the anterior view, which is due to normal synchondrosis.

## 9: Age 6–7 years

## Skull, thorax and upper limbs

*FIG. 1. Anterior view of skull and thorax.*



*FIG. 4. Posterior view of skull and thorax.*

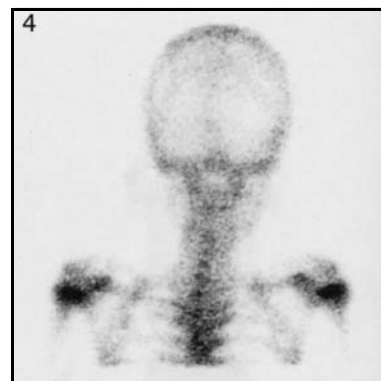


*FIG. 2. Right lateral view of skull and right upper limb.*

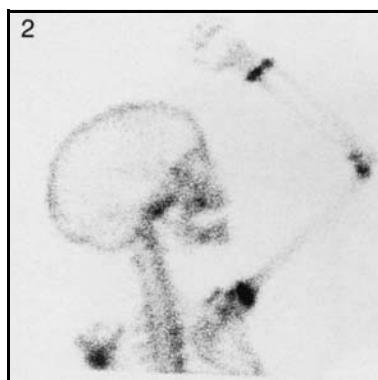
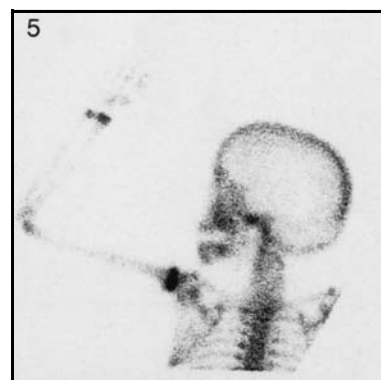


*FIG. 5. Left lateral view of skull and left upper limb.*



### Technical comment

The lateral views of the skull (Figs 2 and 5) were taken posteriorly.

## 9: Age 6–7 years

## Skull and upper limbs

*FIG. 1. Right lateral view of skull and right upper limb.*

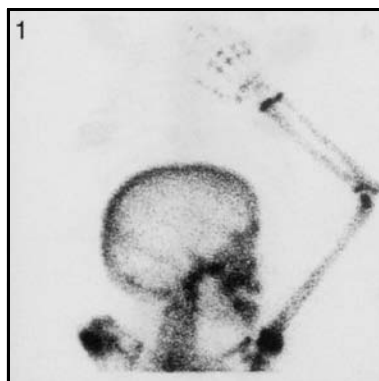


*FIG. 4. Left lateral view of skull and left upper limb.*

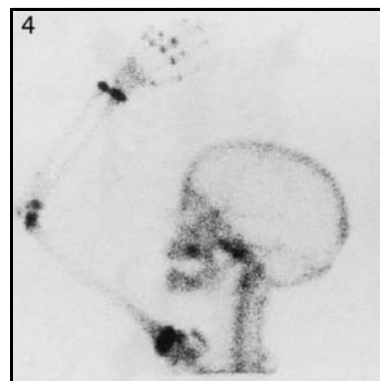


*FIG. 2. Anterior view of both upper limbs.*



### Technical comments

Note the extravasation of isotope at the site of injection in the elbow in Fig. 2. The lateral views of the skull (Figs 1 and 4) were taken posteriorly.

## 9: Age 6–7 years

## Thorax, spine and pelvis

*FIG. 1. Anterior view of thorax, spine and pelvis.*

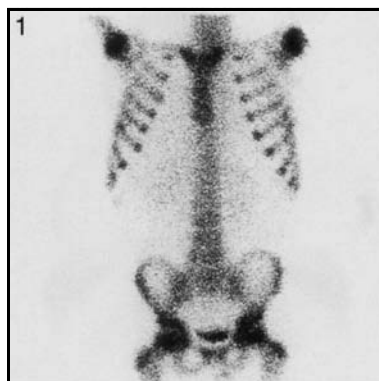


*FIG. 4. Anterior view of thorax and spine.*

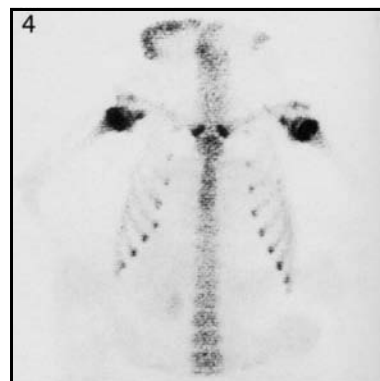


*FIG. 2. Anterior view of thorax, spine and upper pelvis.*

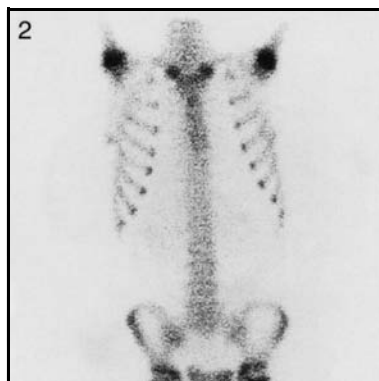
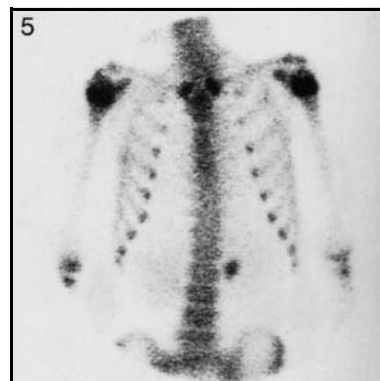


*FIG. 5. Anterior view of thorax and spine.*



### Technical comments

The lower lumbar spine is well seen on these anterior views.

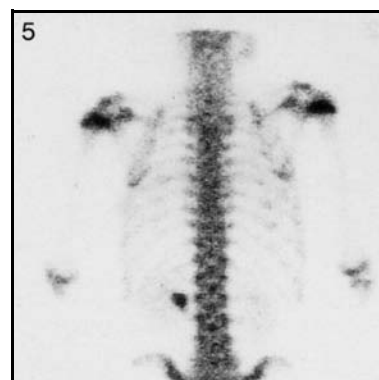
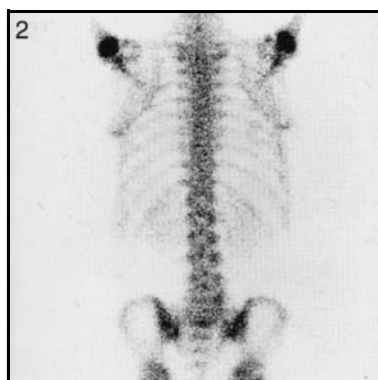
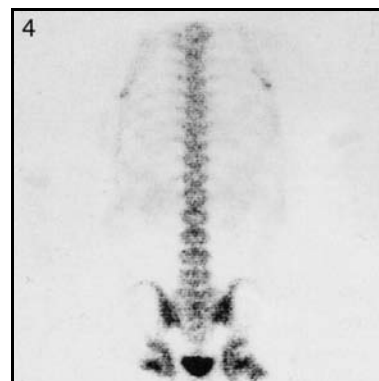
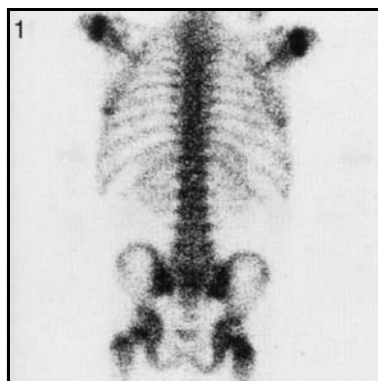
The difference between the two kidneys in Fig. 5 is within normal limits.

*FIG. 1. Posterior view of thorax, spine and pelvis.*

*FIG. 4. Posterior view of thorax, spine and upper pelvis.*

*FIG. 2. Posterior view of thorax, spine and upper pelvis.*

*FIG. 5. Posterior view of thorax and spine.*



These images are from the same four children as seen in Figs 1, 2, 4 and 5 on p.123.

**Technical comment**

There is accumulation of isotope in the renal pelvis of the left kidney in Fig. 5. This is still within normal limits (same child as in Fig. 5, p.123).

**Potential pitfall**

Increased activity over the line of the ribs in the posterior axillary portion, best seen in Fig. 5 on the right are not due to fractures but reflect shine through from the anterior costochondral junctions.



**9: Age 6–7 years**

**Thorax, spine and pelvis**

*FIG. 1. Anterior view of spine, pelvis and femora.*

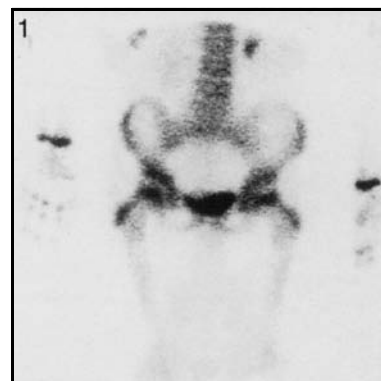
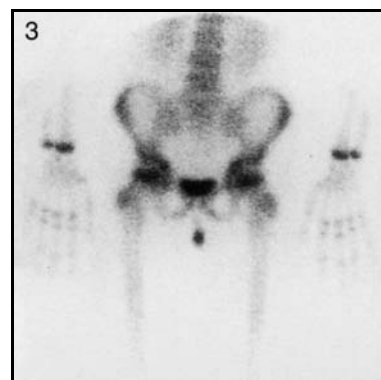


*FIG. 2. Anterior view of spine, pelvis and femora.*



*FIG. 3. Anterior view of spine, pelvis, femora and hands.*



**Technical comment**

Urine contamination below the pelvis is seen in Fig. 3.

## 9: Age 6–7 years

## Spine, pelvis and femora

FIG. 1. Posterior view of spine, pelvis, femora and hands.



FIG. 2. Posterior view of spine, pelvis and femora.

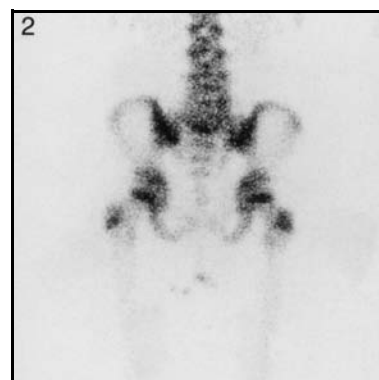


FIG. 3. Posterior view of spine and pelvis.



### Technical comment

Urine contamination below the pelvis is seen in Fig. 2.

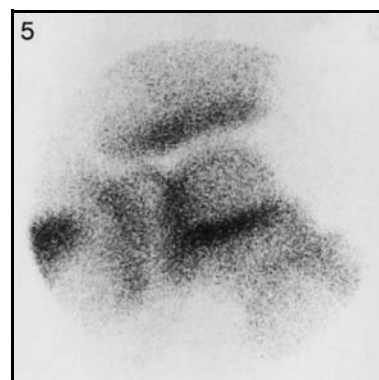
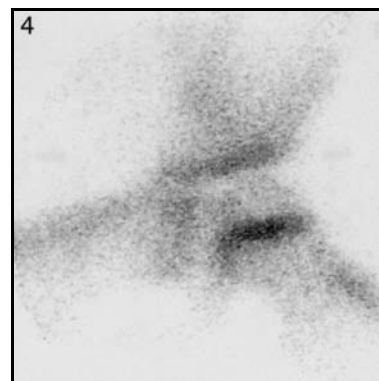
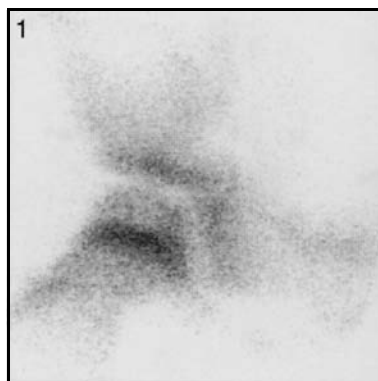
### Potential pitfall

Note the increased activity in Fig. 3 at the junction of the left ischial tuberosity and the posterior pubic ramus, which is due to normal synchondrosis at the site.

*FIG. 1. Pinhole view of right hip.*

*FIG. 4. Pinhole view of left hip.*

*FIG. 5. Pinhole view of left hip.*



**Technical comment**

The larger size of the hip is due to the size of the pinhole insert used compared with Figs 1 and 4.

*FIG. 1. Posterior view of femora and knees.*

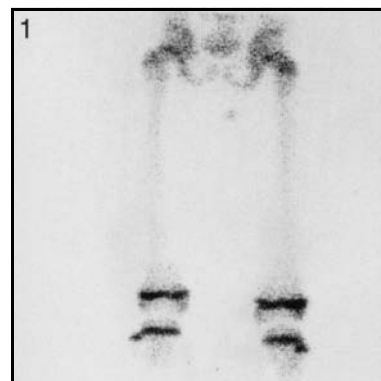


*FIG. 2. Posterior view of knees, tibia, fibula and ankles.*

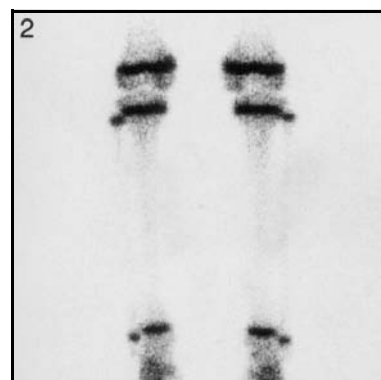
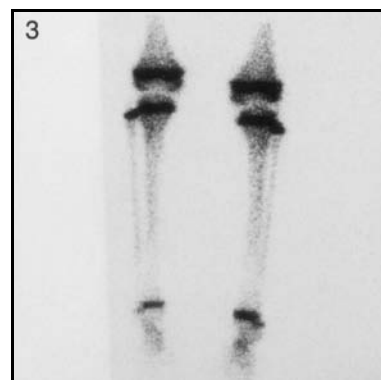


*FIG. 3. Posterior view of knees, tibia, fibula and ankles.*



### **Technical comments**

Note the good positioning of the feet, resulting in clear separation of the fibula from the tibia in Fig. 2.  
Note the different visualization of the ankles in Fig. 3. This is due to different positioning of the feet.

### **Potential pitfall**

Note the slight but definite increased activity in the mid-portion of the tibial shafts, best seen in Fig. 3. As the child grows, this will become more obvious and potentially confusing.

*FIG. 1. Posterior magnified view of knees.*

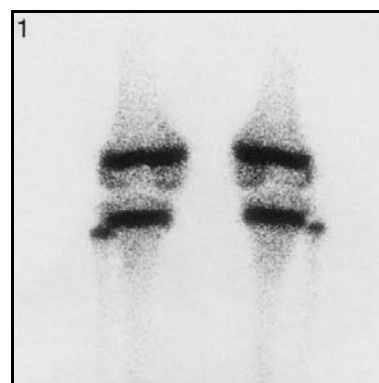


*FIG. 2. Posterior view of knees.*



**Technical comment**

Note the clear definition of the growth plate from the adjacent metaphyses.

**9: Age 6–7 years**

**Ankles and feet**

*FIG. 1. Anterior view of ankles and feet.*



*FIG. 2. Lateral view of feet.*



## **10. AGE 7–8 YEARS**





**10: Age 7–8 years**

**Blood pool images**

*FIG. 1. Posterior view of thorax and spine.*

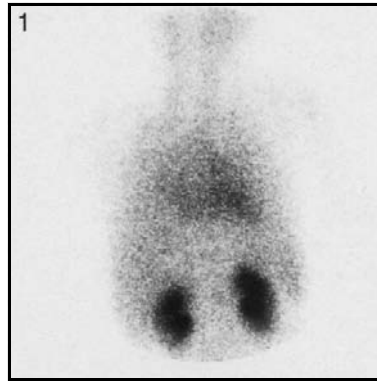


*FIG. 2. Posterior view of spine and pelvis.*

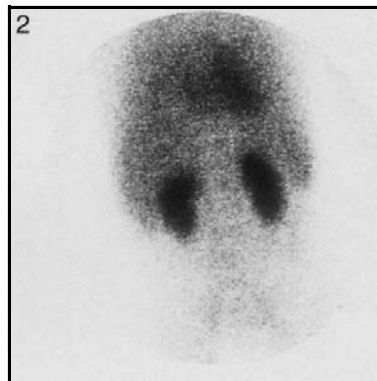


*FIG. 3. Anterior view of pelvis and femora.*

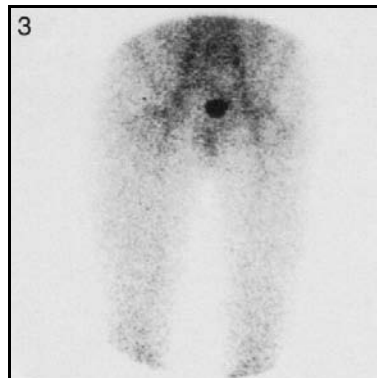
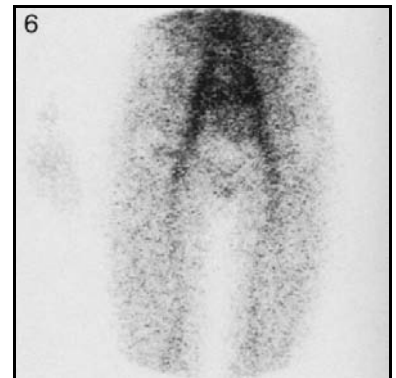


*FIG. 6. Anterior view of pelvis and femora.*



**10: Age 7–8 years**

**Blood pool images**

*FIG. 1. Anterior view of both hands.*

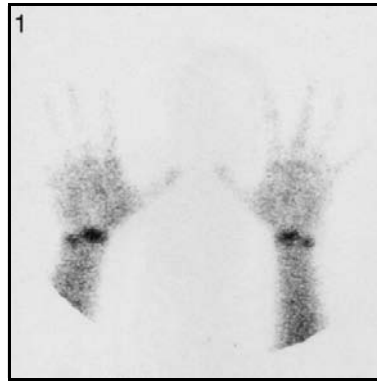


*FIG. 2. Anterior view of knees.*

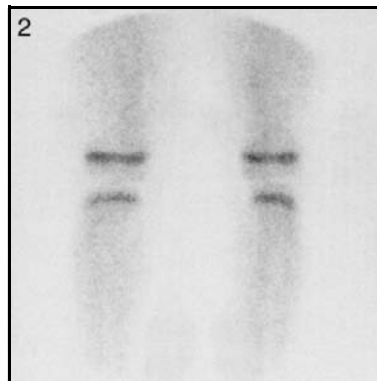


*FIG. 5. Posterior view of tibia and fibula.*

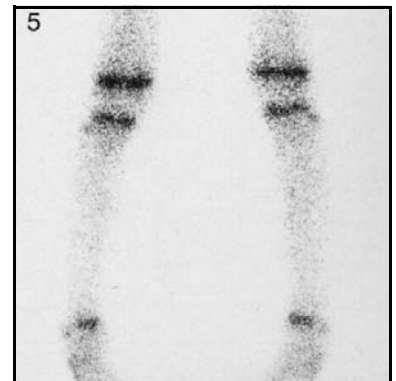


*FIG. 3. Lateral view of feet.*

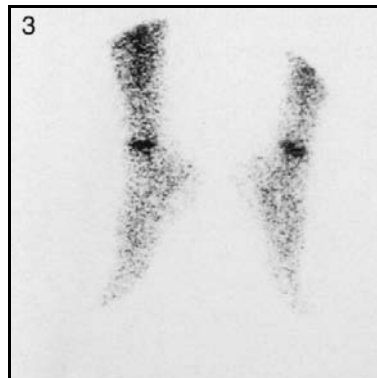


*FIG. 6. Lateral view of feet.*

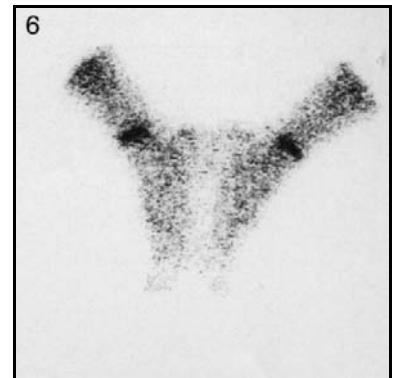


*FIG. 1. A double headed whole body gamma camera was used. Left image is anterior view; right image is posterior view.*



**Technical comments**

Distal end of the left upper limb is not seen due to a lead shield following the extravasation of isotope at the site of injection.

Marker on the right side.

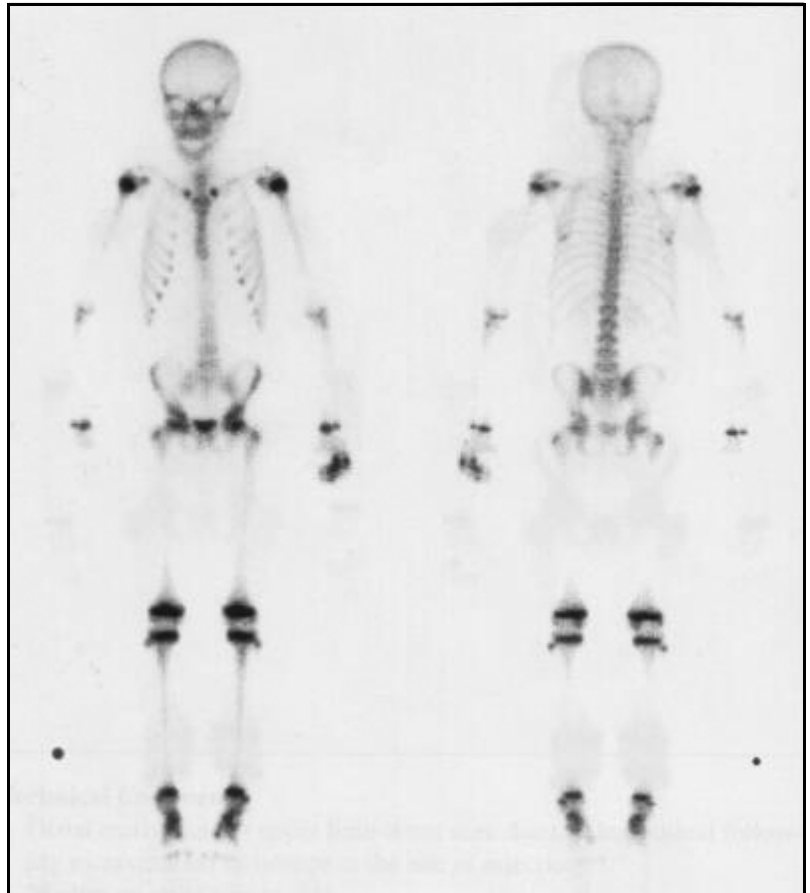
*FIG. 1. A double headed whole body gamma camera was used. Left image is anterior view; right image is posterior view.*



**Technical comments**

Note the extravasation of isotope at the site of injection in the left hand.  
Marker on the right side.

*FIG. 1. A double headed whole body gamma camera was used. Left image is anterior view; right image is posterior view.*



**Technical comments**

Note the extravasation of isotope at the site of injection in the child's left hand.  
Marker on the right side.

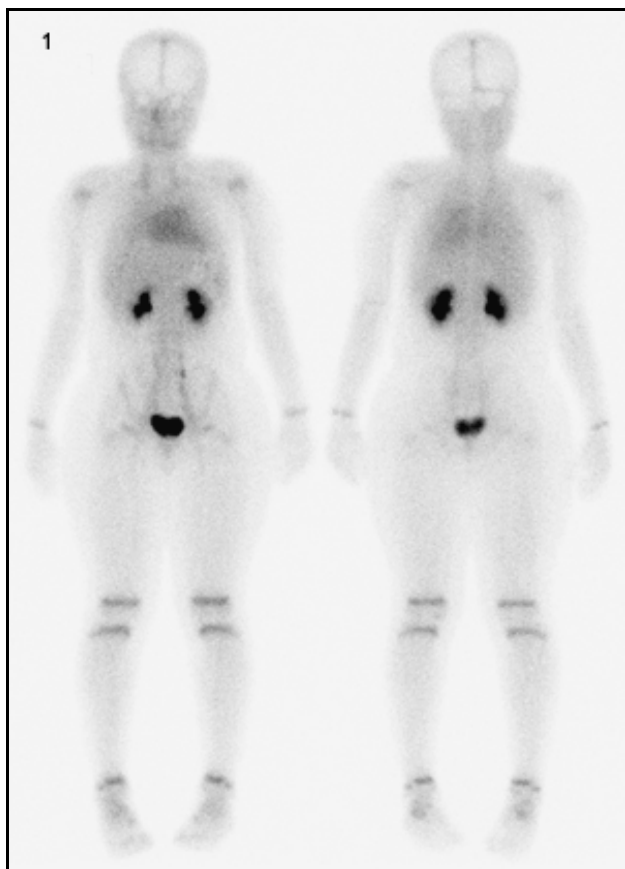


*FIG. 1. Whole body images of an 8-year-old male (40 kg body weight). Anterior and posterior blood pool whole body views.*



*FIG. 2. Whole body images of an 8-year-old male (40 kg body weight). Delayed anterior and posterior whole body bone scan.*

### Technical comments

A double headed digital whole body gamma camera equipped with high resolution low energy collimator was used and the energy window width set to 15%.

Immediately following the intravenous injection of 320 MBq (0.64, fraction of adult administered activity of 500 MBq) of  $^{99m}\text{Tc}$ -MDP, whole body blood pool imaging was started at a camera scanning speed of 17 cm/min. Delayed imaging was started 3 hours p.i. at a camera speed of 10 cm/min.

Note the appearance of the activity in the growing epiphyses of the upper and lower extremities.

*FIG. 1. Anterior view of skull and thorax.*

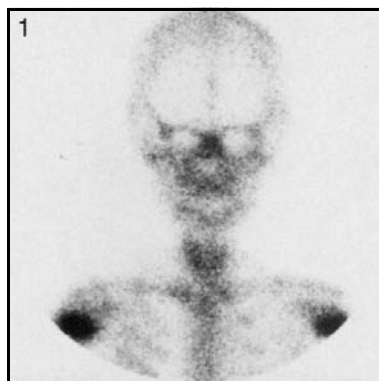


*FIG. 4. Posterior view of skull and thorax.*

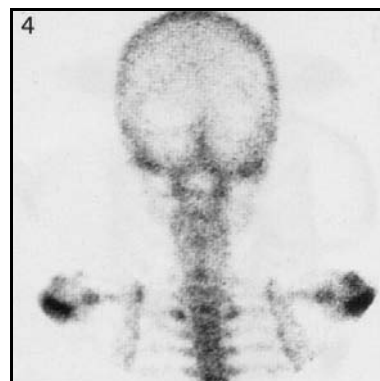


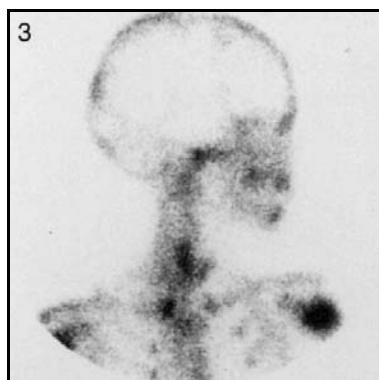
*FIG. 2. Right lateral view of skull and right upper limb.*



*FIG. 5. Left lateral view of skull and left upper limb.*



*FIG. 3. Right lateral view of skull and anterior view of thorax.*



### **Technical comments**

The coronal suture is clearly seen in Fig. 3. This is not the case in Figs 2 and 5. The thyroid gland is seen in Figs 1 and 3 owing to free  $^{99m}\text{TC}$ -pertechnetate. The lateral views of the skull (Figs 2 and 5) were taken posteriorly.

*FIG. 1. Right lateral view of skull and right upper limb.*



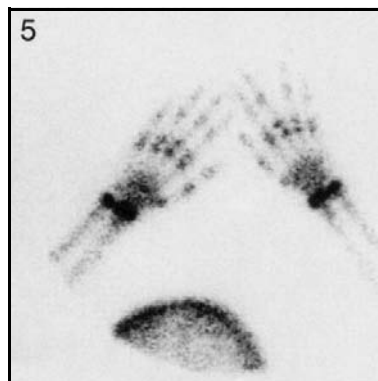
*FIG. 4. Left lateral view of skull and left upper limb.*



*FIG. 2. Anterior view of upper limbs and hands.*



*FIG. 5. Anterior view of hands.*



**Technical comments**

The hands in Fig. 5 are poorly positioned compared with those shown in Fig. 2.

The lateral views of the skull (Figs 1 and 4) were taken posteriorly.

Note that part of the occipital bone in Fig. 4 has been excluded from the field of view.



## 10: Age 7–8 years

## Thorax, spine and pelvis

*FIG. 1. Anterior view of thorax, spine and pelvis.*

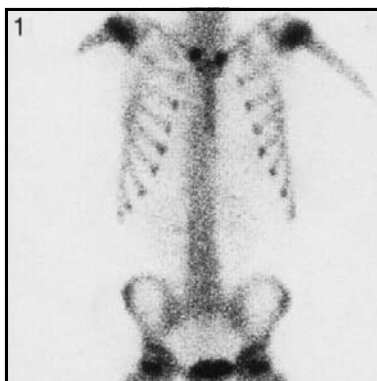


*FIG. 4. Anterior view of thorax and spine.*

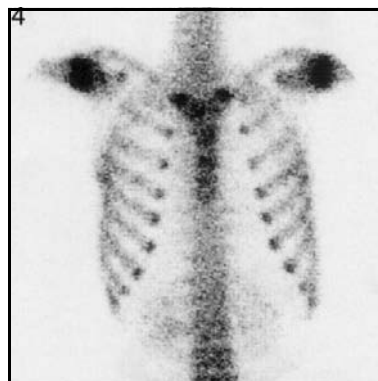


*FIG. 2. Anterior view of thorax and spine.*

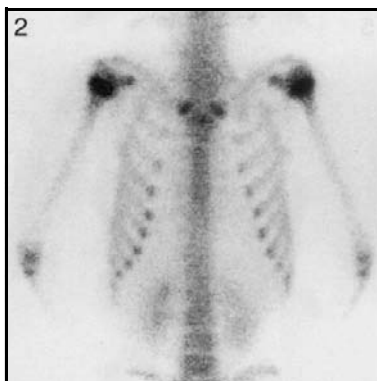
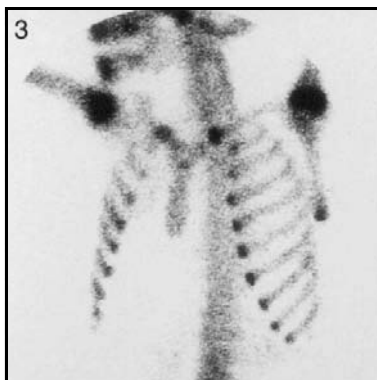


*FIG. 3. Left anterior oblique view of thorax.*



### Technical comments

Note the clarity of the lumbar spine, especially in Fig. 2.

The sternum is best seen with slight obliquity of the thoracic cage, as in Figs 1 and 3.

**10: Age 7–8 years**

**Thorax, spine and pelvis**

*FIG. 1. Posterior view of thorax and spine.*

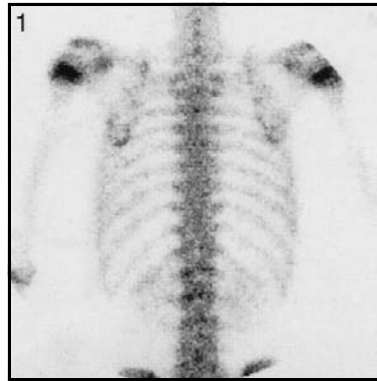


*FIG. 4. Posterior view of thorax and spine.*

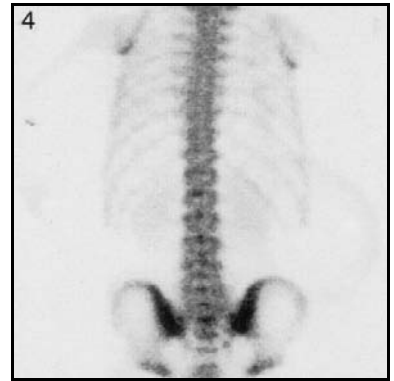


*FIG. 2. Posterior view of thorax, spine and pelvis.*

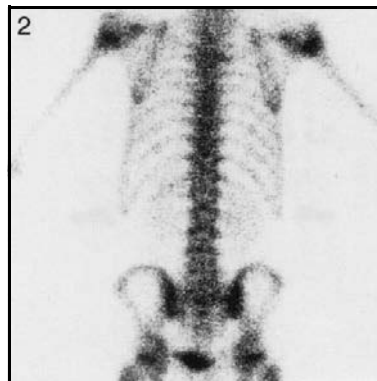
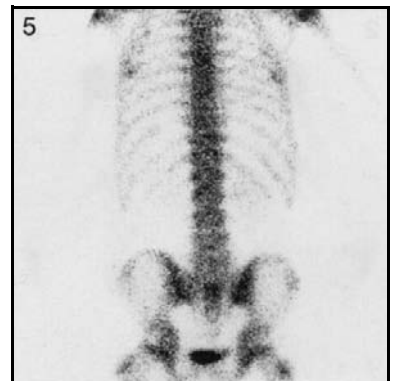


*FIG. 5. Posterior view of thorax, spine and pelvis.*



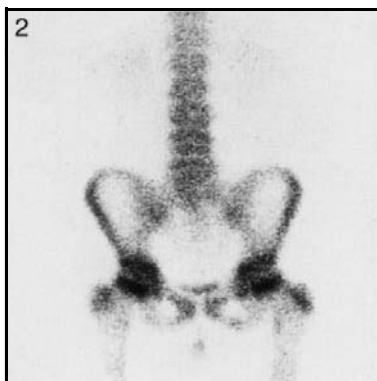
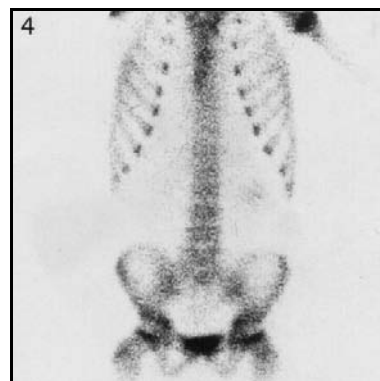
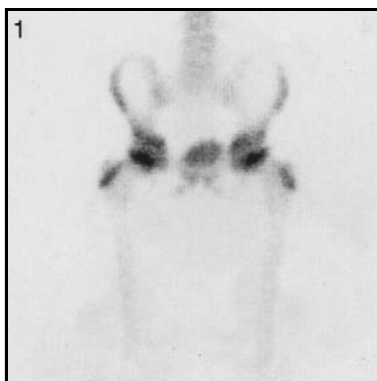
## 10: Age 7–8 years

## Thorax, spine, pelvis and femora

*FIG. 1. Anterior view of pelvis and femora.*

*FIG. 4. Anterior view of thorax, spine and pelvis.*

*FIG. 2. Anterior view of spine and femora.*



### Technical comments

Note that the bladder is virtually empty in all the images.  
Urine contamination below the pelvis is seen in Fig. 2.

## 10: Age 7–8 years

## Spine, pelvis and femora

*FIG. 1. Posterior view of spine, pelvis and femora.*

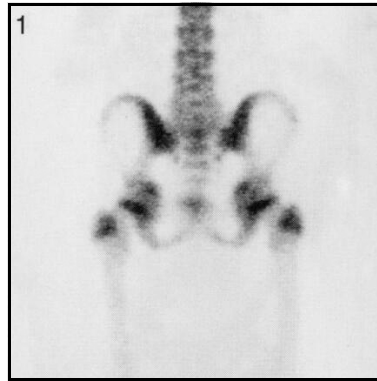


*FIG. 4. Posterior view of spine and pelvis.*

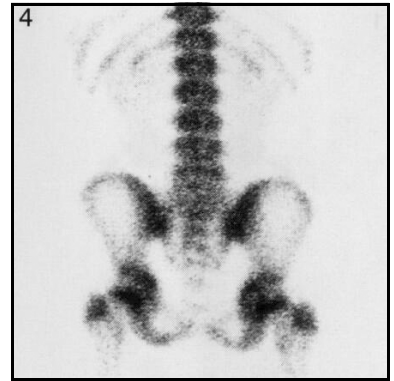


*FIG. 2. Posterior view of pelvis and femora.*



### Technical comment

Urine contamination below the pelvis is seen in Fig. 2.

*FIG. 1. Pinhole view of right hip.*

*FIG. 4. Pinhole view of left hip.*

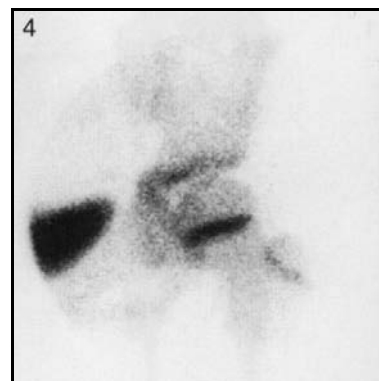
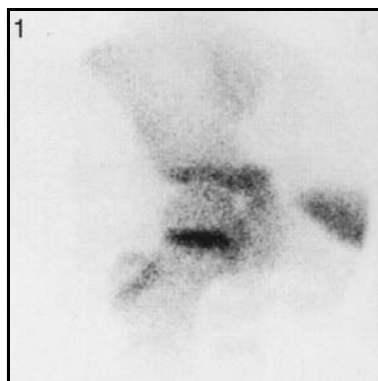


*FIG. 1. Posterior view of femora and knees.*



*FIG. 4. Posterior view of hips, femora and knees.*



*FIG. 2. Posterior view of tibia, fibula and ankles.*

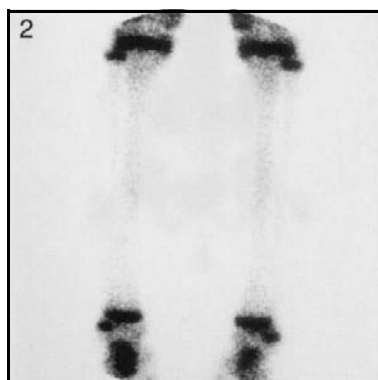
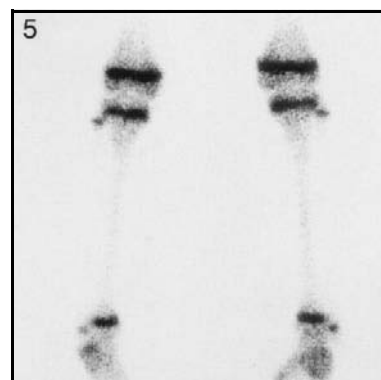


*FIG. 5. Posterior view of knees, tibia, fibula and ankles.*



### **Technical comments**

Note the clarity and the separation of the epiphysis of the fibula from the tibia due to the good positioning of the feet. This is not true for the left knee in Fig. 1, especially when compared with the right knee.

Urine contamination below the pelvis is seen in Fig. 1.

*FIG. 1. Posterior magnified view of knees.*

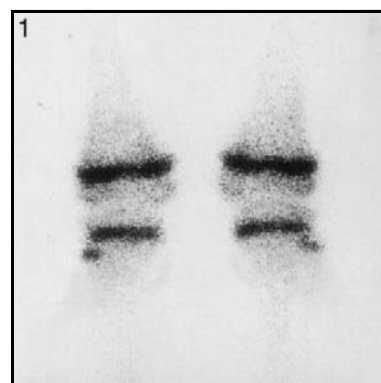


*FIG. 2. Posterior magnified view of knees.*

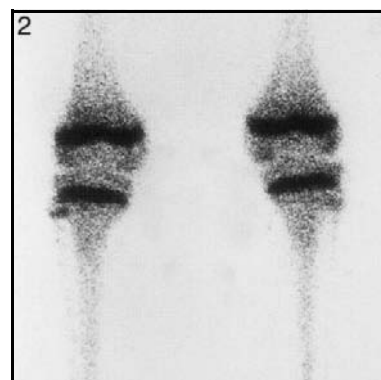
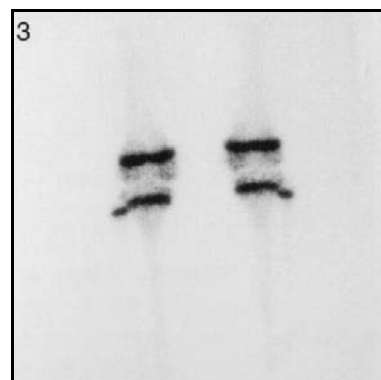


*FIG. 3. Posterior view of knees.*



**Technical comment**

There is clear separation between the upper tibia and the fibula due to good positioning of the feet in all images, apart from the right knee in Fig. 2 where the fibula cannot be clearly seen.

**10: Age 7–8 years**

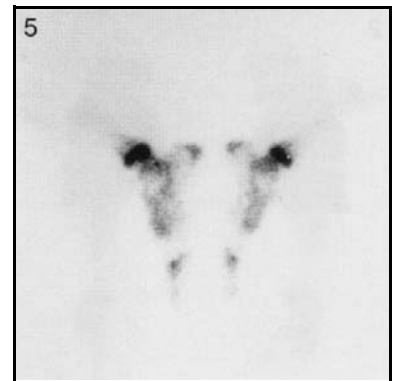
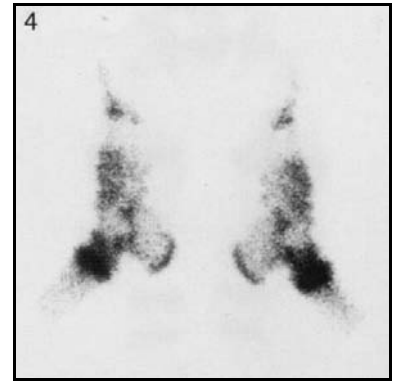
**Ankles and feet**

*FIG. 1. Posterior view of feet.*

*FIG. 4. Lateral view of feet.*

*FIG. 2. Posterior view of feet.*

*FIG. 5. Lateral view of feet.*





## **11. AGE 8–9 YEARS**



**11: Age 8–9 years**

**Blood pool images**

*FIG. 1. Anterior view of pelvis.*

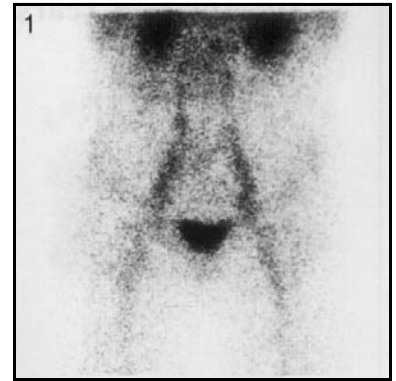


*FIG. 2. Posterior view of knees.*

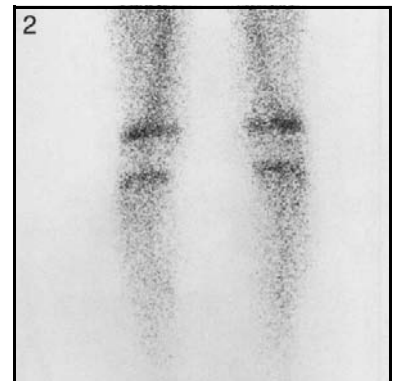


*FIG. 3. Anterior view of tibia, fibula and feet.*

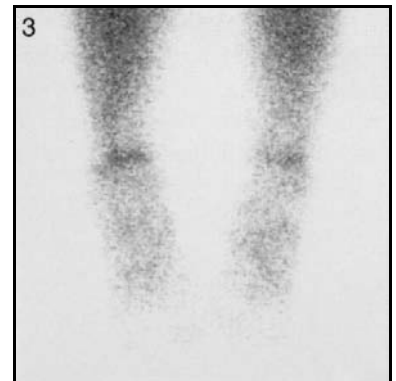


*FIG. 1. A double headed whole body gamma camera was used. Left image is anterior view; right image is posterior view.*



**Technical comments**

Note in the posterior view the difference between the two straight sinuses, with more isotope entering the right than the left. This is a variation of normality.

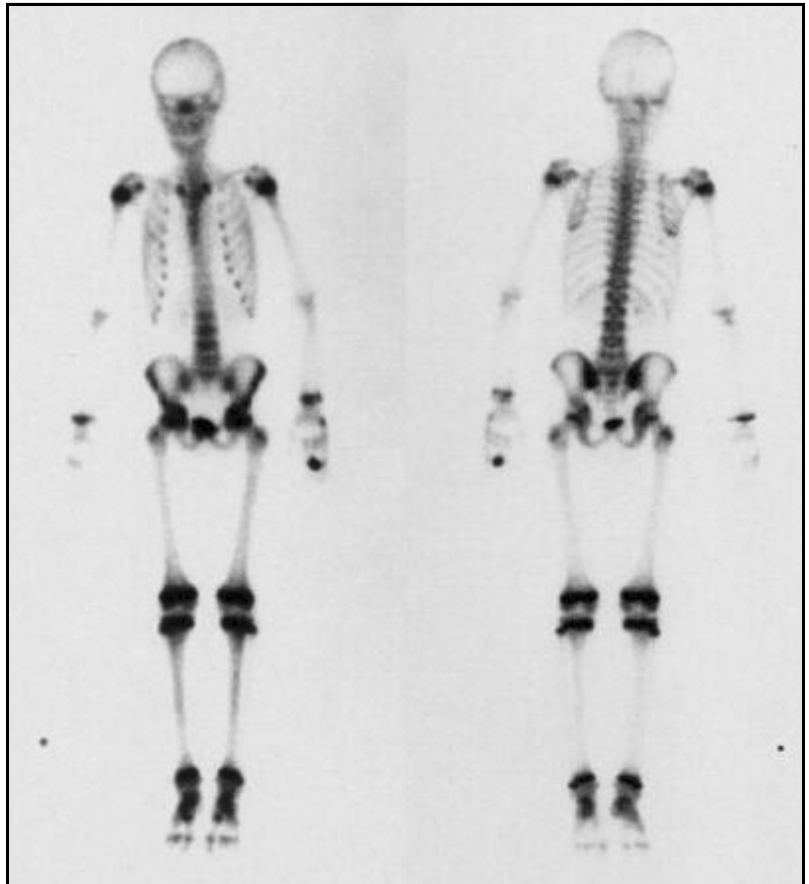
Note the extravasation of isotope at the site of injection in the right hand.

Marker on the right.

**Potential pitfall**

Focal increased uptake of isotope is seen in the anterior view in the region of the maxillary sinus. This is probably due to sinusitis.

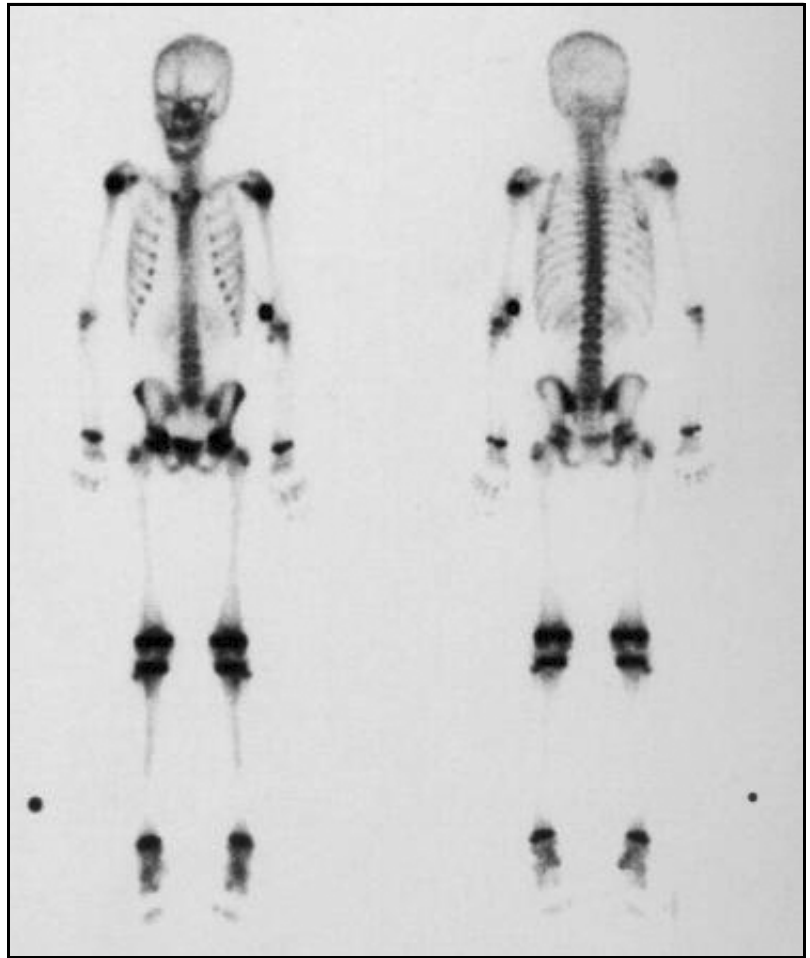
*FIG. 1. A double headed whole body gamma camera was used. Left image is anterior view; right image is posterior view.*



**Technical comments**

Note the extravasation of isotope at the site of injection in the left hand.  
Marker on the right side.

*FIG. 1. A double headed whole body gamma camera was used. Left image is anterior view; right image is posterior view.*



**Technical comments**

The child's head is rotated, causing asymmetry, especially to the facial bones.  
Note the extravasation of isotope at the site of injection in the left elbow.  
Marker on the right side.

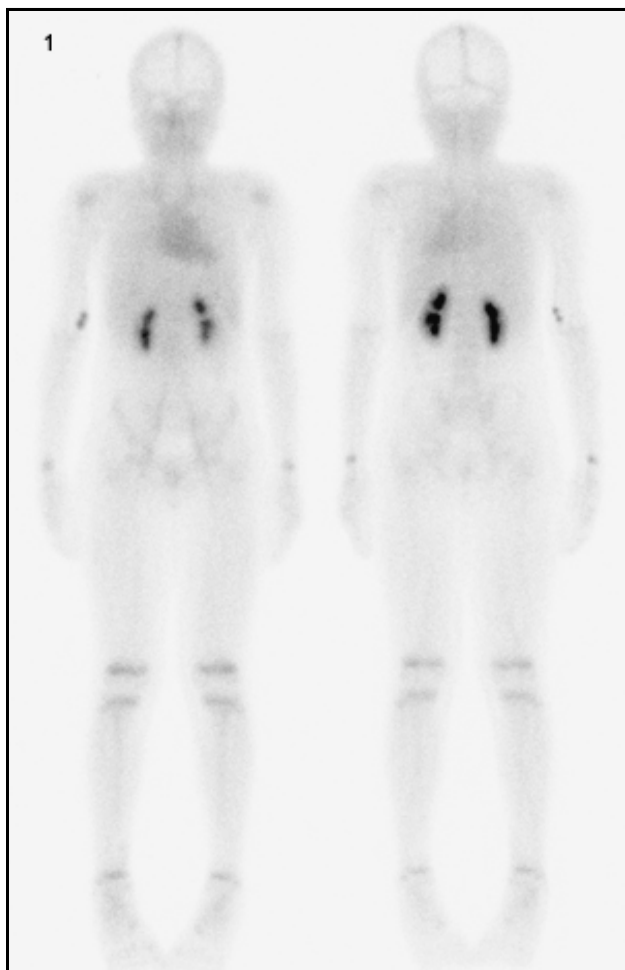


*FIG. 1. Whole body images of a 9-year-old male (38 kg body weight). Anterior and posterior blood pool whole body views.*

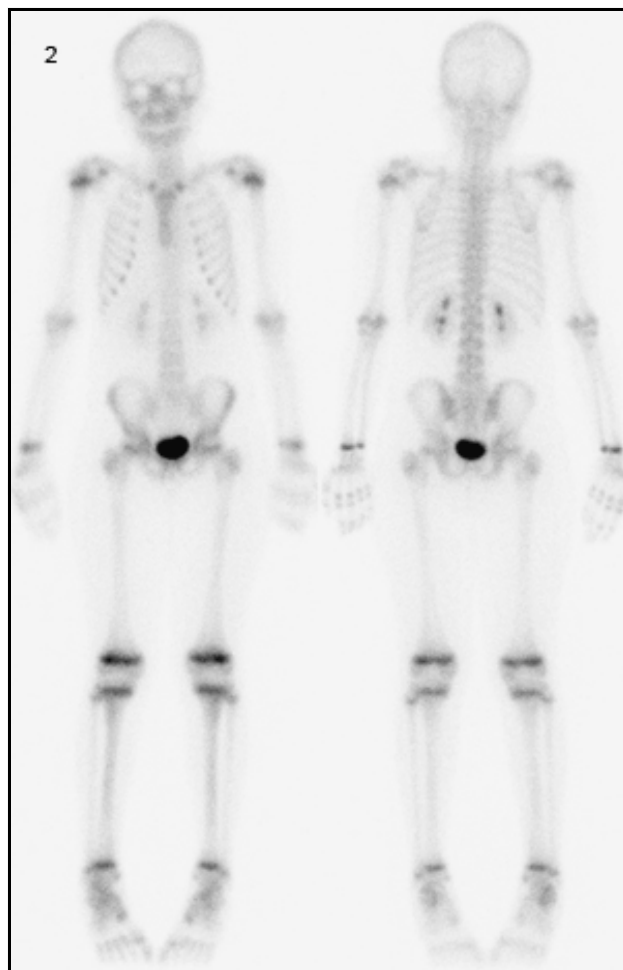


*FIG. 2. Whole body images of a 9-year-old male (38 kg body weight). Delayed anterior and posterior whole body bone scan.*

### Technical comments

A double headed digital whole body gamma camera equipped with high resolution low energy collimator was used and the energy window width set to 15%.

Immediately following the intravenous injection of 320 MBq (0.64, fraction of adult administered activity of 500 MBq) of  $^{99m}\text{Tc}$ -MDP, whole body blood pool imaging was started at a camera scanning speed of 19.5 cm/min. Delayed imaging was started 3 hours p.i. at a camera speed of 11 cm/min.

Note the appearance of the activity in the growing epiphyses of the upper and lower extremities.

## 11: Age 8–9 years

## Skull and thorax

*FIG. 1. Anterior view of skull and thorax.*

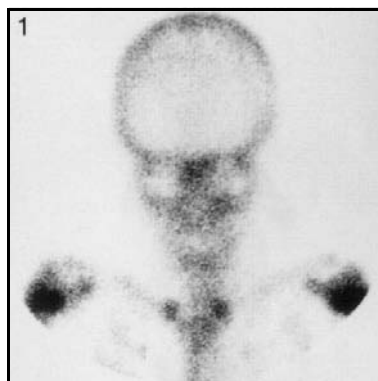


*FIG. 4. Posterior view of skull and thorax.*

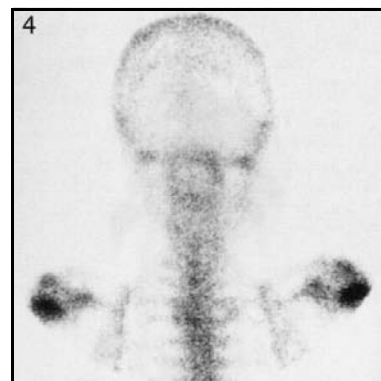


*FIG. 2. Right lateral view of skull.*

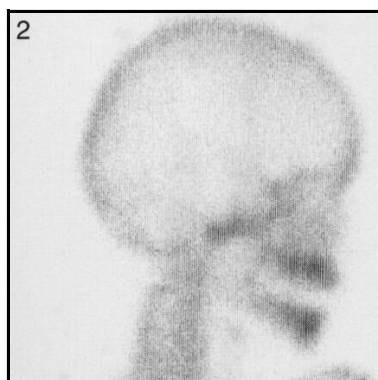


*FIG. 5. Left lateral view of skull.*

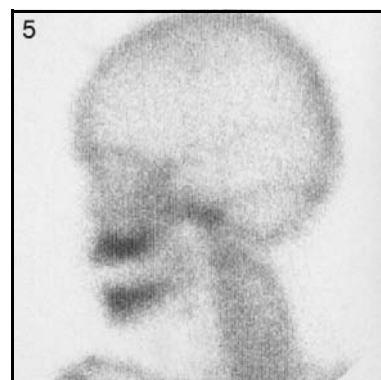
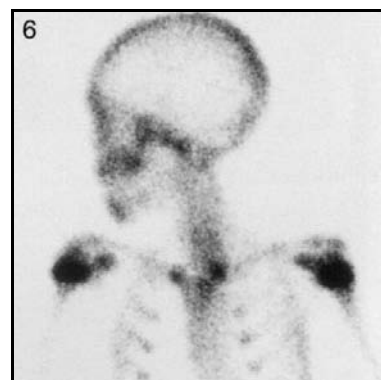


*FIG. 6. Left lateral view of skull and anterior view of thorax.*



### Technical comments

Note the sternoclavicular joints in Figs 1 and 6. The asymmetry of the joints is due to the rotation of the patient. The lateral views of the skull (Figs 2 and 5) were taken anteriorly.



*FIG. 1. Anterior view of hands.*

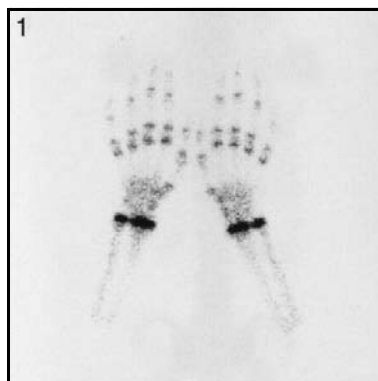


*FIG. 4. Anterior view of hands and upper limbs.*

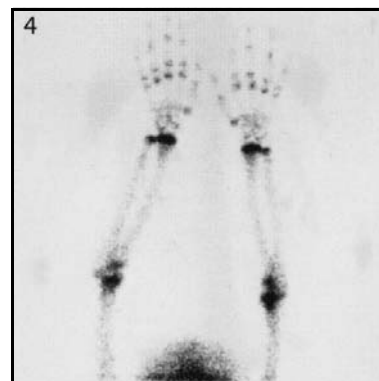


*FIG. 1. Anterior view of thorax and spine.*

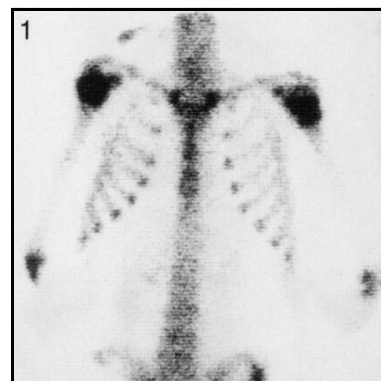


*FIG. 2. Anterior view of thorax and spine.*

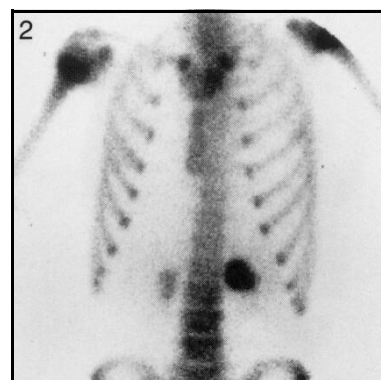
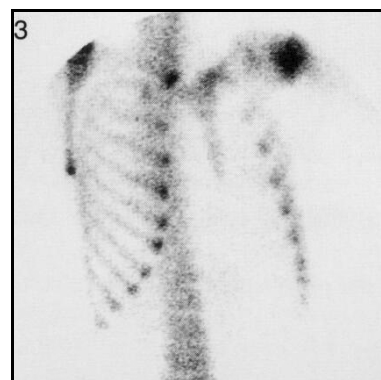


*FIG. 3. Right anterior oblique view of thorax.*



**Technical comments**

The lumbar spine in Fig. 2 is clearly seen.

The asymmetry of the sternoclavicular joints shown in Fig. 2 is due to slight rotation.

Note the abnormal accumulation of the isotope in a dilated left renal pelvis in Fig. 2.

*FIG. 1. Posterior view of thorax, spine and upper pelvis.*

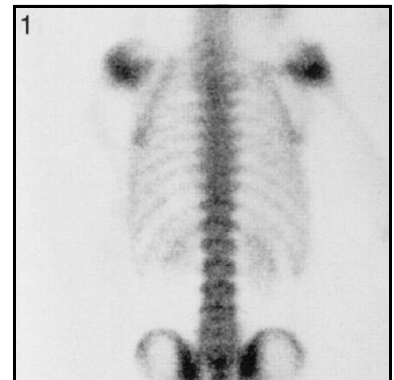
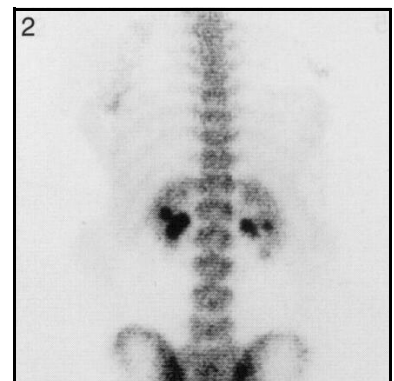


*FIG. 2. Posterior view of thorax, spine and upper pelvis.*



**Potential pitfall**

The tracer is seen in abnormal calyces and the renal pelvis of both kidneys in Fig. 2.

## 11: Age 8–9 years

## Spine, pelvis and femora

*FIG. 1. Anterior view of spine, pelvis and femora.*



*FIG. 4. Anterior view of spine, pelvis and femora.*

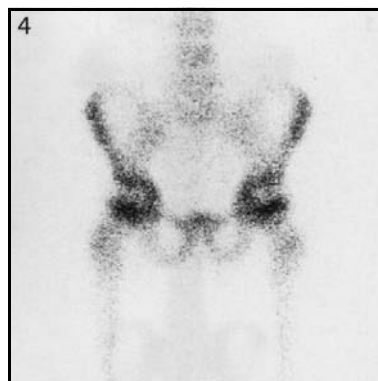


*FIG. 2. Anterior view of spine and pelvis.*

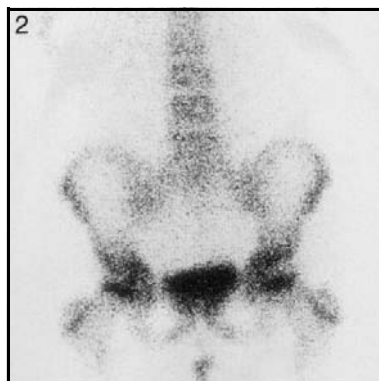
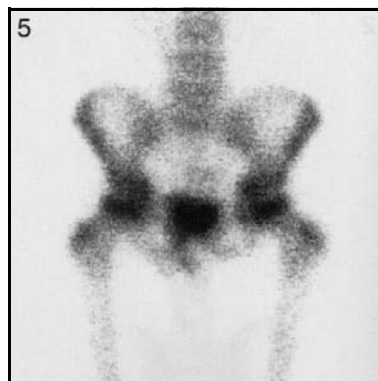


*FIG. 5. Anterior view of spine, pelvis and femora.*



### Technical comment

Urine contamination below the pelvis is seen in Figs 1, 2 and 5.

## 11: Age 8–9 years

## Spine, pelvis and femora

*FIG. 1. Posterior view of spine, pelvis and femora.*



*FIG. 4. Posterior view of spine and pelvis.*

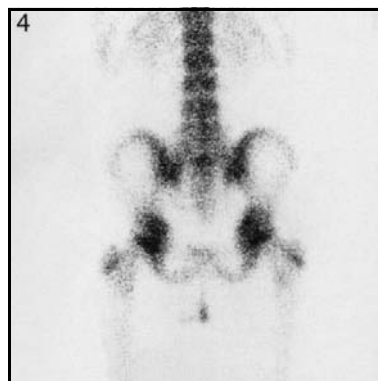


*FIG. 2. Posterior view of spine, pelvis and femora.*

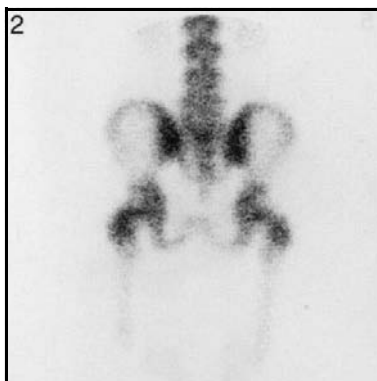


*FIG. 3. Pelvic inlet view. This view is infrequently used in paediatrics.*



### Technical comment

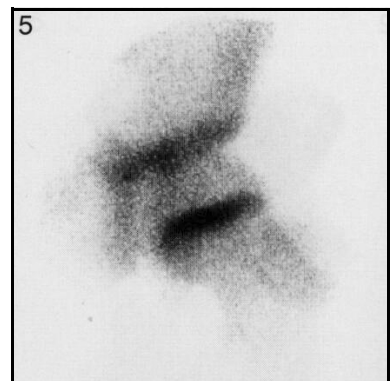
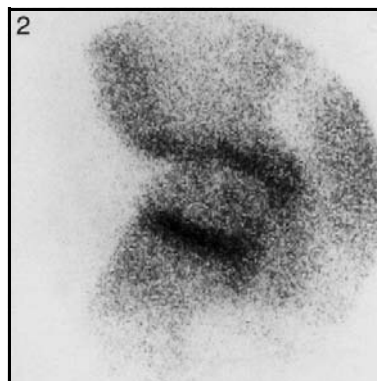
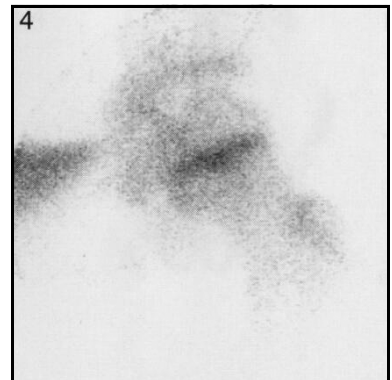
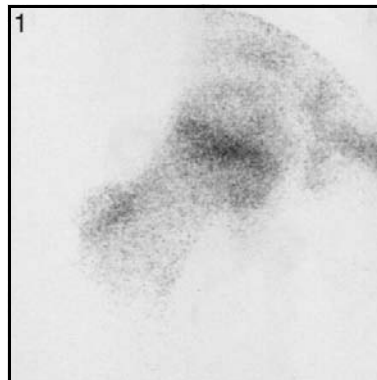
Urine contamination below the pelvis is seen in Figs 3 and 4.

*FIG. 1. Pinhole view of right hip.*

*FIG. 4. Pinhole view of left hip.*

*FIG. 2. Pinhole view of right hip.*

*FIG. 5. Pinhole view of left hip.*



**Technical comment**

Figures 2 and 5 show a change in magnification, creating an apparent difference in the sizes of the two hips.

*FIG. 1. Posterior view of femora and knees.*

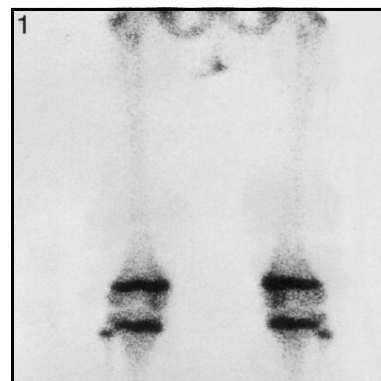
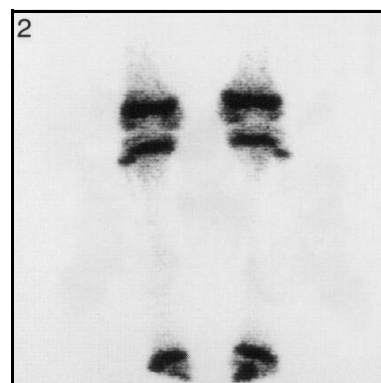


*FIG. 2. Posterior view of knees, tibia and fibula.*



**Technical comment**

Urine contamination below the pelvis is seen in Fig. 1.

FIG. 1. Posterior view of knees.



FIG. 4. Anterior view of knees.

FIG. 2. Medial lateral view of left knee.

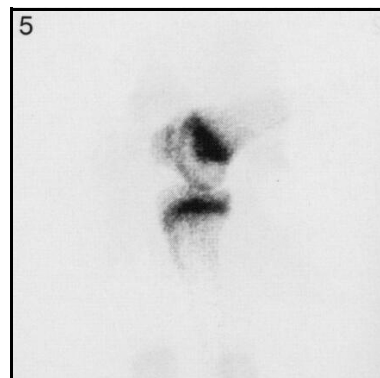
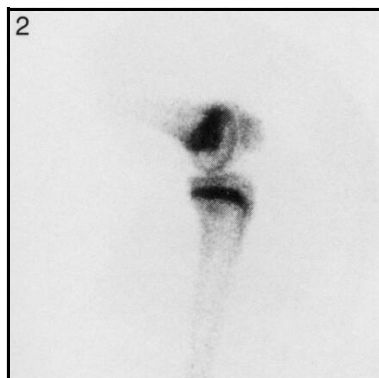


FIG. 5. Medial lateral view of right knee.

FIG. 3. Lateral lateral view of right knee.

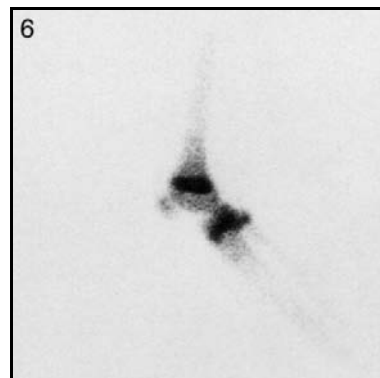
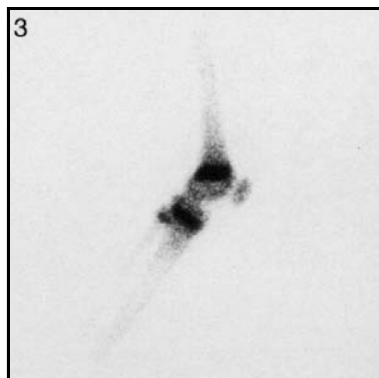


FIG. 6. Lateral lateral view of left knee.

### Technical comment

The pair of lateral knees in Figs 2 and 5 represents the medial lateral knees, while Figs 3 and 6 represent lateral knees in lateral projection. This accounts for the clarity of the fibula in the lower series and the difficulties in seeing the fibula in the upper series.



## 11: Age 8–9 years

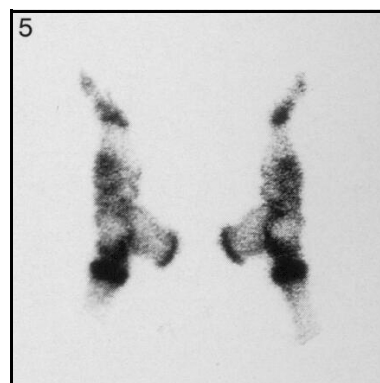
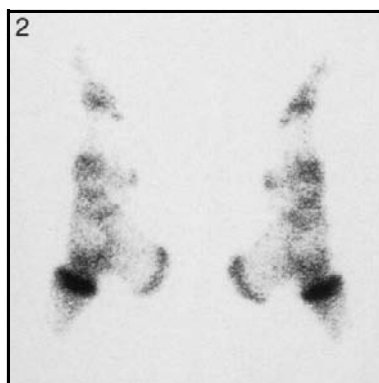
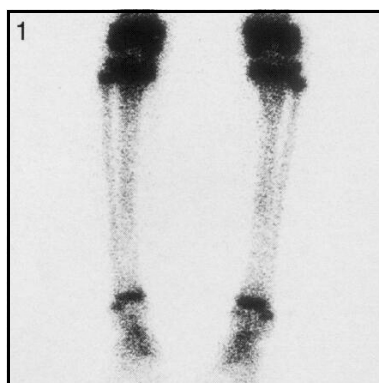
## Tibia, fibula, ankles and feet

*FIG. 1. Posterior view of tibia, fibula and ankles.*

*FIG. 4. Posterior view of feet.*

*FIG. 2. Lateral view of feet.*

*FIG. 5. Lateral view of feet.*



### Potential pitfalls

Note the slightly increased activity in the mid-shaft of the tibia is more marked in the right than in the left in Fig. 1. This is a variation of normality.

The lack of clarity of the epiphyseal plates around the knees in Fig. 1 is due to overexposure during acquisition.



## **12. AGE 9–10 YEARS**



## 12: Age 9–10 years

## Blood pool images

*FIG. 1. Anterior view of thorax, spine and pelvis.*

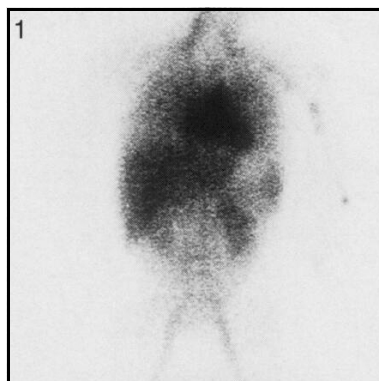


*FIG. 4. Posterior view of thorax and spine.*

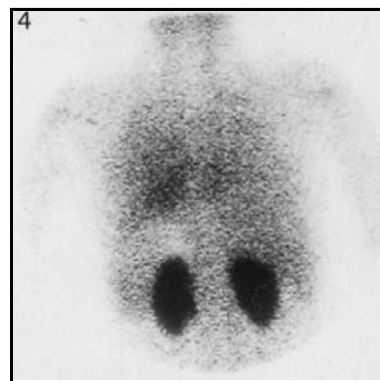


*FIG. 2. Anterior view of pelvis and femora.*

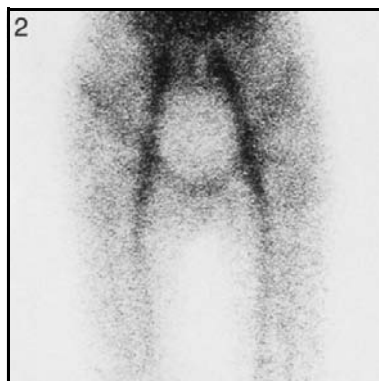


*FIG. 5. Posterior view of pelvis and femora.*

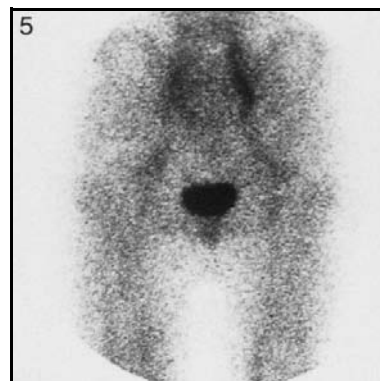
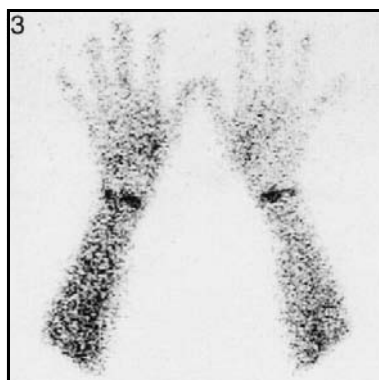


*FIG. 3. Anterior view of hands.*



### Technical comments

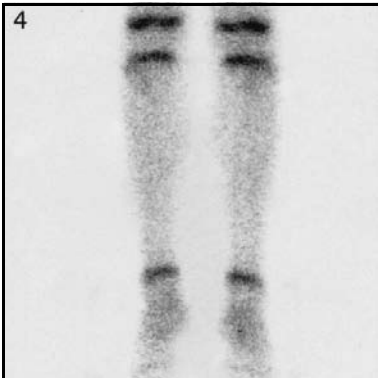
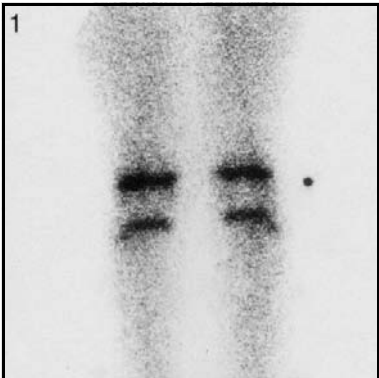
Figure 2 shows a photon deficient area which is due to a bladder full of urine at the time of injection of the radiotracer.

The photon deficient area above the kidney in Figs 1 and 4 is due to a full stomach.

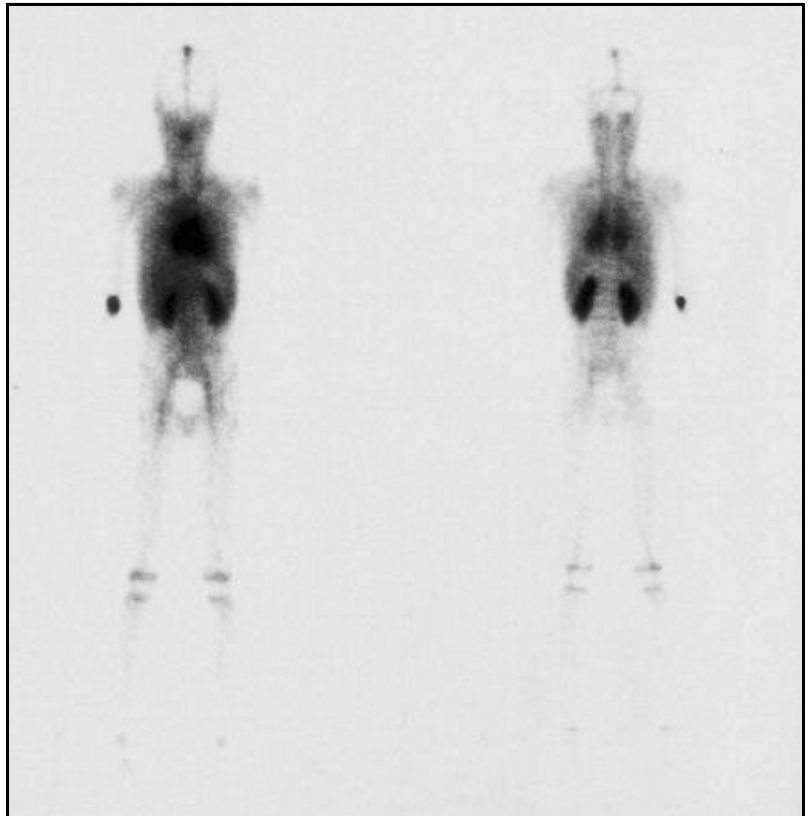
FIG. 1. Posterior view of knees.

FIG. 4. Anterior view of knees, tibia and ankles.

FIG. 2. Posterior view of feet.



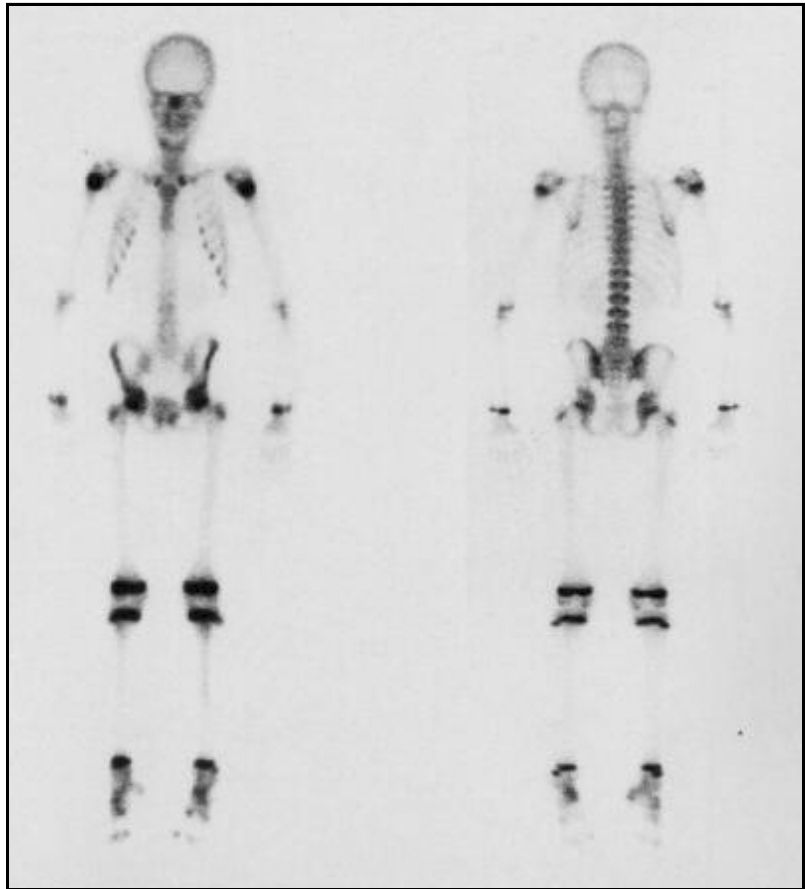
*FIG. 1. A double headed whole body gamma camera was used. Left image is anterior view; right image is posterior view.*



**Technical comments**

Note the extravasation of isotope at the site of injection in the right elbow.  
The photon deficient area in the anterior view is due to a bladder full of urine at the time of injection of radiotracer.  
Marker on the right side.

*FIG. 1. A double headed whole body gamma camera was used. Left image is anterior view; right image is posterior view.*



**Technical comments**

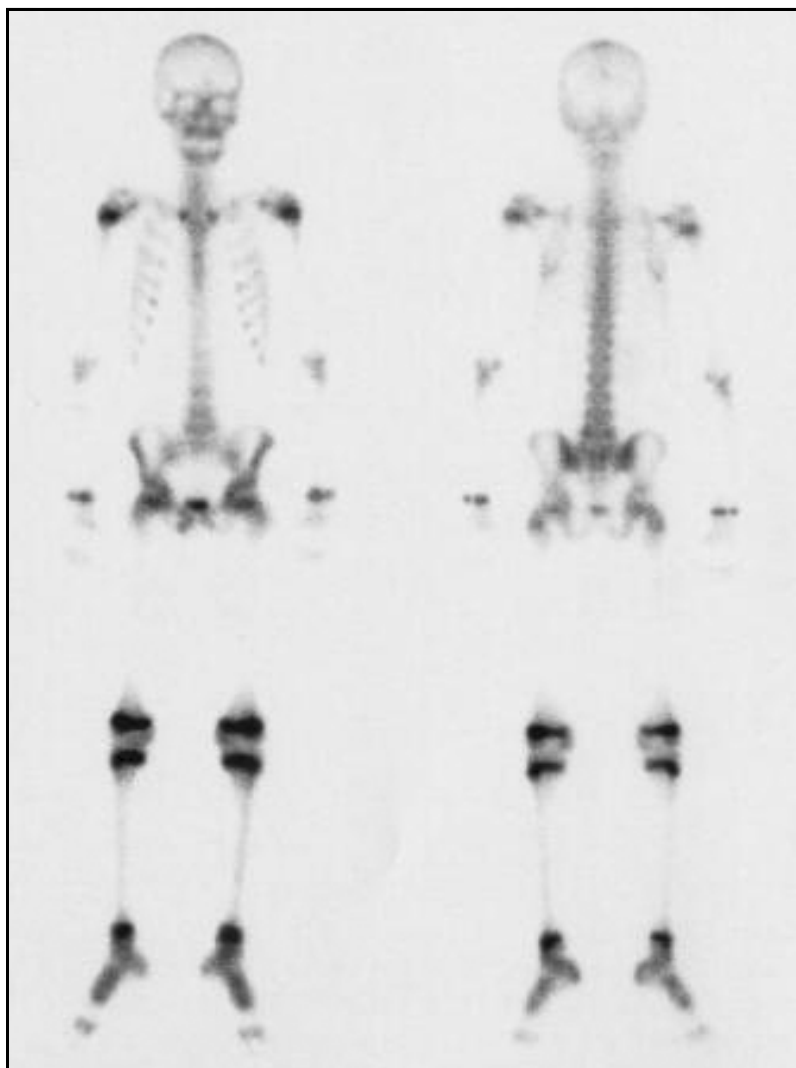
There is better positioning of the left foot, with the toes turned inwards compared with the right foot. The consequently improved images of the left knee are noted.

The child's pelvis is rotated, causing asymmetry.

Marker on the right side, posterior view only.



*FIG. 1. A double headed whole body gamma camera was used. Left image is anterior view; right image is posterior view.*



**Technical comment**

There is poor positioning of the feet, with the toes turned outwards.

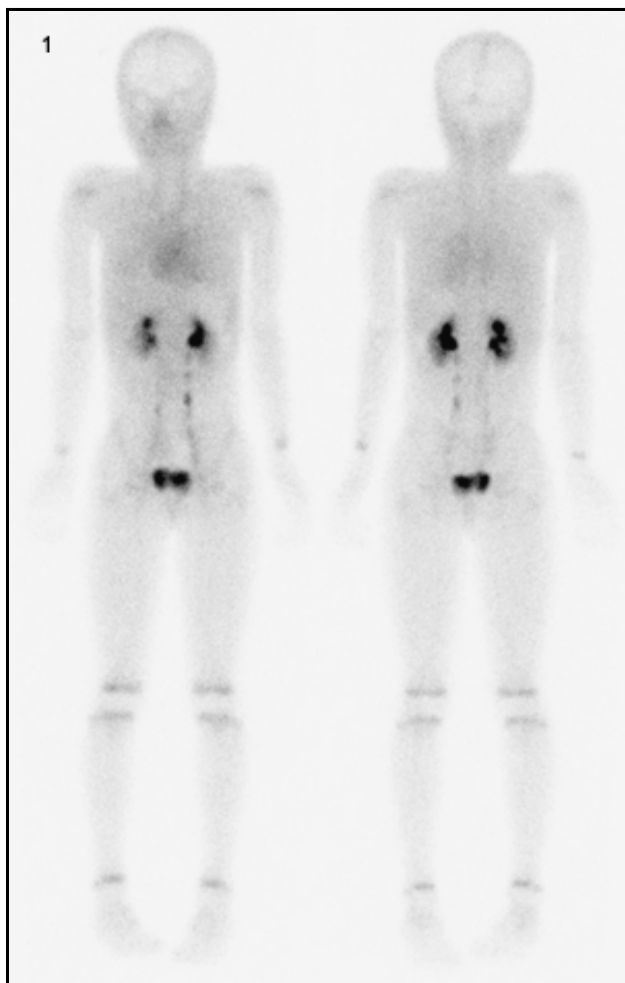


*FIG. 1. Whole body images of a 10-year-old female (20 kg body weight, height 140 cm). Anterior and posterior blood pool whole body views.*



*FIG. 2. Whole body images of a 10-year-old female (20 kg body weight, height 140 cm). Delayed anterior and posterior whole body bone scan.*

#### Technical comments

A double headed digital whole body gamma camera equipped with a high resolution low energy collimator was used and the energy window width set to 15%.

Immediately following the intravenous injection of 2600 MBq (0.52, fraction of adult administered activity of 500 MBq) of  $^{99m}\text{Tc}$ -MDP, whole body blood pool imaging was started at a camera scanning speed of 19.5 cm/min. Delayed imaging was started 3 hours p.i. at a camera speed of 11 cm/min.

Note the appearance of the activity in the growing epiphyses of the upper and lower extremities.

## 12: Age 9–10 years

## Skull, thorax and upper limbs

*FIG. 1. Anterior view of skull and thorax.*

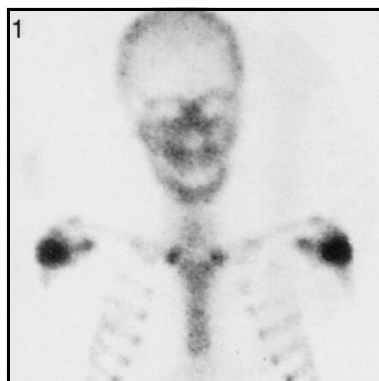


*FIG. 4. Posterior view of skull and thorax.*

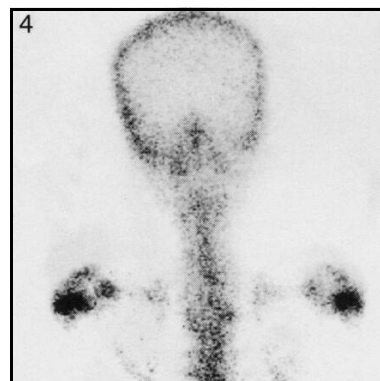


*FIG. 2. Right lateral view of skull and right upper limb.*

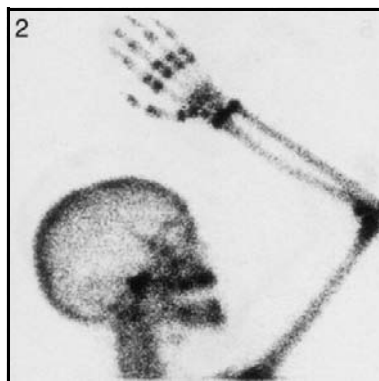
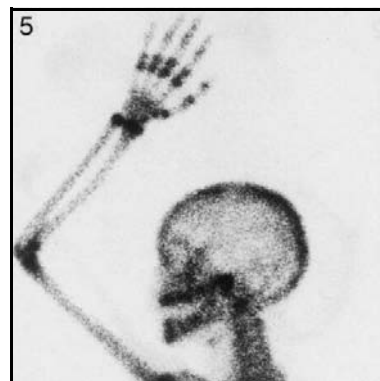


*FIG. 5. Left lateral view of skull and left upper limb.*



### Technical comments

Note the slightly increased activity in the right maxillary region in Fig. 1. This is due to rotation of the head. The lateral views of the skull (Figs 2 and 5) were taken posteriorly.

## 12: Age 9–10 years

## Skull, thorax and upper limbs

*FIG. 1. Anterior view of skull and thorax.*

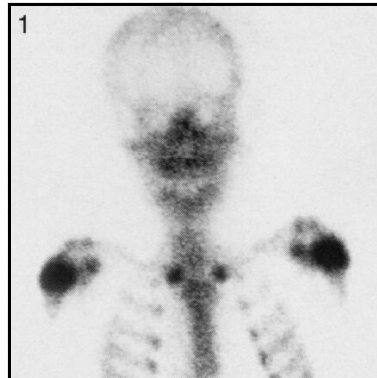


*FIG. 2. Right lateral view of skull and right upper limb.*

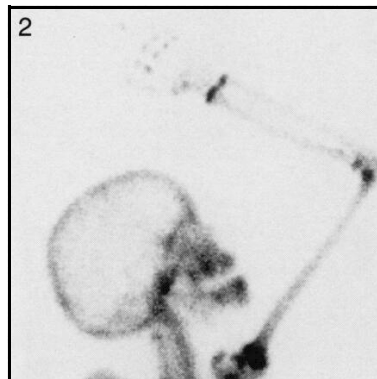


*FIG. 5. Left lateral view of skull and left upper limb.*



### Technical comment

The lateral views of the skull (Figs 2 and 5) were taken posteriorly.

*FIG. 1. Anterior view of right hemithorax and right upper limb.*

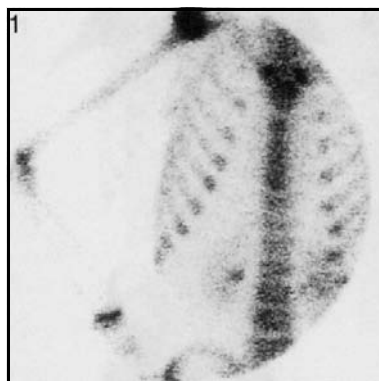


*FIG. 4. Anterior view of left hemithorax and left upper limb.*

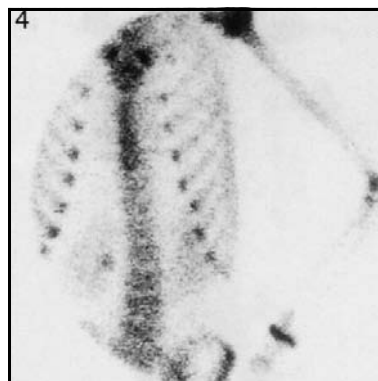


*FIG. 2. Right anterior oblique view of thorax.*



*FIG. 5. Left anterior oblique view of thorax.*



**Technical comments**

Figures 1 and 4 illustrate the difficulty in obtaining good images of the upper limbs with the anterior thoracic views. The upper limbs should be imaged at the same time as the lateral skull images. Retention of the tracer is noted in the detailed right renal pelvis in Fig. 2.

## 12: Age 9–10 years

## Thorax, spine and pelvis

*FIG. 1. Anterior view of thorax, spine and upper pelvis.*

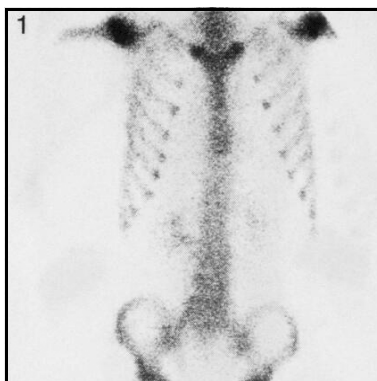


*FIG. 4. Anterior view of thorax, spine and pelvis.*

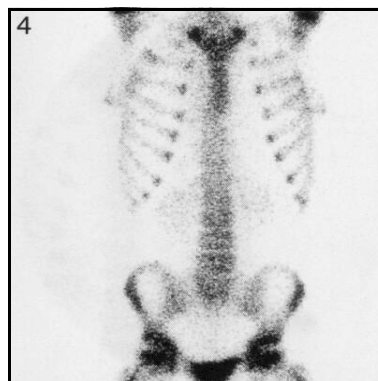


*FIG. 2. Anterior view of thorax, spine and upper pelvis.*

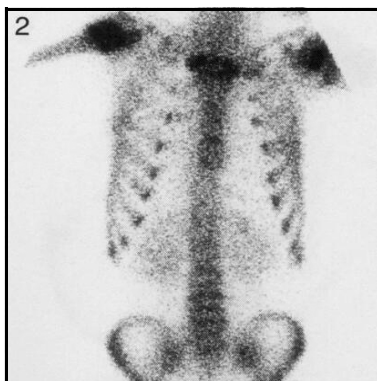
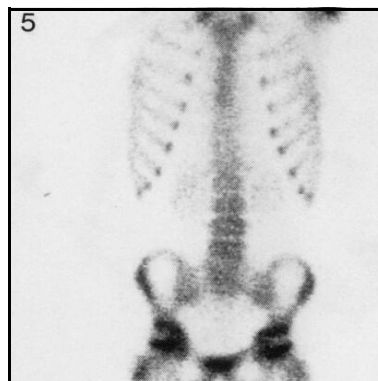


*FIG. 5. Anterior view of thorax, spine and pelvis.*



### Technical comment

The lower lumbar spine is clearly seen in the anterior views in Figs 2, 4 and 5.

## 12: Age 9–10 years

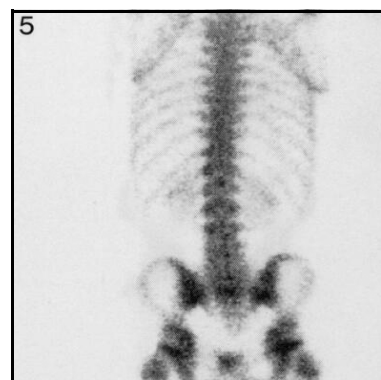
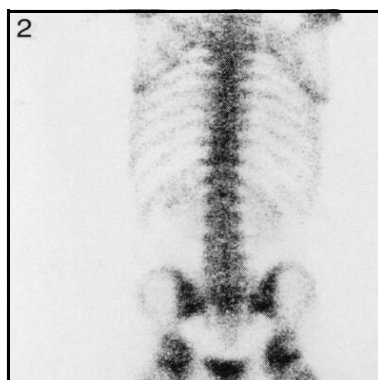
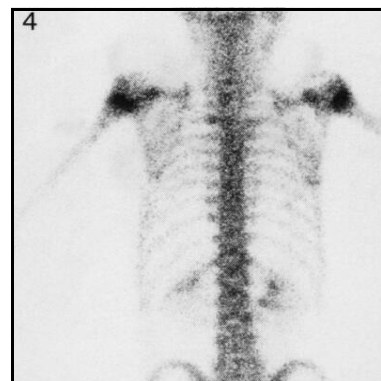
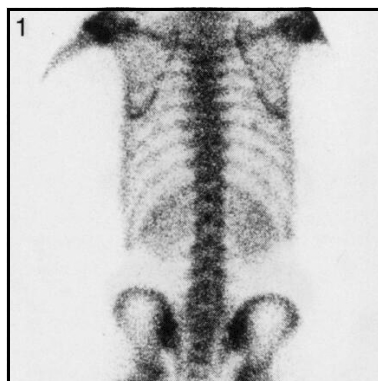
## Thorax, spine and pelvis

*FIG. 1. Posterior view of thorax, spine and upper pelvis.*

*FIG. 4. Posterior view of thorax and spine.*

*FIG. 2. Posterior view of thorax, spine and pelvis.*

*FIG. 5. Posterior view of thorax, spine and pelvis.*



### Technical comment

The scapula is clearly seen in all images. The differences are due to the varying positions of the upper limbs.

### Potential pitfall

The focal increased activity is seen in the region of the posterior aspect of the left 3rd rib in Fig. 4. This is due to the activity from the overlying left sternoclavicular joint shining through.

## 12: Age 9–10 years

## Spine, pelvis and femora

*FIG. 1. Anterior view of pelvis and femora.*



*FIG. 2. Anterior view of spine, pelvis and femora.*

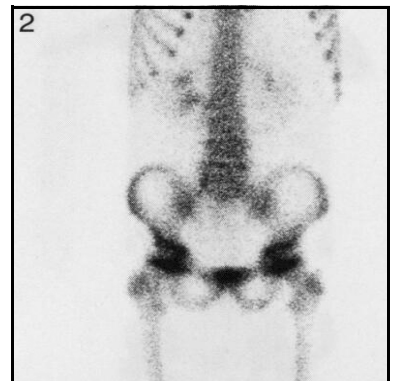
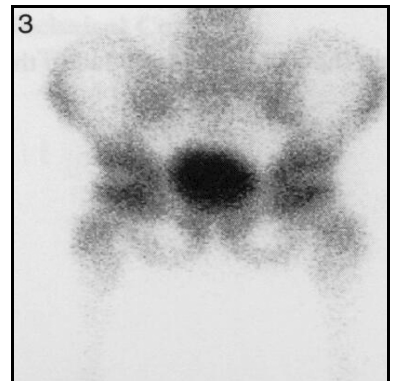


*FIG. 3. Anterior magnified view of pelvis and femora.*



### Technical comments

Urine contamination below the pelvis is seen in Fig. 1.  
The bladder is full of isotope in Fig. 3.



*FIG. 1. Posterior view of spine and pelvis.*

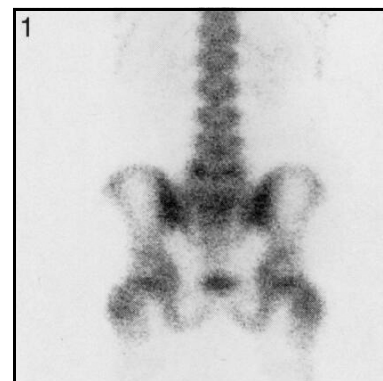


*FIG. 2. Posterior view of spine and pelvis.*

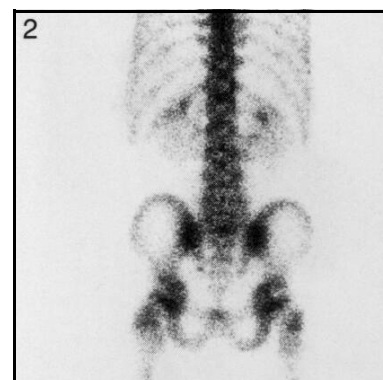
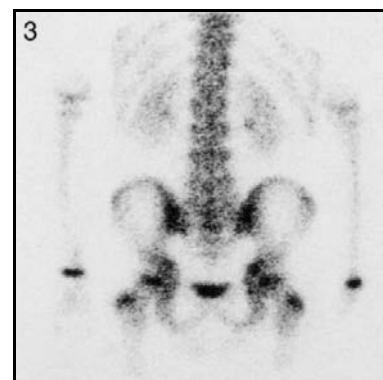


*FIG. 3. Posterior view of spine and pelvis.*



**Technical comment**

Note the slightly different rotation of the greater trochanter in Fig. 2, which is not seen separately on the left but is seen to overly the femoral neck. This is due to poor positioning of the left knee and foot.

**Potential pitfall**

The increased activity seen over the lower ribs in Fig. 2 is due to retention of tracer in the collecting system of the 'horseshoe' kidney.

*FIG. 1. Pinhole view of right hip.*

*FIG. 4. Pinhole view of left hip.*

*FIG. 2. Pinhole view of right hip.*

*FIG. 5. Pinhole view of left hip.*

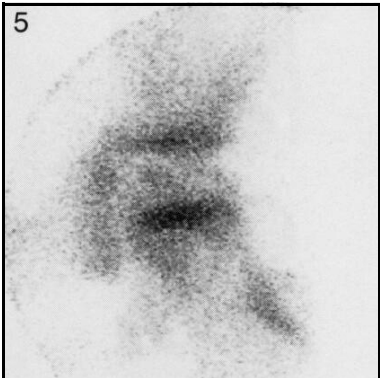
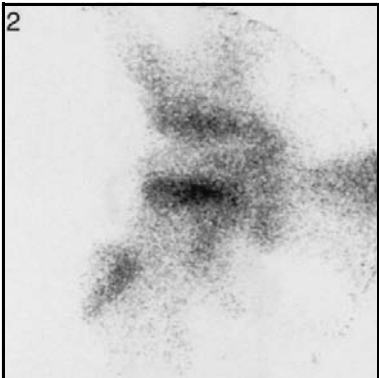
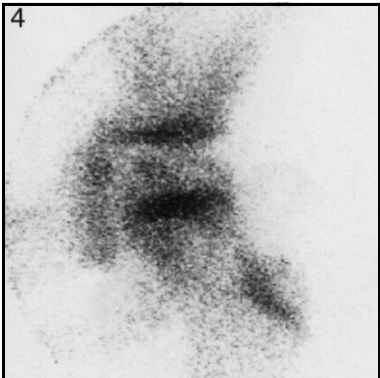
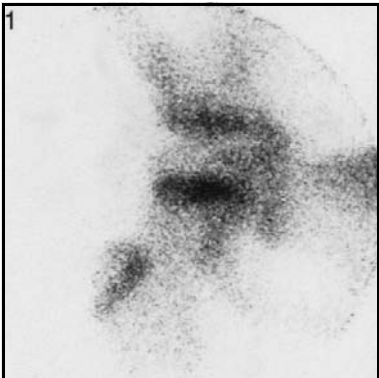


*FIG. 1. Posterior view of femora and knees.*

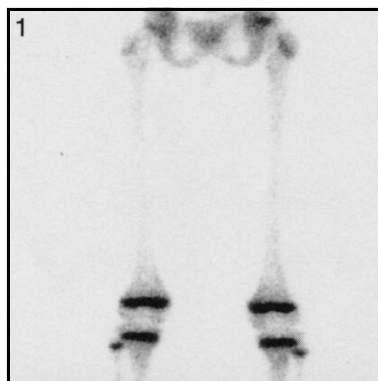


*FIG. 4. Posterior view of femora and knees.*

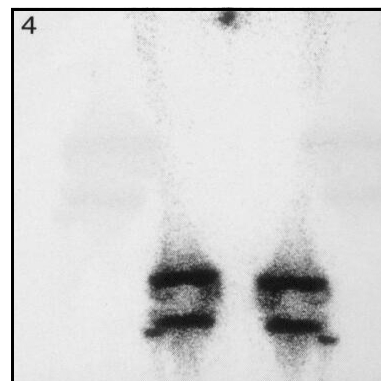


*FIG. 2. Posterior view of knees, tibia, fibula and ankles.*

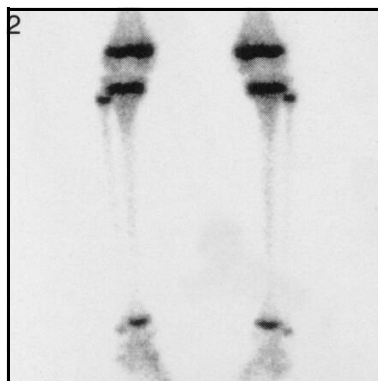
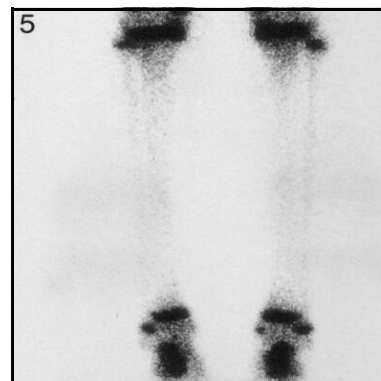


*FIG. 5. Posterior view of knees, tibia, fibula and ankles.*



### **Technical comments**

Note the in-turning of the feet in Figs 2 and 5 into the radiographic neutral position. The difference between greater trochanters in Fig. 1 is a variation of normality. Urine contamination between the femora is seen in Fig. 4.

*FIG. 1. Posterior view of knees.*

*FIG. 4. Posterior view of knees.*

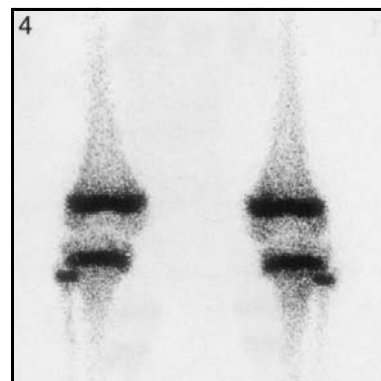
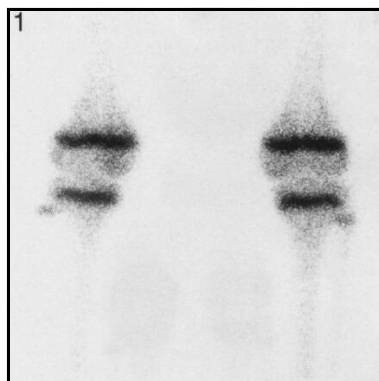


*FIG. 2. Posterior view of knees.*

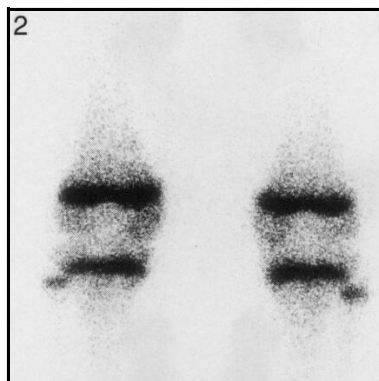


*FIG. 3. Anterior oblique view of knees.*



### Technical comments

Figure 3 is an oblique view of the knees obtained when the medial femoral condyles need to be imaged; not frequently used in paediatrics.

The patella is seen overlying the lateral aspect of the femoral epiphyseal plate in Fig. 3.

**12: Age 9–10 years**

**Tibia, fibula, ankles and feet**

*FIG. 1. Posterior view of knees, tibia, fibula and ankles.*

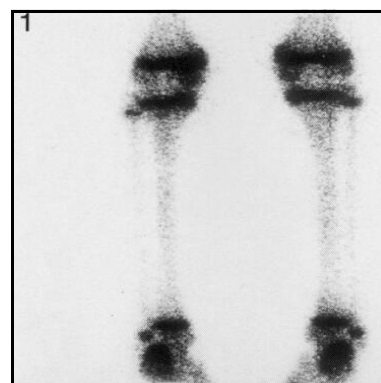


*FIG. 2. Lateral view of foot.*

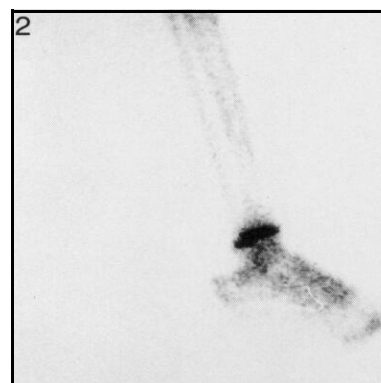
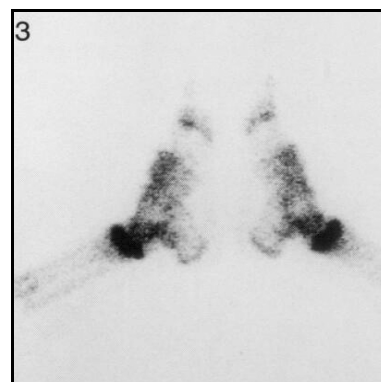


*FIG. 3. Lateral view of feet.*





## **13. AGE 10–11 YEARS**





*FIG. 1. Posterior view of skull and thorax.*



*FIG. 2. Anterior view of skull and thorax.*

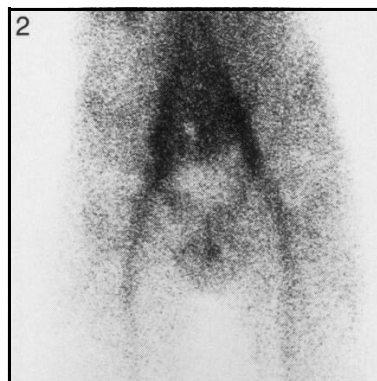


*FIG. 5. Anterior view of lower limbs.*



*FIG. 3. Posterior view of spine and pelvis.*

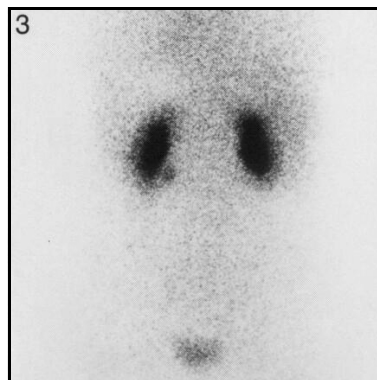
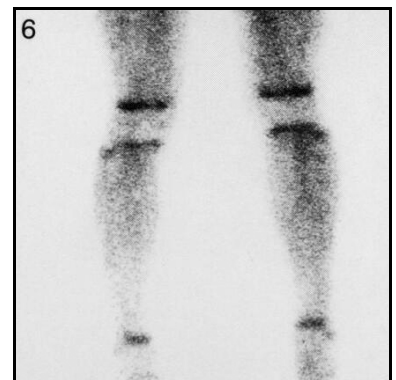


*FIG. 6. Anterior view of lower limbs.*



**Technical comment**

The skull is rotated in Fig. 1; the sagittal sinus to appear off-centre.

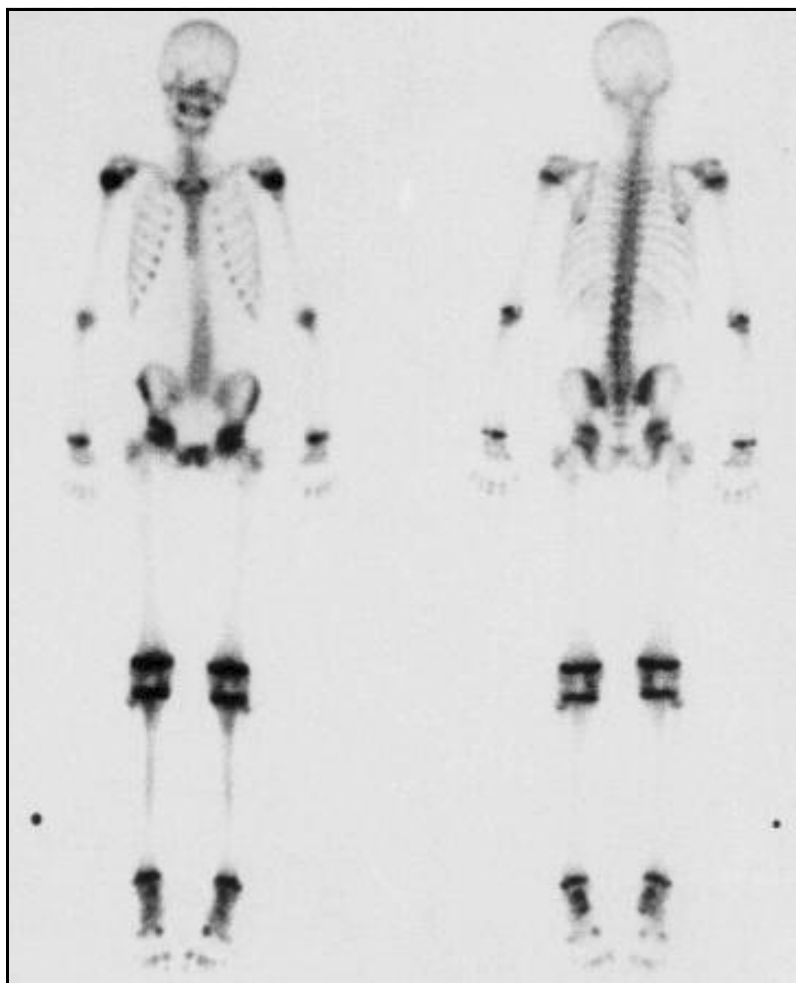
*FIG. 1. A double headed whole body gamma camera was used. Left image is anterior view; right image is posterior view.*



**Technical comments**

Note the extravasation of isotope at the site of injection.  
Marker on the right side.

*FIG. 1. A double headed whole body gamma camera was used. Left image is anterior view; right image is posterior view.*



**Technical comment**

Marker on the right side.

### 13: Age 10–11 years

### Skull, thorax and upper limb

*FIG. 1. Anterior view of skull and thorax.*

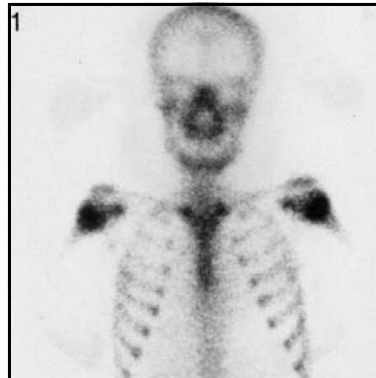


*FIG. 4. Posterior view of skull.*

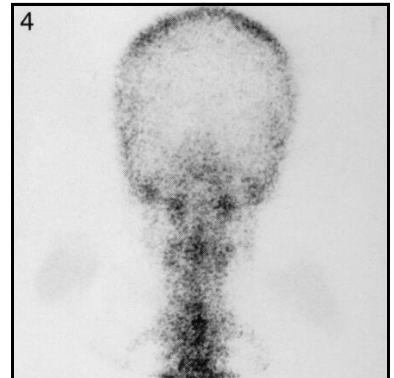


*FIG. 2. Right lateral view of skull and right upper limb.*

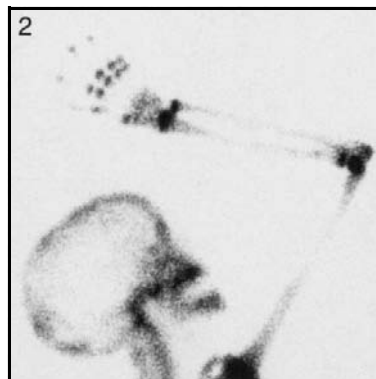
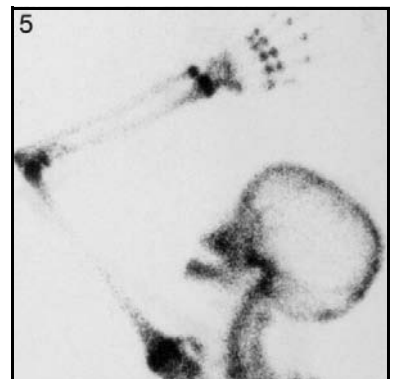


*FIG. 5. Left lateral view of skull and left upper limb.*



#### Technical comment

The lateral views of the skull (Figs 2 and 5) were taken posteriorly.

### 13: Age 10–11 years

### Skull, thorax and upper limb

*FIG. 1. Anterior view of skull and thorax.*



*FIG. 4. Posterior view of skull.*

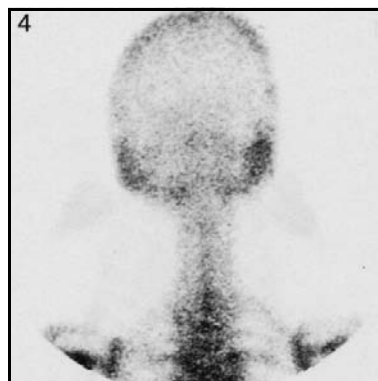


*FIG. 2. Right lateral view of skull and right upper limb.*

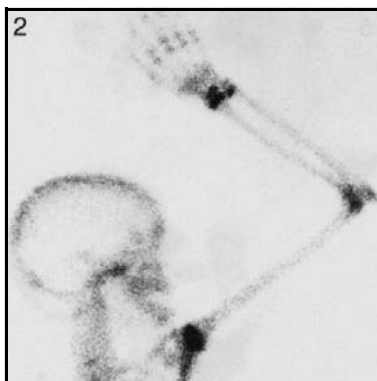


*FIG. 5. Left lateral view of skull and left upper limb.*

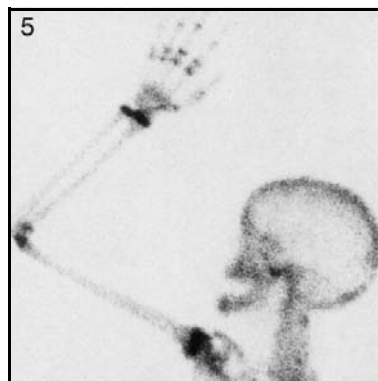
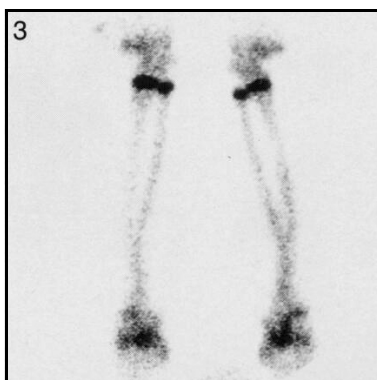


*FIG. 3. Forearms.*



#### Technical comments

The image of the forearms in Fig. 3 reveals overlap of the upper radius and ulna. This should be compared with Figs 2 and 5, which show a clear separation of radius and ulna.

The differences between the mastoid areas in Fig. 4 are due to rotation.

The lateral views of the skull (Figs 2 and 5) were taken posteriorly.

*FIG. 1. Anterior view of thorax.*



*FIG. 2. Anterior view of thorax, spine and upper pelvis.*

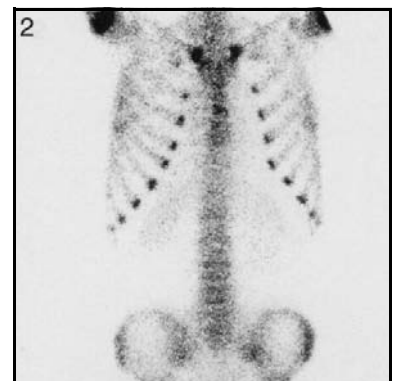
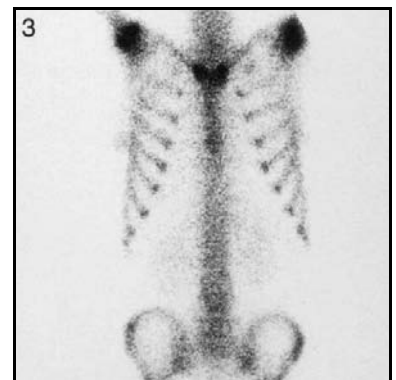


*FIG. 3. Anterior view of thorax, spine and upper pelvis.*



**Potential pitfall**

Note the sternum in Fig. 1 where increased activity is noted in two areas. This represents normal growth centres of the sternum and should not be confused with a fracture.

### 13: Age 10–11 years

### Skull, thorax and upper limb

*FIG. 1. Anterior view of thorax.*



*FIG. 2. Anterior view of thorax, spine and upper pelvis.*

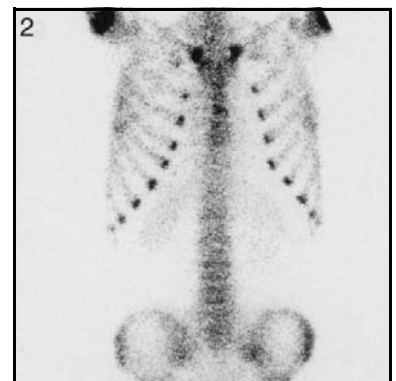
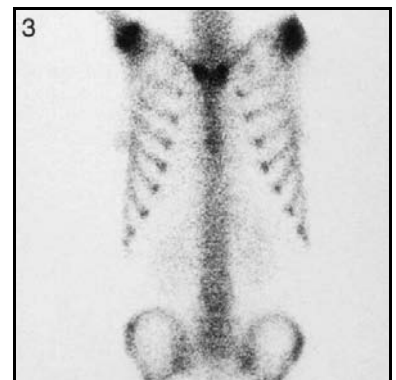


*FIG. 3. Anterior view of thorax, spine and upper pelvis.*



#### **Potential pitfall**

Note the sternum in Fig. 1 where increased activity is evident in two areas. This represents normal growth centres of the sternum and should not be confused with a fracture.

*FIG. 1. Right anterior oblique view of thorax.*

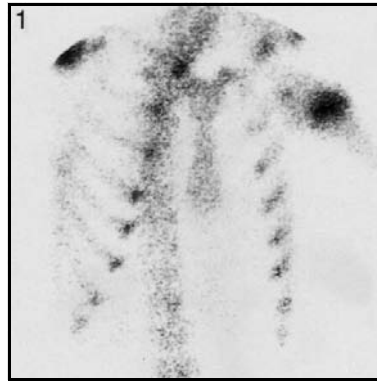


*FIG. 4. Left anterior oblique view of thorax.*

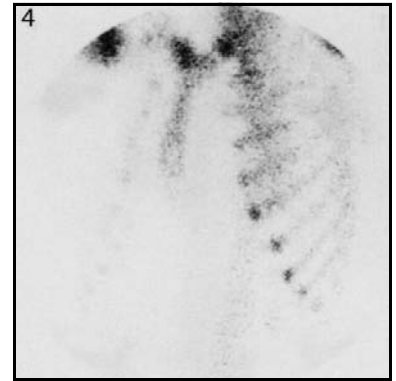
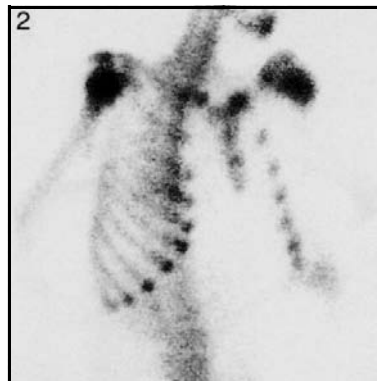


*FIG. 2. Right anterior oblique view of thorax.*



**Technical comment**

Note the different appearances of the sternum owing to different degrees of obliquity.



**13: Age 10–11 years**

**Thorax, spine and upper pelvis**

*FIG. 1. Posterior view of thorax, spine and upper pelvis.*

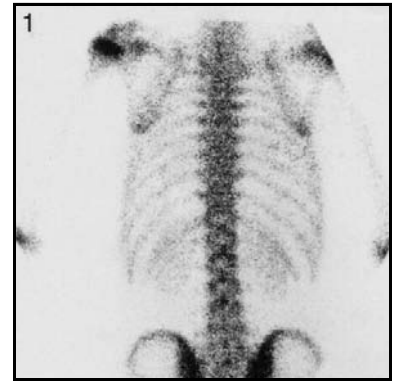


*FIG. 2. Posterior view of thorax, spine and upper pelvis.*

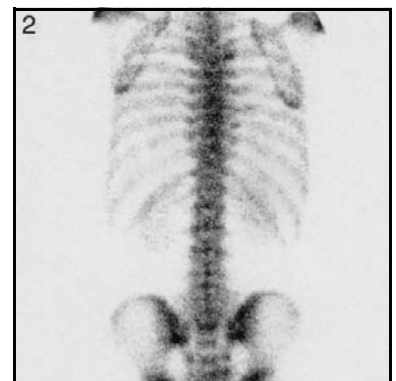
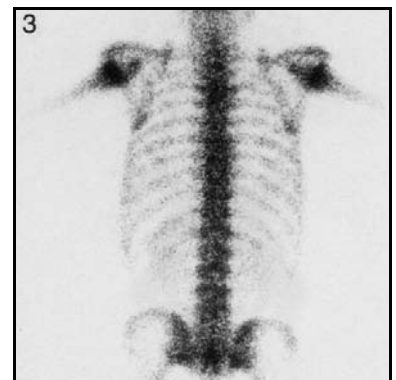


*FIG. 3. Posterior view of thorax, spine and upper pelvis.*



**13: Age 10–11 years**

**Pelvis and femora**

*FIG. 1. Anterior view of pelvis and femora.*

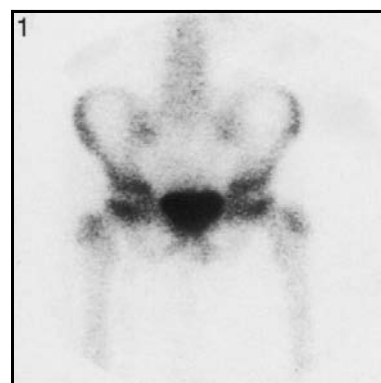


*FIG. 2. Anterior view of pelvis and femora.*



### 13: Age 10–11 years

### Spine, pelvis and femora

*FIG. 1. Posterior view of spine, pelvis and femora.*



*FIG. 2. Posterior view of pelvis and femora.*

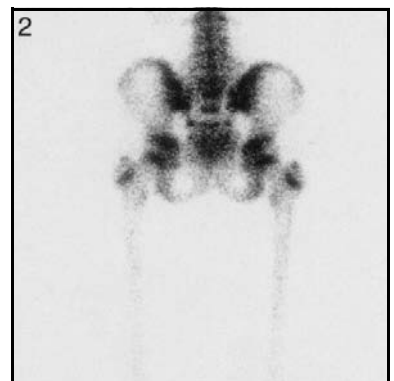
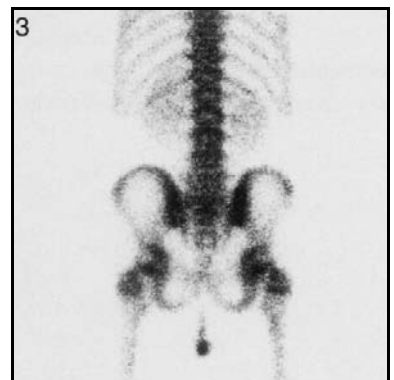


*FIG. 3. Posterior view of spine, pelvis and femora.*



#### Technical comment

Urine contamination below the pelvis is seen in Fig. 3.

### 13: Age 10–11 years

### Spine and pelvis

*FIG. 1. Pelvic inlet view.*

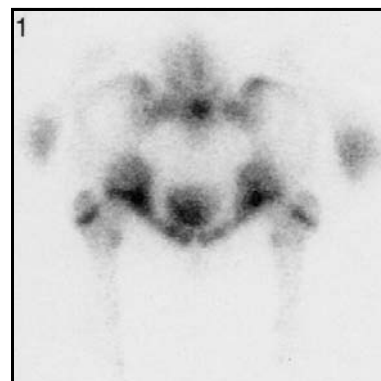


*FIG. 2. Sitting view of spine and pelvis.*

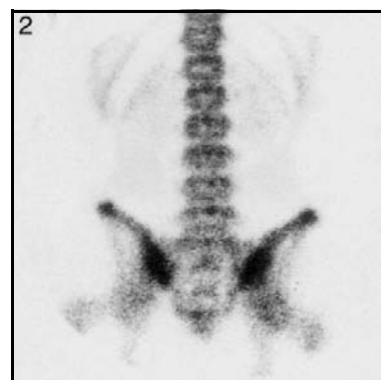


*FIG. 1. Pinhole view of right hip.*

*FIG. 4. Pinhole view of left hip.*

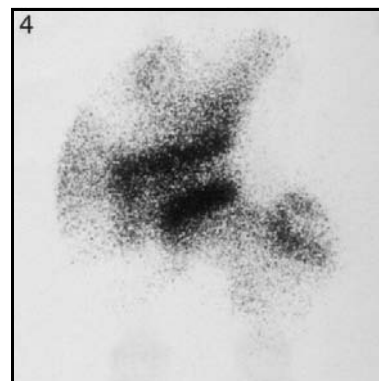
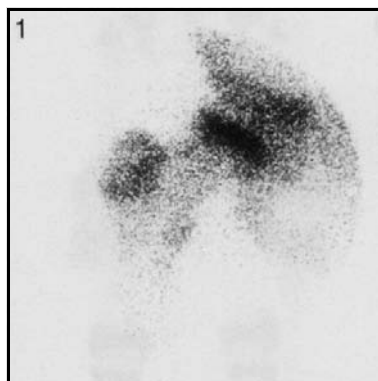


*FIG. 1. Posterior view of femora.*

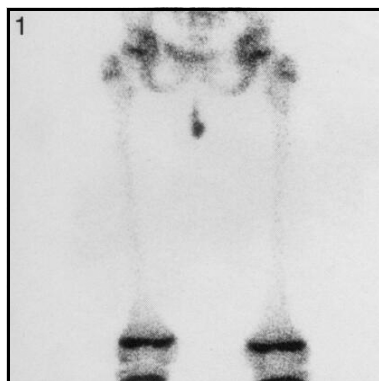


*FIG. 4. Posterior view of femora and knees.*

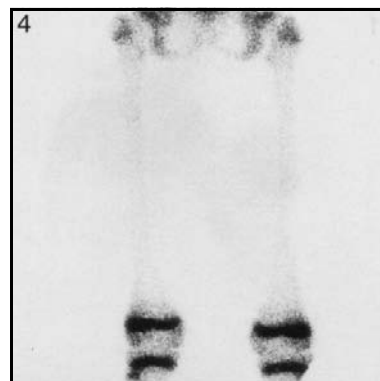


*FIG. 2. Posterior view of knees, tibia, fibula and ankles.*

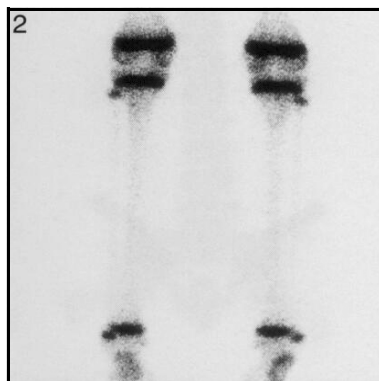
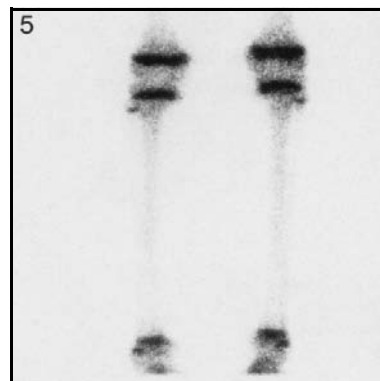


*FIG. 5. Posterior view of knees, tibia, fibula and ankles.*



**Technical comment**

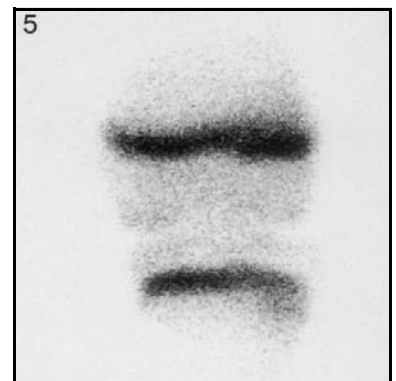
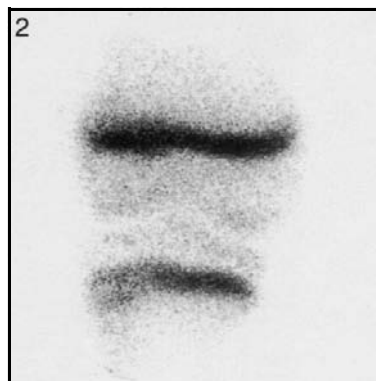
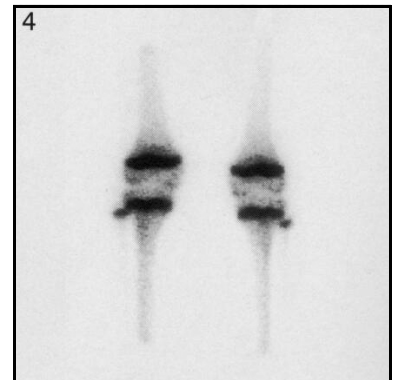
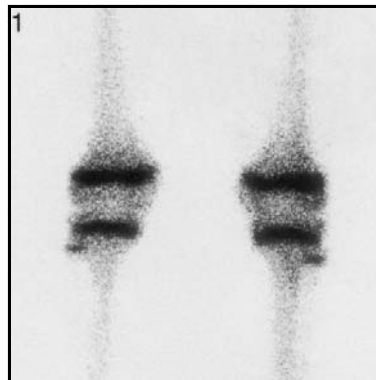
Urine contamination below the pelvis is seen in Fig. 1.

*FIG. 1. Posterior magnified view of knees.*

*FIG. 4. Posterior view of knees.*

*FIG. 2. Anterior pinhole view of right knee.*

*FIG. 5. Anterior pinhole view of left knee.*



**Technical comment**

Note that the fibula is better seen in the posterior views in Figs 1 and 4 than in the anterior pinhole views in Figs 2 and 5.

### 13: Age 10–11 years

### Knees, tibia, fibula and feet

*FIG. 1. Posterior view of knees, tibia, fibula and ankles.*

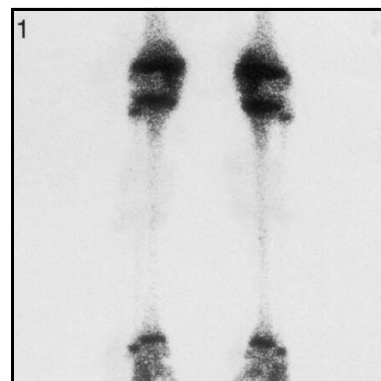


*FIG. 2. Lateral view of feet.*

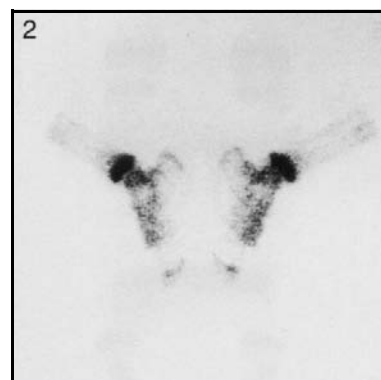
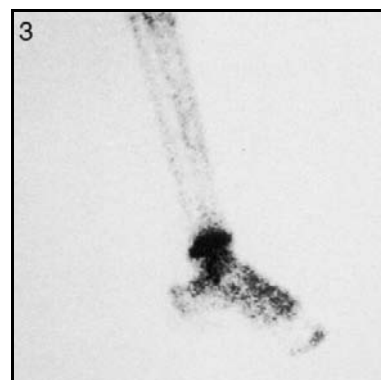


*FIG. 3. Lateral view of foot.*





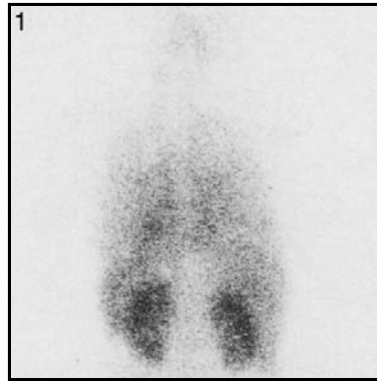
## **14. AGE 11–12 YEARS**



## 14: Age 11–12 years

## Blood pool images

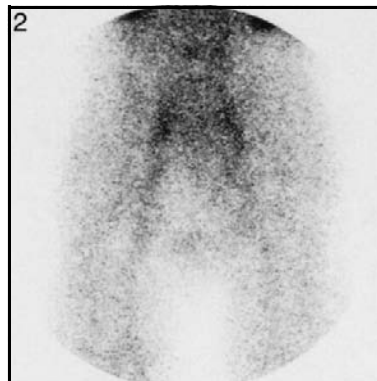
*FIG. 1. Posterior view of thorax and spine.*



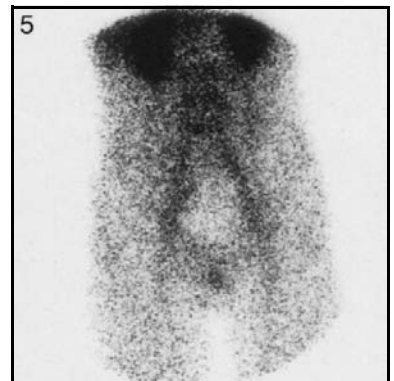
*FIG. 4. Right lateral view of skull and posterior view of upper limbs.*



*FIG. 2. Posterior view of pelvis.*



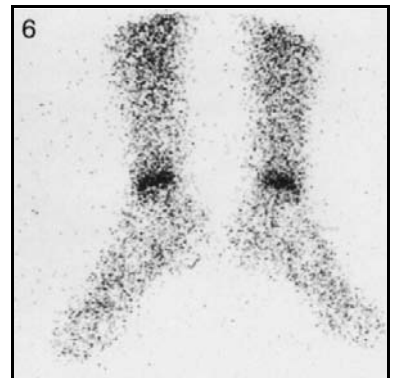
*FIG. 5. Anterior view of pelvis.*



*FIG. 3. Posterior view of knees.*



*FIG. 6. Lateral view of feet.*



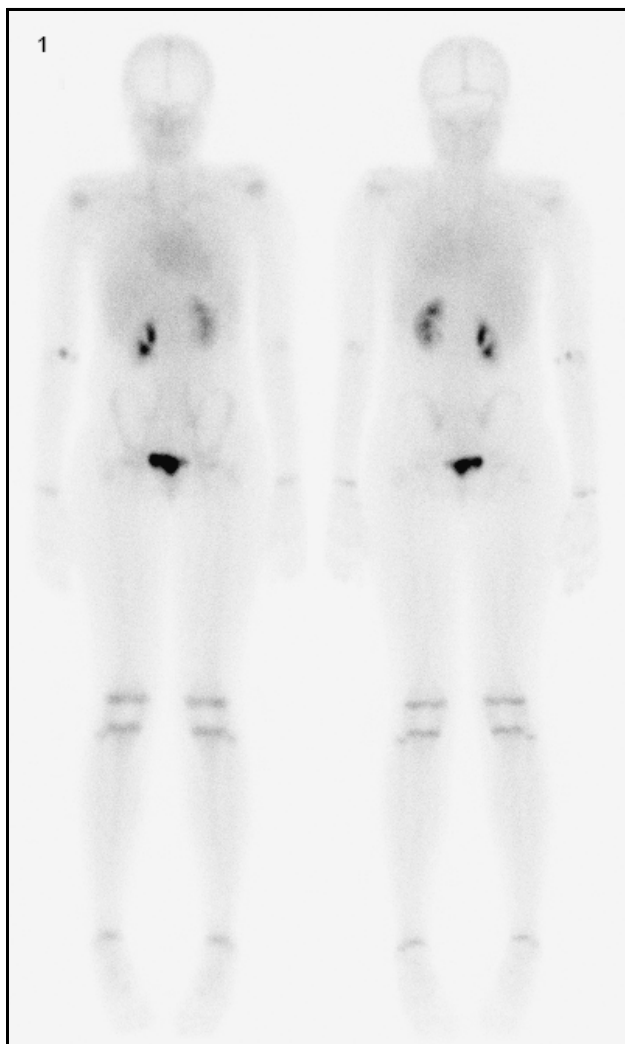


*FIG. 1. Whole body images of a 12-year-old male (35 kg body weight, height 155 cm). Anterior and posterior whole body blood pool views.*

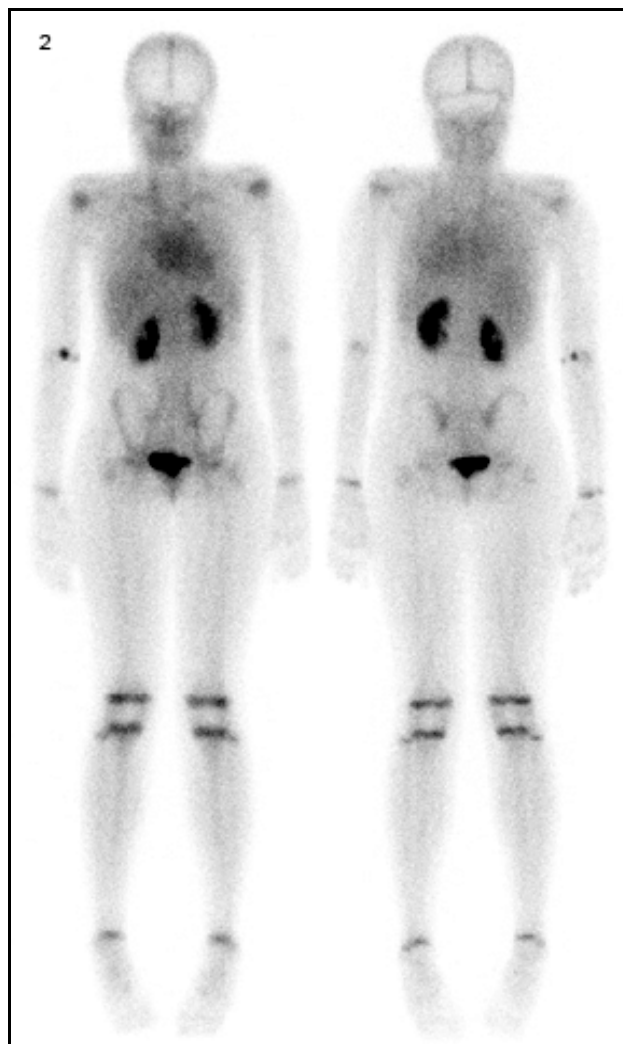


*FIG. 2. Whole body images of a 12-year-old male (35 kg body weight, height 155 cm). Anterior and posterior whole body blood pool views.*

#### Technical comments

The study was acquired with a double headed digital whole body gamma camera equipped with high resolution low energy collimators.

Figures 1 and 2 are anterior and posterior whole body blood pool views presented at different levels of intensity. Note the early intense trace accumulation in the metaphysis growth plates corresponding to high blood flow to this metabolically active tissue.



*FIG. 1. Whole body images of a 12-year-old male (35 kg body weight, height 155 cm). Delayed anterior and posterior whole body scans presented for the same study with different intensity levels.*

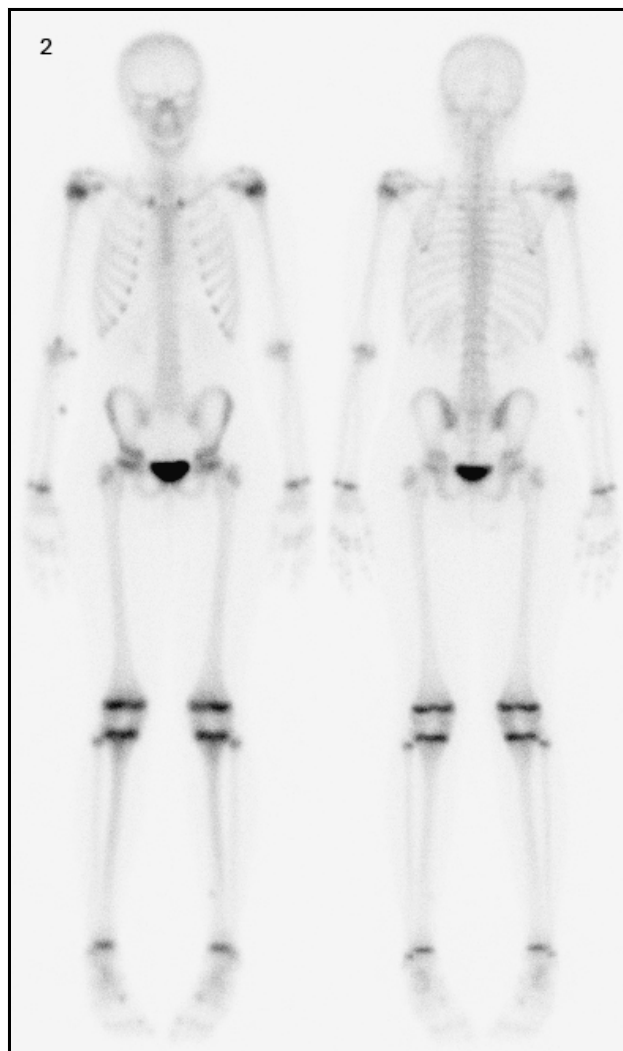


*FIG. 2. Whole body images of a 12-year-old male (35 kg body weight, height 155 cm). Delayed anterior and posterior whole body scans presented for the same study with different intensity levels.*

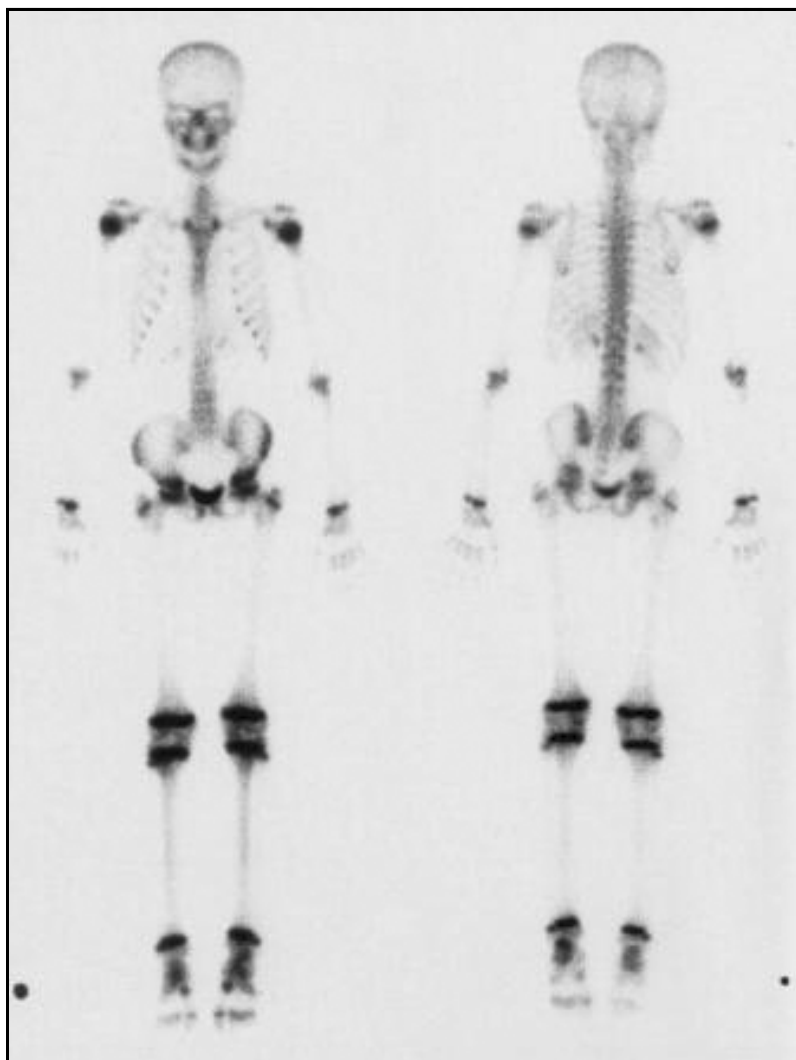
#### Technical comments

A double headed digital whole body gamma camera equipped with high resolution low energy collimator was used and the energy window width set to 15%.

Immediately following the intravenous injection of 360 MBq (0.72, fraction of adult administered activity of 500 MBq) of  $^{99m}\text{Tc}$ -MDP, whole body blood pool imaging was started at a camera scanning speed of 19.5 cm/min. Delayed imaging was started 3 hours p.i. at a camera speed of 11 cm/min.

Note the appearance of the activity in the growing epiphyses of the upper and lower extremities.

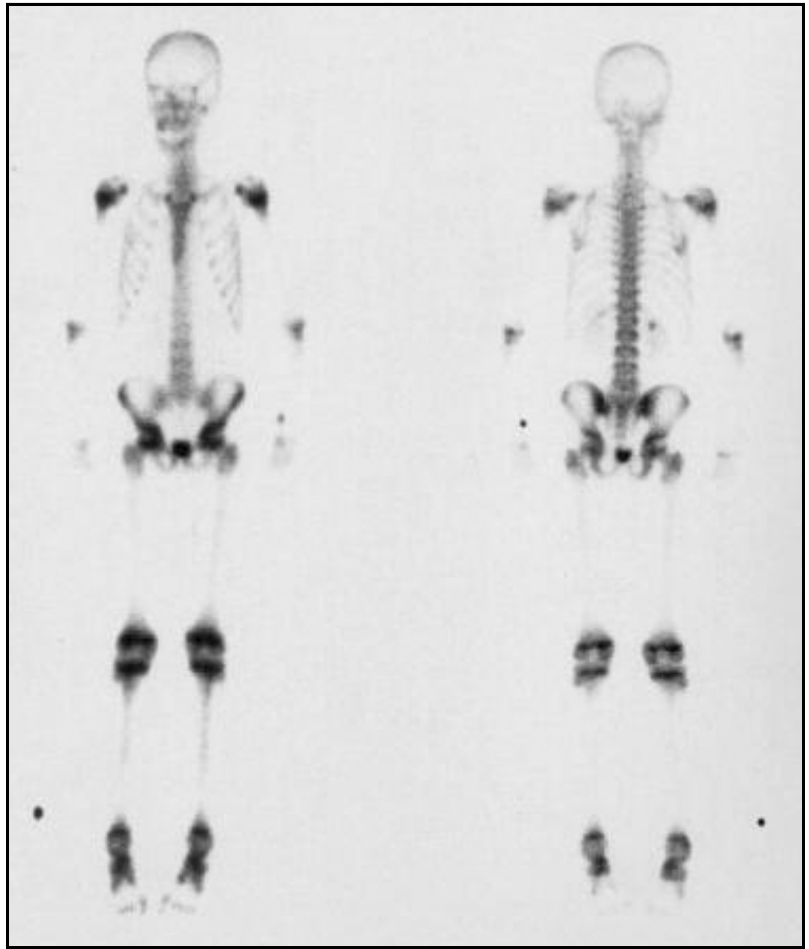
*FIG. 1. A double headed whole body gamma camera was used. Left image is anterior view; right image is posterior view.*



**Technical comment**

Marker on the right side.

*FIG. 1. A double headed whole body gamma camera was used. Left image is anterior view; right image is posterior view.*



**Technical comments**

Note the extravasation of isotope at the site of injection in the left hand.  
Marker on the right side.

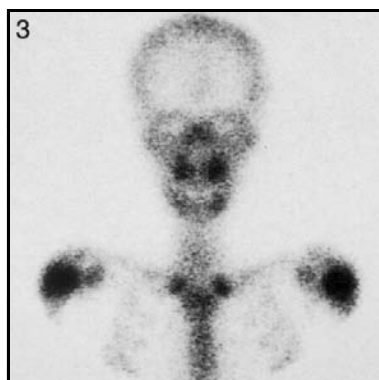
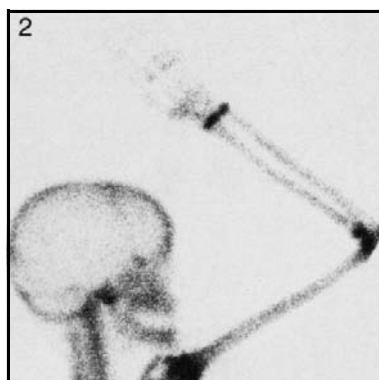
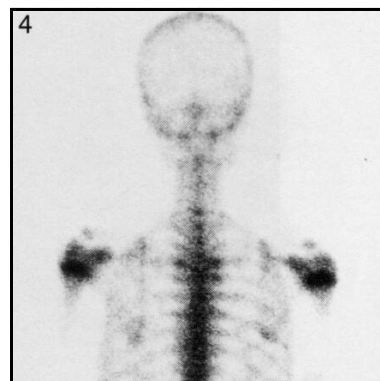
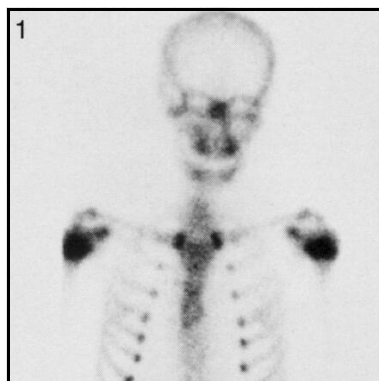
*FIG. 1. Anterior view of skull and thorax.*

*FIG. 4. Posterior view of skull and thorax.*

*FIG. 2. Right lateral view of skull and right upper limb.*

*FIG. 5. Left lateral view of skull and left upper limb.*

*FIG. 3. Anterior view of skull and thorax.*



### **Technical comments**

In the posterior view of the thorax in Fig. 4, the angles of the scapulae show up as focal areas of increased activity, especially on the right; this is normal.

Focal increased activity is noted on the left of the midline in the mandible in Fig. 3. The cause for this is uncertain but may be related to the teeth.

The distal end of the humerus has been excluded from the field of view in Figs 2 and 5. This is due to the difficulty in positioning both the skull and the upper limb at the same time in children of this age.

The lateral views of the skull (Figs 2 and 5) were taken posteriorly.



*FIG. 1. Anterior view of hands.*



*FIG. 2. Anterior view of part of right thorax and right upper limb.*

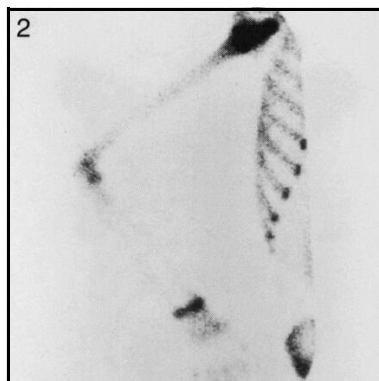
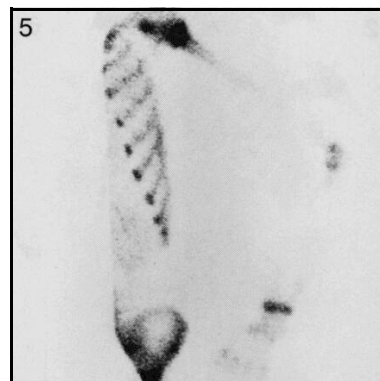


*FIG. 5. Anterior view of part of left thorax and left upper limb.*



**Technical comment**

Figures 2 and 5 show the difficulty of obtaining high quality images of the upper limbs adjacent to the thorax. Compare with the images on p. 177.

*FIG. 1. Anterior view of thorax.*

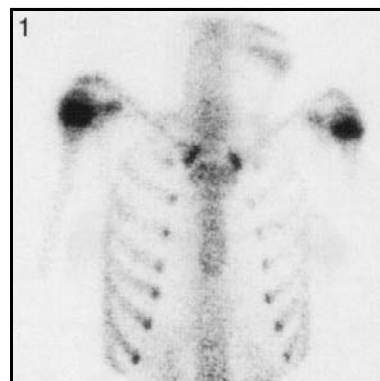


*FIG. 2. Anterior view of thorax, spine and upper pelvis.*

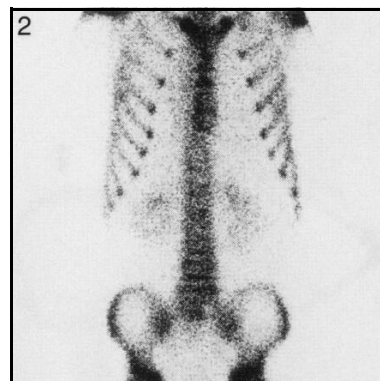


*FIG. 3. Anterior view of thorax and spine.*



**Technical comments**

The unusual activity in the neck and in the left hypochondrium in Fig. 3 suggests  $^{99m}\text{Tc}$ -pertechnetate in both the stomach and the thyroid gland.

The clarity of the lower lumbar spine in the anterior views in Figs 2 and 3 is again noted.

*FIG. 1. Posterior view of thorax and spine.*



*FIG. 4. Posterior view of thorax and spine.*

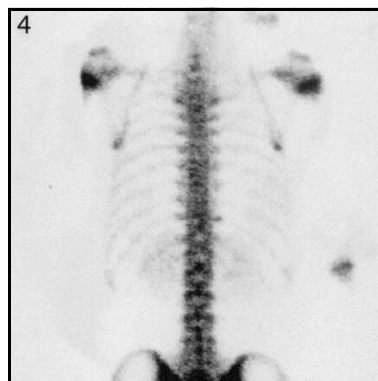


*FIG. 2. Posterior view of thorax and spine.*

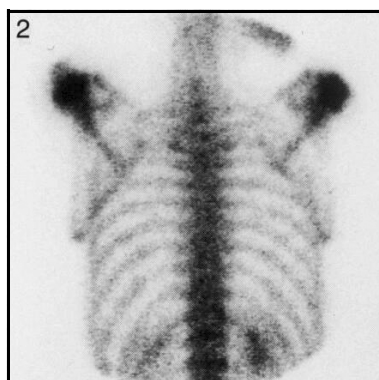
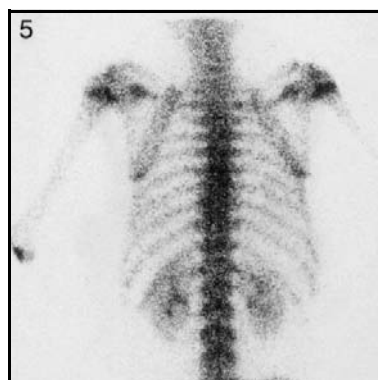


*FIG. 5. Posterior view of thorax and spine.*



### **Technical comments**

The scapulae appear different owing to the varying positions of the humeri in these images.  
There is retention of isotope in the right kidney in Fig. 2.

*FIG. 1. Right anterior oblique view of thorax.*

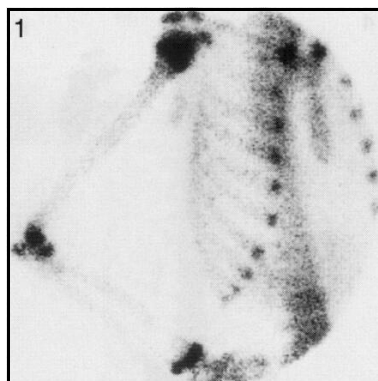
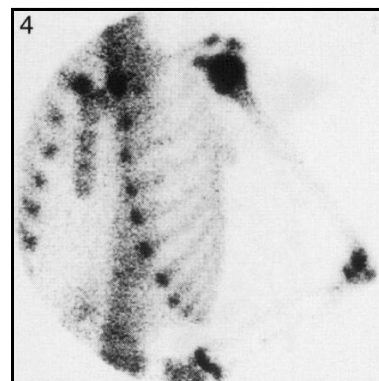


*FIG. 4. Left anterior oblique view of thorax.*



## 14: Age 11–12 years

## Spine, pelvis and femora

*FIG. 1. Anterior view of spine, pelvis and femora.*

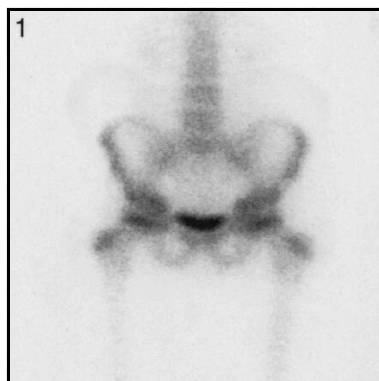


*FIG. 4. Anterior view of spine, pelvis and femora.*



*FIG. 2. Anterior view of pelvis and femora.*



*FIG. 5. Anterior view of spine, pelvis and femora.*



### Technical comment

Urine contamination below the pelvis is seen in Fig. 4.

### Potential pitfall

Focal increased activity is noted in the region of the right synchondrosis (a cartilaginous joint) in Fig. 5. This represents contamination and does not represent pathology in the pubic bone.

## 14: Age 11–12 years

## Spine, pelvis and femora

*FIG. 1. Posterior view of spine, pelvis and femora.*



*FIG. 4. Posterior view of spine, pelvis and femora.*

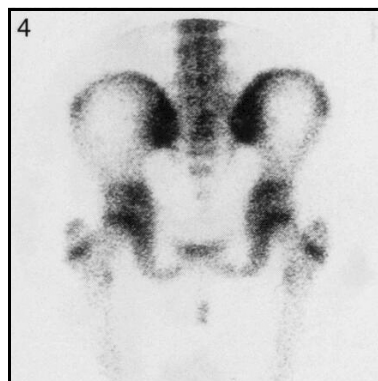


*FIG. 2. Posterior view of spine, pelvis and femora.*

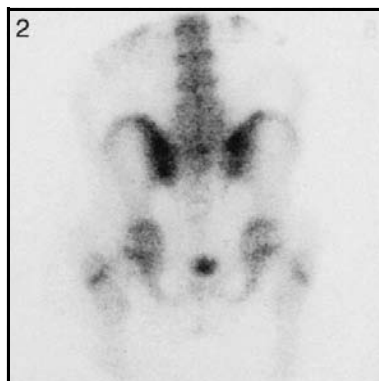
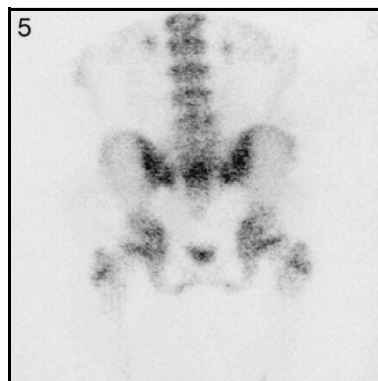


*FIG. 5. Posterior view of spine, pelvis and femora.*



### Technical comment

Urine contamination below the pelvis is seen in Figs 1, 2 and 4.

*FIG. 1. Pinhole view of right hip.*

*FIG. 4. Pinhole view of left hip.*

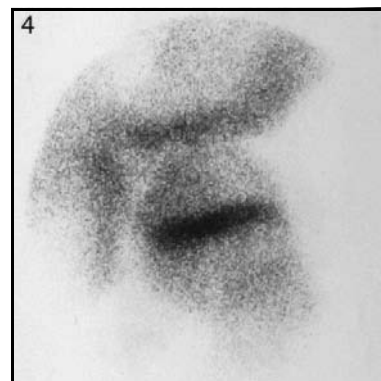
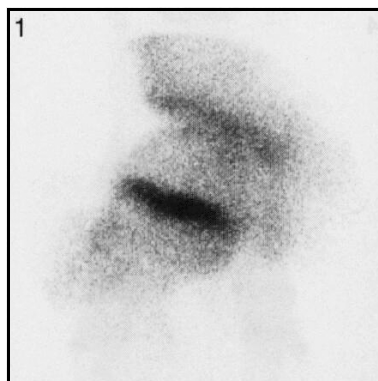
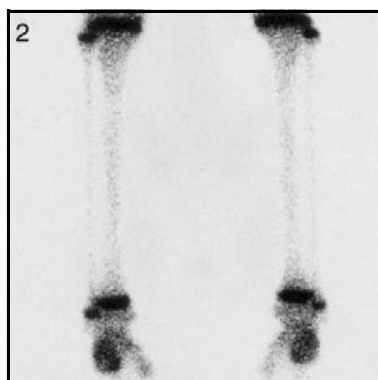
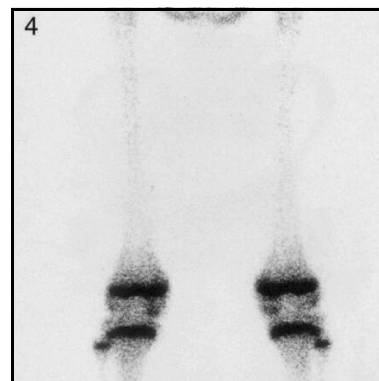
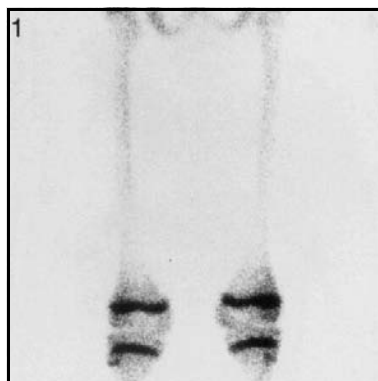


*FIG. 1. Posterior view of femora and knees.*

*FIG. 4. Posterior view of femora and knees.*

*FIG. 2. Posterior view of tibia, fibula and ankles.*

*FIG. 5. Posterior view of tibia, fibula and ankles.*



**Technical comment**

Note the rather patchy asymmetrical distribution of the isotope in the mid-portions of the tibia in Fig. 5. Although the authors are unable to offer a physiological explanation, the observation has been made frequently and has no clinical consequence.

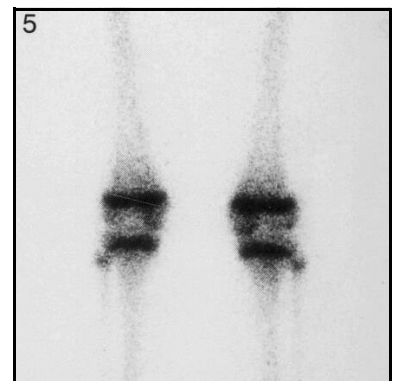
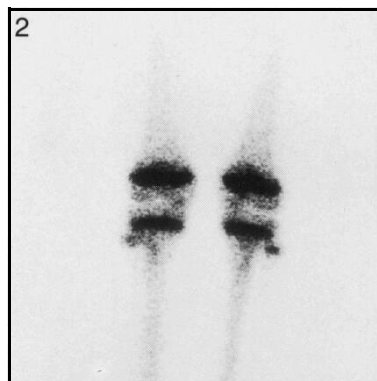
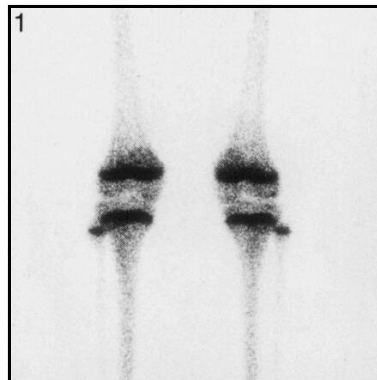


*FIG. 1. Posterior view of knees.*

*FIG. 4. Posterior view of knees.*

*FIG. 2. Anterior view of knees.*

*FIG. 5. Posterior view of knees.*



**Technical comment**

The epiphyseal plate of the femur is not well defined in Fig. 2, the anterior view, because the patella overlies the epiphyseal plate.

**14: Age 11–12 years**

**Tibia, fibula, ankles and femora**

*FIG. 1. Posterior view of tibia, fibula and ankles.*

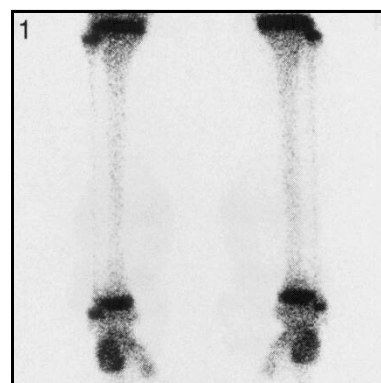
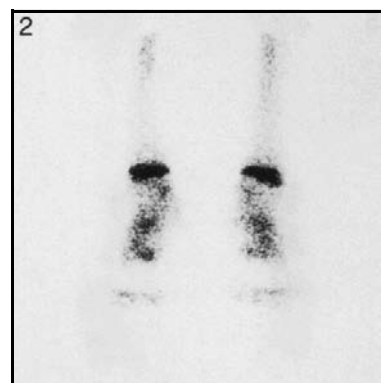


*FIG. 2. Anterior view of ankles and feet.*



## **15. AGE 12–13 YEARS**



**15: Age 12–13 years**

**Blood pool images**

*FIG. 1. Posterior view of thorax and spine.*

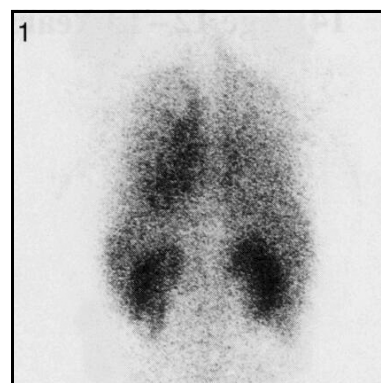


*FIG. 2. Anterior view of knees.*

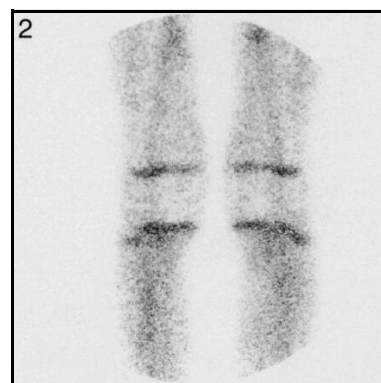
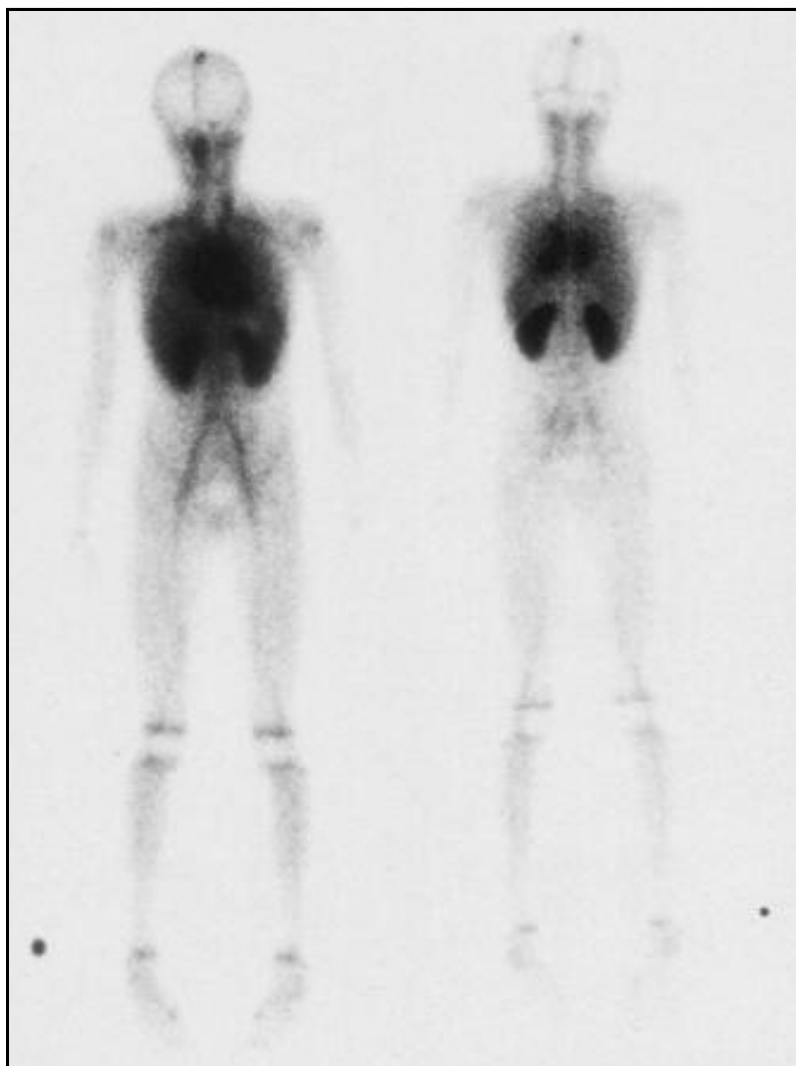


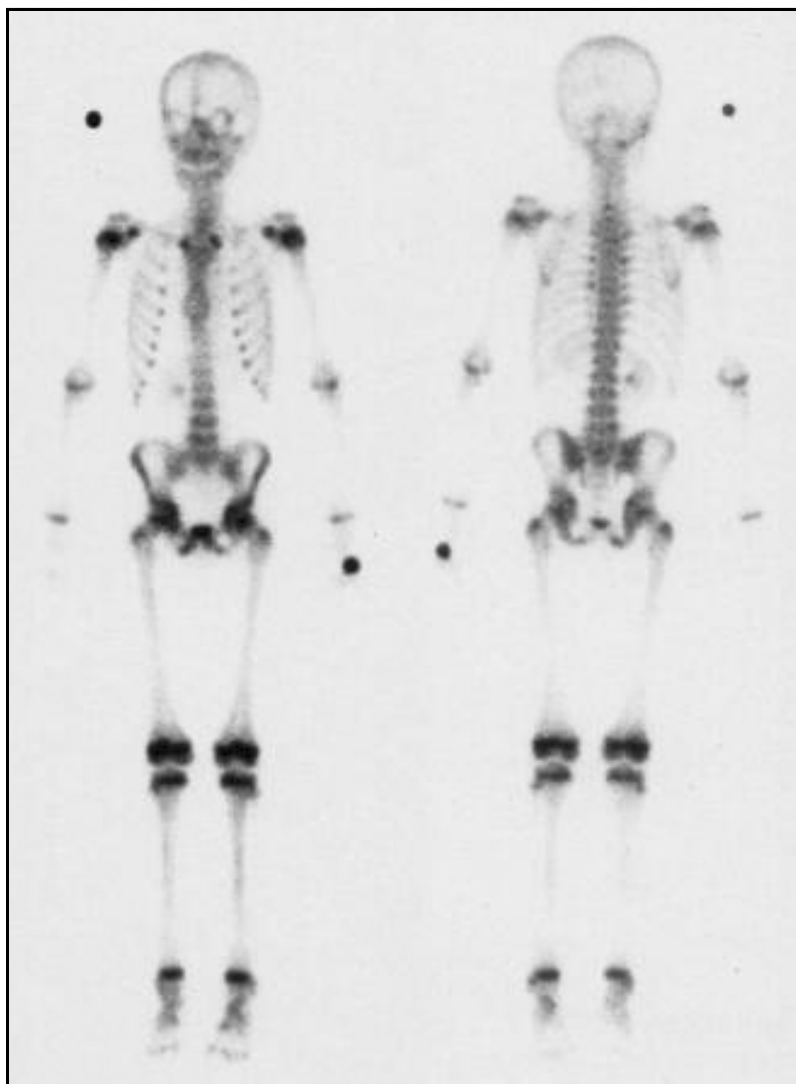
*FIG. 1. A double headed whole body gamma camera was used. Left image is anterior view; right image is posterior view.*



**Technical comment**

Marker on the right side.

*FIG. 1. A double headed whole body gamma camera was used. Left image is anterior view; right image is posterior view.*



**Technical comments**

Note the poor positioning of the right foot.  
Note the extravasation of isotope at the site of injection in the left hand.  
Marker on the right side.

**Potential pitfall**

Increased activity is noted in the inferior pubic ramus owing to the synchondrosis (cartilaginous joint). This should not be mistaken for pathology.

## 15: Age 12–13 years

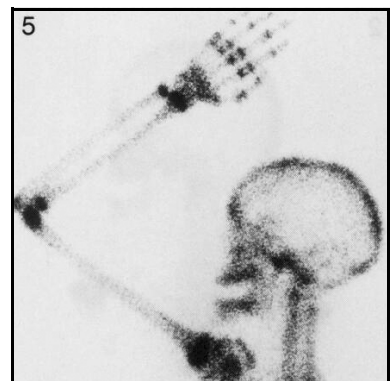
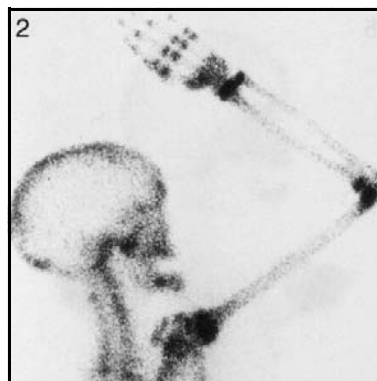
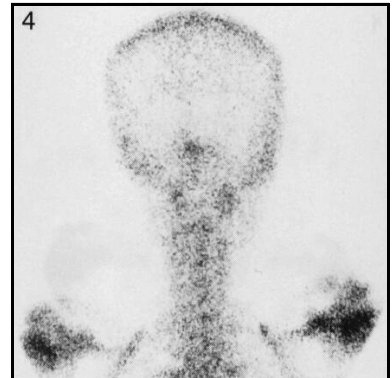
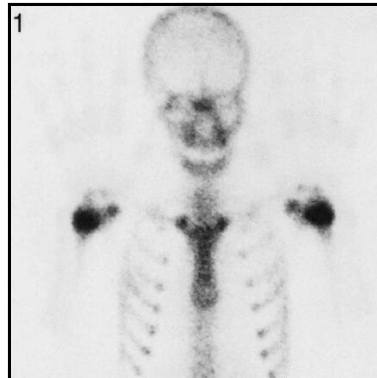
## Skull, thorax and upper limbs

*FIG. 1. Anterior view of skull and thorax.*

*FIG. 4. Posterior view of skull.*

*FIG. 2. Right lateral view of skull and right upper limb.*

*FIG. 5. Left lateral view of skull and left upper limb.*



### Technical comment

The lateral views of the skull (Figs 2 and 5) were taken posteriorly.



*FIG. 1. Anterior view of skull and thorax.*

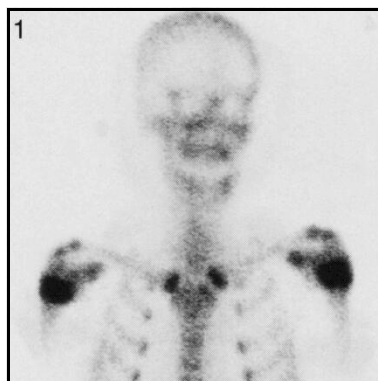


*FIG. 2. Right anterior view of skull and thorax.*

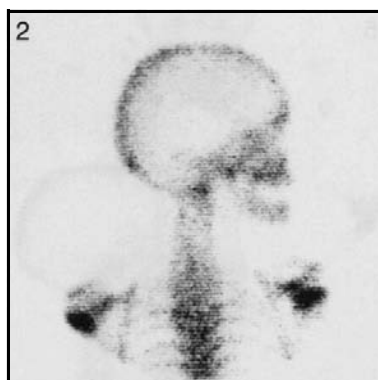


*FIG. 5. Left lateral view of skull and posterior view of thorax.*

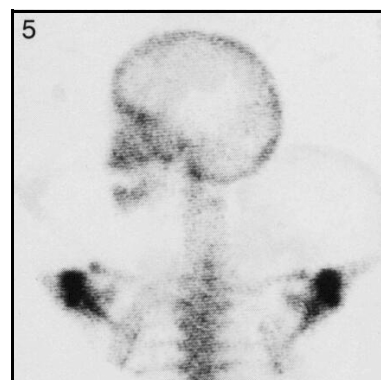


*FIG. 1. Anterior view of hands.*

*FIG. 4. Anterior view of hands.*

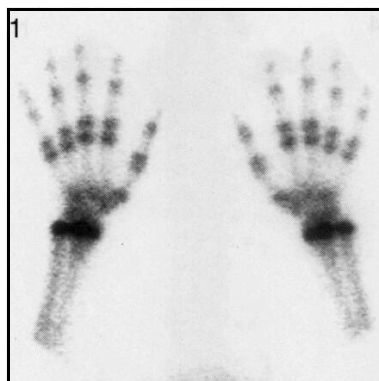


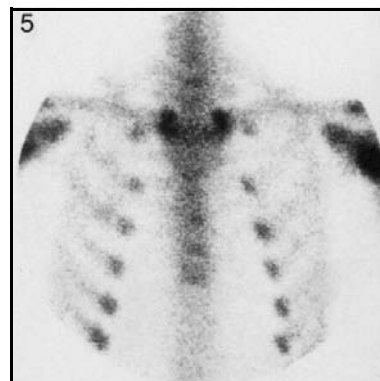
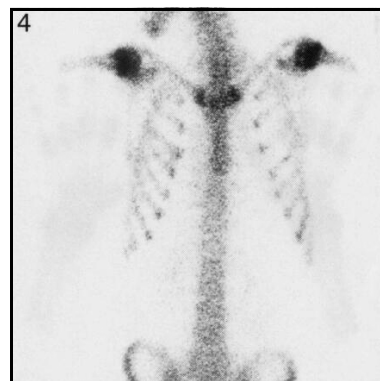
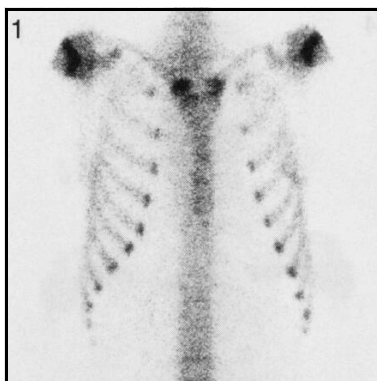
*FIG. 1. Anterior view of thorax and spine.*

*FIG. 4. Anterior view of thorax and spine.*

*FIG. 2. Anterior view of thorax and spine.*

*FIG. 5. Anterior view of spine.*

*FIG. 3. Left anterior oblique view of thorax and spine.*



**Technical comment**

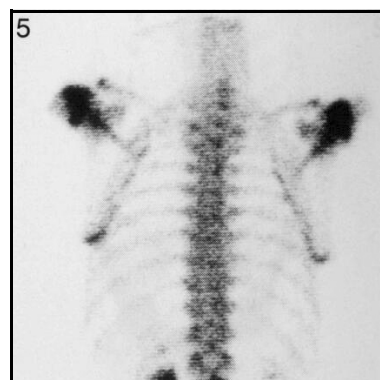
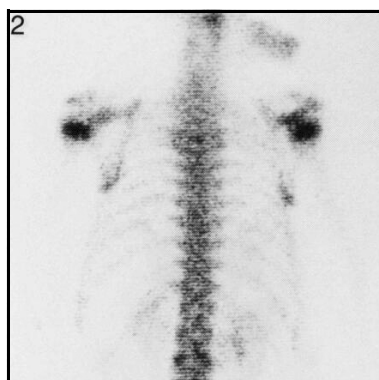
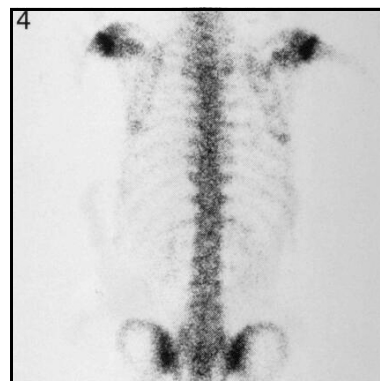
Note the variation of the sternum in these different anterior and oblique anterior projections.

*FIG. 1. Posterior view of thorax and spine.*

*FIG. 4. Posterior view of thorax, spine and upper pelvis.*

*FIG. 2. Posterior view of thorax and spine.*

*FIG. 5. Posterior view of thorax and spine.*



**Technical comments**

Asymmetrical activity in the renal pelvis is noted in Fig. 5. This is within normal limits. Note the appearance of the scapulae with the positioning of the upper limbs.

*FIG. 1. Anterior view of spine and pelvis.*



*FIG. 2. Anterior view of spine and pelvis.*

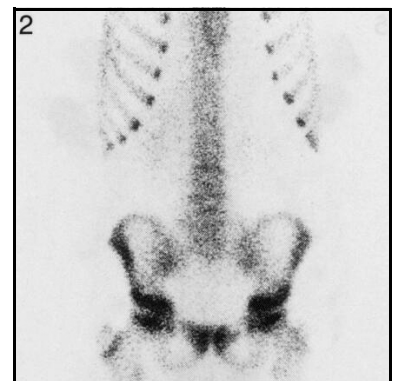
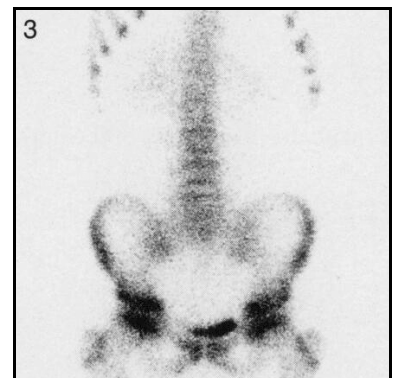


*FIG. 3. Anterior view of spine and pelvis.*



**Technical comments**

Note the clarity of the lumbar spine on these anterior views.  
Urine contamination below the pelvis is seen in Fig. 2.

**Potential pitfall**

The pubic rami show normal increased uptake of tracer in all images.

*FIG. 1. Posterior view of spine and pelvis.*

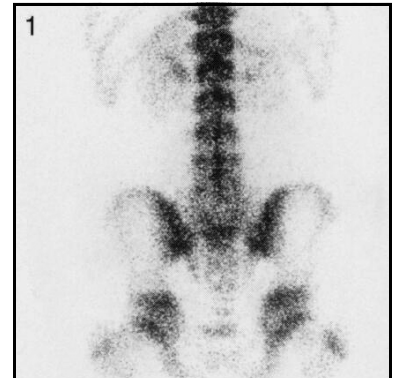


*FIG. 2. Posterior view of spine and pelvis.*

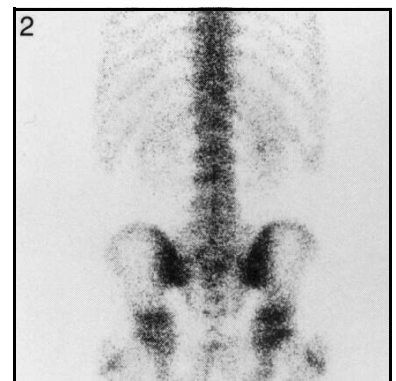


*FIG. 3. Posterior view of spine and pelvis.*



**Technical comments**

Note the isotope in the left renal pelvis in Fig. 3, suggesting dilation of the renal pelvis.  
Urine contamination below the pelvis is seen in Fig. 2.

*FIG. 1. Pinhole view of right hip.*

*FIG. 4. Pinhole view of left hip.*

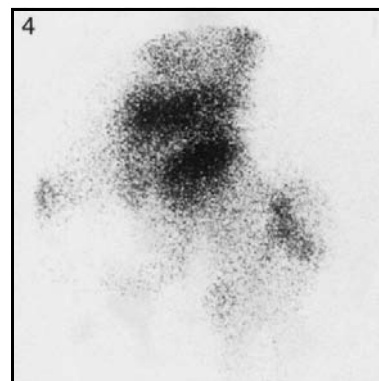
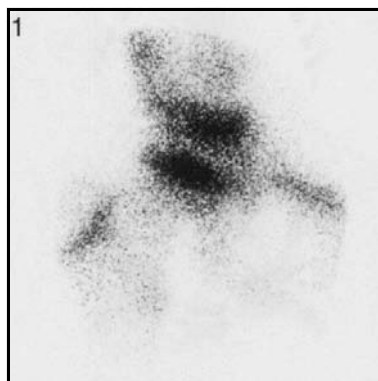


*FIG. 1. Posterior view of femora and knees.*

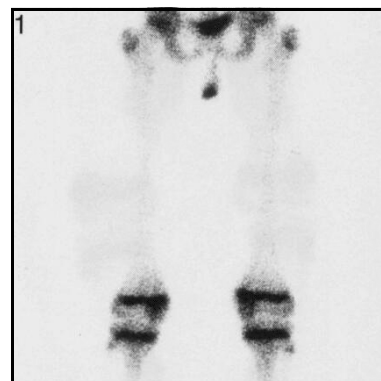
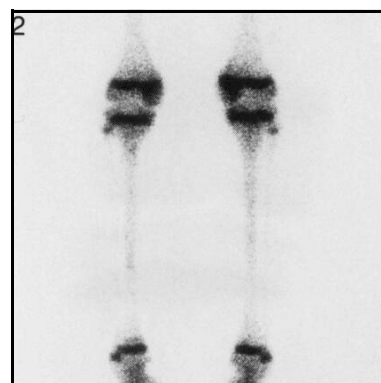


*FIG. 2. Posterior view of knees, tibia, fibula and ankles.*



**Technical comments**

Slight increased activity is noted in the left mid-tibia in Fig. 2, similar to the appearances in Fig. 5, p. 220. Urine contamination below the pelvis is seen in Fig. 1.



*FIG. 1. Anterior view of knees.*

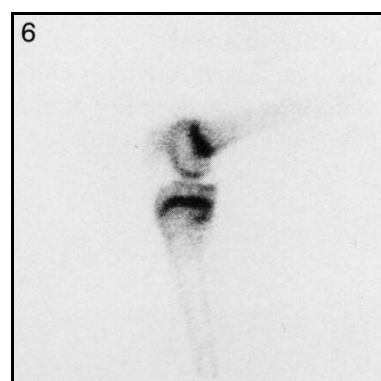
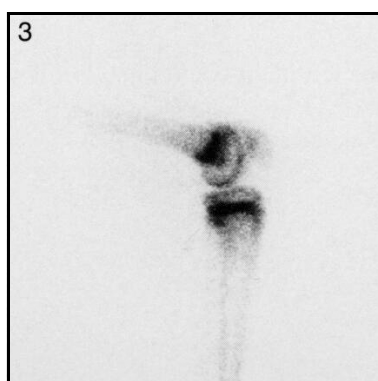
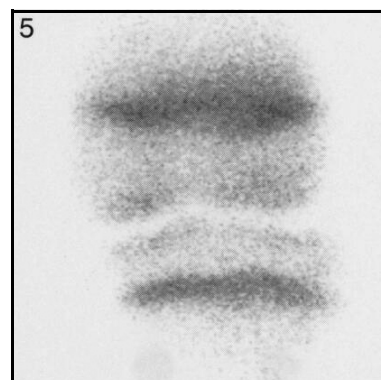
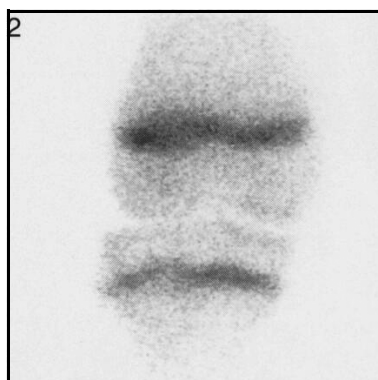
*FIG. 4. Anterior view of knees.*

*FIG. 2. Anterior pinhole view of right knee.*

*FIG. 5. Anterior pinhole view of left knee.*

*FIG. 3. Lateral view of left knee.*

*FIG. 6. Lateral view of right knee.*



**Technical comment**

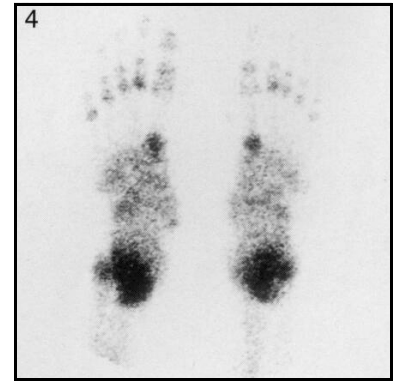
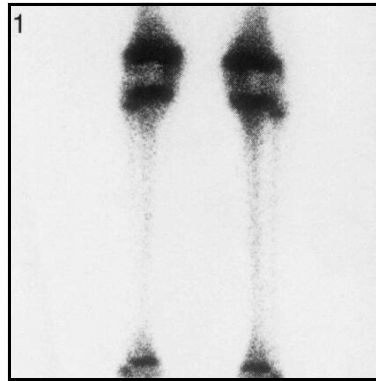
The fibula is not seen in Figs 3 and 6 because the images are medial lateral views.

## 15: Age 12–13 years

## Knees, tibia, fibula, ankles and feet

*FIG. 1. Posterior view of knees, tibia, fibula and ankles.*

*FIG. 4. Anterior view of feet.*



### Potential pitfall

The lack of clarity of the epiphyseal plates around the knees in Fig. 1 is due to overexposure during the acquisition.

## **16. AGE 13–14 YEARS**



## 16: Age 13–14 years

## Blood pool images

*FIG. 1. Posterior view of skull and upper limbs.*

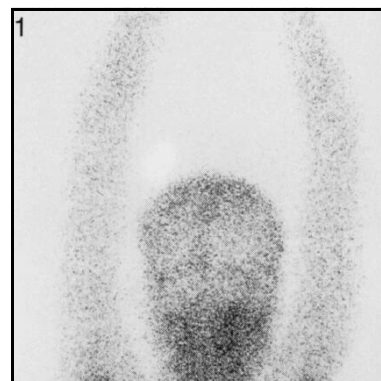


*FIG. 2. Anterior view of spine and pelvis.*

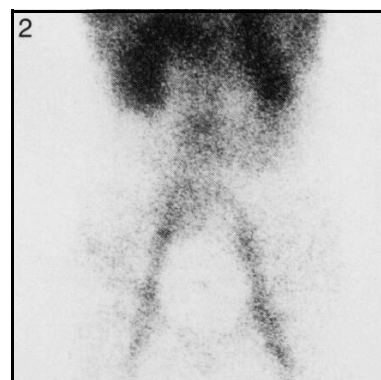
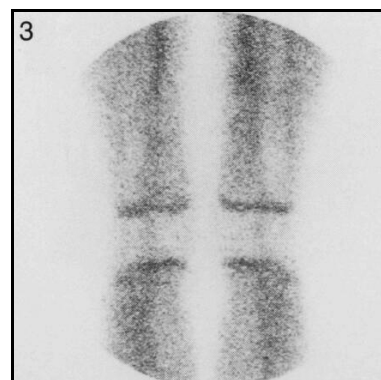


*FIG. 3. Anterior view of knees.*



### Technical comment

The full bladder is seen as a photon deficient area in Fig. 2.

*FIG. 1. A double headed whole body gamma camera was used. Left image is anterior view; right image is posterior view.*



**Technical comments**

Note the extravasation of isotope at the site of injection in the left hand.  
Marker on the right side.

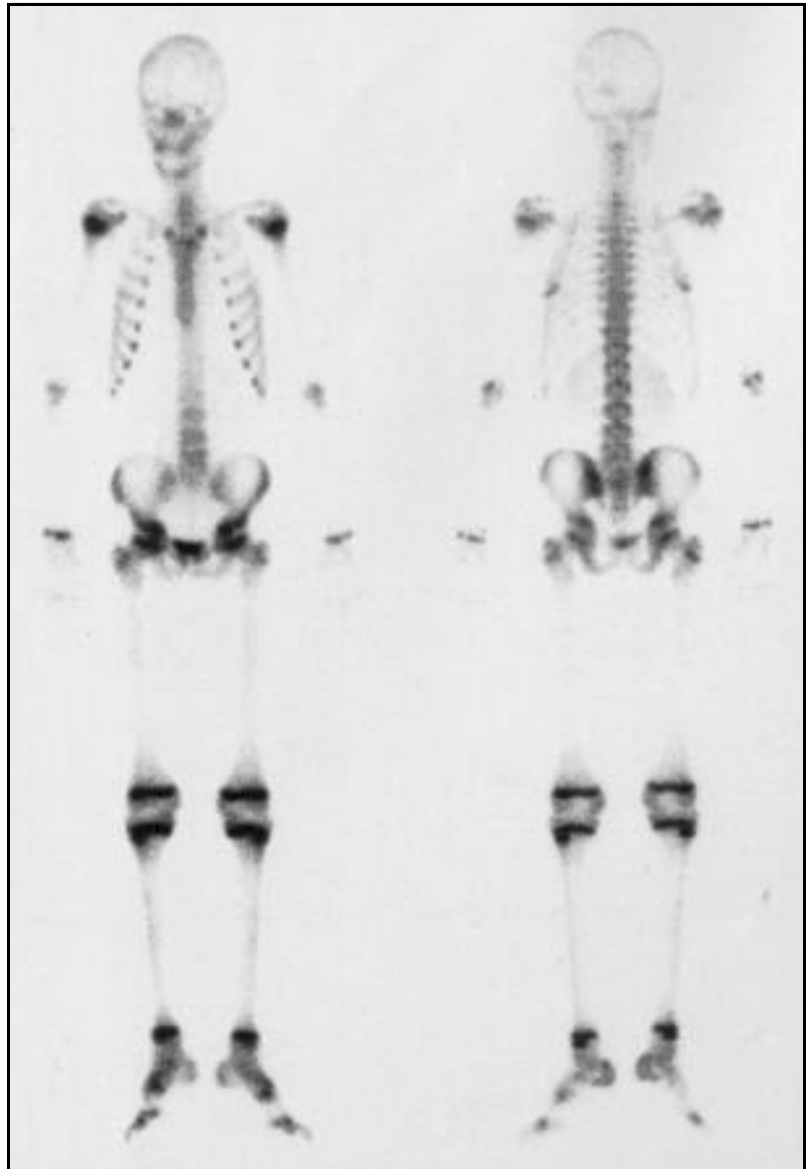
*FIG. 1. A double headed whole body gamma camera was used. Left image is anterior view; right image is posterior view.*



**Technical comments**

Urine contamination below the pelvis is seen.  
Marker on the right side.

*FIG. 1. A double headed whole body gamma camera was used. Left image is anterior view; right image is posterior view.*



**Technical comment**

Both feet are poorly positioned.



## 16: Age 13–14 years

## Skull

*FIG. 1. Anterior view of skull.*

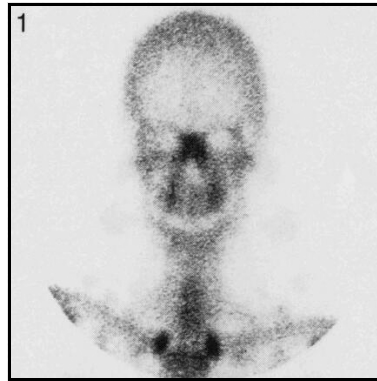


*FIG. 4. Posterior view of skull.*

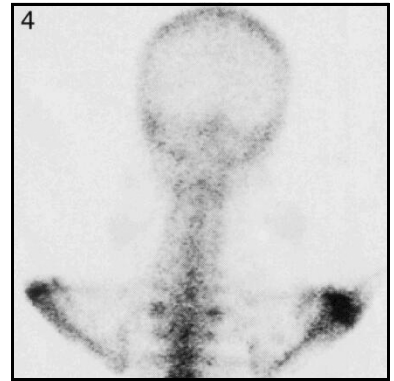


*FIG. 2. Right lateral view of skull.*



*FIG. 5. Left lateral view of skull.*



### Technical comment

The lateral views of the skull (Figs 2 and 5) were taken posteriorly.

## 16: Age 13–14 years

## Skull and upper limbs

*FIG. 1. Right lateral view of skull and right upper limb.*

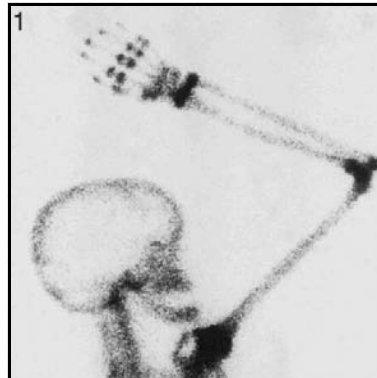


*FIG. 4. Left lateral view of skull and left upper limb.*

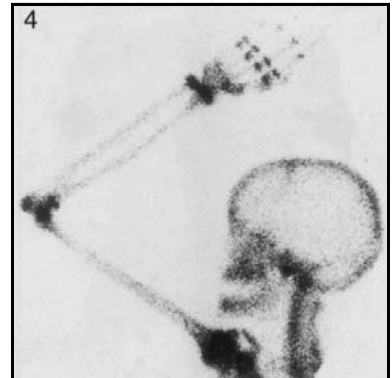


*FIG. 2. Anterior view of right upper limb.*

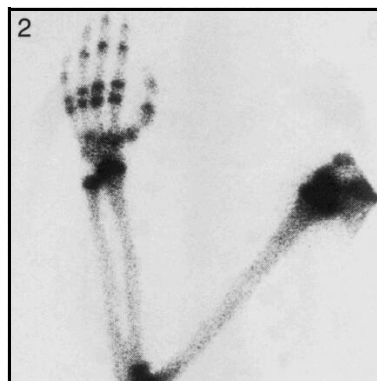
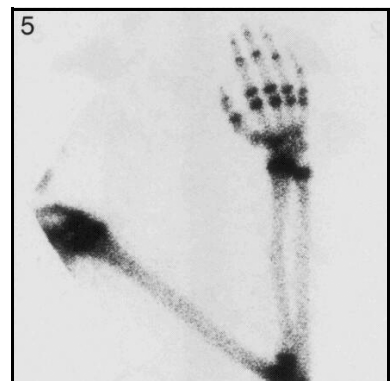


*FIG. 5. Anterior view of left upper limb.*



### Technical comment

The lateral views of the skull (Figs 1 and 4) were taken posteriorly.

*FIG. 1. Anterior view of thorax.*



*FIG. 4. Anterior view of thorax and spine.*

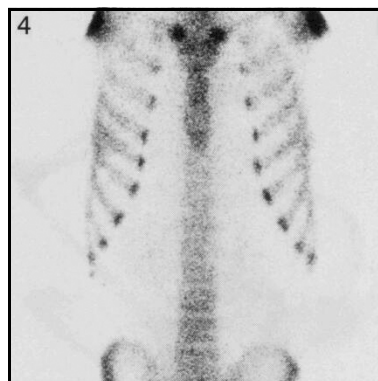


*FIG. 2. Anterior view of thorax and spine.*

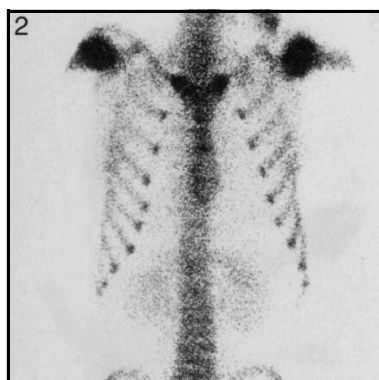


*FIG. 5. Anterior view of thorax.*

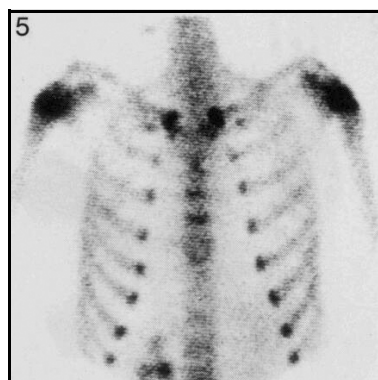
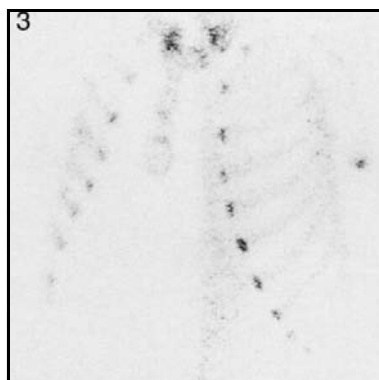


*FIG. 3. Left anterior oblique view of thorax.*



**Technical comments**

Note the differences in the sternum on both the anterior projections and also the anterior oblique.  
 Note the clarity of the lumbar spine in Figs 2 and 4.

*FIG. 1. Posterior view of thorax and spine.*

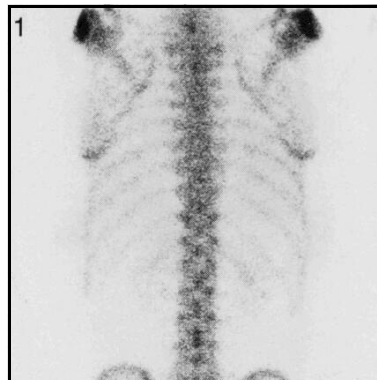


*FIG. 4. Posterior view of thorax and spine.*

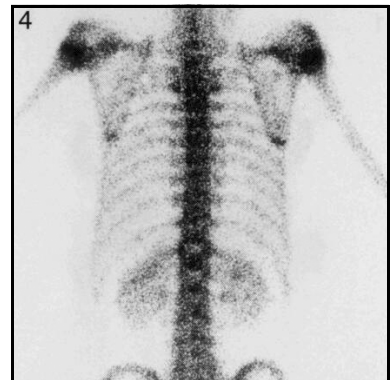


*FIG. 2. Posterior view of thorax and spine.*

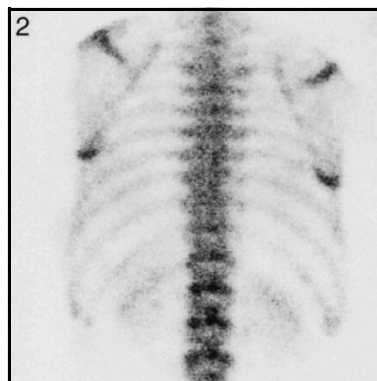
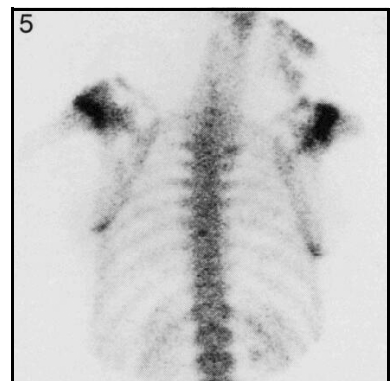


*FIG. 5. Posterior view of thorax and spine.*



**Technical comment**

Note the difference in positions of the scapulae in Fig. 1 compared with Fig. 4. This is due to the different positions of the upper limbs.

## 16: Age 13–14 years

## Spine, pelvis and femora

*FIG. 1. Anterior view of spine, pelvis and femora.*



*FIG. 4. Anterior view of spine, pelvis and femora.*



*FIG. 2. Anterior view of spine, pelvis and femora.*

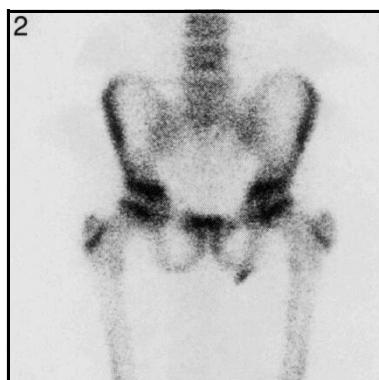
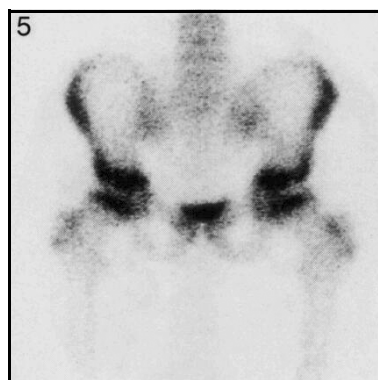


*FIG. 5. Anterior view of spine, pelvis and femora.*



### Technical comments

The lower lumbar spine is again clearly seen in the anterior views in Figs 1, 2 and 4. Urine contamination adjacent to the left ischium is seen in Fig. 2.

**16: Age 13–14 years**

**Spine, pelvis and femora**

*FIG. 1. Posterior view of spine, pelvis and femora.*



*FIG. 4. Posterior view of spine, pelvis and femora.*



*FIG. 2. Posterior view of spine, pelvis and femora.*

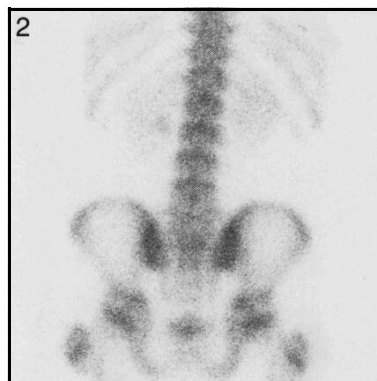


*FIG. 5. Posterior view of spine, pelvis and femora.*

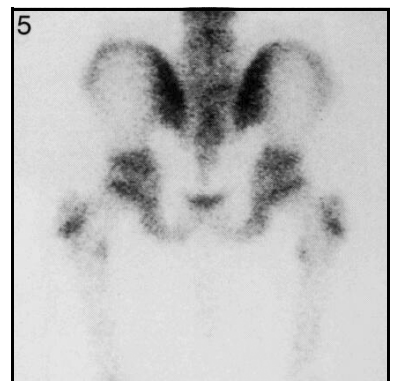
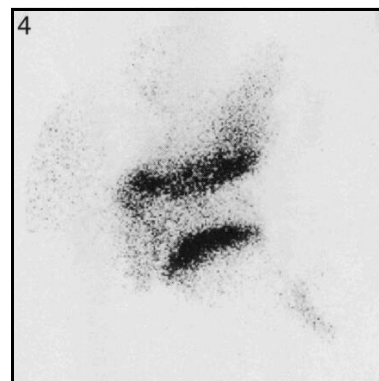
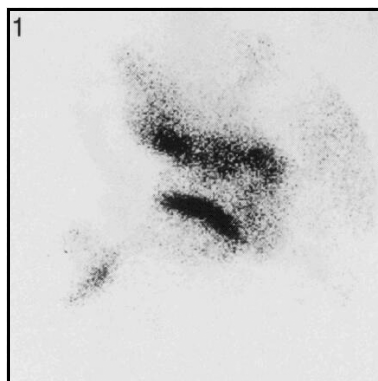


*FIG. 1. Pinhole view of right hip.*

*FIG. 4. Pinhole view of left hip.*



## 16: Age 13–14 years

## Lower limbs

*FIG. 1. Posterior view of femora and knees.*



*FIG. 4. Posterior view of femora and knees.*



*FIG. 2. Posterior view of tibia, fibula and ankles.*

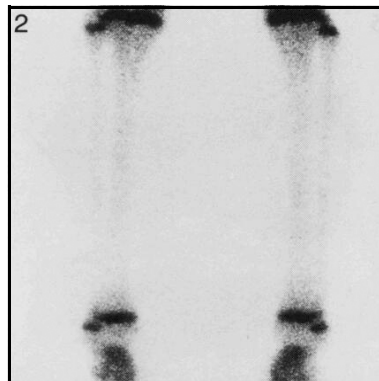


*FIG. 5. Posterior view of tibia, fibula and ankles.*

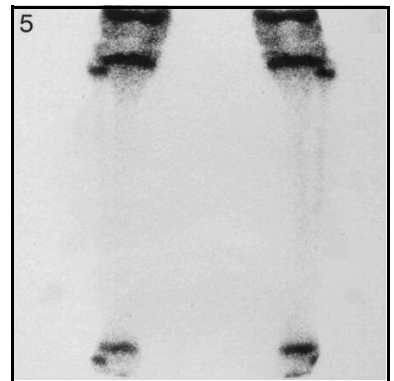




FIG. 1. Anterior view of knees.

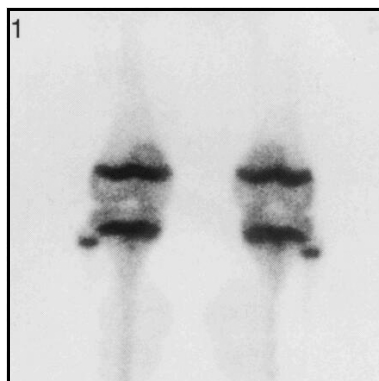


FIG. 4. Posterior view of knees.



FIG. 2. Anterior pinhole view of right knee.

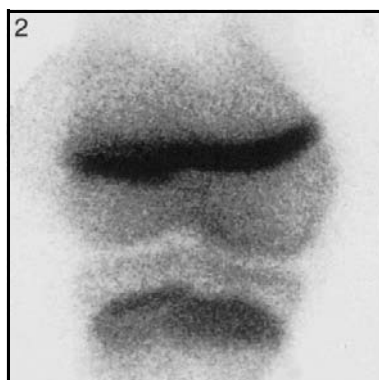


FIG. 5. Anterior pinhole view of left knee.

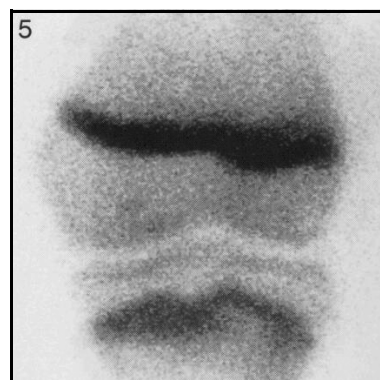


FIG. 3. Lateral view of knees.

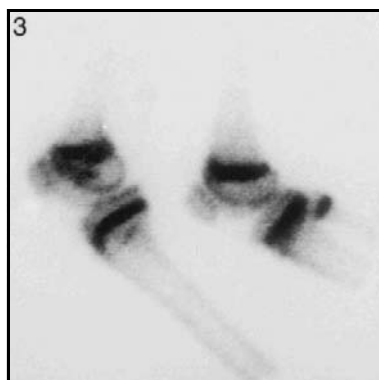
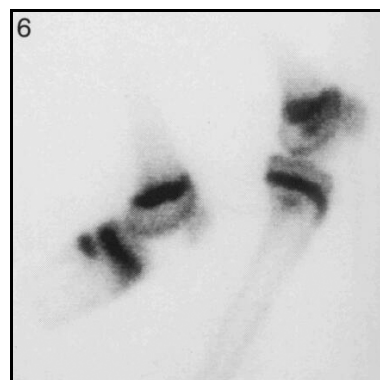


FIG. 6. Lateral view of knees.



### Technical comment

Figures 3 and 6 represent lateral images of the knees, on the left there is a medial lateral and a lateral lateral while on the right it is the reverse order. The lateral lateral images show the head of the fibula clearly while the medial lateral show the head of the fibula within the tibia but below the epiphyseal plate.

**16: Age 13–14 years**

**Tibia, ankles and feet**

*FIG. 1. Lateral view of tibia and ankles.*

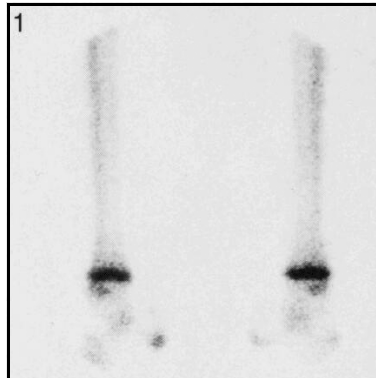


*FIG. 2. Anterior view of feet.*

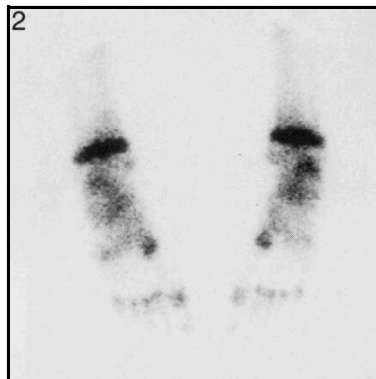
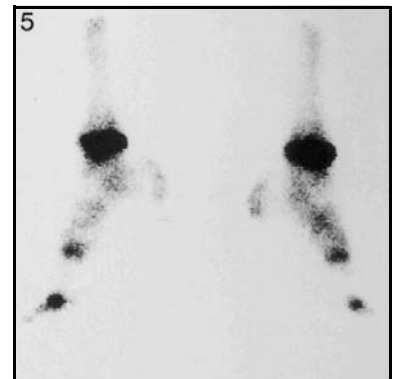


*FIG. 5. Lateral view of feet.*



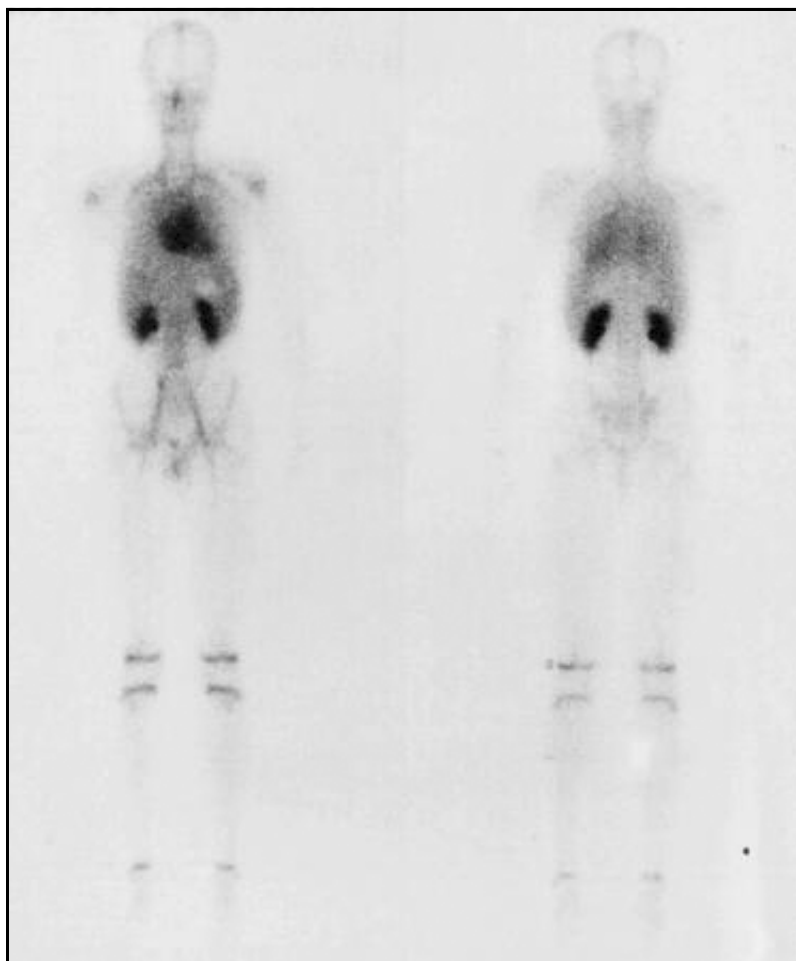
**Technical comment**

Note external rotation of the feet in Fig. 1, resulting in non-visualization of the epiphyseal plate at the distal end of the fibula.

## **17. AGE 14–15 YEARS**



*FIG. 1. A double headed whole body gamma camera was used. Left image is anterior view; right image is posterior view.*



**Technical comment**

Marker on the right side.

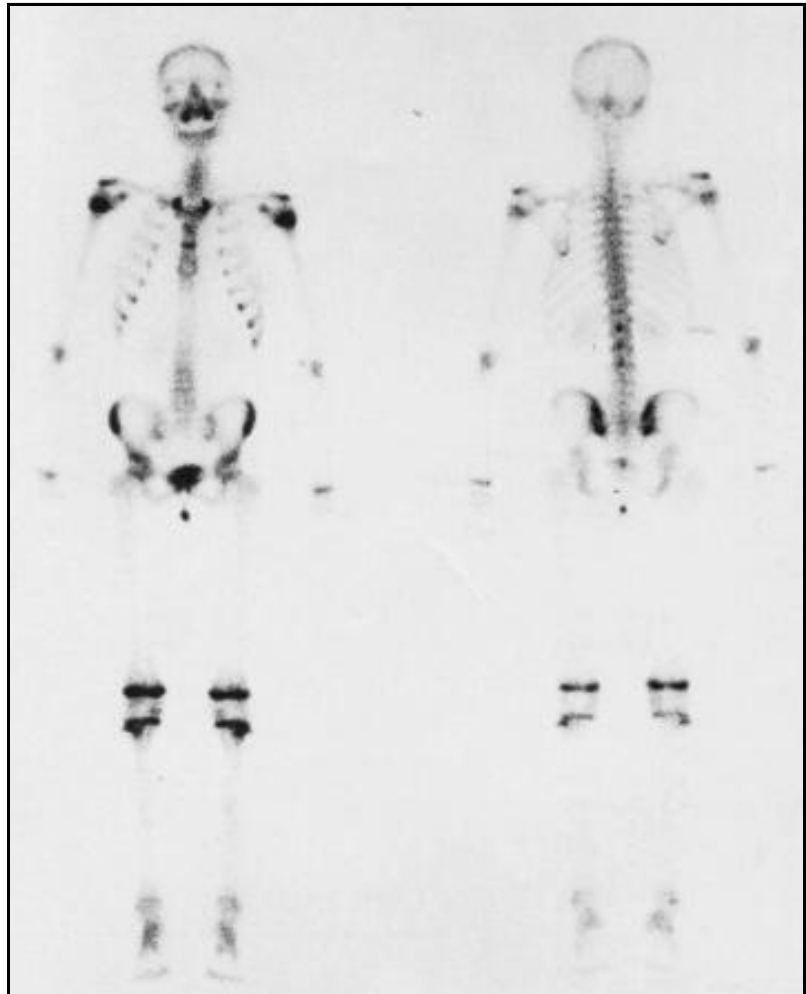
*FIG. 1. A double headed whole body gamma camera was used. Left image is anterior view; right image is posterior view.*



**Technical comments**

Note that in the anterior projection (on the left) the epiphyseal plates at the elbow, wrists and knees are not as distinct as in the posterior view (on the right). This is due to the greater distance of the patient from the detector. Marker on the right side.

*FIG. 1. A double headed whole body gamma camera was used. Left image is anterior view; right image is posterior view.*



**Technical comments**

Note the increased activity in the sternum in the anterior view. This is within the normal range. Sternal fusion has not yet occurred.

Urine contamination below the pelvis is seen.

Marker on the right side.

## 17: Age 14–15 years

## Skull, thorax and upper limb

*FIG. 1. Anterior view of skull and thorax.*

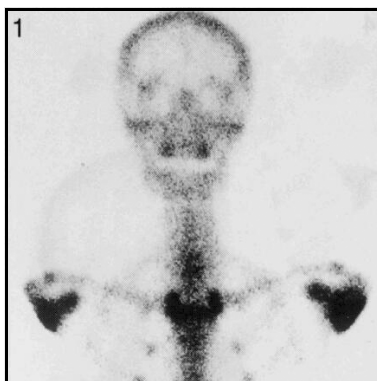


*FIG. 4. Posterior view of skull and thorax.*

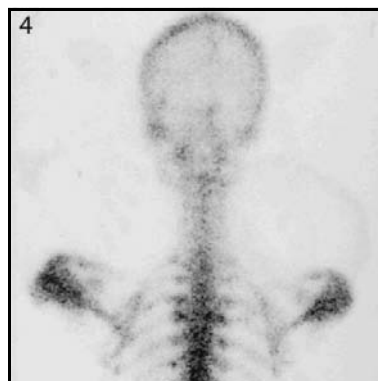


*FIG. 2. Right lateral view of skull and right upper limb.*

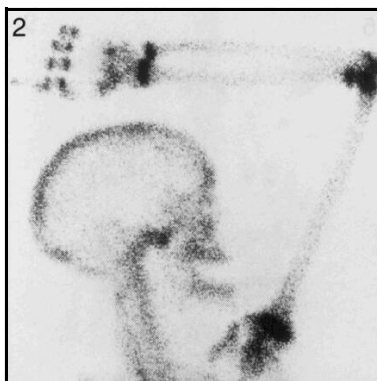
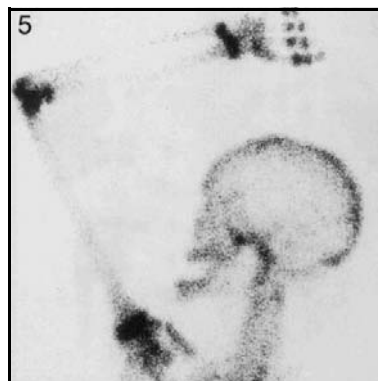


*FIG. 5. Left lateral view of skull and left upper limb.*



### Technical comments

The fingers of the hand in Figs 2 and 5 have been excluded from the field of view of the child's size. The lateral views of the skull (Figs 2 and 5) were taken posteriorly.



## 17: Age 14–15 years

## Skull and upper limbs

*FIG. 1. Right lateral view of skull and right upper limb.*

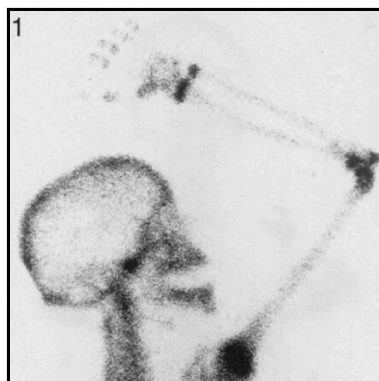


*FIG. 4. Left lateral view of skull and left upper limb.*



*FIG. 2. Anterior (upper) view of hands.*

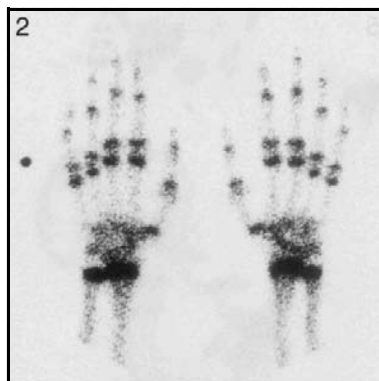
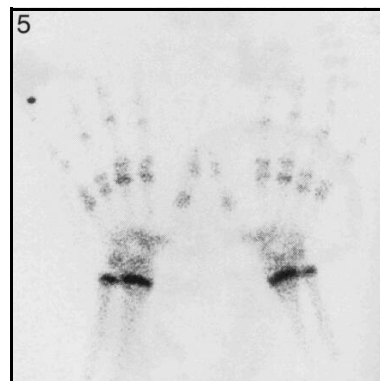


*FIG. 5. Anterior (upper) view of hands.*



### Technical comments

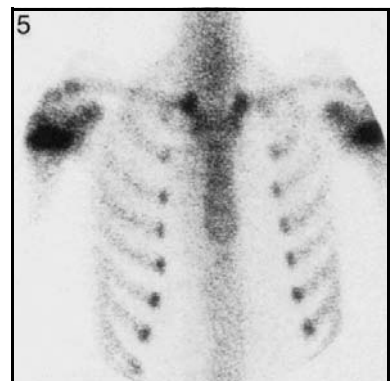
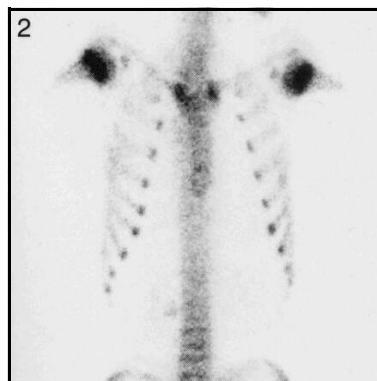
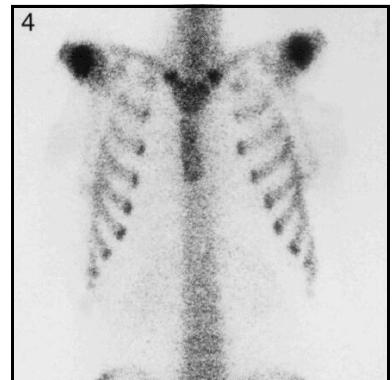
Note that part of the occipital bone in Fig. 1 has been excluded from the field of view.  
The lateral views of the skull (Figs 1 and 4) were taken posteriorly.  
The marker is adjacent to the right hand in Figs 2 and 5.

*FIG. 1. Anterior view of thorax.*

*FIG. 4. Anterior view of thorax and spine.*

*FIG. 2. Anterior view of thorax and spine.*

*FIG. 5. Anterior view of thorax.*



**Technical comment**

Note the variation of the sternum in these four children, but all within the normal range.

*FIG. 1. Right anterior oblique view of thorax.*



*FIG. 4. Left anterior oblique view of thorax.*

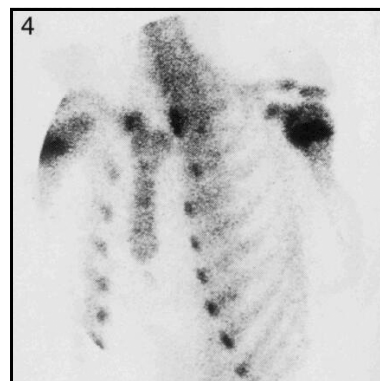
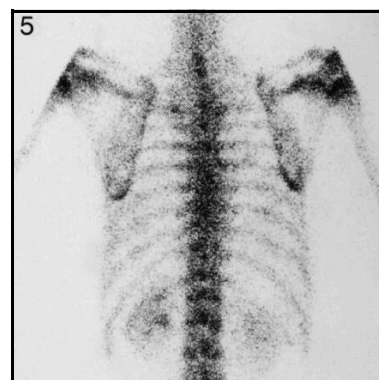
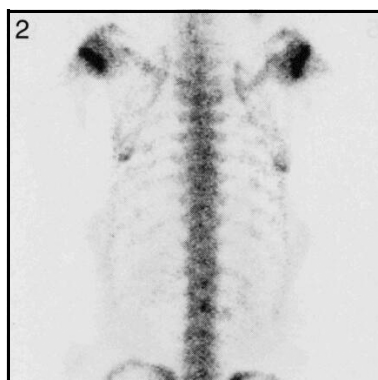
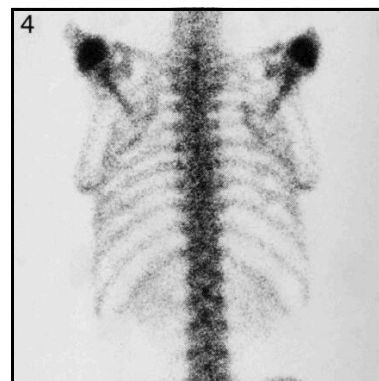
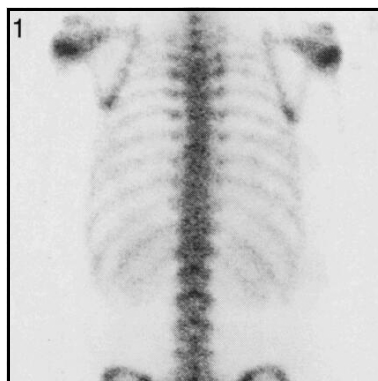


FIG. 1. Posterior view of thorax and spine.

FIG. 4. Posterior view of thorax and spine.

FIG. 2. Posterior view of thorax and spine.

FIG. 5. Posterior view of thorax and spine.



#### Technical comment

Note the variation of the appearances of the scapulae.

#### Potential pitfall

Focal increased activity is noted in Fig. 5 in the region of the mid-portion of the left third rib. This represents activity from the sternoclavicular joint, not a fracture of the rib.

## 17: Age 14–15 years

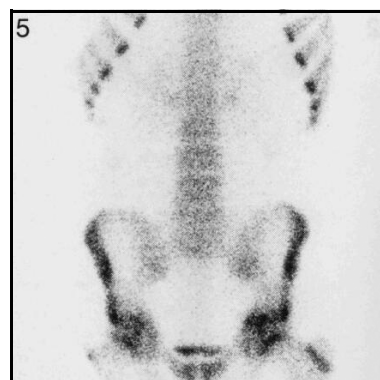
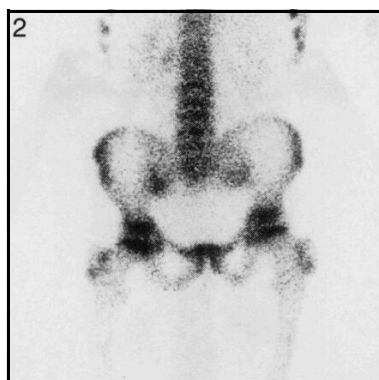
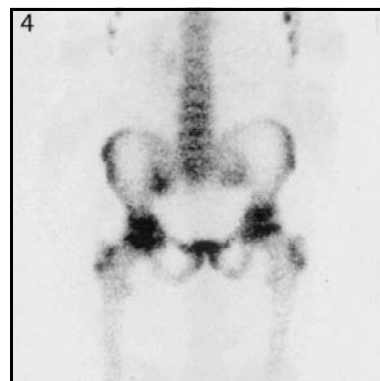
## Spine, pelvis and femora

*FIG. 1. Anterior view of spine and pelvis.*

*FIG. 4. Anterior view of spine, pelvis and femora.*

*FIG. 2. Anterior view of spine and pelvis.*

*FIG. 5. Anterior view of spine and pelvis.*



### Technical comment

Urine contamination to the left of the pubic bone is seen in Fig. 1.

## 17: Age 14–15 years

## Spine, pelvis and femora

*FIG. 1. Posterior view of spine, pelvis and femora.*



*FIG. 4. Posterior view of spine, pelvis and femora.*

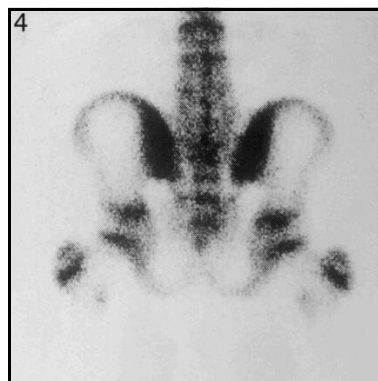


*FIG. 2. Posterior view of spine, pelvis and femora.*

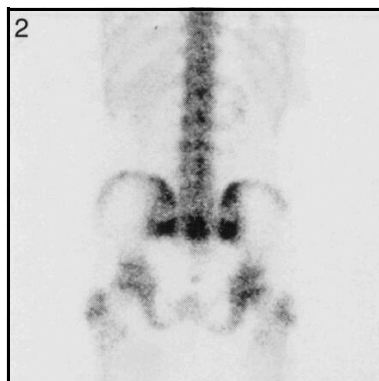
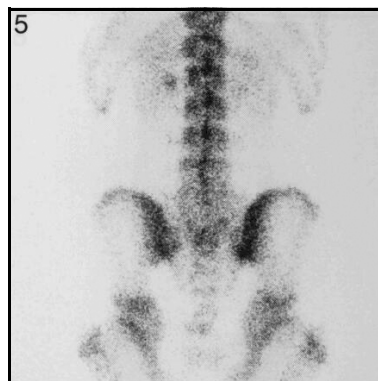


*FIG. 5. Posterior view of spine, pelvis and femora.*



### Technical comment

Note the non-uniformity of activity in Fig. 2 in both sacroiliac joints, with a relatively cool area in the mid-portion of the joints. This is within the normal range.

*FIG. 1. Pinhole view of right hip.*

*FIG. 4. Pinhole view of left hip.*

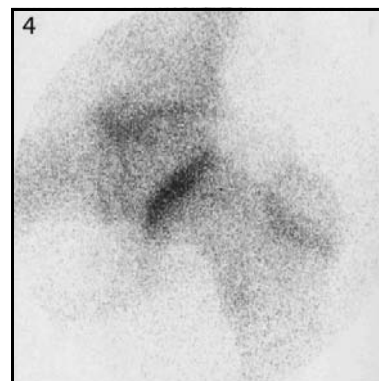
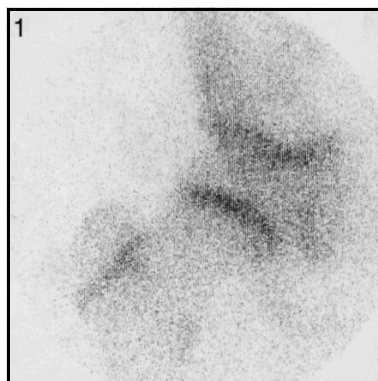
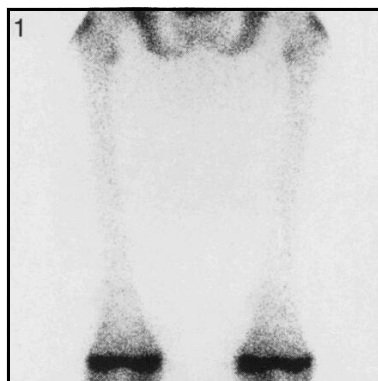


*FIG. 1. Posterior view of femora.*

*FIG. 4. Posterior view of femora and knees.*

*FIG. 2. Posterior view of tibia, fibula and ankles.*

*FIG. 5. Posterior view of tibia, fibula and ankles.*



**Technical comment**

Note the non-homogeneous distribution of isotope in the tibia with apparent slight increase in the mid-portion in Figs 2 and 5. Both of these children underwent 10 year follow-up and no abnormality was detected (see also pp. 220 and 236).



*FIG. 1. Posterior view of knees.*

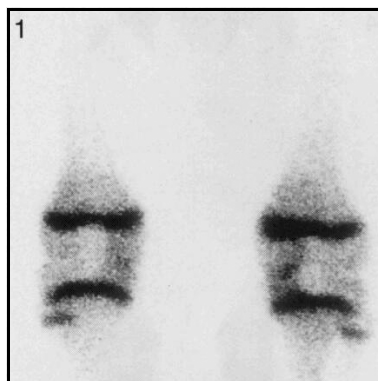


*FIG. 2. Anterior pinhole view of right knee.*

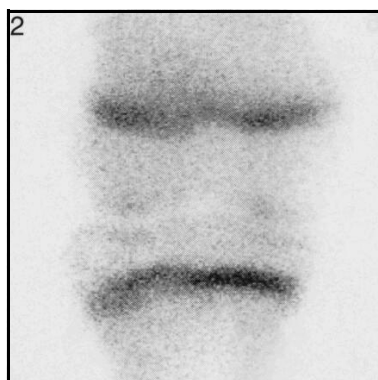


*FIG. 5. Anterior pinhole view of left knee.*

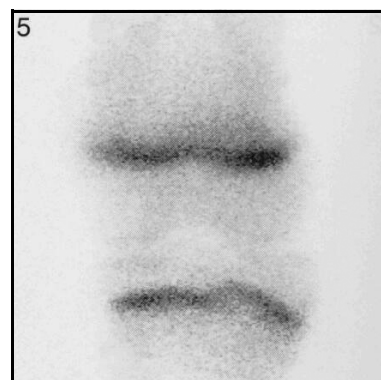
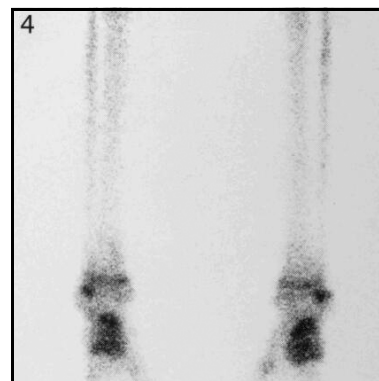
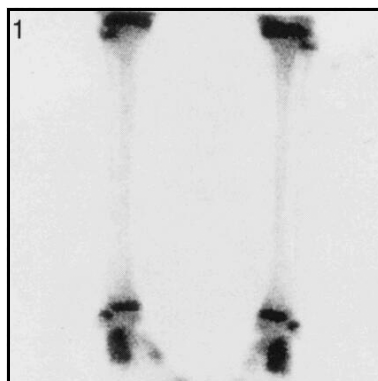


*FIG. 1. Posterior view of tibia, fibula and ankles.*

*FIG. 4. Posterior view of tibia, fibula and ankles.*



**Technical comment**

Note the patchy distribution of the isotope in the fibulae in Fig. 4.

## **18. AGE 15–17 YEARS**



**18: Age 15–17 years**

**Blood pool images**

*FIG. 1. Posterior view of pelvis.*

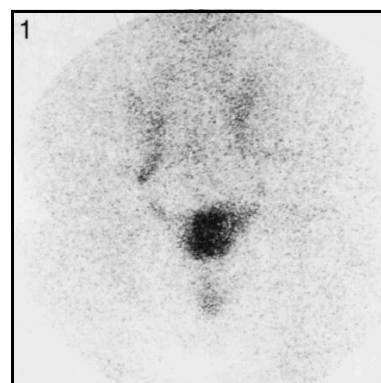


*FIG. 2. Anterior view of knees.*

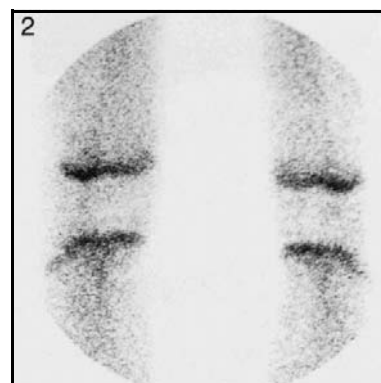
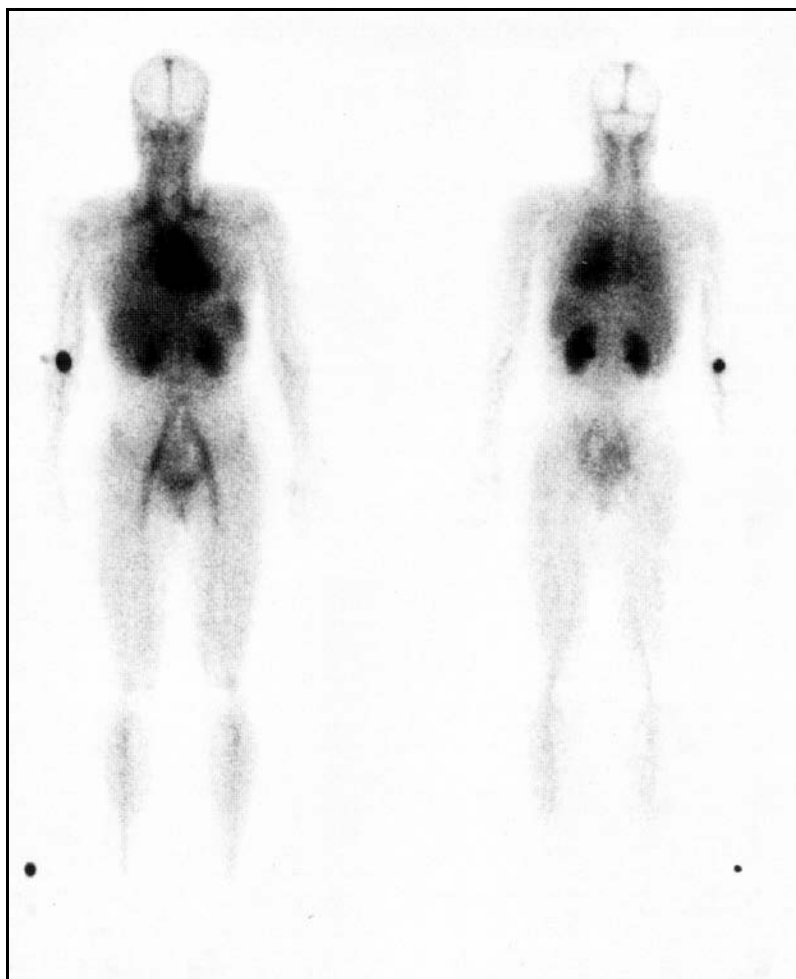


*FIG. 1. A double headed whole body gamma camera was used. Left image is anterior view; right image is posterior view.*



**Technical comments**

Note the extravasation of isotope at the site of injection in the right elbow.  
Marker on the right side.

*FIG. 1. A double headed whole body gamma camera was used. Left image is anterior view; right image is posterior view.*



**Technical comments**

Isotope in the breasts causes indistinctness of the ribs in the anterior view.  
Marker on the right side.

*FIG. 1. A double headed whole body gamma camera was used. Left image is anterior view; right image is posterior view.*



**Technical comments**

Isotope in the breasts causes indistinctness of the ribs in the anterior view.  
Marker on the right side.



*FIG. 1. Anterior view of skull.*

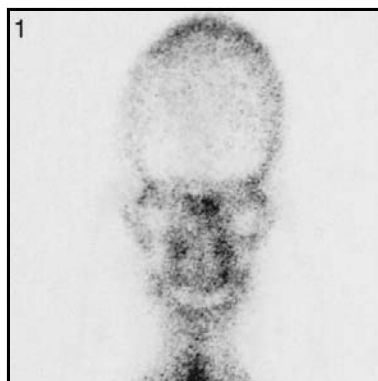


*FIG. 4. Posterior view of skull.*

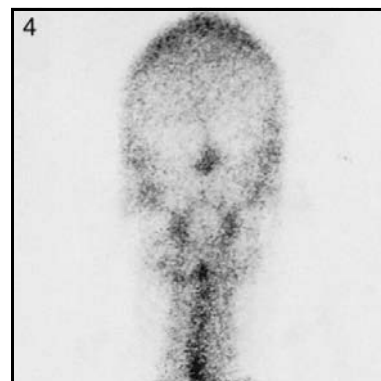


*FIG. 2. Right lateral view of skull and right upper limb.*

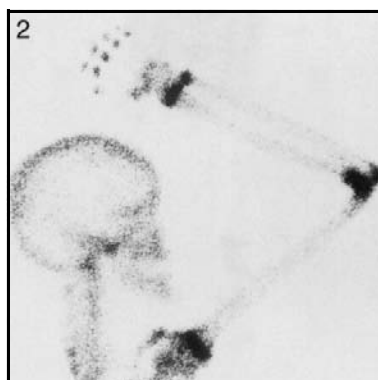


*FIG. 5. Left lateral view of skull and left upper limb.*

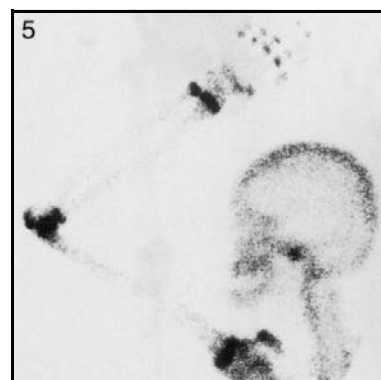


*FIG. 3. Anterior view of hands.*



**Technical comments**

Note the significant difference between the activity in the epiphyseal plates of the wrist in Figs 2, 3 and 5. The lateral views of the skull (Figs 2 and 5) were taken posteriorly. The tips of the fingers have not been included in the field of view of the gamma camera in Figs 2 and 5.

*FIG. 1. Anterior view of skull.*

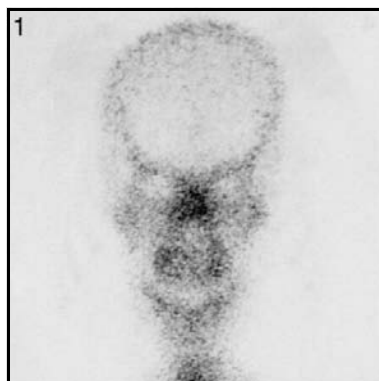


*FIG. 4. Posterior view of skull.*

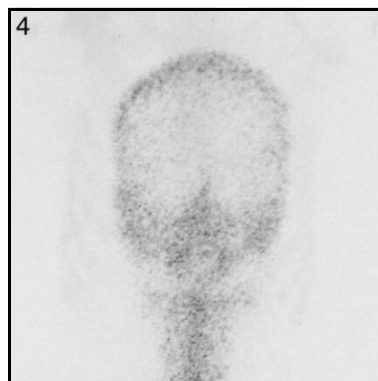
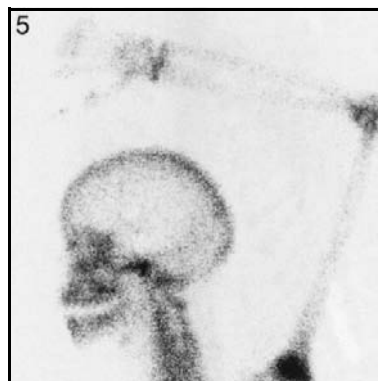


*FIG. 2. Right lateral view of skull and right upper limb.*



*FIG. 5. Left lateral view of skull and left upper limb.*



**Technical comments**

The lateral views of the skull (Figs 2 and 5) were taken anteriorly.

The tips of the fingers have not been included in the field of view of the gamma camera in Figs 2 and 5.

**18: Age 15–17 years**

**Thorax and spine**

*FIG. 1. Anterior view of thorax and spine.*

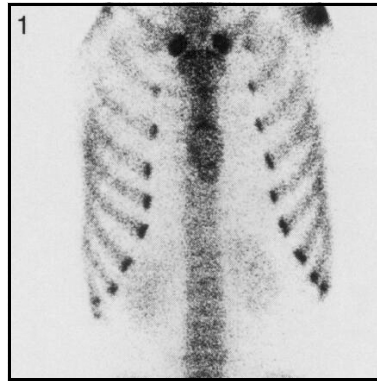


*FIG. 4. Anterior view of thorax and spine.*

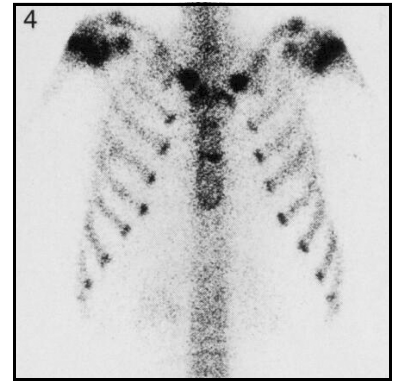


*FIG. 2. Anterior view of thorax and spine.*

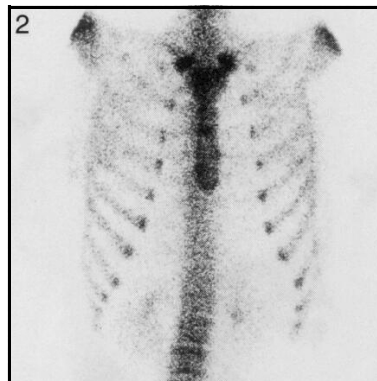
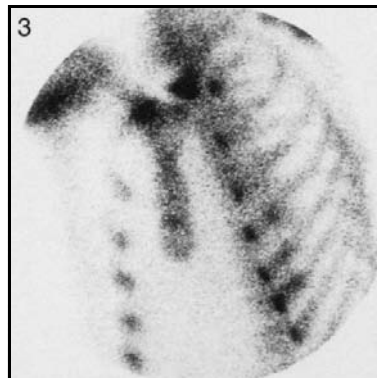


*FIG. 3. Left anterior oblique view of thorax.*



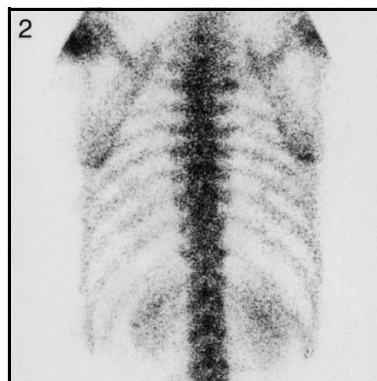
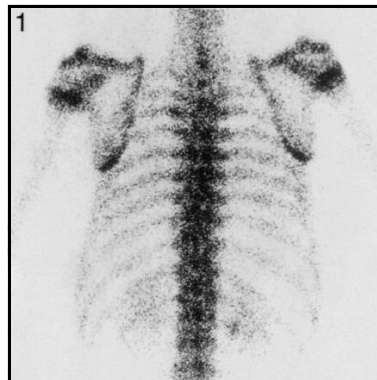
**18: Age 15–17 years**

**Thorax and spine**

*FIG. 1. Posterior view of thorax and spine.*

*FIG. 4. Posterior view of thorax and spine.*

*FIG. 2. Posterior view of thorax and spine.*



## 18: Age 15–17 years

## Spine, pelvis and femora

*FIG. 1. Anterior view of spine, pelvis and femora.*



*FIG. 4. Posterior view of spine, pelvis and femora.*



*FIG. 2. Anterior view of spine, pelvis and femora.*



*FIG. 5. Posterior view of spine and pelvis.*



### Technical comment

Urine contamination below the pelvis is seen in Fig. 2.

*FIG. 1. Pinhole view of right hip.*

*FIG. 4. Pinhole view of left hip.*

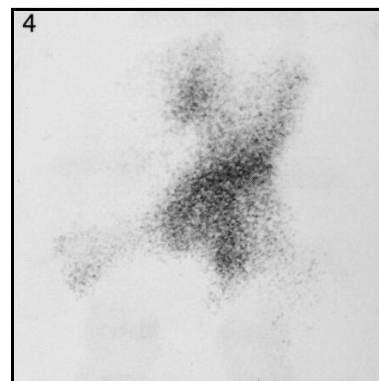
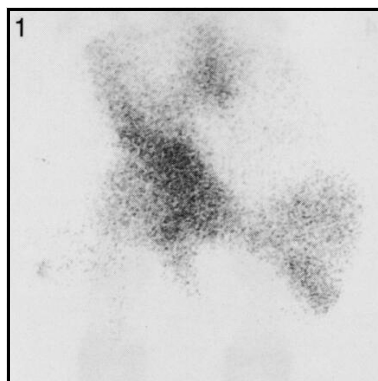


*FIG. 1. Posterior view of femora.*

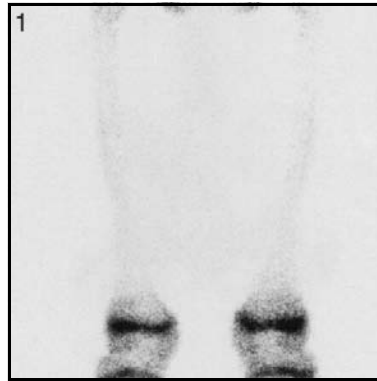


*FIG. 4. Posterior view of femora.*

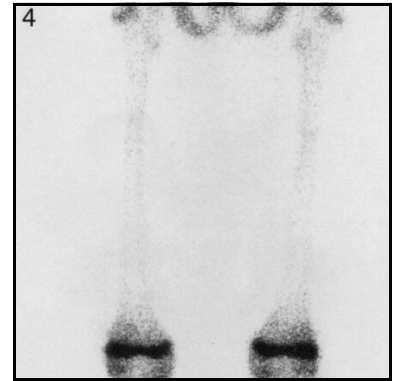


*FIG. 2. Posterior view of tibia, fibula and ankles.*

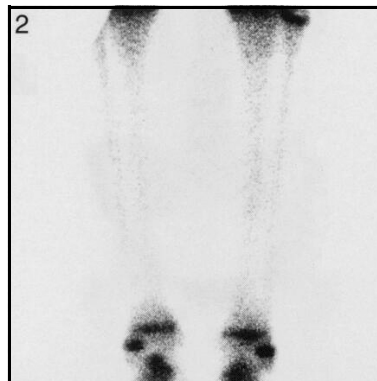


*FIG. 5. Posterior view of tibia, fibula and ankles.*

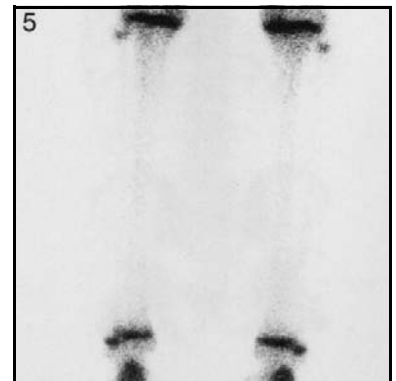


*FIG. 1. Posterior view of knees.*

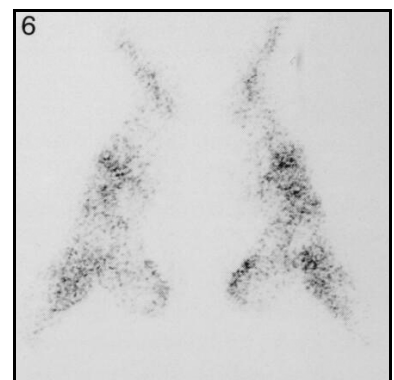
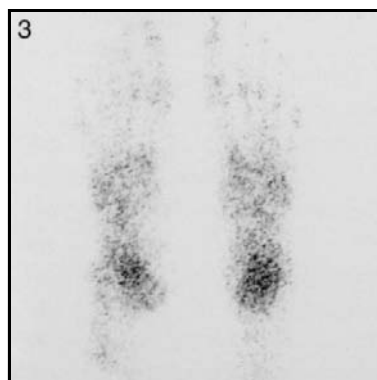
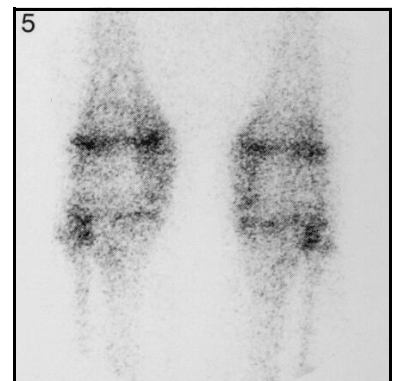
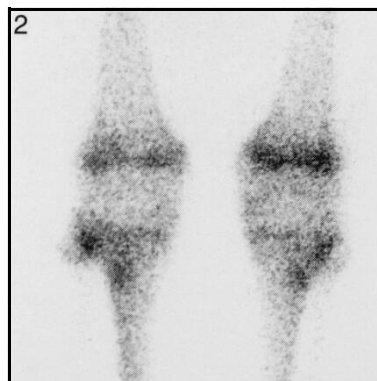
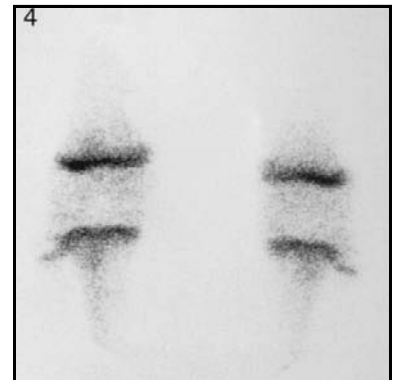
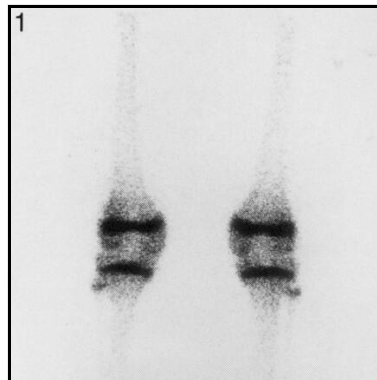
*FIG. 4. Posterior view of knees.*

*FIG. 2. Anterior view of knees.*

*FIG. 5. Posterior view of knees.*

*FIG. 3. Posterior view of feet.*

*FIG. 6. Lateral view of feet.*



**Technical comment**

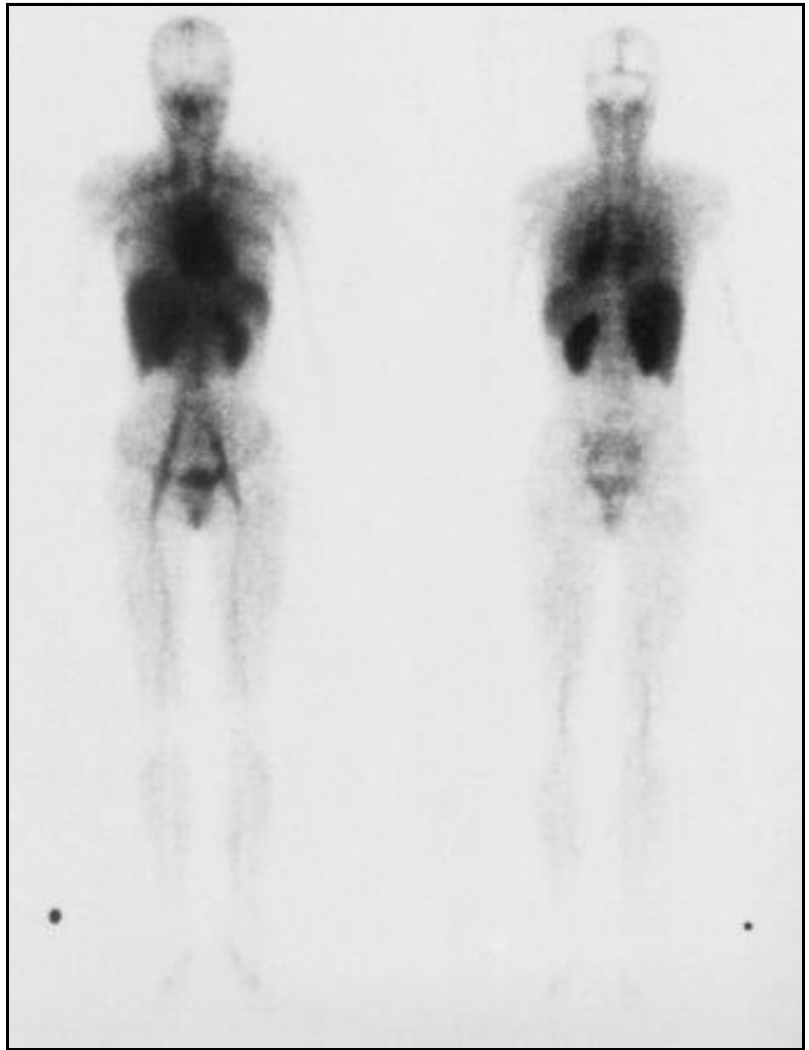
Note the difference in maturation of the epiphyseal plates in Figs 1, 2, 4 and 5.



## **19. AGE 17–22 YEARS**



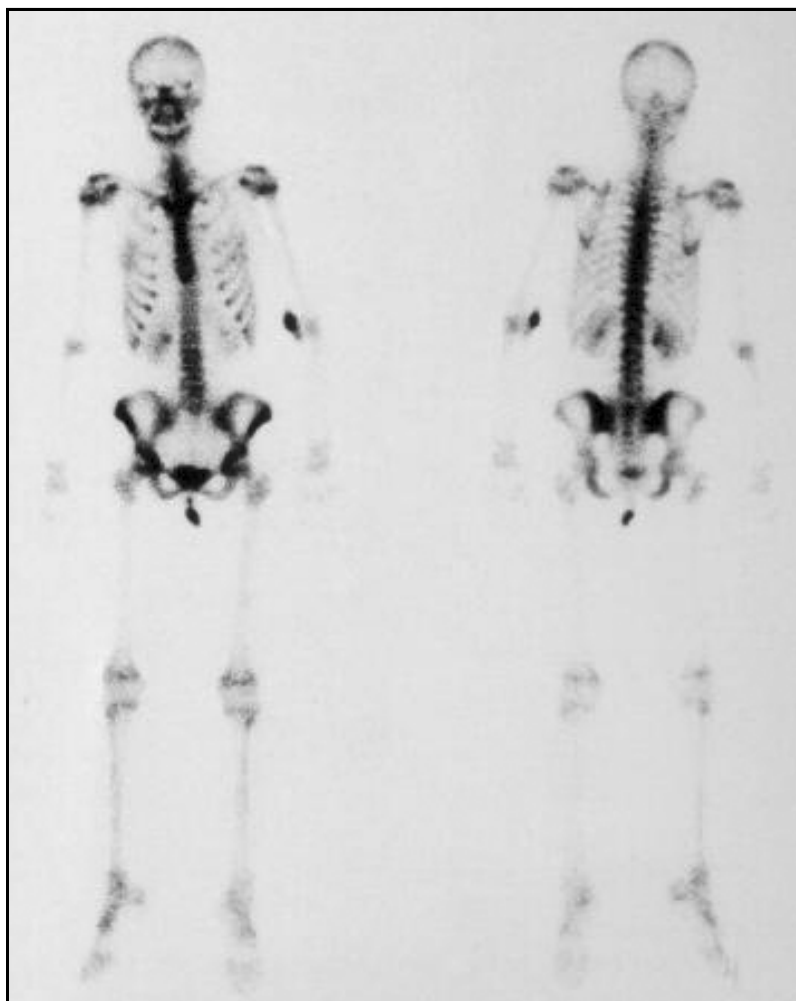
*FIG. 1. A double headed whole body gamma camera was used. Left image is anterior view; right image is posterior view.*



**Technical comments**

Note the mature skeleton with no visualization of epiphyseal plates.  
Marker on the right side.

*FIG. 1. A double headed whole body gamma camera was used. Left image is anterior view; right image is posterior view.*



**Technical comments**

Isotope in the breasts causes indistinctness of the ribs in the anterior view.

Note the poor positioning of the feet.

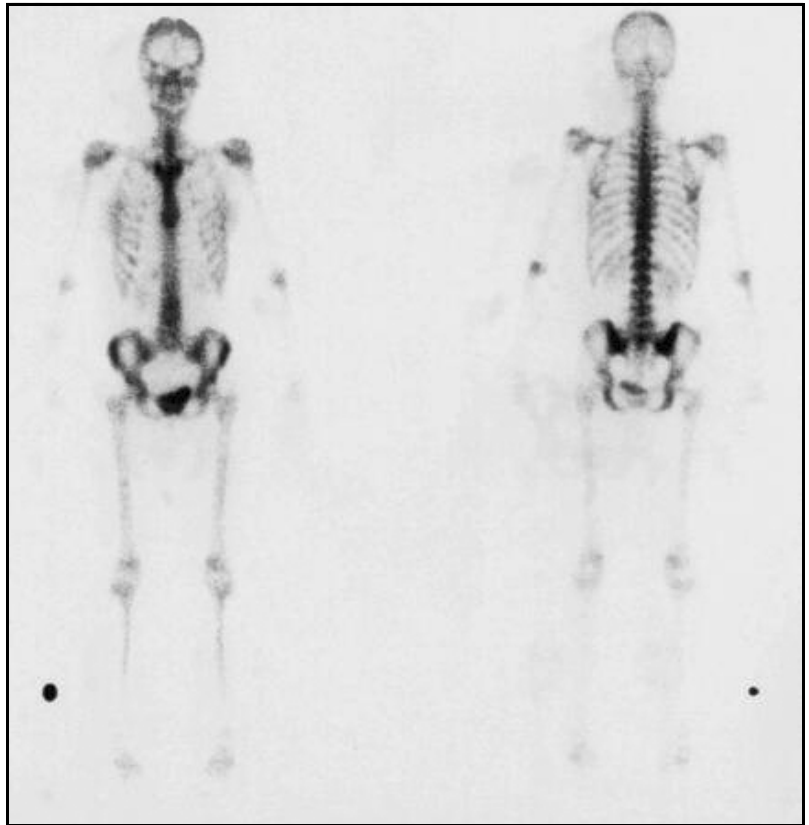
The focal area of apparent increased uptake in the left orbital region seen only in the anterior is probably due to rotation of the head.

Note the mature skeleton with no visualization of the epiphyseal plates.

Note the extravasation of isotope at the site of injection in the left elbow.

Urine contamination below the pelvis is seen.

*FIG. 1. A double headed whole body gamma camera was used. Left image is anterior view; right image is posterior view.*



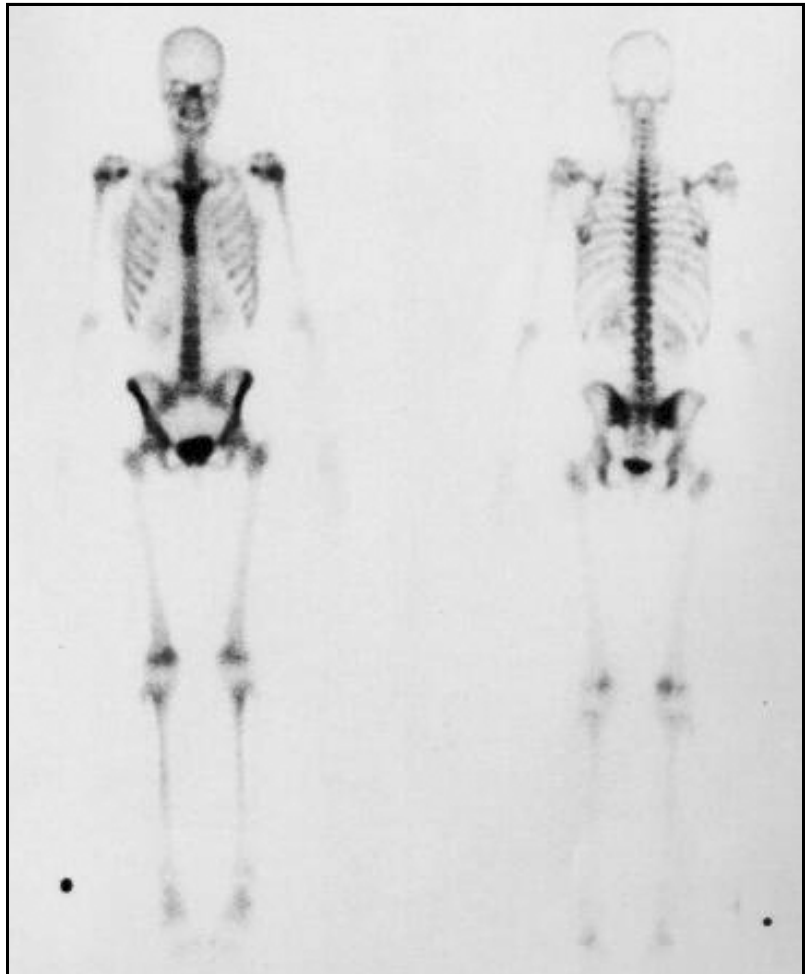
**Technical comments**

Isotope in the breasts causes indistinctness of the ribs in the anterior view.

Note the relatively mature skeleton with most of the epiphyseal plates virtually fused.

Marker on the right side.

*FIG. 1. A double headed whole body gamma camera was used. Left image is anterior view; right image is posterior view.*



**Technical comments**

Isotope in the breasts causes indistinctness of the ribs in the anterior view.  
Note the relatively mature skeleton with most of the epiphyseal plates virtually fused.  
Marker on the right side.

*FIG. 1. Anterior view of skull.*

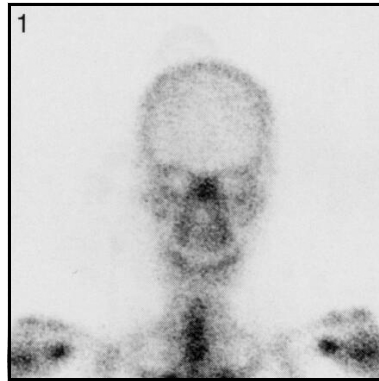


*FIG. 4. Posterior view of skull.*

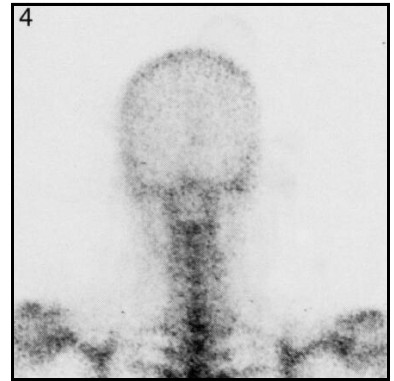


*FIG. 2. Right lateral view of skull.*

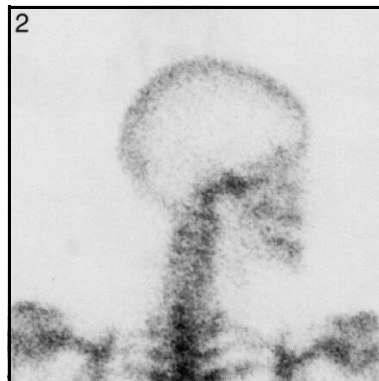
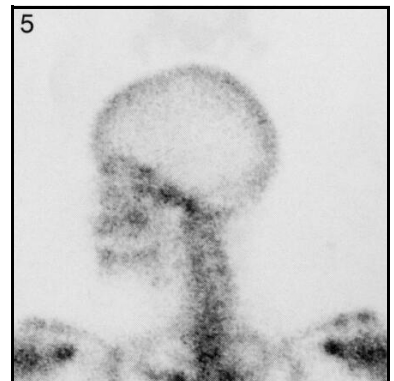


*FIG. 5. Left lateral view of skull.*



## 19: Age 17–22 years

## Skull and upper limbs

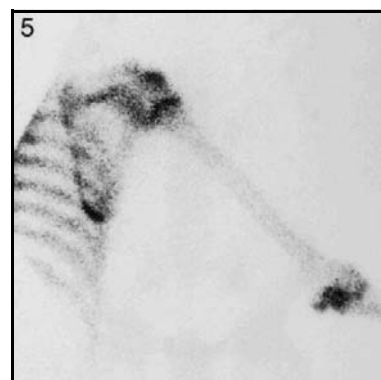
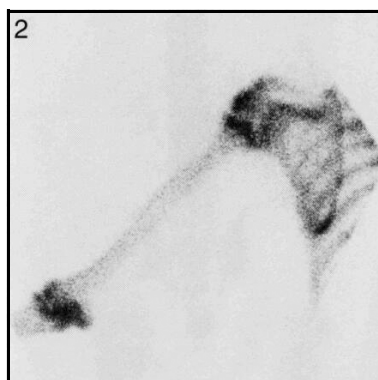
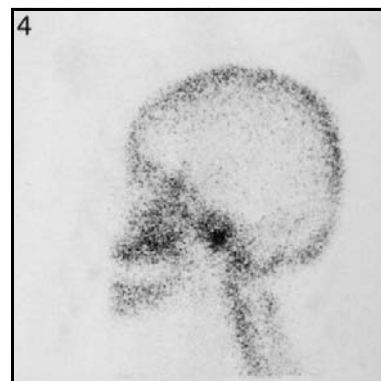
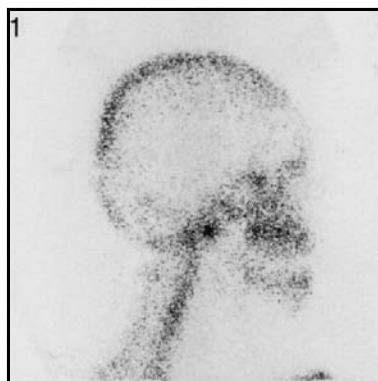
*FIG. 1. Right lateral view of skull.*

*FIG. 4. Left lateral view of skull.*

*FIG. 2. Posterior view of left humerus.*

*FIG. 5. Posterior view of right humerus.*

*FIG. 3. Anterior view of hands.*



### Technical comment

Note the variation in the maturity of the skeleton in this age group. The epiphyses around the hands and wrists are not yet fused in this particular case (Fig. 3).



*FIG. 1. Anterior view of thorax.*

*FIG. 4. Posterior view of thorax and spine.*

*FIG. 2. Anterior view of spine and pelvis.*

*FIG. 5. Posterior view of spine and pelvis.*

*FIG. 3. Pinhole view of right hip.*

*FIG. 6. Pinhole view of left hip.*

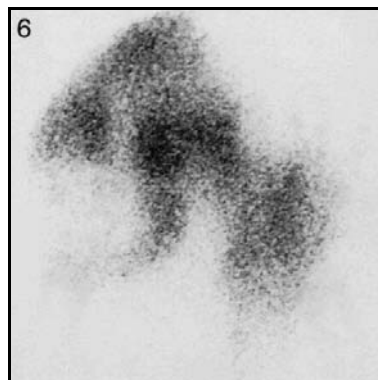
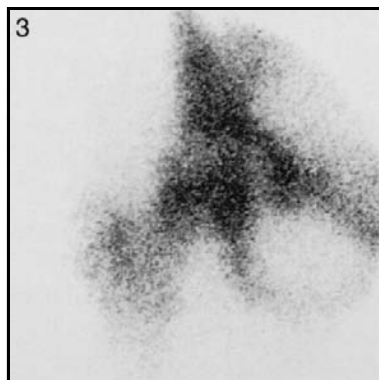
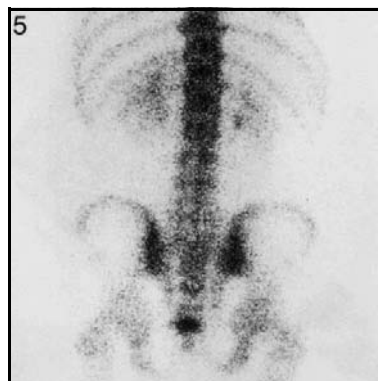
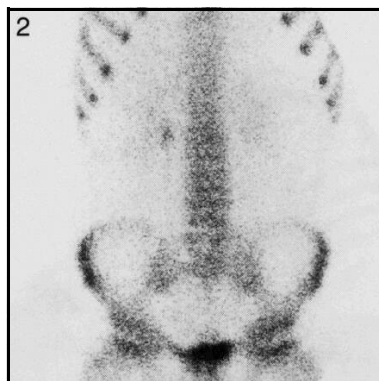
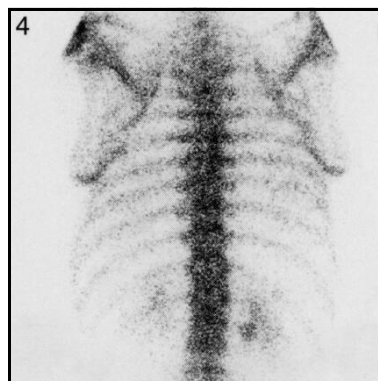
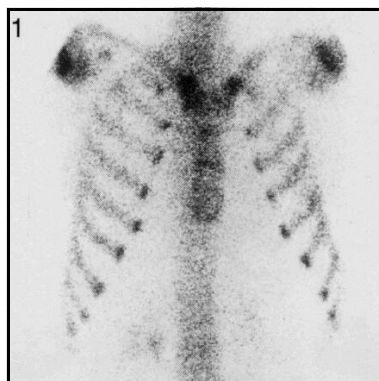


*FIG. 1. Posterior view of femora.*

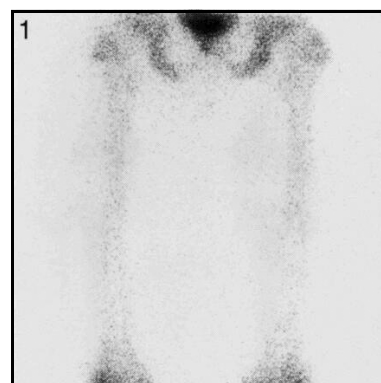
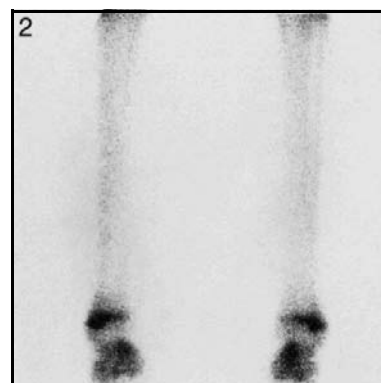


*FIG. 2. Posterior view of tibia, fibula and ankles.*



**19: Age 17–22 years**

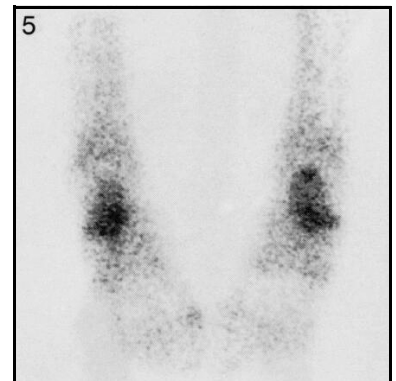
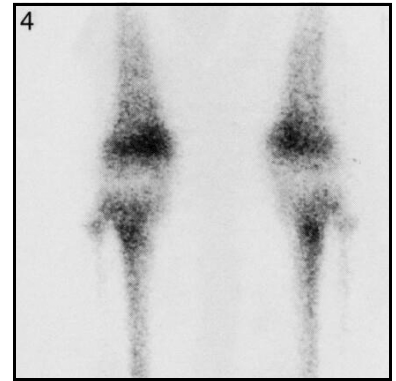
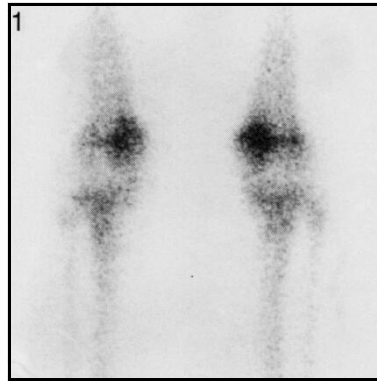
**Knees and feet**

*FIG. 1. Anterior view of knees.*

*FIG. 4. Posterior view of knees.*

*FIG. 2. Anterior view of feet.*

*FIG. 5. Posterior view of feet.*





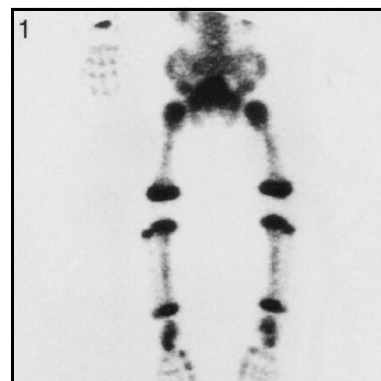
## **20. KNEES**



**20: Age:0–6 months**

**Knees**

*FIG. 1. Anterior view.*



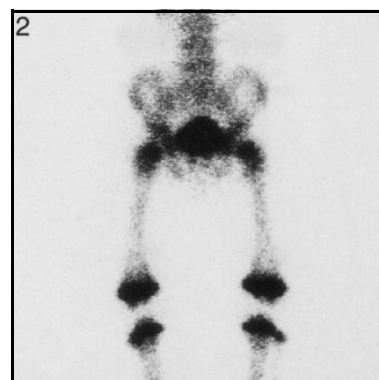
**Technical comment**

The toes are facing medially, in the radiographic neutral position. This is the reason for the fibula being clearly seen.

*FIG. 1. Anterior view.*



*FIG. 2. Anterior view.*



**Technical comments**

Figure 1 shows good positioning of the left knee and foot. This allows visualization of the left fibula. The fibula is not seen on the right due to poor positioning of both the knee and the foot.

Figure 2 shows good positioning of the left knee and foot. This allows visualization of the fibula.

Note the shape of the epiphyseal plates around the knees.

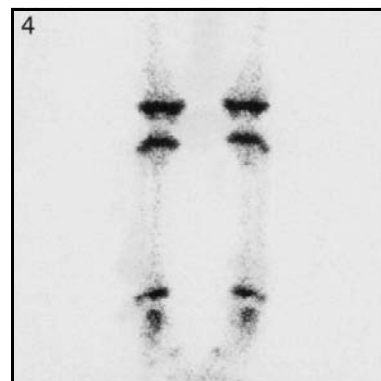
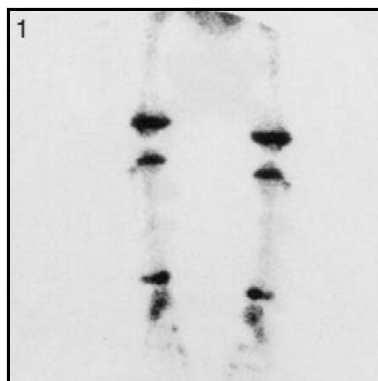


**20: Age: 1–2 years**

**Knees**

*FIG. 1. Anterior view.*

*FIG. 4. Anterior view.*



**Technical comment**

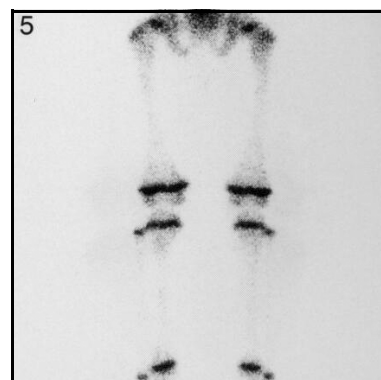
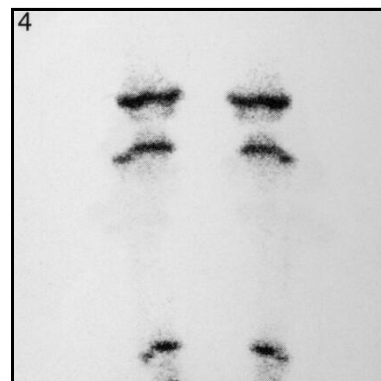
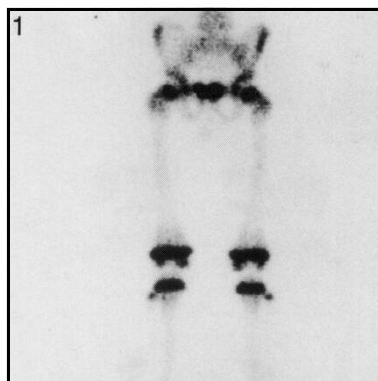
Good positioning for the knees, tibia and fibula. The fibula is clearly seen, separate from the tibia.

*FIG. 1. Anterior view.*

*FIG. 4. Anterior view.*

*FIG. 2. Anterior view.*

*FIG. 5. Anterior view.*



**Technical comments**

Note the clarity of the fibula, separate from the tibia, in Figs 1, 2, 4 and 5. This is due to the radiographic neutral position of the feet.

Note the progressive changes in the epiphyseal plates with maturation.

*FIG. 1. Anterior view.*

*FIG. 4. Anterior view.*

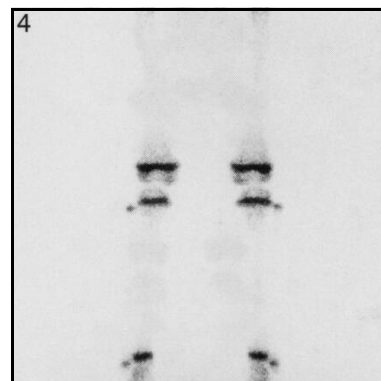
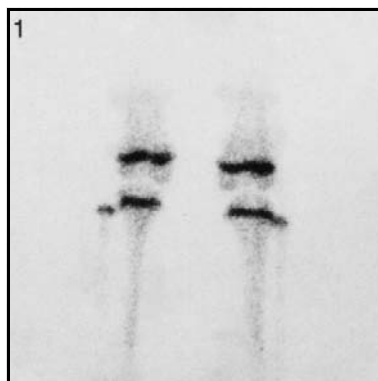
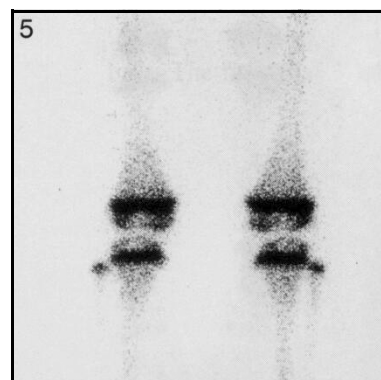


*FIG. 5. Posterior view.*



**Technical comment**

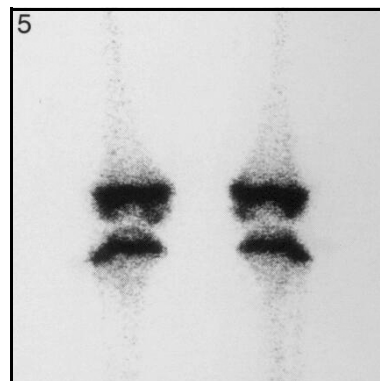
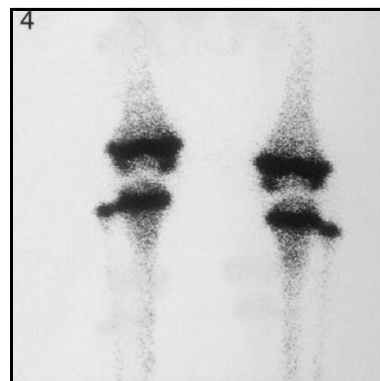
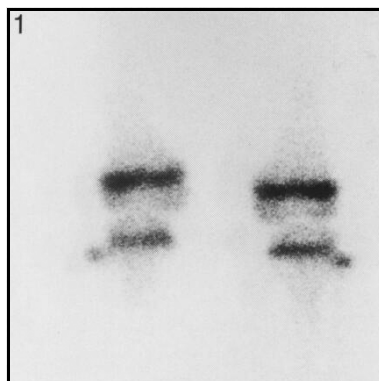
The clarity of the fibula in all images suggests good positioning of the feet.

*FIG. 1. Posterior view.*

*FIG. 4. Posterior view.*

*FIG. 2. Posterior view.*

*FIG. 5. Posterior view.*



**Technical comment**

Note the clarity of the heads of the fibulae in all the images. Also, note the clarity of the epiphyseal plates with their well-defined margins.

*FIG. 1. Posterior view.*

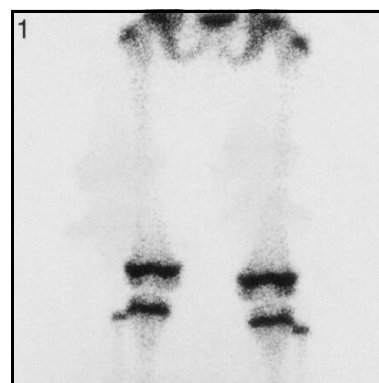
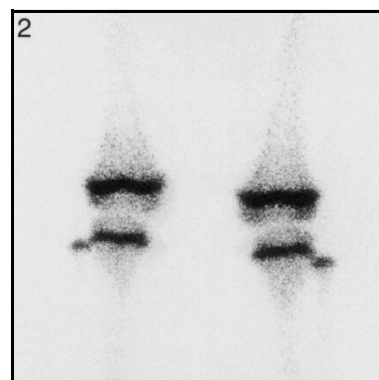


*FIG. 2. Posterior magnified view.*



**Technical comments**

The magnified view (Fig. 2) shows the epiphyseal plates to best advantage.

The fibula is clearly seen in both figures because the toes were turned inwards during image acquisition.

*FIG. 1. Posterior magnified view.*

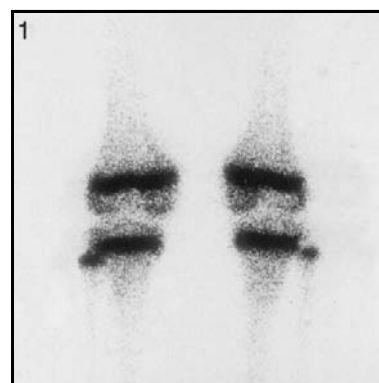
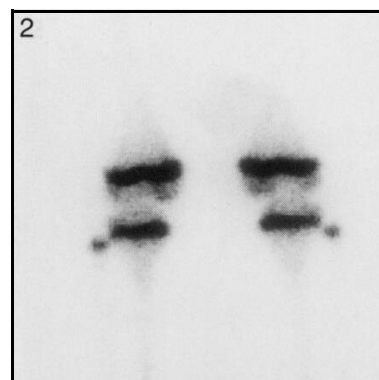


*FIG. 2. Posterior view.*



**Technical comment**

Note the clear definition of the growth plate from the adjacent metaphyses.

*FIG. 1. Posterior magnified view.*

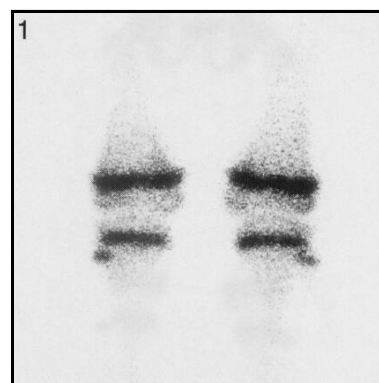


*FIG. 2. Posterior magnified view.*

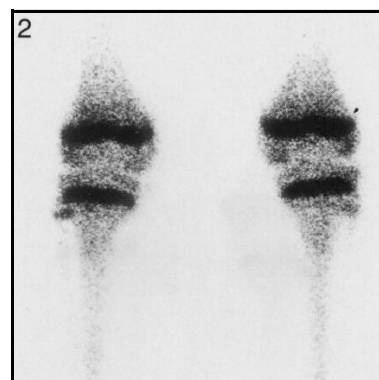
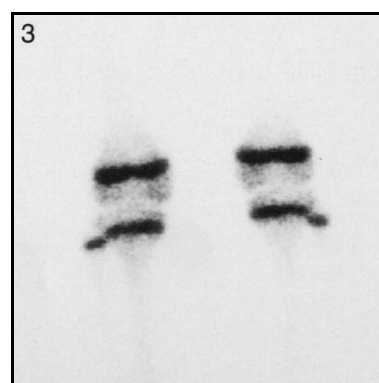


*FIG. 3. Posterior view.*



**Technical comments**

There is clear separation between the upper tibia and the fibula due to good positioning. Slight overexposure is seen in Fig. 2, which shows the tibia better but causes overexposure of the epiphyseal plates. This is the reason for the different appearance of this image compared with Figs 1 and 3.

FIG. 1. Posterior view.

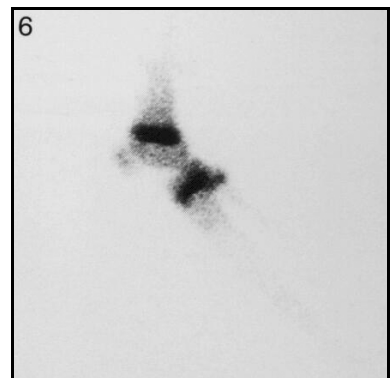
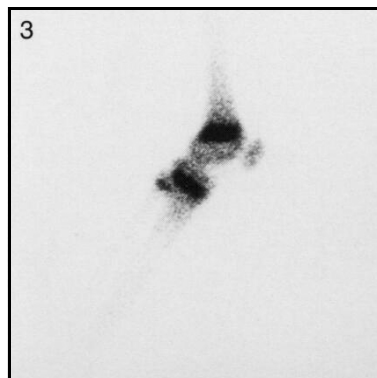
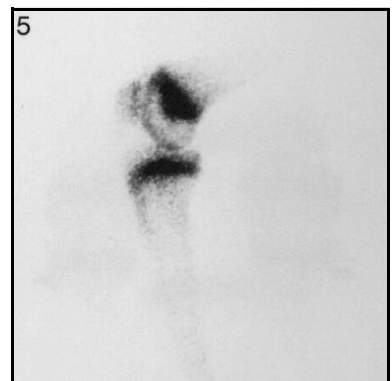
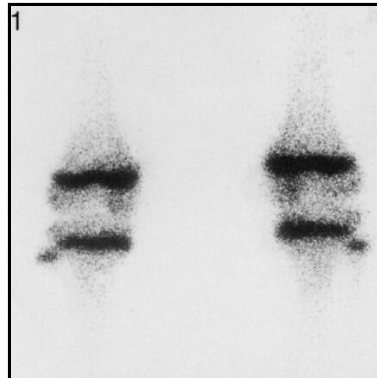
FIG. 4. Anterior view.

FIG. 2. Medial lateral view of left knee.

FIG. 5. Medial lateral view of right knee.

FIG. 3. Lateral lateral view of right knee.

FIG. 6. Lateral lateral view of left knee.



### Technical comment

The pair of lateral knees shown in Figs 2 and 5 represents medial lateral knees while Figs 3 and 6 represent lateral knees in the lateral projection. This accounts for the clarity of the fibula in the lower series and the difficulty in seeing the fibula in the upper series.



*FIG. 1. Posterior view.*

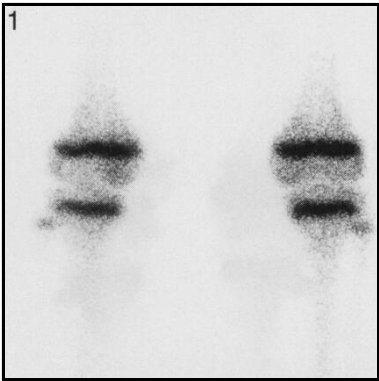


*FIG. 4. Posterior view.*

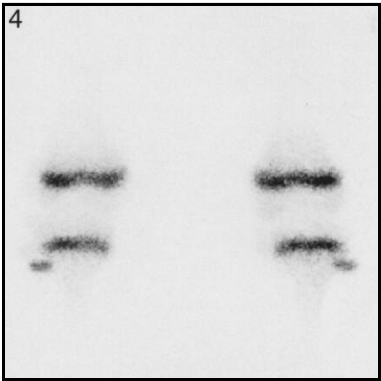


*FIG. 2. Posterior view.*

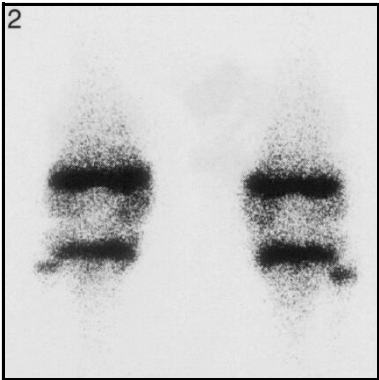
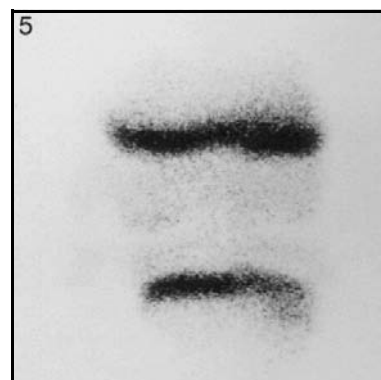
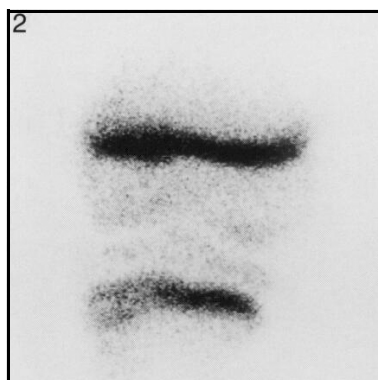
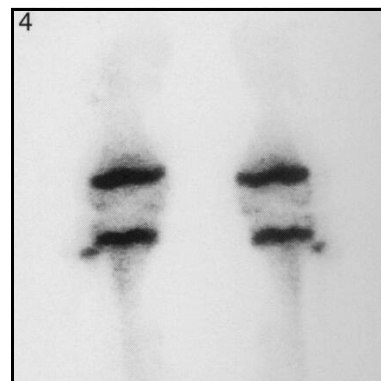
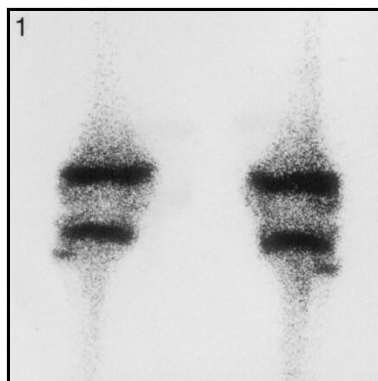


*FIG. 1. Posterior magnified view.*

*FIG. 4. Posterior view.*

*FIG. 2. Anterior pinhole view of right knee.*

*FIG. 5. Anterior pinhole view of left knee.*



**Technical comment**

Note that the fibula is better seen in the posterior views in Figs 1 and 4 than in the anterior pinhole views in Figs 2 and 5.

*FIG. 1. Posterior view.*

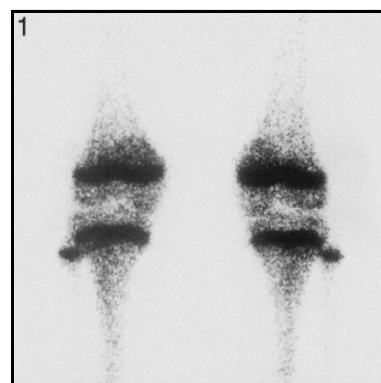


*FIG. 2. Posterior view.*

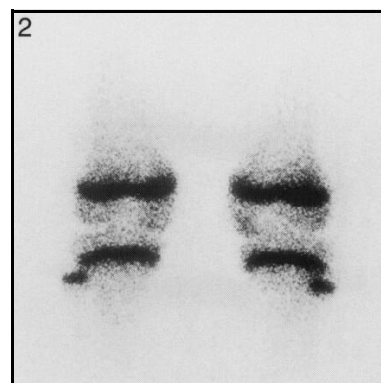


FIG. 1. Anterior view.

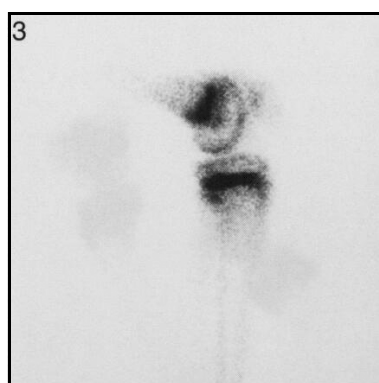
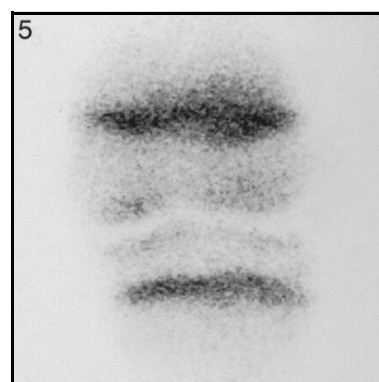
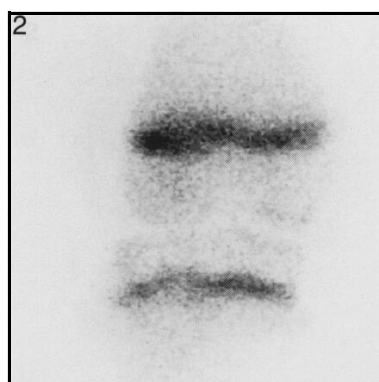
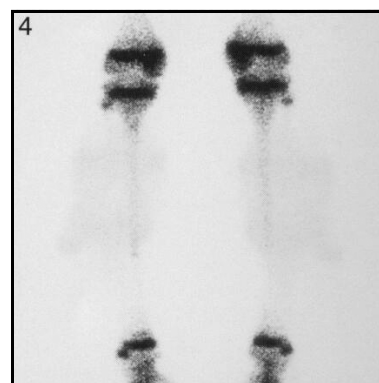
FIG. 4. Posterior view.

FIG. 2. Anterior pinhole view of right knee.

FIG. 5. Anterior pinhole view of right knee.

FIG. 3. Lateral view of left knee.

FIG. 6. Lateral view of right knee.



### Technical comment

The fibula is not seen in Figs 3 and 6 because the images are medial lateral views.

FIG. 1. Anterior view.

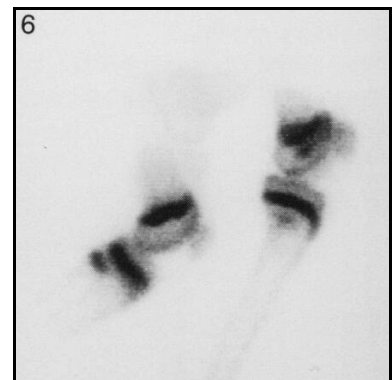
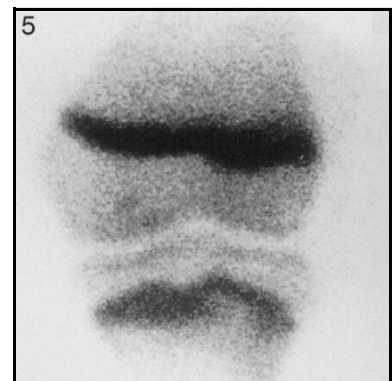
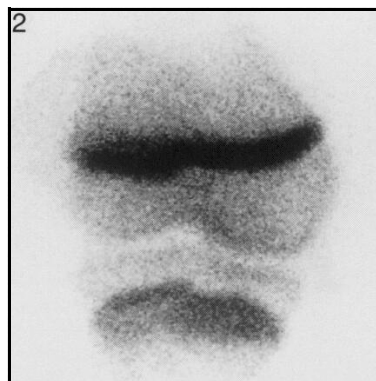
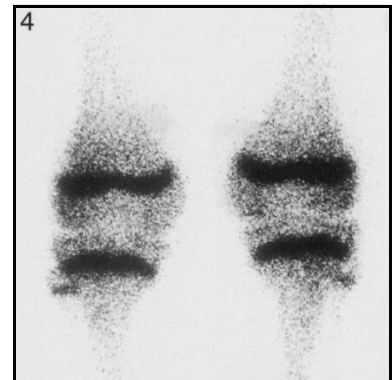
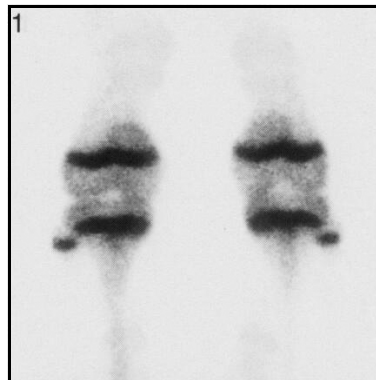
FIG. 4. Posterior view.

FIG. 2. Anterior pinhole view of right knee.

FIG. 5. Anterior pinhole view of left knee.

FIG. 3. Lateral view.

FIG. 6. Lateral view.



### Technical comment

Figures 3 and 6 represent lateral images of knees. On the left there is a medial lateral and a lateral lateral (Fig. 3), while on the right it is in reverse order (Fig. 6). The lateral lateral images show the head of the fibula clearly while the medial lateral images show the head of the fibula within the tibia but below the epiphyseal plate.

*FIG. 1. Posterior view.*

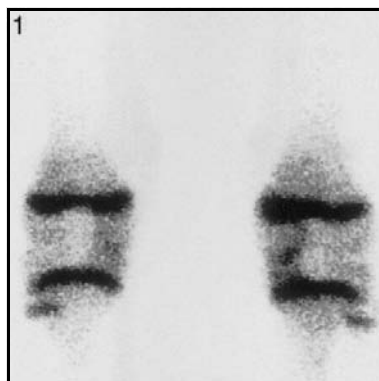


*FIG. 2. Anterior pinhole view of right knee.*

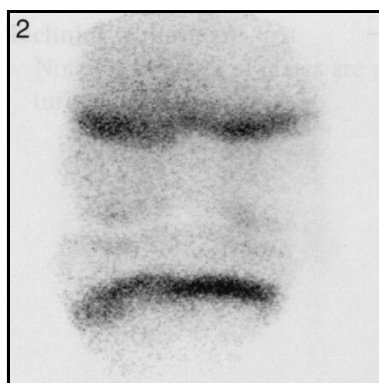


*FIG. 5. Anterior pinhole view of left knee.*

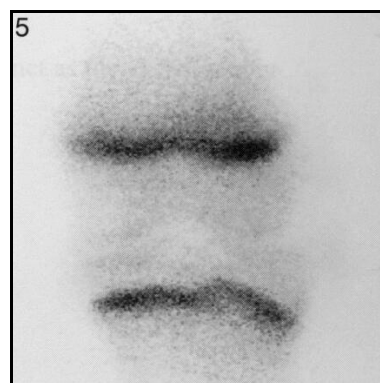
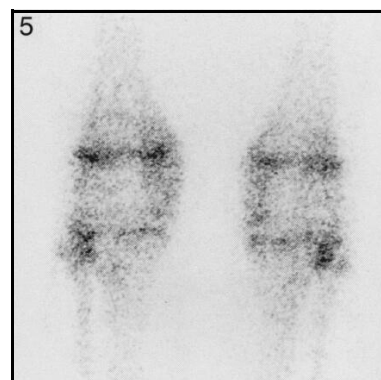
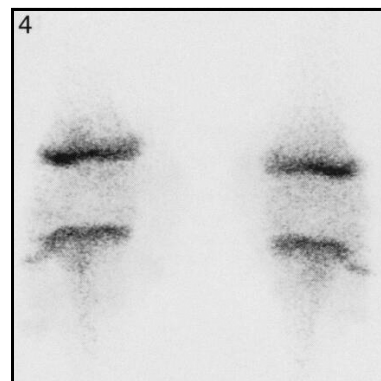
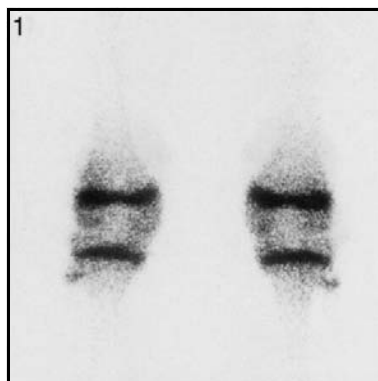


*FIG. 1. Posterior view.*

*FIG. 4. Posterior view.*

*FIG. 2. Anterior view.*

*FIG. 5. Posterior view.*

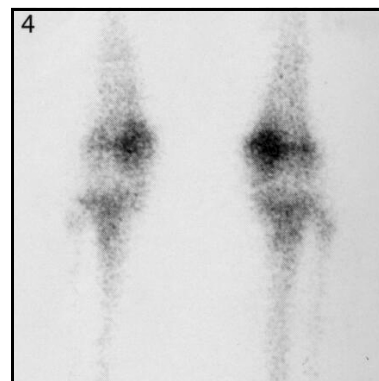


**Technical comment**

Note the differences in maturation of the epiphyseal plates in Figs 1, 2, 4 and 5.

*FIG. 1. Anterior view.*

*FIG. 4. Posterior view.*



**Technical comment**

Note the epiphyseal plates are distinct as the skeleton approaches maturity.



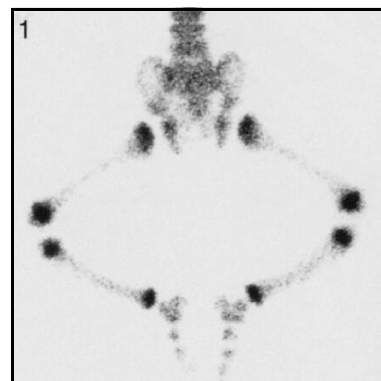
## **21. HIPS**



**21: Age: 0–6 months**

**Hips**

*FIG. 1. Posterior view.*



**21: Age: 6–12 months**

**Hips**

*FIG. 1. Posterior view.*

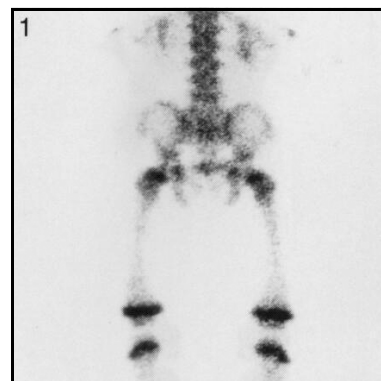


*FIG. 1. Posterior view.*



*FIG. 2. Pinhole view of right hip.*

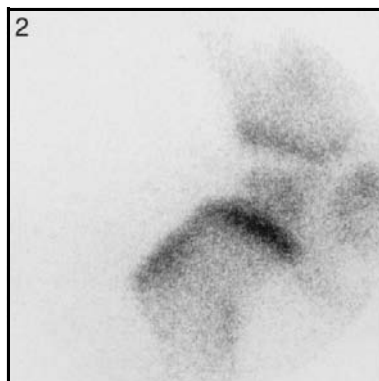


*FIG. 5. Pinhole view of left hip.*

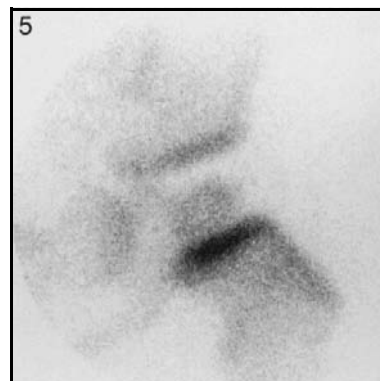
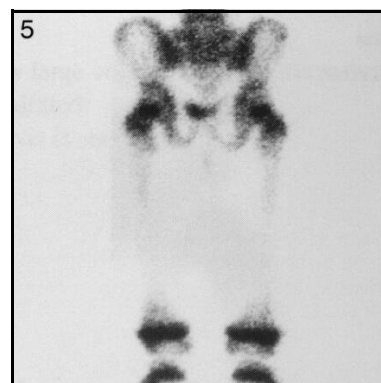
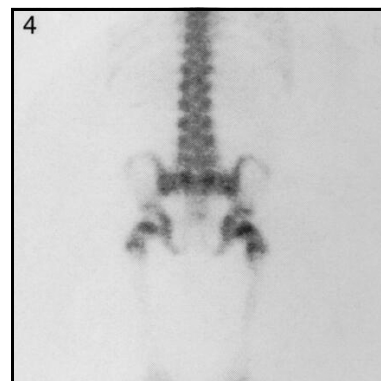


*FIG. 1. Anterior view.*

*FIG. 4. Posterior view.*

*FIG. 5. Posterior view.*



**Technical comments**

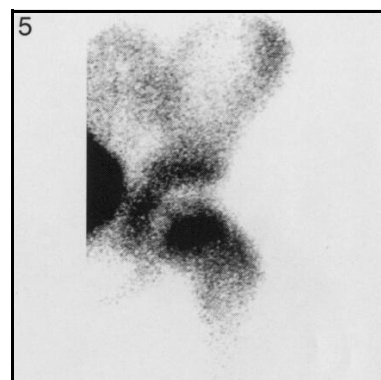
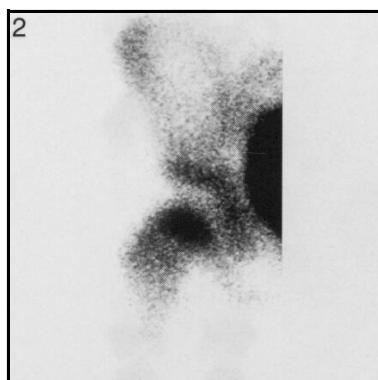
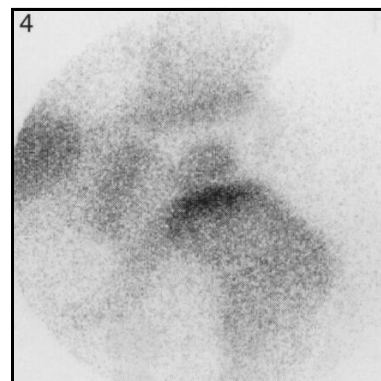
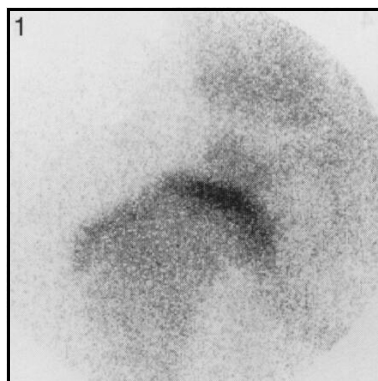
Note that the bladder is virtually empty in all three images; an ideal situation. Urine contamination below the pelvis is seen in Figs 1 and 5.

*FIG. 1. Pinhole view of right hip.*

*FIG. 4. Pinhole view of left hip.*

*FIG. 2. Pinhole view of right hip.*

*FIG. 5. Pinhole view of left hip.*

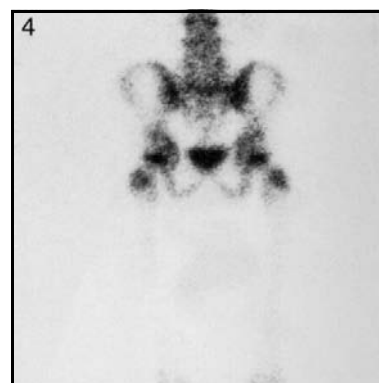
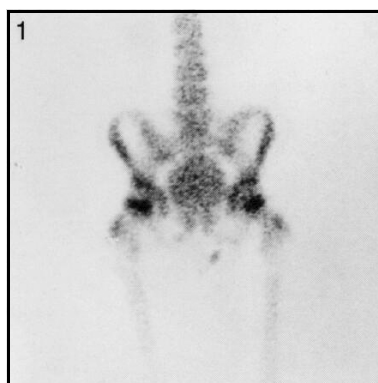


**Technical comment**

The femoral heads are well seen in Figs 1 and 4, while poor visualization is noted in Figs 2 and 5 because of poor positioning of the knees and feet.

*FIG. 1. Posterior view.*

*FIG. 4. Posterior view.*



**Technical comments**

The bladder in Fig. 1 is of relatively large volume but has little activity, suggesting that the child is well hydrated. Urine contamination below the pelvis is seen in Fig. 1.



*FIG. 1. Pinhole view of right hip.*

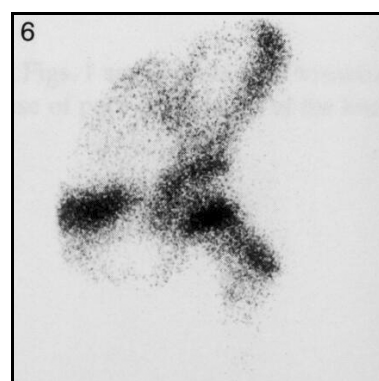
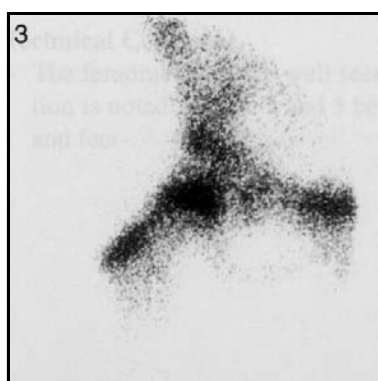
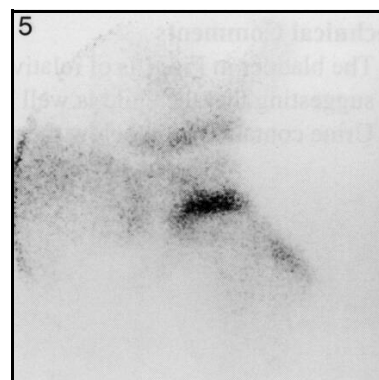
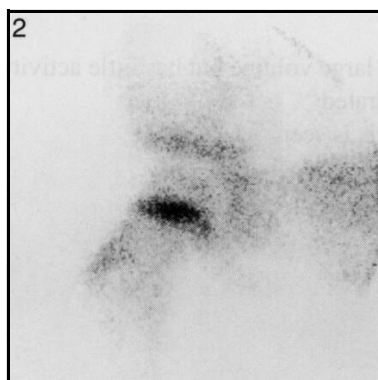
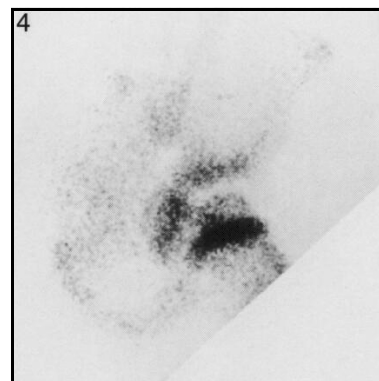
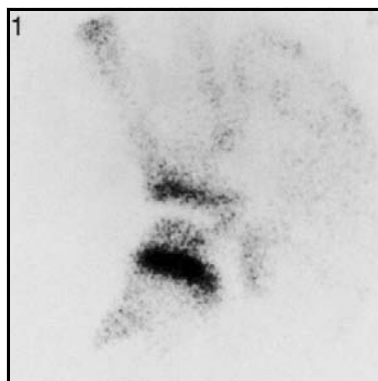
*FIG. 4. Pinhole view of left hip.*

*FIG. 2. Pinhole view of right hip.*

*FIG. 5. Pinhole view of left hip.*

*FIG. 3. Pinhole view of right hip.*

*FIG. 6. Pinhole view of left hip.*



### **Technical comments**

Different sizes of pinhole insert give different degrees of magnification.

The position of the hips in Figs 3 and 6 is not as good as in Figs 1, 2, 4 and 5. This is related to the positioning of the knees and the lack of turning in of the feet. The radiographic neutral position of the feet and knees is essential when doing pinholes of the hips.

*FIG. 1. Anterior view.*

*FIG. 4. Posterior view.*

*FIG. 2. Pinhole view of right hip.*

*FIG. 5. Pinhole view of left hip.*

*FIG. 3. Pinhole view of right hip.*

*FIG. 6. Pinhole view of left hip.*

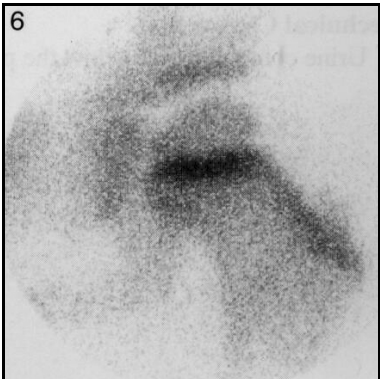
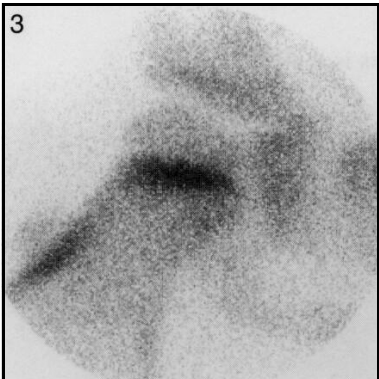
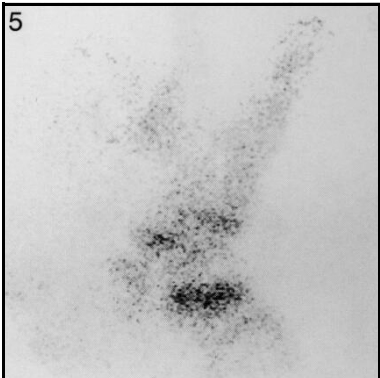
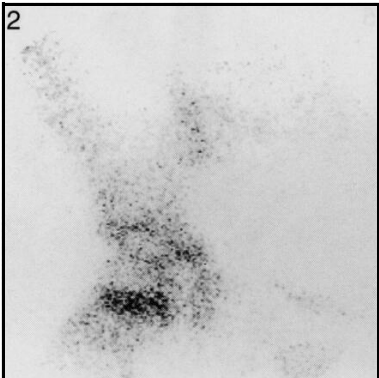
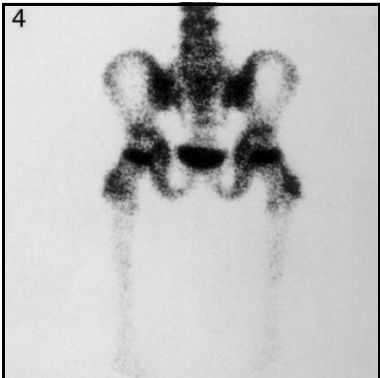
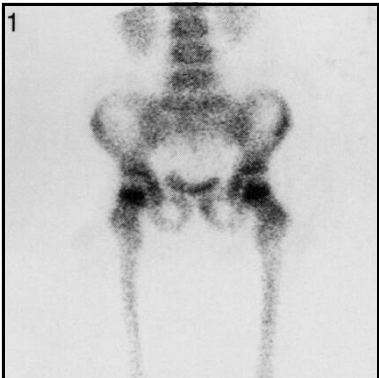


*FIG. 1. Anterior view.*

*FIG. 4. Posterior view.*

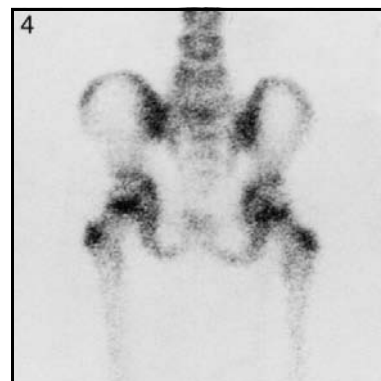
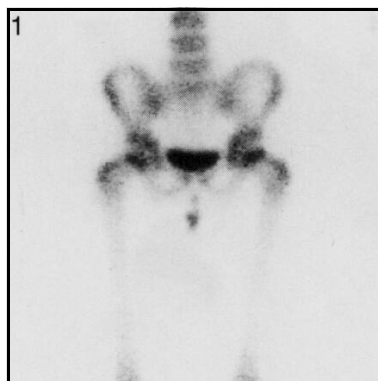
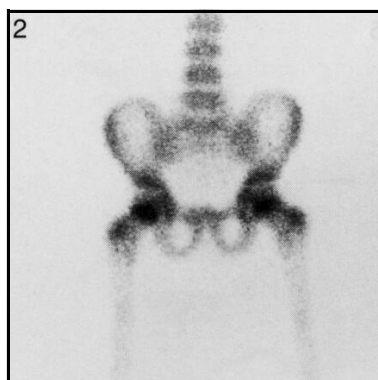


*FIG. 1. Anterior view.*

*FIG. 4. Posterior view.*



**Technical comment**

Urine contamination below the pelvis is seen in Fig. 1.

*FIG. 1. Pinhole view of right hip.*

*FIG. 4. Pinhole view of left hip.*

*FIG. 2. Pinhole view of right hip.*

*FIG. 5. Pinhole view of left hip.*

*FIG. 3. Pinhole view of right hip.*

*FIG. 6. Pinhole view of left hip.*

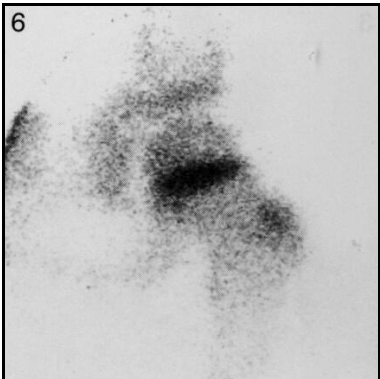
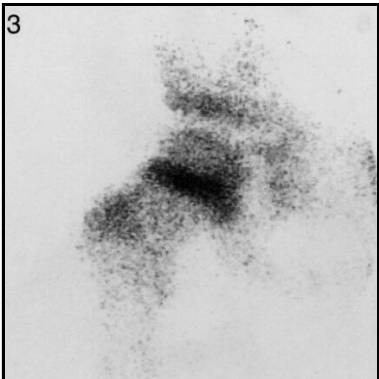
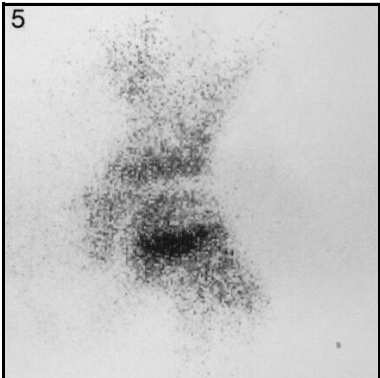
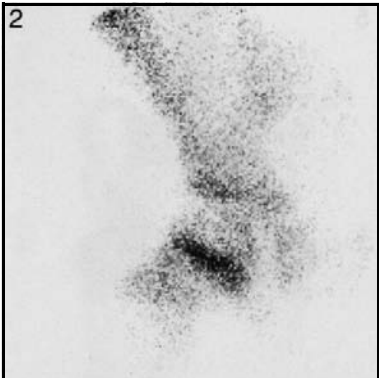
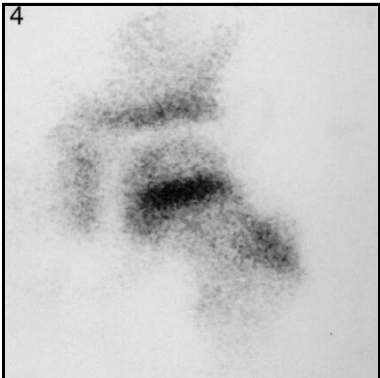
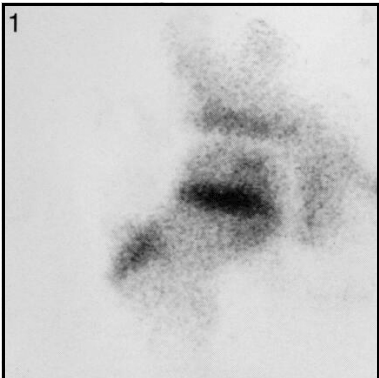


*FIG. 1. Anterior view.*



*FIG. 4. Posterior view.*



*FIG. 5. Posterior view.*

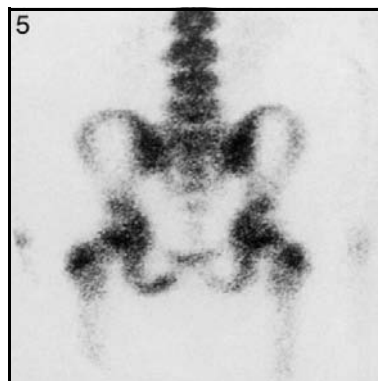


*FIG. 3. Pinhole view of right hip.*

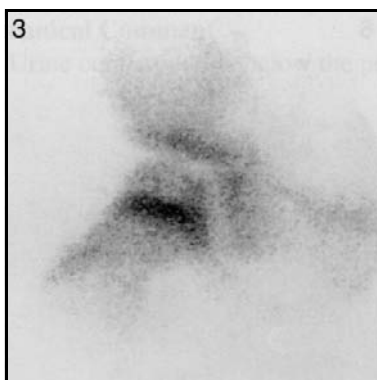
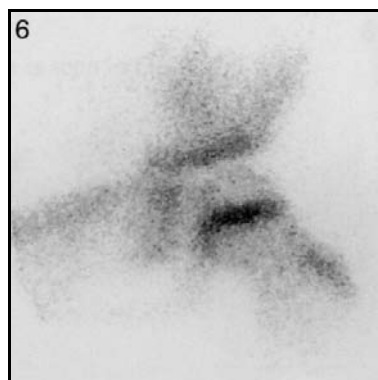


*FIG. 6. Pinhole view of left hip.*



**Technical comment**

Urine contamination below the pelvis is seen in Fig. 4.

**Potential pitfall**

Note the increased activity in Fig. 5 at the junction of the left ischial tuberosity and the posterior pubic ramus. This is due to the normal synchondrosis at this site.

*FIG. 1. Anterior view.*

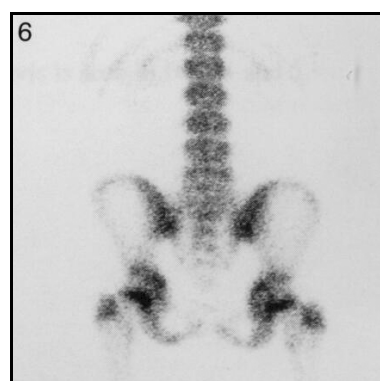
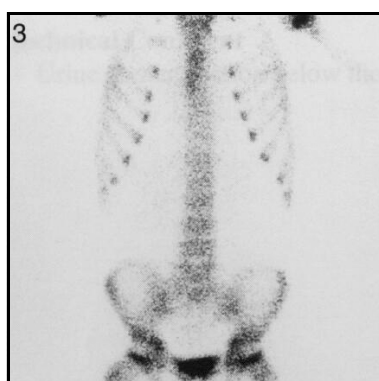
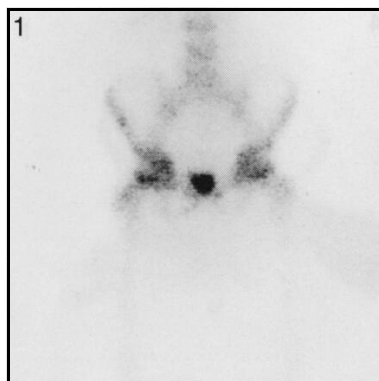
*FIG. 4. Posterior view.*

*FIG. 2. Anterior view.*

*FIG. 5. Posterior view.*

*FIG. 3. Anterior view.*

*FIG. 6. Posterior view.*



**Technical comment**

Urine contamination below the pelvis is seen in Figs 2 and 5.

*FIG. 1. Pinhole view of right hip.*

*FIG. 4. Pinhole view of left hip.*

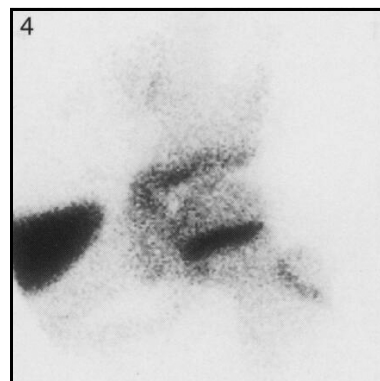
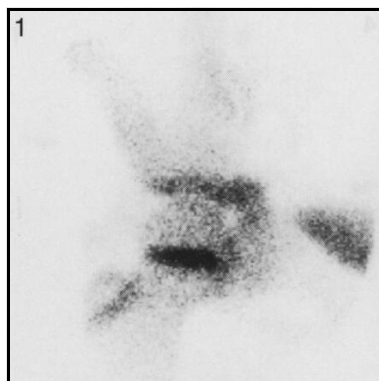
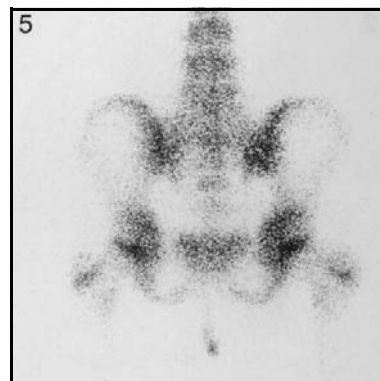
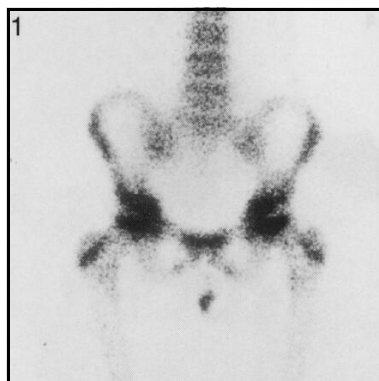


*FIG. 1. Anterior view.*

*FIG. 4. Posterior view.*

*FIG. 2. Anterior view.*

*FIG. 5. Posterior view.*



**Technical comment**

Urine contamination below the pelvis is seen in Figs 1 and 5.

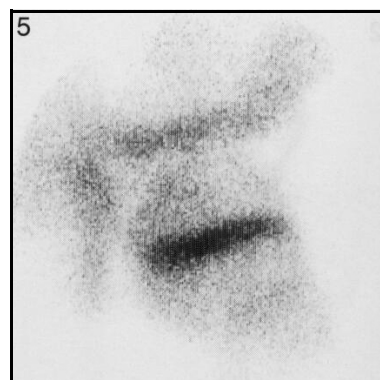
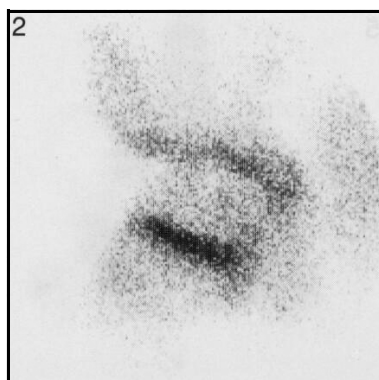
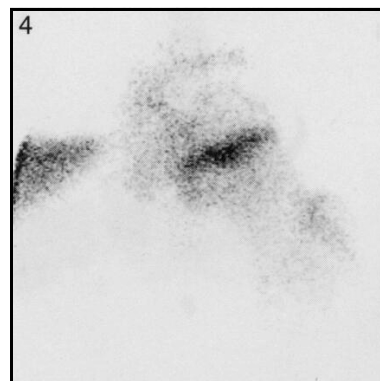
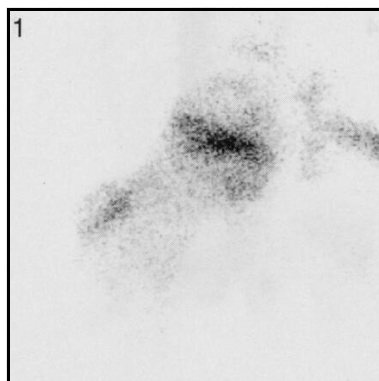


*FIG. 1. Pinhole view of right hip.*

*FIG. 4. Pinhole view of left hip.*

*FIG. 2. Pinhole view of right hip.*

*FIG. 5. Pinhole view of left hip.*



**Technical comment**

Figures 2 and 5 show a change in magnification, creating an apparent difference between the sizes of the hips.

FIG. 1. Anterior view.

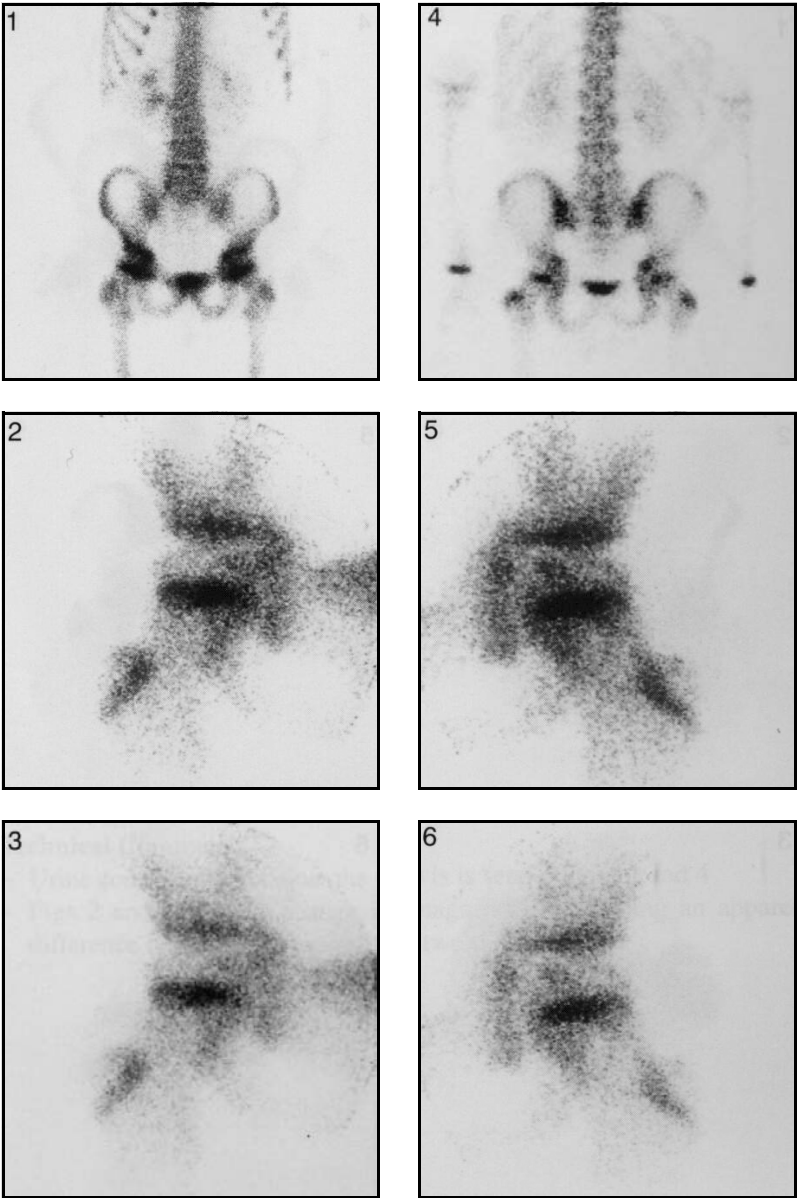
FIG. 4. Posterior view.

FIG. 2. Pinhole view of right hip.

FIG. 5. Pinhole view of left hip.

FIG. 3. Pinhole view of right hip.

FIG. 6. Pinhole view of left hip.



*FIG. 1. Anterior view.*

*FIG. 4. Posterior view.*

*FIG. 2. Anterior view.*

*FIG. 5. Posterior view.*

*FIG. 3. Pinhole view of right hip.*

*FIG. 6. Pinhole view of left hip.*

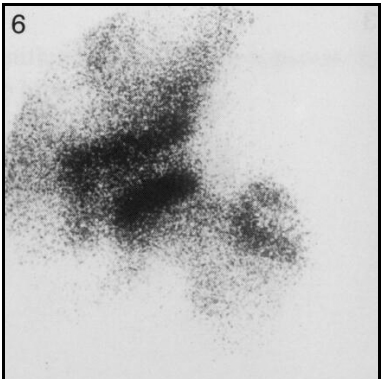
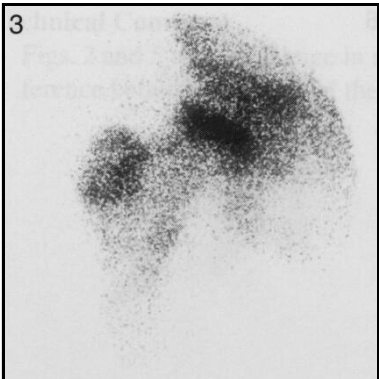
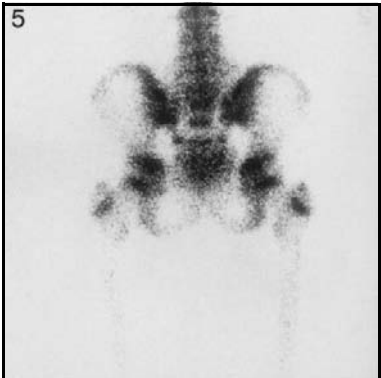
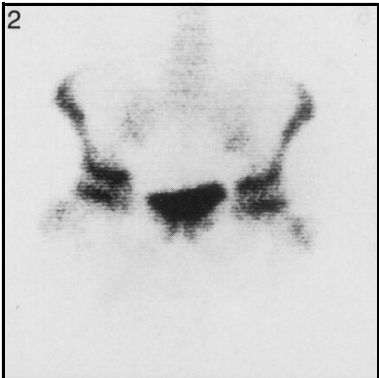
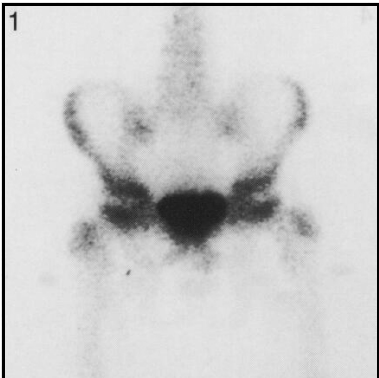
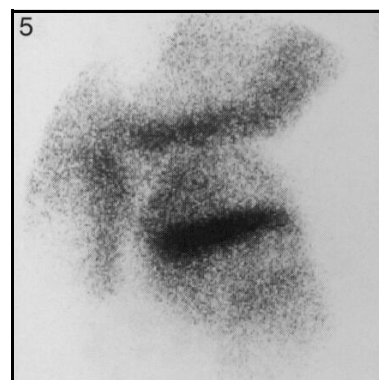
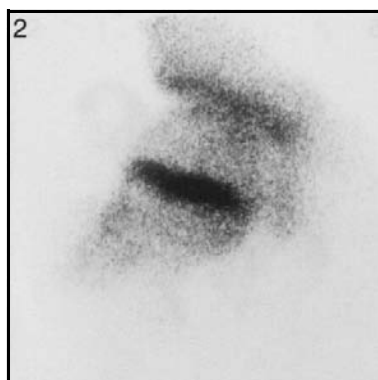
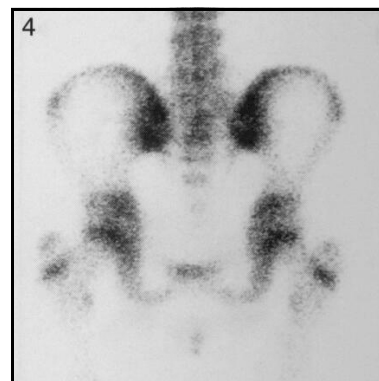


*FIG. 1. Anterior view.*

*FIG. 4. Posterior view.*

*FIG. 2. Pinhole view of right hip.*

*FIG. 5. Pinhole view of left hip.*



### **Technical comments**

Urine contamination below the pelvis is seen in Figs 1 and 4.

Figures 2 and 5 show a change in magnification, creating an apparent difference between the sizes of the hips.

*FIG. 1. Anterior view.*

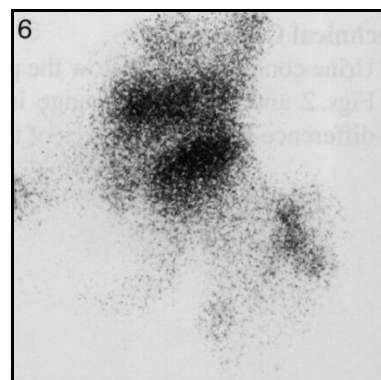
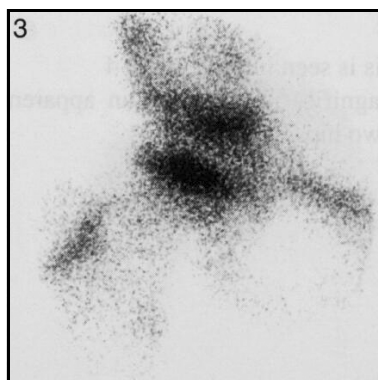
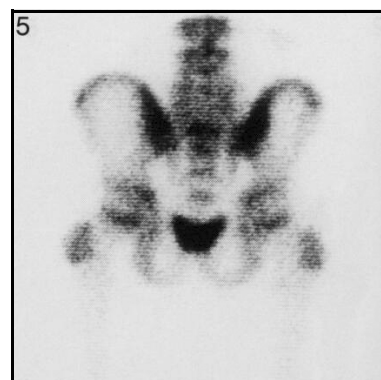
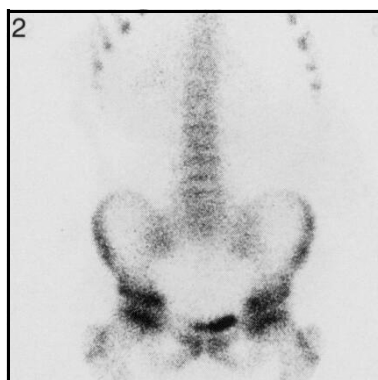
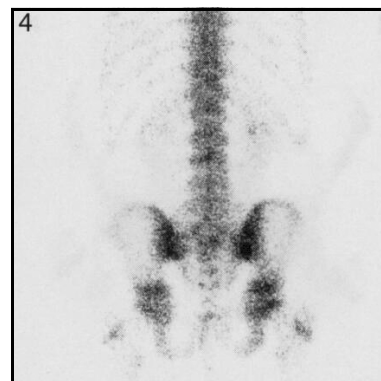
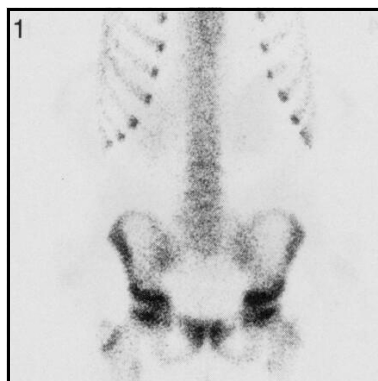
*FIG. 4. Posterior view.*

*FIG. 2. Anterior view.*

*FIG. 5. Posterior view.*

*FIG. 3. Pinhole view of right hip.*

*FIG. 6. Pinhole view of left hip.*



### **Technical comment**

Urine contamination below the pelvis is seen in Figs 1 and 4.

### **Potential pitfall**

The pubic rami show normal increased uptake of tracer in Figs 1 and 2.

*FIG. 1. Anterior view.*

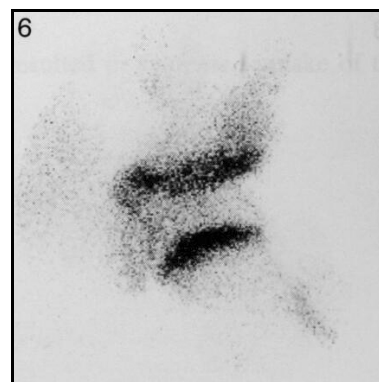
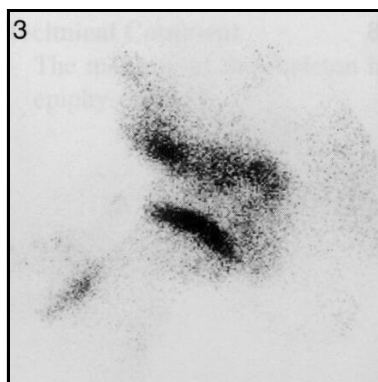
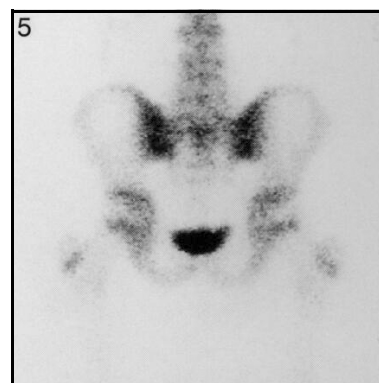
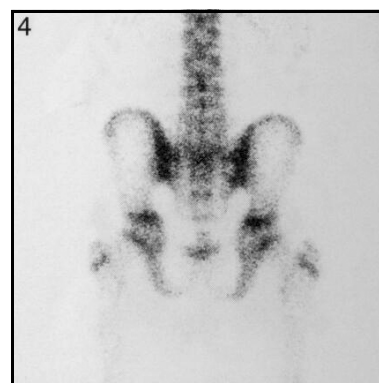
*FIG. 4. Posterior view.*

*FIG. 2. Anterior view.*

*FIG. 5. Posterior view.*

*FIG. 3. Pinhole view of right hip.*

*FIG. 6. Pinhole view of left hip.*



**Technical comment**

Urine contamination adjacent to the left ischium is seen in Fig. 2.

*FIG. 1. Anterior view.*

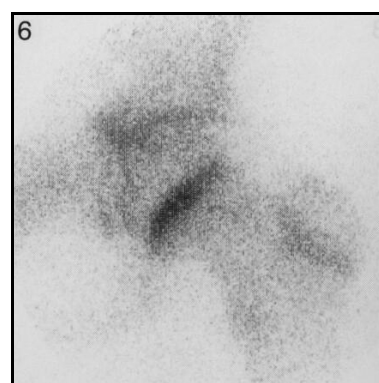
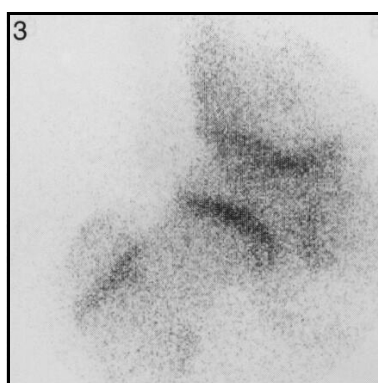
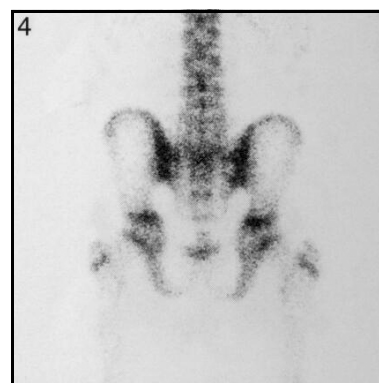
*FIG. 4. Posterior view.*

*FIG. 2. Anterior view.*

*FIG. 5. Posterior view.*

*FIG. 3. Pinhole view of right hip.*

*FIG. 6. Pinhole view of left hip.*



### **Technical comment**

Urine contamination to the left of the pubic bone is seen in Fig. 1.

### **Potential pitfall**

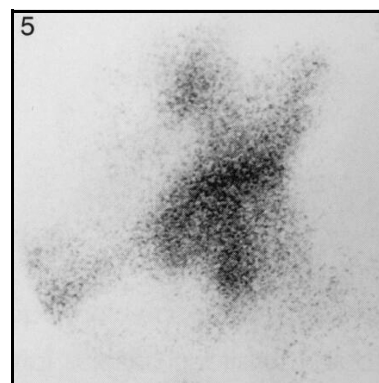
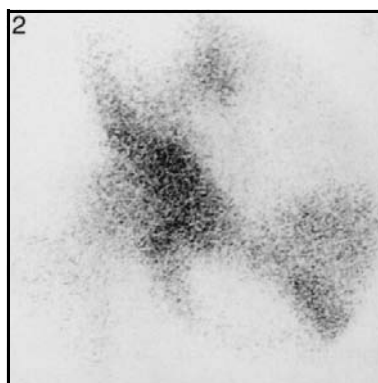
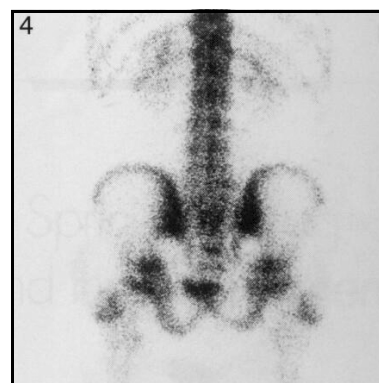
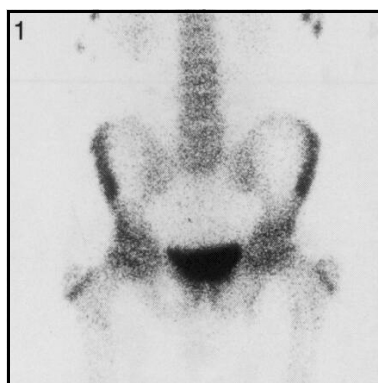
The apparent increased activity in the right sacroiliac joint in Fig. 2 is due to rotation of the pelvis and is not pathological.

*FIG. 1. Anterior view.*

*FIG. 4. Posterior view.*

*FIG. 2. Pinhole view of right hip.*

*FIG. 5. Pinhole view of left hip.*



**Technical comment**

The maturity of the skeleton has resulted in decreased uptake in the epiphyseal plates.

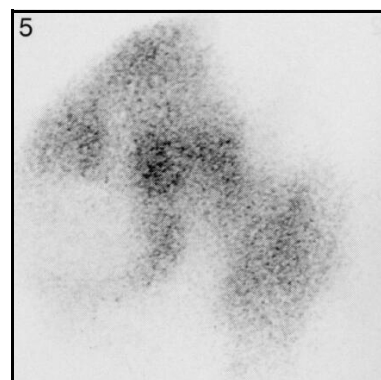
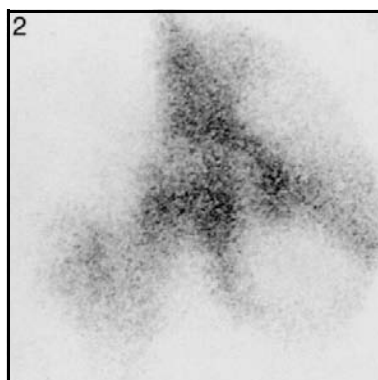
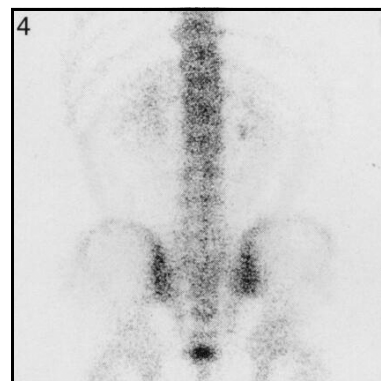
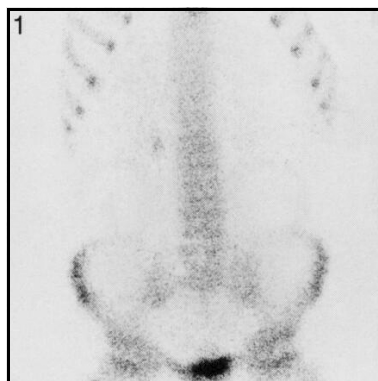


*FIG. 1. Anterior view.*

*FIG. 4. Posterior view.*

*FIG. 2. Pinhole view of right hip.*

*FIG. 5. Pinhole view of left hip.*





## 22. CONCLUDING REMARKS

In developing Member States, a radionuclide bone scan is one of the most commonly requested nuclear medicine procedures, comprising approximately 25–45% of the bulk of in vivo imaging procedures used in general nuclear medicine. These figures underline the clinical importance of bone scanning, as it provides aid in diagnosing bone and soft tissue infection and occult trauma lacking radiographic correlation, assessing post-traumatic injuries and staging of cancer patients. There is an established role for bone scanning in assessing the child with non-accidental injury, such as the child with a limp, for clarifying the underlying etiology as related to infection, inflammation or malignant disease.

Taking the large body of clinical experience, bone scanning is accepted as a safe, simple and reproducible diagnostic procedure, for both children and adults. In combination with early acquisition protocols, both arterial and blood pool imaging, the procedure delivers valuable information on inflammatory or malignant processes, response to therapy or tissue viability as encountered in diabetic patients or in complicated cases of frostbite.

Bone scintigraphy in the paediatric population requires special attention to acquisition techniques and to the patient's correct positioning and comfort during the study, thereby assuring high quality images. Acquiring additional views, image magnification and SPECT studies may be required to identify subtle lesions. The correlation of bone scans with conventional X ray studies is mandatory.

The advent of new hybrid imaging instrumentation (SPECT-CT or PET-CT) with high resolution CT systems and the introduction of PET-CT ( $^{18}\text{F}$ ) for the diagnosis of musculo-skeletal disease bone scans provide new impulses towards enhancing the diagnostic efficacy of bone scanning. Increasing evidence indicates that this is in part attributable to enhancing the specificity and sensitivity of the procedure by improved anatomical location and improved spatial resolution.

The endeavour to produce an atlas of the scintigraphic features of the usual developing skeleton required a review of over 1800 bone scans considered normal, which were provided by the following centres: Hospital for Sick Children, Department of Radiology, London, United Kingdom; Service de Biophysique, Centre Hospitalier d'Agen, Agen, France; Klinik und Poliklinik für Nuklearmedizin der Universität Mainz, Mainz, Germany; Hospital St. Pierre, Akademisch Ziekenhuis, Department of Radiology, Brussels, Belgium; Hospital General Vall d'Hebron, Department of Nuclear Medicine, Barcelona, Spain; Assistance Publique, Hôpitaux de Paris, Saint-Antoine, Service de Médecine Nucléaire, Paris, France, and the Red Cross War Memorial Children's Hospital, Department of Paediatrics and Child Health, Cape Town, South Africa.

We are indebted to the medical professionals for their invaluable contribution.



## Appendix I

### PAEDIATRIC DOSAGE OF RADIOPHARMACEUTICALS

This appendix provides two tables for calculating the age adjusted dosing of injected radiopharmaceuticals, as recommended by EANM with respect to paediatrics and dosimetry. Tables 1 and 2 are the revised versions of the prior, more simplified version that is provided as Table 3 for comparison.

The minimum recommended injected activity for  $^{99m}\text{Tc}$ -MDP is 40 MBq (Table 2). This is the activity that is recommended for the lowest body weight of 3 kg while assuring good quality images. For higher body weight (e.g. a child weighing 12 kg undergoing a bone scan with  $^{99m}\text{Tc}$ -MDP), first identify from Table 2 the Class and the Baseline Activity (Class B and 35 MBq for MDP). From Table 1 identify the weight factor and multiply by the Baseline Activity ( $35 \text{ MBq} \times 3.14$ ). Therefore, the amount of  $^{99m}\text{Tc}$ -MDP activity to be injected is 109.9 MBq.

Always be sure to choose the appropriate Class (A, B or C) from Table 2 to avoid errors in reading the multiplication factor from Table 1.<sup>1</sup>

For a copy of the dosage card please follow the link provided herewith:

<https://www.eanm.org/committees/dosimetry/dosagecard.pdf>

The radiopharmaceuticals, their corresponding class, baseline activity for calculating total injected activity and the minimum recommended activity.

The minimum recommended activity for each radiopharmaceutical should guarantee good image quality at the lowest acceptable radiation burden. Table 2 provides a list for 39 procedures. The alphabetic class designations A, B and C identify radiopharmaceuticals delivering higher radiation burdens for equal units of injected activity.

TABLE 1. THE EANM PAEDIATRIC DOSAGE CARD (VERSION 1.5.2008)

#### Multiple of Baseline Activity

Weight kg	Class A	Class B	Class C	Weight kg	Class A	Class B	Class C
3	1	1	1	32	3.77	7.29	14.00
4	1.12	1.14	1.33	34	3.88	7.72	15.00
6	1.47	1.71	2.00	36	4.00	8.00	16.00
8	1.71	2.14	3.00	38	4.18	8.43	17.00
10	1.94	2.71	3.67	40	4.29	8.86	18.00
12	2.18	3.14	4.67	42	4.41	9.14	19.00
14	2.35	3.57	5.67	44	4.53	9.57	20.00
16	2.53	4.00	6.33	46	4.65	10.00	21.00
18	2.71	4.43	7.33	48	4.77	10.29	22.00
20	2.88	4.86	8.33	50	4.88	10.71	23.00
22	3.06	5.29	9.33	52-54	5.00	11.29	24.67
24	3.18	5.71	10.00	56-58	5.24	12.00	26.67
26	3.35	6.14	11.00	60-62	5.47	12.71	28.67
28	3.47	6.43	12.00	64-66	5.65	13.43	31.00
30	3.65	6.86	13.00	68	5.77	14.00	32.33

<sup>1</sup> Adapted from: LASSMANN, M., BIASSONI, L., MONSIEURS, M., FRANZIUS, C., JACOBS, F., The new EANM paediatric dosage card, Eur. J. Nucl. Med. Mol. Imaging **35** (2008) 1748, and from the EANM Dosimetry and Paediatrics Committees.

Note that in special cases identical radiopharmaceutical might be assigned to a higher ‘class’ if organ dysfunction or disease exist, e.g.  $^{123}\text{I}$  Hippuran. Adapted from: LASSMANN, M., BIASSONI, L., MONSIEURS, M., FRANZIUS, C., JACOBS, F., The new EANM paediatric dosage card, Eur. J. Nucl. Med. Mol. Imaging **35** (2008) 1748, and from the EANM Dosimetry and Paediatrics Committees.

TABLE 2. RECOMMENDED MINIMUM AND BASELINE RADIOACTIVITIES FOR 39 DIAGNOSTIC PROCEDURES (MBq)

Radiopharmaceutical	Class	Baseline activity (for calculation purposes only) (MBq)	Minimum recommended activity <sup>a</sup> (MBq)
$^{123}\text{I}$ (thyroid)	C	0.6	3
$^{123}\text{I}$ Amphetamine (brain)	B	13.0	18
$^{123}\text{I}$ HIPPURAN (abnormal renal function)	B	5.3	10
$^{123}\text{I}$ HIPPURAN (normal renal function)	A	12.8	10
$^{123}\text{I}$ mIBG	B	28.0	80
$^{131}\text{I}$ mIBG	B	5.6	35
$^{18}\text{F}$ FDG (2-D) <sup>4</sup>	B	25.9	26
$^{18}\text{F}$ FDG (3-D), recommended in children <sup>b</sup>	B	14.0	14
$^{18}\text{F}$ Fluorine (2-D)	B	25.9	26
$^{18}\text{F}$ Fluorine (3-D), recommended in children	B	14.0	14
$^{67}\text{Ga}$ Citrate	B	5.6	10
$^{99\text{m}}\text{Tc}$ ALBUMIN (cardiac)	B	56.0	80
$^{99\text{m}}\text{Tc}$ COLLOID (gastric reflux)	B	2.8	10
$^{99\text{m}}\text{Tc}$ COLLOID (liver/spleen)	B	5.6	15
$^{99\text{m}}\text{Tc}$ COLLOID (marrow)	B	21.0	20
$^{99\text{m}}\text{Tc}$ DMSA	A	17.0	15
$^{99\text{m}}\text{Tc}$ DTPA (abnormal renal function)	B	14.0	20
$^{99\text{m}}\text{Tc}$ DTPA (normal renal function)	A	34.0	20
$^{99\text{m}}\text{Tc}$ ECD (brain perfusion)	B	32.0	110
$^{99\text{m}}\text{Tc}$ HMPAO (brain)	B	51.8	100
$^{99\text{m}}\text{Tc}$ HMPAO (WBC)	B	35.0	40
$^{99\text{m}}\text{Tc}$ IDA (biliary)	B	10.5	20
$^{99\text{m}}\text{Tc}$ MAA/microspheres	B	5.6	10
$^{99\text{m}}\text{Tc}$ MAG3	A	11.9	15
$^{99\text{m}}\text{Tc}$ MDP	B	35.0	40
$^{99\text{m}}\text{Tc}$ Pertechnetate (cystography)	B	1.4	20
$^{99\text{m}}\text{Tc}$ Pertechnetate (ectopic gastric mucosa)	B	10.5	20
$^{99\text{m}}\text{Tc}$ Pertechnetate (cardiac first pass)	B	35.0	80
$^{99\text{m}}\text{Tc}$ Pertechnetate (thyroid)	B	5.6	10
$^{99\text{m}}\text{Tc}$ RBC (blood pool)	B	56.0	80
$^{99\text{m}}\text{Tc}$ SestaMIBI/Tetrofosmin (cancer seeking agent)	B	63.0	80
$^{99\text{m}}\text{Tc}$ SestaMIBI/Tetrofosmin <sup>c</sup> (cardiac rest scan 2-day protocol min.)	B	42.0	80
$^{99\text{m}}\text{Tc}$ SestaMIBI/Tetrofosmin <sup>c</sup> (cardiac rest scan 2-day protocol max.)	B	63.0	80

TABLE 2. RECOMMENDED MINIMUM AND BASELINE RADIOACTIVITIES FOR 39 DIAGNOSTIC PROCEDURES (MBq) (cont.)

Radiopharmaceutical	Class	Baseline activity (for calculation purposes only) (MBq)	Minimum recommended activity <sup>a</sup> (MBq)
<sup>99m</sup> Tc SestaMIBI/Tetrofosmin <sup>c</sup> (cardiac stress scan 2-day protocol min.)	B	42.0	80
<sup>99m</sup> Tc SestaMIBI/Tetrofosmin <sup>c</sup> (cardiac stress scan 2-day protocol max.)	B	63.0	80
<sup>99m</sup> Tc SestaMIBI/Tetrofosmin <sup>c</sup> (cardiac rest scan 1-day protocol)	B	28.0	80
<sup>99m</sup> Tc SestaMIBI/Tetrofosmin <sup>c</sup> (cardiac stress scan 1-day protocol)	B	84.0	80
<sup>99m</sup> Tc Spleen (denatured RBC)	B	2.8	20
<sup>99m</sup> Tc TECHNEGAS (lung ventilation) <sup>d</sup>	B	70.0	100


<sup>a</sup> The minimum recommended activities are calculated for commonly used gamma cameras or positron emission tomographs. Lower activities could be administered when using systems with higher counting efficiency.

<sup>b</sup> For brain imaging using the FDG, the maximum injected activity recommended by EANM is within the range of 300–600 MBq (typically 370 MBq) for 2-D and 125–250 MBq (typically 150 MBq) for 3-D. See guideline Brain Imaging Using [18F]FDG on [www.eanm.org](http://www.eanm.org) (section Publications/Guidelines).

<sup>c</sup> The minimum and maximum values correspond to the recommended administered activities discussed in the EANM/ESC procedural guidelines: HESSE, B., et al., EANM/ESC procedural guidelines for myocardial perfusion imaging in nuclear cardiology, *Eur. J. Nucl. Med. Mol. Imaging* **32** (2005) 855–897.

<sup>d</sup> This is the activity load needed to prepare the TECHNEGAS device. The amount of retained activity in the lung will be significantly lower, typically, for adults it will be in the range 15–60 MBq.

TABLE 3. FRACTION OF ADULT ADMINISTERED ACTIVITY AND THE MINIMUM RECOMMENDED ACTIVITY OF THE OLD PAEDIATRIC DOSAGE CARD (MBq)

			Recommended adult and minimum amount (MBq)		
Paediatric Task Group			Radiopharmaceutical	Adult	Minimum activity
<b>Fraction of Adult Administered Activity</b>			<sup>99m</sup> Tc DTPA	200	20
			<sup>99m</sup> Tc DMSA	100	15
			<sup>99m</sup> Tc MAG3	70	15
			<sup>99m</sup> Tc Pertechnetate (cystography)	20	20
			<sup>99m</sup> Tc MDP	500	40
			<sup>99m</sup> Tc COLLOID (liver/spleen)	80	15
			<sup>99m</sup> Tc COLLOID (marrow)	300	20
			<sup>99m</sup> Tc Denaturated RBC (spleen)	40	20
			<sup>99m</sup> Tc RBC (blood pool)	800	80
			<sup>99m</sup> Tc ALBUMIN (cardiac)	800	80
			<sup>99m</sup> Tc Pertechnetate (cardiac first pass)	500	80
			<sup>99m</sup> Tc MAA/Microspheres	80	10
			<sup>99m</sup> Tc Pertechnetate (ectopic gastric)	150	20
			<sup>99m</sup> Tc COLLOID (gastric reflux)	40	10
			<sup>99m</sup> Tc IDA (biliary)	150	20
			<sup>99m</sup> Tc Pertechnetate (thyroid)	80	10
			<sup>99m</sup> Tc HMPAO (brain)	740	100
			<sup>99m</sup> Tc HMPAO (WBC)	500	40
			<sup>123</sup> I HIPURAN	75	10
			<sup>123</sup> I NaI (thyroid)	20	3
			<sup>123</sup> I mIBG	200	35
			<sup>131</sup> I mIBG	80	35
			<sup>67</sup> Ga-Citrate	80	10

This first and simplified version of the dosage card was recommended earlier by the EANM's Paediatric Task Group. It should be noted that this table resembles an outdated version of the dosage card. It is strongly recommended that the combined information provided in Tables 1 and 2 be used to calculate the patient's injected activity dose.



## CONTRIBUTORS TO DRAFTING AND REVIEW

Fischer, S.	Klinik und Poliklinik für Nuklearmedizin der Universität Mainz, Germany
Gilday, D.L.	The Hospital for Sick Children, Canada
Gordon, I.	Hospital for Sick Children, United Kingdom
Guillet, J.	Centre Hospitalier d'Agen, France
Hahn, K.	Klinik und Poliklinik für Nuklearmedizin der Universität Mainz, Germany
Mann, M.D.	Red Cross War Memorial Children's Hospital, South Africa
Piepsz, A.	CHU Saint-Pierre, Belgium
Roca, I.	Hospital Vall d'Hebron, Spain
Wioland, M.	Hôpitaux de Paris, Saint-Antoine, France
Zaknun, J.J.	International Atomic Energy Agency





# IAEA

International Atomic Energy Agency

No. 22

## Where to order IAEA publications

In the following countries IAEA publications may be purchased from the sources listed below, or from major local booksellers. Payment may be made in local currency or with UNESCO coupons.

### AUSTRALIA

DA Information Services, 648 Whitehorse Road, MITCHAM 3132  
Telephone: +61 3 9210 7777 • Fax: +61 3 9210 7788  
Email: [service@dadirect.com.au](mailto:service@dadirect.com.au) • Web site: <http://www.dadirect.com.au>

### BELGIUM

Jean de Lannoy, avenue du Roi 202, B-1190 Brussels  
Telephone: +32 2 538 43 08 • Fax: +32 2 538 08 41  
Email: [jean.de.lannoy@infoboard.be](mailto:jean.de.lannoy@infoboard.be) • Web site: <http://www.jean-de-lannoy.be>

### CANADA

Bernan Associates, 4501 Forbes Blvd, Suite 200, Lanham, MD 20706-4346, USA  
Telephone: 1-800-865-3457 • Fax: 1-800-865-3450  
Email: [customercare@bernan.com](mailto:customercare@bernan.com) • Web site: <http://www.bernan.com>

Renouf Publishing Company Ltd., 1-5369 Canotek Rd., Ottawa, Ontario, K1J 9J3  
Telephone: +613 745 2665 • Fax: +613 745 7660  
Email: [order.dept@renoufbooks.com](mailto:order.dept@renoufbooks.com) • Web site: <http://www.renoufbooks.com>

### CHINA

IAEA Publications in Chinese: China Nuclear Energy Industry Corporation, Translation Section, P.O. Box 2103, Beijing

### CZECH REPUBLIC

Suweco CZ, S.R.O., Klecakova 347, 180 21 Praha 9  
Telephone: +420 26603 5364 • Fax: +420 28482 1646  
Email: [nakup@suweco.cz](mailto:nakup@suweco.cz) • Web site: <http://www.suweco.cz>

### FINLAND

Akateeminen Kirjakauppa, PO BOX 128 (Keskuskatu 1), FIN-00101 Helsinki  
Telephone: +358 9 121 41 • Fax: +358 9 121 4450  
Email: [akatilais@akateeminen.com](mailto:akatilais@akateeminen.com) • Web site: <http://www.akateeminen.com>

### FRANCE

Form-Edit, 5, rue Janssen, P.O. Box 25, F-75921 Paris Cedex 19  
Telephone: +33 1 42 01 49 49 • Fax: +33 1 42 01 90 90  
Email: [formedit@formedit.fr](mailto:formedit@formedit.fr) • Web site: <http://www.formedit.fr>  
  
Lavoisier SAS, 145 rue de Provigny, 94236 Cachan Cedex  
Telephone: + 33 1 47 40 67 02 • Fax +33 1 47 40 67 02  
Email: [romuald.verrier@lavoisier.fr](mailto:romuald.verrier@lavoisier.fr) • Web site: <http://www.lavoisier.fr>

### GERMANY

UNO-Verlag, Vertriebs- und Verlags GmbH, Am Hofgarten 10, D-53113 Bonn  
Telephone: + 49 228 94 90 20 • Fax: +49 228 94 90 20 or +49 228 94 90 222  
Email: [bestellung@uno-verlag.de](mailto:bestellung@uno-verlag.de) • Web site: <http://www.uno-verlag.de>

### HUNGARY

Librotrade Ltd., Book Import, P.O. Box 126, H-1656 Budapest  
Telephone: +36 1 257 7777 • Fax: +36 1 257 7472 • Email: [books@librotrade.hu](mailto:books@librotrade.hu)

### INDIA

Allied Publishers Group, 1st Floor, Dubash House, 15, J. N. Heredia Marg, Ballard Estate, Mumbai 400 001,  
Telephone: +91 22 22617926/27 • Fax: +91 22 22617928  
Email: [alliedpl@vsnl.com](mailto:alliedpl@vsnl.com) • Web site: <http://www.alliedpublishers.com>  
  
Bookwell, 2/72, Nirankari Colony, Delhi 110009  
Telephone: +91 11 23268786, +91 11 23257264 • Fax: +91 11 23281315  
Email: [bookwell@vsnl.net](mailto:bookwell@vsnl.net)

### ITALY

Libreria Scientifica Dott. Lucio di Biasio "AEIOU", Via Coronelli 6, I-20146 Milan  
Telephone: +39 02 48 95 45 52 or 48 95 45 62 • Fax: +39 02 48 95 45 48  
Email: [info@libreriaaeiou.eu](mailto:info@libreriaaeiou.eu) • Website: [www.libreriaaeiou.eu](http://www.libreriaaeiou.eu)

## **JAPAN**

Maruzen Company, Ltd., 13-6 Nihonbashi, 3 chome, Chuo-ku, Tokyo 103-0027  
Telephone: +81 3 3275 8582 • Fax: +81 3 3275 9072  
Email: journal@maruzen.co.jp • Web site: <http://www.maruzen.co.jp>

## **REPUBLIC OF KOREA**

KINS Inc., Information Business Dept. Samho Bldg. 2nd Floor, 275-1 Yang Jae-dong SeoCho-G, Seoul 137-130  
Telephone: +02 589 1740 • Fax: +02 589 1746 • Web site: <http://www.kins.re.kr>

## **NETHERLANDS**

De Lindeboom Internationale Publicaties B.V., M.A. de Ruyterstraat 20A, NL-7482 BZ Haaksbergen  
Telephone: +31 (0) 53 5740004 • Fax: +31 (0) 53 5729296  
Email: books@delindeboom.com • Web site: <http://www.delindeboom.com>

Martinus Nijhoff International, Koraalrood 50, P.O. Box 1853, 2700 CZ Zoetermeer  
Telephone: +31 793 684 400 • Fax: +31 793 615 698  
Email: info@nijhoff.nl • Web site: <http://www.nijhoff.nl>

Swets and Zeitlinger b.v., P.O. Box 830, 2160 SZ Lisse  
Telephone: +31 252 435 111 • Fax: +31 252 415 888  
Email: info@swets.nl • Web site: <http://www.swets.nl>

## **NEW ZEALAND**

DA Information Services, 648 Whitehorse Road, MITCHAM 3132, Australia  
Telephone: +61 3 9210 7777 • Fax: +61 3 9210 7788  
Email: service@dadirect.com.au • Web site: <http://www.dadirect.com.au>

## **SLOVENIA**

Cankarjeva Založba d.d., Kopitarjeva 2, SI-1512 Ljubljana  
Telephone: +386 1 432 31 44 • Fax: +386 1 230 14 35  
Email: import.books@cankarjeva-z.si • Web site: <http://www.cankarjeva-z.si/uvvoz>

## **SPAIN**

Díaz de Santos, S.A., c/ Juan Bravo, 3A, E-28006 Madrid  
Telephone: +34 91 781 94 80 • Fax: +34 91 575 55 63  
Email: compras@diazdesantos.es, carmela@diazdesantos.es, barcelona@diazdesantos.es, julio@diazdesantos.es  
Web site: <http://www.diazdesantos.es>

## **UNITED KINGDOM**

The Stationery Office Ltd, International Sales Agency, PO Box 29, Norwich, NR3 1 GN  
Telephone (orders): +44 870 600 5552 • (enquiries): +44 207 873 8372 • Fax: +44 207 873 8203  
Email (orders): book.orders@tso.co.uk • (enquiries): book.enquiries@tso.co.uk • Web site: <http://www.tso.co.uk>

### **On-line orders**

DELTA Int. Book Wholesalers Ltd., 39 Alexandra Road, Addlestone, Surrey, KT15 2PQ  
Email: info@profbooks.com • Web site: <http://www.profbooks.com>

### **Books on the Environment**

Earthprint Ltd., P.O. Box 119, Stevenage SG1 4TP  
Telephone: +44 1438748111 • Fax: +44 1438748844  
Email: orders@earthprint.com • Web site: <http://www.earthprint.com>

## **UNITED NATIONS**

Dept. I004, Room DC2-0853, First Avenue at 46th Street, New York, N.Y. 10017, USA  
(UN) Telephone: +800 253-9646 or +212 963-8302 • Fax: +212 963-3489  
Email: publications@un.org • Web site: <http://www.un.org>

## **UNITED STATES OF AMERICA**

Bernan Associates, 4501 Forbes Blvd., Suite 200, Lanham, MD 20706-4346  
Telephone: 1-800-865-3457 • Fax: 1-800-865-3450  
Email: customercare@bernan.com • Web site: <http://www.bernan.com>

Renouf Publishing Company Ltd., 812 Proctor Ave., Ogdensburg, NY, 13669  
Telephone: +888 551 7470 (toll-free) • Fax: +888 568 8546 (toll-free)  
Email: order.dept@renoufbooks.com • Web site: <http://www.renoufbooks.com>

**Orders and requests for information may also be addressed directly to:**

### **Marketing and Sales Unit, International Atomic Energy Agency**

Vienna International Centre, PO Box 100, 1400 Vienna, Austria  
Telephone: +43 1 2600 22529 (or 22530) • Fax: +43 1 2600 29302  
Email: sales.publications@iaea.org • Web site: <http://www.iaea.org/books>

Bone scintigraphy is a widely accepted method for the evaluation of paediatric bone metabolism. Its strengths are high sensitivity and the capability to investigate the entire skeleton in a single examination. The interpretation of bone scanning in children is challenging and requires knowledge of the appearance of the maturing skeleton. The atlas provides an overview of issues related to the bone physiology and variants, and points out pitfalls that might be encountered in daily routine work. Specific suggestions and hints assist in establishing adequate imaging protocols to deliver optimal image quality adjusted to the needs of each age group. The atlas will serve as a valuable reference for nuclear medicine physicians, radiologists and orthopaedic surgeons and those involved in teaching and performing paediatric bone scan imaging.

## IAEA HUMAN HEALTH SERIES

INTERNATIONAL ATOMIC ENERGY AGENCY

VIENNA

ISBN 978-92-0-112710-5

ISSN 2075-3772